Designed Degradation of a Specific Protein in the Cell

Dissertation

zur

Erlangung der naturwissenschaftlichen Doktorwürde (Dr. sc. nat.)

vorgelegt der

Mathematisch-naturwissenschaftlichen Fakultät

der

Universität Zürich

von

Myriam Vincent

aus

Frankreich

Promotionskomitee

Prof. Dr. Andreas Plückthun (Vorsitz)

Prof. Dr. Peter Sonderegger

Prof. Dr. Matthias Peter

Dr. Olivier Coux

Zürich, 2010

To my grand-mother,

Sans qui je ne serais pas arrivée jusque là.

Table of contents

Abstract

In eukaryotes, the majority of intracellular proteins are degraded by a 2.5 megadaltons multimeric assembly, the proteasome. This giant self-compartmentalizing protease ensures the quality of intracellular proteins and controls numerous cellular processes by regulating the break-down of key regulatory proteins. Selectively depleting intracellular proteins could open a new avenue for protein function analysis and therapeutic applications. It can be achieved by specifically leading the protein of interest to the proteasome for degradation. Several protein knock-out techniques were developed, but engineered degradation has so far been successfully applied to very few proteins only, and every time redesigned case by case. To further assess the potential of protein knock-out, we chose to use a common binding scaffold, DARPins, for the design of diverse generalizable effector proteins, meant to degrade any kind of target protein.

The proteasome functions primarily to break down proteins which have been covalently modified with a polyubiquitin tag. Ubiquitin protein ligases (E3) are the enzymes responsible for the substrate specificity of the ubiquitination reaction. We aimed at altering their recognition function to ubiquitinate selected proteins. SCF (Skp1 - Cullin - F-Box protein) ubiquitin ligases, a well characterized family of multisubunit E3 enzymes, were exploited to achieve designed degradation. They contain a core enzymatic structure and an interchangeable F-Box protein subunit, which is responsible for the SCF substrate specificity. A chimeric F-box protein was engineered using DARPin to provide an artificial specificity domain. In *S. cerevisiae*, a chimeric F-box protein could specifically destabilize a cognate target protein in a SCF- and proteasome-dependent manner. The chimeric F box protein was further reengineered in order to better investigate how F-box proteins mediate ubiquitination. A deeper understanding of the ubiquitination machinery was gained but the target protein degradation efficiency stayed limited.

An ubiquitin free route was also used as an alternative strategy for degrading selected proteins. A small subset of proteins is degraded by the proteasome without prior ubiquitination. These proteins contain a degradation signal, named degron, enabling a direct interaction with the proteasome. The ODC and NYV degron sequences, originating from the mouse ornithine decarboxylase and the G1 glycoprotein of NY-1V hantavirus, respectively, were evaluated in *S. cerevisiae*. Different kinds of target proteins, among which highly stable ones like DARPins, were very rapidly degraded by the proteasome, when the ODC- or NYV-degron was fused to their C termini. We then assessed if a degron could work in trans to induce degradation of a binding partner. A DARPin-degron was co-expressed with a cognate target protein in *S. cerevisiae*. Whereas the DARPin-degron was quickly degraded, the levels of the target protein were not affected. In mammalian cells, DARPin-degron constructs could be targeted to the proteasome with a lower rate than in *S. cerevisiae*. In spite of more favorable interaction conditions and complex formation, a co-expressed cognate target protein was still not co-degraded.

Targeted degradation may be very valuable for the complete removal of proteins potentially toxic for the cell such as oncoproteins, viral proteins and stabilized proteins in neurodegenerative diseases. Our experimental data indicate that targeting a selected protein to the proteasome might not be enough to turn it into an eligible substrate. The proteasome might require specific substrate characteristics to achieve efficient degradation, making the development of a general protein knock-out strategy more challenging than it was previously assumed.

Zusammenfassung

In Eukaryoten wird die Merheit der intrazellulären Proteine vom Proteasom, einem 2.5 Megadalton multimerischen Komplex abgebaut. Diese gigantische Protease ist verantwortlich für die Qualität der intrazellulären Proteine und kontrolliert zahlreiche zelluläre Prozesse durch den Abbau von Proteinen mit Schlüsselfunktionen. Der spezifische Abbau von intrazellulären Proteinen könnte einen neuen Weg für die Funktionsanalyse von Proteinen eröffnen und zudem eine therapeutische Anwedung haben. Eine Möglichkeit, um ein bestimmtes Zielprotein abzubauen, ist es dieses spezifisch zum Proteasom zu führen. Mehrere Protein-knock-out-Techniken/Strategien wurden entwickelt, konnten bis zum jetzigen Zeitpunkt aber nur für ein begrenzte Reihe von Proteinen bewiesen werden. Zudem musste das Verfahren für jedes Zielprotein einzeln optimiert werden. Um das Potenzial von Protein-knock-out-Strategien richtig einzuschätzen, haben wir ein generelles proteinbindendes Molekül, DARPIns, zu Hilfe genommen. Mithilfe dieser DARPins wurden verschiedene Effektor moleküle hergestellt, welche den Abbau von beliebigen Protein ermöglichen sollten.

Das Proteasom zerstört hauptsächlich Proteine, an die eine Polyubiquitinkette angehängt wurde. Ubiquitin-Protein-Ligasen (E3) sind diejenigen Enzyme, die für die Spezifizität der Ubiquitinierungsreaktion verantwortlich sind. Eine Strategie verfolgte die Modifizierung der Erkennungsfunktion der E3-Ligasen, so dass diese ein Zielprotein für die Ubiquitinierungsreaktion auswählen würden. SCF (Skp1 - Cullin - F-Box protein)- Ubiquitin-Ligasen, eine Familie von multimerischen E3-Enzymen, wurden genutzt um spezifischen Abbau zu ermöglichen. Der SCF Komplex besteht aus einer enzymatischen Kernstruktur und einem austauschbaren Faktor, dem F-box-Protein. Dieses funktioniert wie ein Adaptor, der spezifisch Substrate in der Zelle rekrutiert. Mithilfe von DARPins wurde ein chimäres F-box-Protein konstruiert, welches eine künstlichen Substraterkennungsstruktur besitzt. In Anwesenheit eines chimären F-box Proteins konnte ein bestimmtes Zielprotein spezifisch durch die SCF-Ligase und das Proteasom abgebaut werden, falls beide in *S. cerevisiae* coexprimiert wurden. Das chimäre F-box Protein wurde weiterentwickelt, um genauer zu analysieren, wie F-box-Proteine den Proteinabbau steuern. Die erhaltenen Ergebnisse führten zu einem besseren Verständnis des Ubiquitinierungsprozesses; die Effizienz des Proteinabbaus blieb jedoch begrenzt.

Eine alternativer Ansatz nutzte einen Ubiquitin-freien Weg, um ein Zielprotein zum Proteasom zu bringen. Eine kleine Gruppe von Proteinen benötigt keine Ubiquitinierung, um abgebaut zu werden. Sie erhalten eine kleine Sequenz – Degron genannt - die direkt mit dem Proteasom interagiert. Die Effekte des ODC(Maus Ornithine Decarboxylase)-Degrons und des NYV(G1 Glycoprotein des NY-1V Hantaviruses)-Degrons wurden im *S. cerevisiae* untersucht. Verschiedene Proteine, unter diesen hoch stabile Proteine wie DARPins, wurden sehr schnell durch das Proteasom abgebaut, falls eine dieser Degron-Sequenzen am C-Terminus fusioniert wurde. Ein DARPin-Degron-Fusionsprotein wurde mit einem bindenden Zielprotein in *S. cerevisiae* exprimiert. Das DARPin-degron wurde schnell abgebaut, während das bindende Zielprotein stabil blieb. In humanen Zellen wurden die DARPin-degron-Fusionen weniger schnell als in *S. cerevisiae* abgebaut. Die Vorraussetzungen für Interaktionen mit dem Zielprotein und den Komplexeinbau waren gegeben, jedoch wurde das Zielprotein dennoch nicht abgebaut.

Gezielter Abbau von Proteinen wäre ein wertvolles Werkzeug um toxische Proteine, die Krankheiten verursachen (zum Beispiel Onkoproteine, virale Proteine, oder stabile Proteine typisch für neurodegenerative Erkrankungen), zu entfernen. Unsere Ergebnisse zeigen, dass es nicht ausreicht ein beliebendes Protein zum Proteasom zu schicken um seinen Abbau auszulösen. Der Proteinabbau durch das Proteasom erfordert vielleicht zusätzliche Proteineigenschaften, damit es als Substrat behandelt wird. Unter diesen Bedingungen ist die Entwicklung einer generellen Protein-knock-out-Strategie herausfordernder als vorausgesetzt.

Introduction

Proteins are in a dynamic state

The concept of protein degradation is about 70 years old. Earlier, dietary proteins were believed to function primarily as energy-providing fuel and the protein components of the body were considered as stable constituents [1]. Between 1937 and 1941, Rudolf Schönheimer studied protein metabolism; using 15N-labelled amino-acids he showed that bodily protein components were turning over. In his posthum book " The Dynamic State of Body Constituents" [2], he proposed the concept of metabolic regeneration and wrote: " The simile of the combustion engine pictured the steady state flow of fuel into a fixed system, and the conversion of this fuel into waste products. The new results imply that not only fuel, but the structural materials are in steady state of flux. The classical doctrine (of metabolism) must thus be replaced by one which takes account of the dynamic state of body structure." Under physiological conditions, whole body protein degradation is approximately equivalent to whole body protein synthesis for a human adult [3]. These are mostly intracellular proteins which account for the vast bulk of body protein turnover. All intracellular proteins are in a dynamic state, they are continuously degraded with half-lives ranging from a few minutes to more than 60 h. Two major intracellular proteolysis systems co-exist. The lysosome, an organelle which contains a broad array of varying proteases, is responsible for the non-selective degradation of intracellular proteins. By a process of autophagy, a portion of cytoplasm or organelle is sequestered within a membrane sac which then fuses with the lysosome. Lysosomal enzymes disintegrate the sac and digest its content. Regulated degradation of intracellular proteins is performed by the proteasome. This multimeric assembly of approximately 2.5 megadaltons functions primarily to break down proteins which have been covalently modified with a polyubiquitin tag [4]. Polymerization of ubiquitin and conjugation to the target protein is achieved by concerted actions of a cascade of enzymes: ubiquitin activating enzyme, ubiquitin conjugating enzyme and ubiquitin protein ligase [5]. The mechanism underlying the ubiquitylation reaction will be more deeply described in the introduction of chapter 1. The proteasome is a giant self-compartmentalizing protease which structurally consists of a proteolytic chamber (20S core particle) and an ATP dependent regulatory machinery (19S regulatory particle), functionally linked by a gated protein translocation channel [6]. Substrates are degraded via a multistep mechanism involving distinct proteasome subunits. The 19S regulatory particle (RP) mediates substrate recognition, preparation, unfolding and translocation into the 20S core particle [7]. The 20S core particle processively digests substrates in a highly heterogeneous mixture of peptides ranging from 3 to 22 residues [8]. An overview of the proteasome's architecture is given; identified subunits give insights into its mechanism.

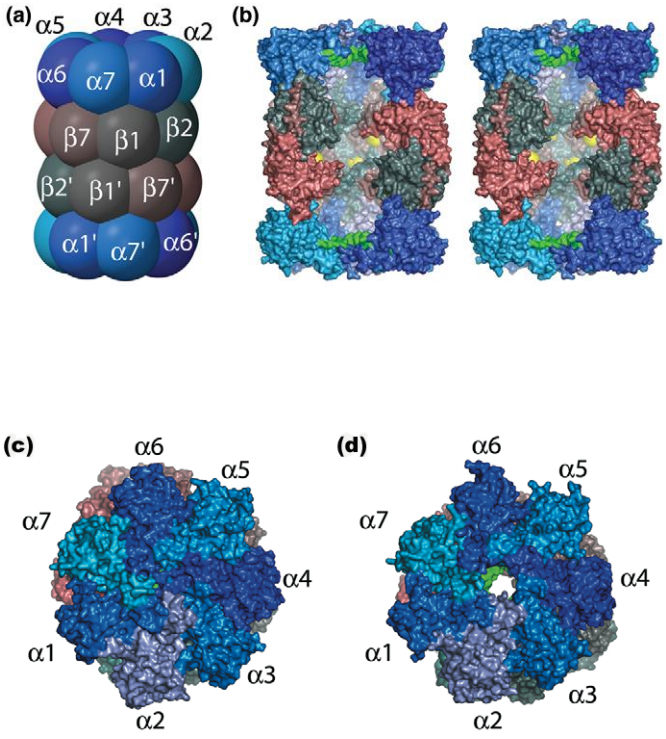

Figure 1: Architecture of the yeast 20S proteasome. (a) Side view of the proteasome. Active sites are formed at the N-termini of β1, β2 and β5. (b) Cutaway stereoview showing how the active sites (yellow) are sequestered within a central catalytic chamber formed by the two β-rings. Substrates and products pass through the α-annulus (green) through the middle of α-rings. (c) Top view of the proteasome in the closed conformation. (d) Top view of the proteasome in the open conformation. Adapted from Rechtsteiner & Hill, 2005 [9].

The proteasome, an elaborate proteolytic machinery

20S core particle (CP)

The CP is made of 28 subunits arranged into four stacked heteroheptameric rings: two inner β-rings and two α-outer rings made up of seven similar yet distinguishable β- and α-subunits [10] (Fig. 1a). This assembly builds a barrel-shaped complex which encloses three internal cavities interconnected by a narrow channel with restricted orifices (Fig. 2) [11]. The central cavity formed by the β-rings is the proteolytic chamber (Fig. 1b). Three beta subunits harbor the catalytic active sites; β1, β2 and β5 are associated with caspase-like, trypsin-like and chymotrypsine-like activities respectively, which confer the ability to cleave peptide bonds on the C-terminal side of acidic, basic and hydrophobic residues respectively [12]. The two outer cavities are antechambers formed jointly by one α- and one β-ring. Antechambers may be used to keep substrates in storage prior to their processive degradation in the catalytic chamber [13]. The two α-rings provide a gating mechanism for the degradative chamber (Fig. 1c). α-subunits converge axially at their N-termini in an interdigitated network that closes the entrance of the channel [14]. On the regulatory particle (RP) facing surface of the ring, they form α-pockets; when the RP binds on these α-pockets, it triggers opening of the channel (Fig. 1d) [15].

19S regulatory particle

The 19S regulatory particle (RP) comprises 19 subunits that are sub-classified in two groups: 6 Regulatory particles of triple- ATPase (Rpt) and 13 Regulatory particles of non-ATPase (Rpn) subunits [16]. Structurally, it consists of two sub-complexes: the lid and base assemblies, which are distal and proximal to the CP, respectively (Glickman, 98).

The base

The base is responsible for capturing client proteins, promoting unfolding and opening the CP channel. This sub-complex contains six homologous AAA-ATPase (Rpt1-6) and four non-ATPase (Rpn1,2,10,13) subunits. Rpts are critical for opening the α-ring channel but also for substrate unfolding. The six ATPases are organized in a hexameric ring; the resulting structure has a hexagonal base and on the top of it a “mouth” [17]. Three of these subunits (Rpt2,3,5) contain a conserved C-terminal hydrophobic-tyrosine-X motif which can insert into the above-described α-pockets of the CP, like a "key in a lock", to induce gate opening. Stabilization of the open gate may be achieved through wobbling of the ATPases [15, 17]. AAA-ATPases are also involved in proteasome assembly, substrate deubiquitination, unfolding and translocation into the CP [18]. Several evidences point towards a coupling of unfolding and translocations events, which would be driven by a same motor [19]. The substrate is, via an “initiation sequence”, pulled within the translocation channel, in an ATP-dependent manner. Unfolding follows, resulting from exposure of previously protected domains of the substrate and/or collisions between the rest of the substrate chain and the entry port of the narrow channel.

Figure 2: Determination of the Drosophila 26S proteasome density by Cryo-electron microscopy. Nickell & colleagues collected a large number of 26S images. A first 3D reconstruction was obtained by using a standard angular refinement procedure; a plain cylinder model was used as an initial reference to assign optimal projection directions and in-plane transformations to all experimental particles, and the model was iteratively refined until no further improvements were observed. Seven different views (from top to bottom) of the 26S proteasome reconstruction rotated around the pseudo-7-fold axis of the 20S CP are presented. The left column shows isosurface representations of the entire 3D reconstruction of the 26S proteasome complex; the second column from the left shows isosurfaces of the reconstruction cut open along the pseudo-7-fold axis of the core particle to display its inner organization. The second column from the right shows central slices in the *x*–*y* plane of the density distribution (mass is white) of the reconstruction. The right column shows a mesh representation of the reconstruction with an overlay isosurface in red highlighting the main variances. Adapted from Nickell & al., 2009 [17].

Rpn1 and Rpn2 function as scaffolding proteins which mediate binding with proteasome associated proteins. All known binding factors are involved in ubiquitin chain recognition [20], disassembly [21] or extension [22]; it seems then that these two subunits play a major role in the proteasome for chain dynamics. Rpn1 and Rpn2 form a stacked double-toroid structure, capable of attaching the CP independently of the Rpt ring and aligning its own channel with the CP's one [23]. It was then proposed that these Rpn1/Rpn2 channel may be a part of the substrate translocation channel of the base. Yet latest structural data of the 26S proteasome do not support this model [17].

Rpn10 and Rpn13 are integral ubiquitin receptors [24, 25]. These subunits respectively trap their substrates via an Ubiquitin Interacting motif (UIM) [26] or pleckstrin-like-receptor for ubiquitin (Pru) domain [27]. Rpt5, another subunit could be an additional ubiquitin receptor as it was reported to bind polyubiquitylated proteins in vitro [28]. In addition to the intrinsic ubiquitin receptors, there are three proteasome-associated ubiquitin receptors: Rad23, Dsk2 and Ddi1 [19, 29, 30]. These proteins, called UBL-UBA proteins, harbor an N-terminal UBL (ubiquitin-like) domain which binds the proteasome and one or two UBA (ubiquitin-associated) domain which bind ubiquitin. These UBL-UBA proteins are thought to function as shuttle proteins which may capture remote substrates and escort them to the proteasome. UBL-UBA proteins can dock ubiquitylated proteins at the proteasome. Moreover, they can interact with ubiquitin ligases, the enzymes involved in the attachment of ubiquitin chains onto the substrate. It is unclear whether these shuttle proteins deliver their bound substrate directly to the proteasome base or if they first hand them off to the intrinsic receptors as their UBL domain can be bound by Rpn10 and Rpn13. Noteworthy, ubiquitin receptors may not have a promiscuous capacity to bind ubiquitylated proteins as UBL-UBA proteins and Rpn10 showed significant substrate selectivity in vivo. What's more, as the five identified ubiquitin receptors are non-essential in yeast, additional receptors remain to be discovered.

The lid

The lid complex is composed of nine non-ATPase subunits (Rpn3,5,6,7,8,9,11,12,15) but only one has a known function. Rpn11 is a deubiquitinating enzyme (DUB), it separates the polyubiquitin chains from the substrate by cleaving them at a proximal site [31, 32]. Its deubiquitination activity requires association with the lid and ATP, suggesting that Rpn11 does only act on substrates which are already proceeding on the pathway of degradation. How the deubiquitination and degradation mechanisms are exactly coupled is unknown but proteasomes function poorly in the absence of Rpn11. It is assumed that ubiquitin chains would obstruct substrate translocation and/or slow down unfolding processes. However it appeared lately that ubiquitin can be degraded along with the substrate protein in a "piggyback" mechanism [33]. Perhaps more importantly, ubiquitin homeostasis is essential for cell viability, and as this protein is transcribed at relatively low levels, it might be crucial to recycle it.

Additionally, ubiquitin chains can be trimmed at their distal end by two other DUBs: Ubp6 (Usp14) and Uch37 [34]. Ubp6 reversibly associates with the proteasome while it is still under debate if Uch37 does so as well or is a stoichiometric component of the 26S proteasome. Associated DUBs may provide an editing function to spare inappropriately or poorly modified substrates from destruction [35]. Besides, these ATP-independent enzymes seem to complement the action of Rpn11, possibly by clearing the

proteasome of bound polyubiquitin chains to create occupancy for new rounds of polyubiquitylated protein binding and proteolysis [34]

Compositional variants of the proteasome

The proteasome has been highly conserved during evolution. However, it appears that its function can be modulated through association of the regulatory particle (RP) with a constellation of specific proteasome interacting proteins. Another regulation mechanism relies on its assembly. The core particle (CP) can associate with different proteasome activators and even some of its subunits can be specifically replaced.

Proteasome interacting proteins (PIPs)

Recent proteomic analyses have led to the discovery of large numbers of auxiliary factors which are physically and /or transiently associated with the 26S proteasome [36, 37]. Many of these proteasome interacting proteins (PIPs) are related to the ubiquitylation system. In addition to the above-discussed UBL-UBA proteins and Ubp6 and Uch37 deubiquitinases, the ubiquitin ligase Hul5 (or E3a) appears to be an additional major component [21]. Hul5 may be acting on ubiquitin conjugates that associate with the proteasome. As longer ubiquitin chains associate more tightly with the proteasome [38], chain extension should increase the residence time of substrates and enhance their degradation. Hul5 chain-extending activity opposes Ubp6 chain-trimming activity in an intimate way as both proteins associate with Rpn2 and Rpn1, respectively [22]. Through dynamic remodeling of ubiquitin chains, proteasomes might actively regulate substrate commitment to degradation. Certain ubiquitin conjugating enzymes and ubiquitin protein ligases also associate with the proteasome, e.g. SCF ubiquitin ligase and its associated ubiquitin conjugating enzyme: cdc34 [39]. Finally, other PIPs seem to regulate the proteasome function or its assembly via direct binding [40]. For instance, Ecm29 enhances the proteasome stability by tethering the CP to the 19S RP [21].

Proteasome activators

In addition to 19S regulatory particle, several other proteasome activators can bind to one or both α-rings of the CP to open its channel [40]. Three are known: PA28 (also called PA28αß, 11S or REG), REGγ (also called PA28γ) and PA200 (also called Blm10). They do not recognize ubiquitin nor utilize ATP.

PA28

PA28 is mostly observed in the cytoplasm in association with CP or CP-RP complex to form a so-called hybrid proteasome. Several observations suggest that it functions in the immune system. It is enriched in immune tissues, its expression is induced by interferon-γ and infection and its presence influences the production of some class I epitopes. The hybrid proteasome enhances the hydrolysis of small peptides but not proteins and generates a pattern of peptides different from those produced by the 26S, without altering the mean product length. This change in peptide profile might account PA28 capacity to enhance antigen presentation.

REGγ

REGγ is most heavily expressed in brain and confined to the nucleus. Its function remains largely unknown; it seems to be involved in apoptosis and cell-cycle regulation. REGγ promotes degradation of loosely folded substrates such as p21 ^{CIP} and the steroid receptor co-activator 3 (SRC-3).

PA200

PA200 is a large nuclear protein which in contrast to the three previously described activators, binds to the CP as a monomer. It is predominantly found as a complex with CP-RP. Like PA28, it stimulates proteasomal hydrolysis of peptides but not proteins. PA200 was suggested to be involved in proteasome assembly and DNA repair but its true role is still an open question and requires further clarification.

As a conclusion, proteasomes can be labile. There is still much to be resolved concerning the biology and biochemistry of proteasome activators, it is possible that they might function primarily in the context of hybrid proteasomes, which tether CP-RP complexes to specific intracellular locations or substrate complexes. In this model, their primary role would be to define a location or association.

Subunit variation

Structural variation can also be achieved at the subunit level, through the replacement of one subunit for another during proteasome de novo assembly [40]. In response to interferon-γ, the active subunits of the CP: β1, β2, β5 are replaced by β1i, β2i, β5i. The resulting proteasomes are called immunoproteasomes and might be more adapted for the immunological processing of antigens. The induced proteolytic subunits have indeed altered cleavage properties; the chymotrypsin- and trypsin-like activites are increased while the caspase-like activity is decreased. The product peptides are more likely to bind in the peptide-binding pocket of MHC class I molecules where peptides usually anchor via basic or mostly hydrophobic carboxyl terminal residues. Similarly, another subunit β5t is assembled with β1i and β2i to form the thymoproteasome, the predominant proteasome species in cortical thymic epithelium. In this case, a more hydrophilic ensemble of peptides is generated, which bind with less affinity to MHC class I clefts. Remarkably, thymoproteasomes are expressed in thymic cortical epithelial cells (cTECs) whereas immnuoproteasomes are constituvely present in thymic medullary epithelial cells (mTECs). As cTECs and mTECs are apparently dedicated to negative and positive T cell selection, β5 cleavage specificity could be linked to the immunological definition of self and non-self. Most likely, other subtypes of proteasomes are about to be discovered. An additional α-subunit, α8, which is expressed in testis, could replace α4 in the proteasome assembly to form a mammalian testis-specific proteasome. Another isoform of Rnp10 is specifically expressed in the embryonic brain in mice, implying the existence of a brain-specific proteasome.

Substrate recognition

All in all, we can nowadays make a sketch of the proteasome and its main components and better understand how this highly elaborated machinery might be functioning but it is still rather unclear on which basis protein substrates are elected as eligible candidates which may enter the core of the CP chamber. The 26S proteasome degrades proteins which have been covalently modified with a polyubiquitin chain. Ubiquitin is a highly conserved 76 amino acid-protein which ends in a diglycine motif. It is attached onto the substrate by covalent bond formation between the carboxyl group of its terminal glycine (G76) and the ε-amino group of a lysine residue belonging to the substrate [41]. Polyubiquitin chain formation is achieved via isopeptide bond formation between G76 carboxyl group of the "n+1" ubiquitin to the ε-amino group of a lysine residue belonging to the preceding ubiquitin. Ubiquitin contains seven lysines: K6, K11, K27, K29, K33, K48 and K63; each of them can be used to form different polyubiquitin chains, which function like stamps for functionally distinct processes. Two kinds of chains have been extensively characterized: K48 and K63 chains. K48 chains are associated with proteasomal degradation; the 26S proteasome recognizes the motif formed by four ubiquitin molecules linked via their lysine 48 [38]. Substrate binding affinity for the proteasome depends on the total number of this motif present at its surface. In contrast, K63 chains provide a signaling function, they are involved in DNA repair, endocytosis and signal transduction pathways [42]. K48 and K63 chains adopt a radically different structural conformation, which was accounted for their dissimilar roles [43-45]. Recent studies have however led to a more complex picture. It seems that linkages other than K48 can occasionally target attached proteins to the proteasome e.g. K63, K29 and K11 [46]. Forked chains, in which one of the ubiquitin moiety is modified by more than one ubiquitin, can also be synthesized; they seem to be unfavorable substrates [47]. Finally, certain substrates can be degraded while being only monoubiquitinated [33, 48]. Ubiquitin chain length and linkage type, along with the affinity for proteasome receptors and ease of deubiquitination, seem to all contribute towards setting substrate hierarchy [49]. Noteworthy, some substrates can bypass the ubiquitin requirement to be processed by the proteasome. The best described ubiquitin-independent proteasome substrate is the Ornithine Decarboxylase (ODC) [50], which is recognized by a degradation signal located at its C terminus. This ubiquitin free route is presented in chapter 2.

The truth of the matter is that we still do not completely understand how substrates make their way to the 26S proteasome. However selective depletion of intracellular proteins could be a powerful tool for protein function analysis and, in the long run, therapeutic applications. We aimed at developing strategies to lead a specific protein to the 26S proteasome. In this respect, we needed a versatile binding scaffold which could be easily expressed in the cytoplasm of cells and armed with different functional protein domains or sequences. For this purpose, we chose to work with DARPIns, an engineered protein scaffold based on the modular architecture of repeat proteins.

DARPIns, a new binding scaffold

Ankyrin repeat

Repeat proteins constitute, next to immunoglobulins, the most abundant natural binding proteins class [51]. Present in all phyla, their most common biological function is to bind to a protein ligand, which translates to different modes of action ranging from anchoring of proteins to each other to enzyme inhibition. Repeat proteins are involved in numerous biological processes such as cell cycle control, transcription regulation, innate immunity and apoptosis, among others. Their favorable binding properties most probably arise from their repetitive architecture [52]. Repeat proteins consist of consecutive homologous structural modules (repeats), which stack to form an elongated non-globular protein domain with a joined hydrophobic core. A repeat is characterized by conserved framework residues which mediate intra- and inter-repeat interactions and variable surface-exposed residues. The juxtaposition of all surface-exposed residues forms the target binding surface, whose size varies according to the number of repeats. The ankyrin repeat characterizes a prominent repeat protein family [53]. One module consists of 33 amino acids forming a well-defined architecture, consisting of a β-turn followed by a pair of anti-parallel α-helices and a loop which bridges to the next module. The overall structure of a fully assembled ankyrin repeat domain is elongated and slightly curved [54]. In most known complexes involving ankyrin repeat proteins, the concave surface formed by the β-turn and the first α-helix is involved in binding the ligand protein. A strategy harnessing the modular architecture of ankyrin repeat proteins was developed for the creation of novel binding molecules [52].

DARPin design and biophysical properties

Information was extracted from natural ankyrin repeat proteins sequences (229 for initial design and 2200 for subsequent refinement) to design an optimal self-compatible repeat module with 26 conserved framework positions and 7 randomized surface-exposed ones (Fig. 3a) [55]. The consensus sequence was finally refined using structural data. Assembling different numbers of the self-compatible repeat module provided a simple means of constructing and evolving new interaction surfaces. To shield the continuous hydrophobic core, special terminal repeats, called capping repeats, were added to yield a novel functional binding protein scaffold: Designed Ankyrin Repeat Proteins (DARPIns) (Fig. 3a) [55]. Combinatorial libraries of DARPins of varying size and randomized potential interaction surfaces were generated, the molecules were denoted as NxC, where x indicates the number of consensus designed ankyrin repeat module, typically ranging between two and four (Fig. 3b). Analysis of unselected members showed very favorable biophysical properties. Proteins were expressed in soluble form in the cytoplasm of *E. coli*; up to 200 mg/L purified protein could be obtained from simple shake flasks cultures in the *E. coli* strain XL1-blue [55]. The crystal structure of the unselected member E3_5 showed a vey regular and ordered ankyrin repeat domain fold with refined intrarepeat and extrarepeat interactions [56]. The design also yielded proteins of remarkable chemical and thermal stabilities; midpoints of

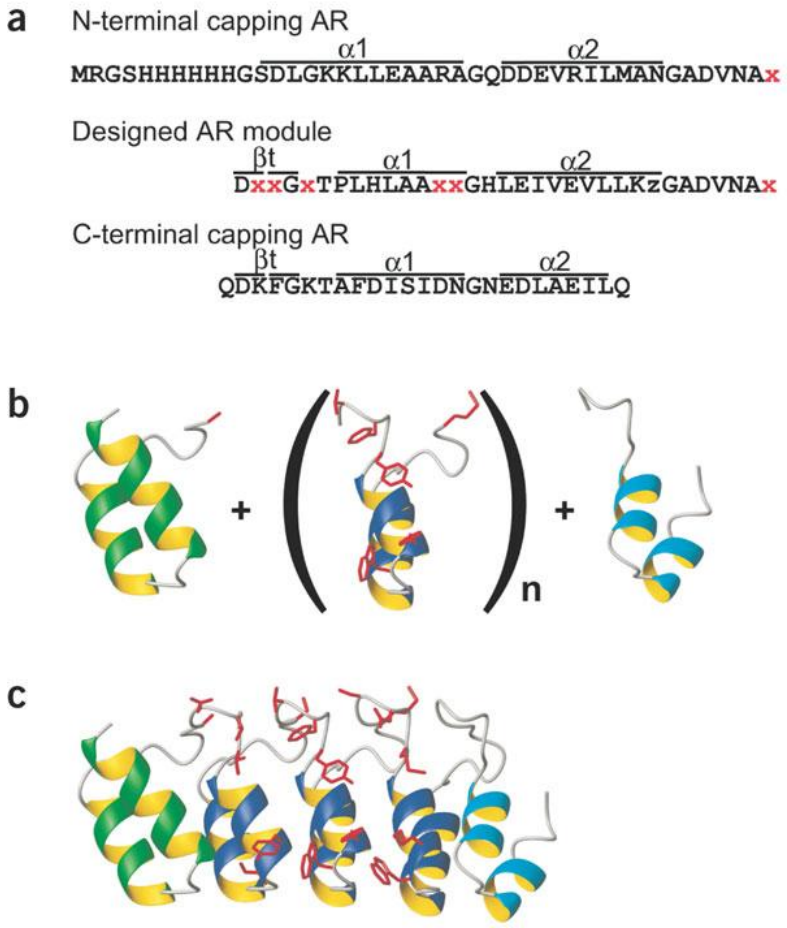

Fig. 3: Construction of DARPin protein libraries. (a) Sequences of the N-terminal capping ankyrin repeat (AR), the designed internal AR module and the C-terminal capping AR. The secondary structure elements are indicated above the sequences. The designed AR module consists of 26 defined framework residues, six randomized potential interaction residues (red x, any of the 20 natural amino acids except cysteine, glycine or proline) and one randomized framework residue (z, any of the amino acids asparagine,histidine or tyrosine). (b) Schematic representation of the library generation of DARPins. This assembly is represented on the protein level, whereas the real library assembly is on the DNA level. By assembling an N-terminal capping AR (green), varying numbers of the designed AR module (blue) and a C-terminal capping AR (cyan), combinatorial libraries of DARPins of different repeat numbers were generated (side chains of the randomized potential interaction residues are shown in stick-mode in red). (c) Ribbon representation of the selected MBP binding DARPin protein off7 (colors as in b). This binder is derived from a N3C library, consisting of a N-terminal capping AR, three designed AR modules and a C-terminal capping AR. Adapted from Binz *et al*, 2004 [57].

denaturation ranged between 2.9 and 5 M guanidine chloride or between 66°C and more than 95°C, respectively [55, 56]. Thermodynamic properties of full consensus DARPins were even more impressive with melting temperatures above 100°C for proteins with three or more repeat modules; their full denaturation required their heating in 5 M guanidine chloride [58].

DARPin selection

DARPin libraries were used as a source for generating new specific binders by directed evolution. Directed evolution mimics natural evolution but in a test tube format. The procedure relies on iterative cycles of selection and amplification of selected molecules, creating a new enriched pool as start for the next round. Using a diverse starting population and a suitable selection method which allows coupling of the genotype and phenotype, new molecules with desired properties can emerge from the procedure and be easily retrieved. Two selection systems were successfully applied for the selection of DARPins: ribosome display [59, 60] and phage display [61]. Ribosome display was the most frequently used one, it is a complete in vitro selection system (Fig. 4). It relies on in vitro translation and production of non-covalent ternary complexes consisting of mRNA, ribosome and the nascent polypeptide chain. Such complexes are “locked” in this configuration by absence of a stop codon, thus preventing dissociation of the mRNA and the polypeptide chain. In addition, a C-terminal spacer at the end of the protein coding sequence allows the nascent polypeptide chain to fold in a functional protein. Complexes can be selected against an immobilized target protein, non-binding ones are washed away and the DNA is recovered by reverse transcription PCR after disassembly of the complexes by depletion of magnesium. New diversity can be directly generated during amplification of the genetic material of the selected molecules. Phage display is a semi-in vitro and semi-in vivo selection method. The protein (phenotype) is displayed on the surface of a bacteriophage particle while the respecting DNA (genotype) is encapsulated inside. The selection step against immobilized target is still performed in vitro but the DNA is replicated inside bacterial cells. The original method was adapted to DARPins, which were directed to the cotranslational signal recognition particle (SRP) translocation pathway instead of the conventional post-translational Sec translocation pathway [62]. SRP phage display is more efficient in displaying very stable and fast folding proteins. Both directed evolution techniques could, in a few selection rounds only, yield several DARPins with affinities ranging from pM to low nM [57, 63, 64]. Maltose Binding Protein (MBP) from *E. coli* was chosen as target for the first selection of DARPins. Using ribosome-display, low nanomolar binders were rapidly isolated. A selected DARPin named off7 was crystallized in complex with MBP, the X-ray structure showed that library modules with their randomized positions were responsible for the interaction (Fig. 3c). After validation of the strategy, numerous binders could be selected against various intracellular proteins.

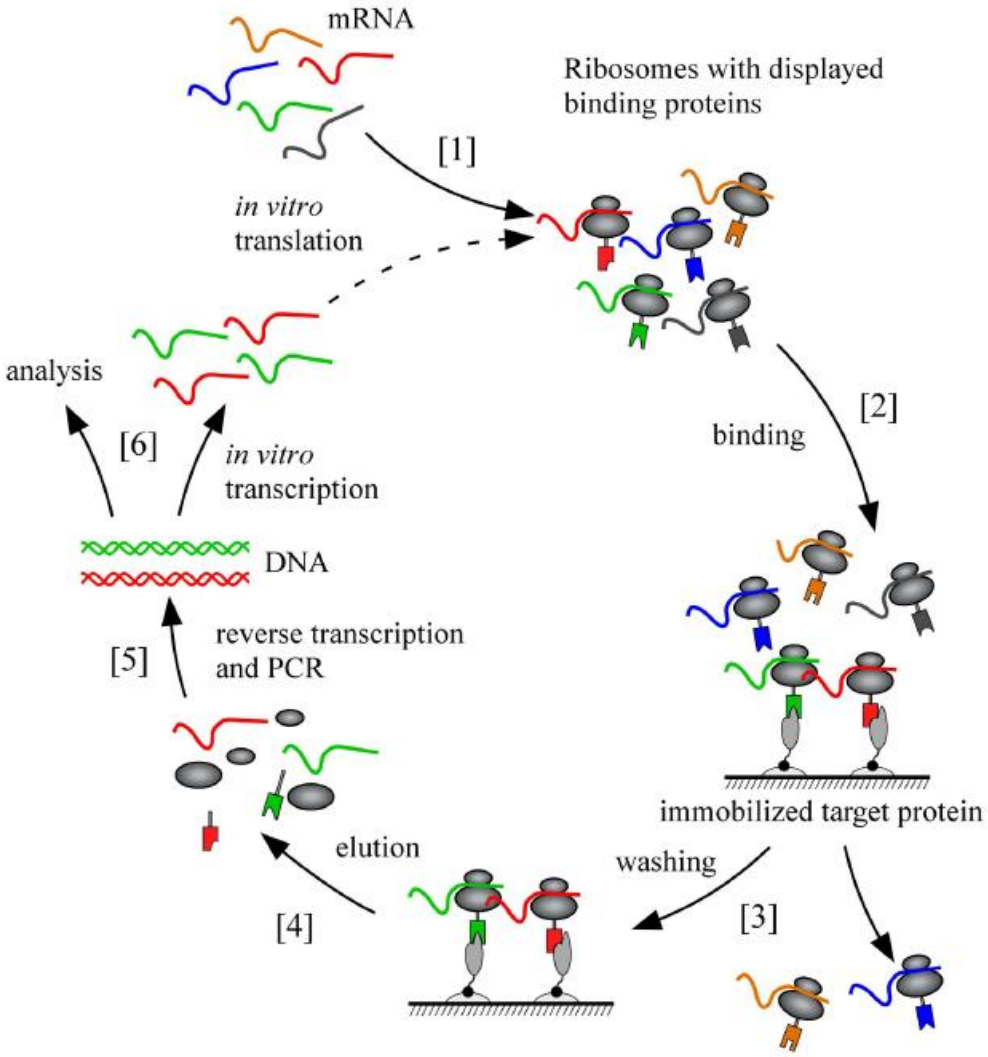

Figure 4: Schematic representation of a ribosome display selection cycle. An mRNA library encoding the proteins of interest without stop codon is translated *in vitro* [1]. After cooling, the translation yields stable ternary complexes of mRNA, ribosomes and nascent polypeptides. These complexes are used for the binding selection on the immobilized target [2]. After binding of the polypeptides to the target protein, unbound complexes are washed away [3]. The mRNA of the bound complex is eluted by dissociating the ribosomal complex with EDTA [4]. A reverse transcription reaction followed by PCR yields the genetic information of the selected clones [5]. The amplified genes can then be used as input for the next selection round starting with *in vitro* transcription [6] or cloned into plasmids for analysis. Adapted from Daniel Steiner dissertation, 2007.

DARPin applications

In combination with in vivo activity screening, DARPIns revealed to be valuable tools which could fulfill various functions. Several inhibitors could be identified against diverse enzymes. A very potent intracellular kinase inhibitor, named 3a, was able to trap the bacterial kinase aminoglycoside phosphotransferase IIIa (APH) in an inactive conformation [65, 66]. An intracellular inhibitor was selected against the NIa^{pro}, the main proteinase responsible for tobacco etch virus maturation, a major plant pathogen [67]. Finally, the first specific caspase-2 inhibitor could be produced; its binding caused allosteric inhibition [68]. DARPins could also be successfully selected against various cell-surface receptors, e.g. members of the ErbB receptor family [63, 69] (Jost & Tamaskovic, in preparation). EGFR (ErbB1) specific DARPins exhibited a cytostatic effect on EGFR-overexpressing A431 cells (Boersma, in preparation). Her2 (ErbB2) specific bivalent DARPIns were constructed and depending on their format (homo-/hetero-specificity and flexible/rigid linker), they could have cytotoxic or proliferative effects on Her2-overexpressing BT474 cells (Jost & Tamaskovic, in preparation). CD4-specific DARPins could compete with the HIV envelope protein gp120 and potently block HIV entry in both cell line and primary cell-based infection systems [70]. Recently, immunoglobulin E receptor was blocked by a bispecific DARPin preventing the release of proinflammatory mediators and potentially allergic reaction [71]. Alternatively DARPins binding activity could also be exploited to facilitate crystallization of arduous proteins [72]. A better resolution could be obtained for the structure of the bacterial multidrug exporter AcrB and allowed a better understanding of its mechanism [73]. The first structure of wild-type apo Plk-1, a well-validated drug target in cancer therapy, could be determined by co-crystallization with a DARPin [74]. Owing to their robust biophysical properties and highly specific binding capacity, DARPins constitute very promising protein based drugs.

PhD project

We propose to expand the formerly described portfolio of applications and use DARPIns as tools to engineer effector proteins able to lead a specific target to the 26S proteasome for degradation. Several strategies were employed and will be described in the following chapters. First, DARPins were exploited to alter the recognition function of an ubiquitin ligase, the enzymes responsible for the ubiquitin-proteasome pathway specificity (chapter 1). We aimed to better understand how ubiquitin ligases were mediating ubiquitination and degradation of a substrate and then apply this knowledge to design “tailored” ubiquitin ligases. Next, DARPins were armed with different sequences enabling a direct interaction with the 26S proteasome, the proteasomal degradation of a complex was investigated (chapter 2). Finally, techniques which have been described so far to achieve targeted protein degradation were reviewed and both DARPin-strategies were, after being developed in a yeast system, evaluated in mammalian cells (chapter 3).

References

1. Ciechanover, A., *Proteolysis: from the lysosome to ubiquitin and the proteasome.* Nat Rev Mol Cell Biol, 2005. **6**(1): p. 79-87.
2. Schönheimer, R., *The Dynamic State of Body Constituents*. 1942, Cambridge, Massachusetts, USA: Harvard University Press.
3. Schwartz, A.L. and A. Ciechanover, *Targeting proteins for destruction by the ubiquitin system: implications for human pathobiology.* Annu Rev Pharmacol Toxicol, 2009. **49**: p. 73-96.
4. Coux, O., K. Tanaka, and A.L. Goldberg, *Structure and functions of the 20S and 26S proteasomes.* Annu Rev Biochem, 1996. **65**: p. 801-47.
5. Pickart, C.M. and M.J. Eddins, *Ubiquitin: structures, functions, mechanisms.* Biochim Biophys Acta, 2004. **1695**(1-3): p. 55-72.
6. Voges, D., P. Zwickl, and W. Baumeister, *The 26S proteasome: a molecular machine designed for controlled proteolysis.* Annu Rev Biochem, 1999. **68**: p. 1015-68.
7. Bajorek, M. and M.H. Glickman, *Keepers at the final gates: regulatory complexes and gating of the proteasome channel.* Cell Mol Life Sci, 2004. **61**(13): p. 1579-88.
8. Kisselev, A.F., et al., *The sizes of peptides generated from protein by mammalian 26 and 20 S proteasomes. Implications for understanding the degradative mechanism and antigen presentation.* J Biol Chem, 1999. **274**(6): p. 3363-71.
9. Rechsteiner, M. and C.P. Hill, *Mobilizing the proteolytic machine: cell biological roles of proteasome activators and inhibitors.* Trends Cell Biol, 2005. **15**(1): p. 27-33.
10. Groll, M., et al., *Structure of 20S proteasome from yeast at 2.4 A resolution.* Nature, 1997. **386**(6624): p. 463-71.
11. Baumeister, W., et al., *The proteasome: paradigm of a self-compartmentalizing protease.* Cell, 1998. **92**(3): p. 367-80.
12. Arendt, C.S. and M. Hochstrasser, *Identification of the yeast 20S proteasome catalytic centers and subunit interactions required for active-site formation.* Proc Natl Acad Sci U S A, 1997. **94**(14): p. 7156-61.
13. Sharon, M., et al., *20S proteasomes have the potential to keep substrates in store for continual degradation.* J Biol Chem, 2006. **281**(14): p. 9569-75.
14. Groll, M., et al., *A gated channel into the proteasome core particle.* Nat Struct Biol, 2000. **7**(11): p. 1062-7.
15. Smith, D.M., et al., *Docking of the proteasomal ATPases' carboxyl termini in the 20S proteasome's alpha ring opens the gate for substrate entry.* Mol Cell, 2007. **27**(5): p. 731-44.
16. Finley, D., et al., *Unified nomenclature for subunits of the Saccharomyces cerevisiae proteasome regulatory particle.* Trends Biochem Sci, 1998. **23**(7): p. 244-5.
17. Nickell, S., et al., *Insights into the molecular architecture of the 26S proteasome.* Proc Natl Acad Sci U S A, 2009. **106**(29): p. 11943-7.
18. Liu, C.W., et al., *ATP binding and ATP hydrolysis play distinct roles in the function of 26S proteasome.* Mol Cell, 2006. **24**(1): p. 39-50.
19. Finley, D., *Recognition and processing of ubiquitin-protein conjugates by the proteasome.* Annu Rev Biochem, 2009. **78**: p. 477-513.
20. Elsasser, S., et al., *Proteasome subunit Rpn1 binds ubiquitin-like protein domains.* Nat Cell Biol, 2002. **4**(9): p. 725-30.
21. Leggett, D.S., et al., *Multiple associated proteins regulate proteasome structure and function.* Mol Cell, 2002. **10**(3): p. 495-507.

22. Crosas, B., et al., *Ubiquitin chains are remodeled at the proteasome by opposing ubiquitin ligase and deubiquitinating activities.* Cell, 2006. **127**(7): p. 1401-13.
23. Rosenzweig, R., et al., *The central unit within the 19S regulatory particle of the proteasome.* Nat Struct Mol Biol, 2008. **15**(6): p. 573-80.
24. Husnjak, K., et al., *Proteasome subunit Rpn13 is a novel ubiquitin receptor.* Nature, 2008. **453**(7194): p. 481-8.
25. Deveraux, Q., et al., *A 26 S protease subunit that binds ubiquitin conjugates.* J Biol Chem, 1994. **269**(10): p. 7059-61.
26. Fujiwara, K., et al., *Structure of the ubiquitin-interacting motif of S5a bound to the ubiquitin-like domain of HR23B.* J Biol Chem, 2004. **279**(6): p. 4760-7.
27. Schreiner, P., et al., *Ubiquitin docking at the proteasome through a novel pleckstrin-homology domain interaction.* Nature, 2008. **453**(7194): p. 548-52.
28. Lam, Y.A., et al., *A proteasomal ATPase subunit recognizes the polyubiquitin degradation signal.* Nature, 2002. **416**(6882): p. 763-7.
29. Elsasser, S. and D. Finley, *Delivery of ubiquitinated substrates to protein-unfolding machines.* Nat Cell Biol, 2005. **7**(8): p. 742-9.
30. Farras, R., et al., *Mechanisms of delivery of ubiquitylated proteins to the proteasome: new target for anti-cancer therapy?* Crit Rev Oncol Hematol, 2005. **54**(1): p. 31-51.
31. Verma, R., et al., *Role of Rpn11 metalloprotease in deubiquitination and degradation by the 26S proteasome.* Science, 2002. **298**(5593): p. 611-5.
32. Yao, T. and R.E. Cohen, *A cryptic protease couples deubiquitination and degradation by the proteasome.* Nature, 2002. **419**(6905): p. 403-7.
33. Shabek, N., Y. Herman-Bachinsky, and A. Ciechanover, *Ubiquitin degradation with its substrate, or as a monomer in a ubiquitination-independent mode, provides clues to proteasome regulation.* Proc Natl Acad Sci U S A, 2009. **106**(29): p. 11907-12.
34. Koulich, E., X. Li, and G.N. DeMartino, *Relative structural and functional roles of multiple deubiquitylating proteins associated with mammalian 26S proteasome.* Mol Biol Cell, 2008. **19**(3): p. 1072-82.
35. Lam, Y.A., et al., *Editing of ubiquitin conjugates by an isopeptidase in the 26S proteasome.* Nature, 1997. **385**(6618): p. 737-40.
36. Guerrero, C., et al., *An integrated mass spectrometry-based proteomic approach: quantitative analysis of tandem affinity-purified in vivo cross-linked protein complexes (QTAX) to decipher the 26 S proteasome-interacting network.* Mol Cell Proteomics, 2006. **5**(2): p. 366-78.
37. Wang, X., et al., *Mass spectrometric characterization of the affinity-purified human 26S proteasome complex.* Biochemistry, 2007. **46**(11): p. 3553-65.
38. Thrower, J.S., et al., *Recognition of the polyubiquitin proteolytic signal.* Embo J, 2000. **19**(1): p. 94-102.
39. Verma, R., et al., *Proteasomal proteomics: identification of nucleotide-sensitive proteasome-interacting proteins by mass spectrometric analysis of affinity-purified proteasomes.* Mol Biol Cell, 2000. **11**(10): p. 3425-39.
40. Tanaka, K., *The proteasome: overview of structure and functions.* Proc Jpn Acad Ser B Phys Biol Sci, 2009. **85**(1): p. 12-36.
41. Pickart, C.M., *Mechanisms underlying ubiquitination.* Annu Rev Biochem, 2001. **70**: p. 503-33.
42. Pickart, C.M. and D. Fushman, *Polyubiquitin chains: polymeric protein signals.* Curr Opin Chem Biol, 2004. **8**(6): p. 610-6.
43. Datta, A.B., G.L. Hura, and C. Wolberger, *The Structure and Conformation of Lys63-Linked Tetraubiquitin.* J Mol Biol, 2009.

44. Tenno, T., et al., *Structural basis for distinct roles of Lys63- and Lys48-linked polyubiquitin chains.* Genes Cells, 2004. **9**(10): p. 865-75.
45. Weeks, S.D., et al., *Crystal structures of Lys-63-linked tri- and di-ubiquitin reveal a highly extended chain architecture.* Proteins, 2009.
46. Saeki, Y., et al., *Lysine 63-linked polyubiquitin chain may serve as a targeting signal for the 26S proteasome.* Embo J, 2009. **28**(4): p. 359-71.
47. Kim, H.T., et al., *Certain pairs of ubiquitin-conjugating enzymes (E2s) and ubiquitin-protein ligases (E3s) synthesize nondegradable forked ubiquitin chains containing all possible isopeptide linkages.* J Biol Chem, 2007. **282**(24): p. 17375-86.
48. Boutet, S.C., et al., *Regulation of Pax3 by proteasomal degradation of monoubiquitinated protein in skeletal muscle progenitors.* Cell, 2007. **130**(2): p. 349-62.
49. Ziv, I., O. Kleifeld, and M. Glickman, *Nonconformity in ubiquitin compliance.* Embo J, 2009. **28**(13): p. 1825-7.
50. Bercovich, Z., et al., *Degradation of ornithine decarboxylase in reticulocyte lysate is ATP-dependent but ubiquitin-independent.* J Biol Chem, 1989. **264**(27): p. 15949-52.
51. Andrade, M.A., C. Perez-Iratxeta, and C.P. Ponting, *Protein repeats: structures, functions, and evolution.* J Struct Biol, 2001. **134**(2-3): p. 117-31.
52. Forrer, P., et al., *A novel strategy to design binding molecules harnessing the modular nature of repeat proteins.* FEBS Lett, 2003. **539**(1-3): p. 2-6.
53. Bork, P., *Hundreds of ankyrin-like repeats in functionally diverse proteins: mobile modules that cross phyla horizontally?* Proteins, 1993. **17**(4): p. 363-74.
54. Sedgwick, S.G. and S.J. Smerdon, *The ankyrin repeat: a diversity of interactions on a common structural framework.* Trends Biochem Sci, 1999. **24**(8): p. 311-6.
55. Binz, H.K., et al., *Designing repeat proteins: well-expressed, soluble and stable proteins from combinatorial libraries of consensus ankyrin repeat proteins.* J Mol Biol, 2003. **332**(2): p. 489-503.
56. Kohl, A., et al., *Designed to be stable: crystal structure of a consensus ankyrin repeat protein.* Proc Natl Acad Sci U S A, 2003. **100**(4): p. 1700-5.
57. Binz, H.K., et al., *High-affinity binders selected from designed ankyrin repeat protein libraries.* Nat Biotechnol, 2004. **22**(5): p. 575-82.
58. Wetzel, S.K., et al., *Folding and unfolding mechanism of highly stable full-consensus ankyrin repeat proteins.* J Mol Biol, 2008. **376**(1): p. 241-57.
59. Hanes, J. and A. Pluckthun, *In vitro selection and evolution of functional proteins by using ribosome display.* Proc Natl Acad Sci U S A, 1997. **94**(10): p. 4937-42.
60. Zahnd, C., P. Amstutz, and A. Pluckthun, *Ribosome display: selecting and evolving proteins in vitro that specifically bind to a target.* Nat Methods, 2007. **4**(3): p. 269-79.
61. Smith, G.P., *Filamentous fusion phage: novel expression vectors that display cloned antigens on the virion surface.* Science, 1985. **228**(4705): p. 1315-7.
62. Steiner, D., et al., *Signal sequences directing cotranslational translocation expand the range of proteins amenable to phage display.* Nat Biotechnol, 2006. **24**(7): p. 823-31.
63. Steiner, D., P. Forrer, and A. Pluckthun, *Efficient selection of DARPins with sub-nanomolar affinities using SRP phage display.* J Mol Biol, 2008. **382**(5): p. 1211-27.
64. Zahnd, C., et al., *A designed ankyrin repeat protein evolved to picomolar affinity to Her2.* J Mol Biol, 2007. **369**(4): p. 1015-28.
65. Amstutz, P., et al., *Intracellular kinase inhibitors selected from combinatorial libraries of designed ankyrin repeat proteins.* J Biol Chem, 2005. **280**(26): p. 24715-22.
66. Kohl, A., et al., *Allosteric inhibition of aminoglycoside phosphotransferase by a designed ankyrin repeat protein.* Structure, 2005. **13**(8): p. 1131-41.

67. Kawe, M., et al., *Isolation of intracellular proteinase inhibitors derived from designed ankyrin repeat proteins by genetic screening.* J Biol Chem, 2006. **281**(52): p. 40252-63.
68. Schweizer, A., et al., *Inhibition of caspase-2 by a designed ankyrin repeat protein: specificity, structure, and inhibition mechanism.* Structure, 2007. **15**(5): p. 625-36.
69. Zahnd, C., et al., *Selection and characterization of Her2 binding-designed ankyrin repeat proteins.* J Biol Chem, 2006. **281**(46): p. 35167-75.
70. Schweizer, A., et al., *CD4-specific designed ankyrin repeat proteins are novel potent HIV entry inhibitors with unique characteristics.* PLoS Pathog, 2008. **4**(7): p. e1000109.
71. Eggel, A., et al., *DARPins as Bispecific Receptor Antagonists Analyzed for Immunoglobulin E Receptor Blockage.* J Mol Biol, 2009.
72. Sennhauser, G. and M.G. Grutter, *Chaperone-assisted crystallography with DARPins.* Structure, 2008. **16**(10): p. 1443-53.
73. Sennhauser, G., et al., *Drug export pathway of multidrug exporter AcrB revealed by DARPin inhibitors.* PLoS Biol, 2007. **5**(1): p. e7.
74. Bandeiras, T.M., et al., *Structure of wild-type Plk-1 kinase domain in complex with a selective DARPin.* Acta Crystallogr D Biol Crystallogr, 2008. **64**(Pt 4): p. 339-53.

Insights into the mechanism of F-box proteins using a chimeric F-box protein

Chapter 1

A

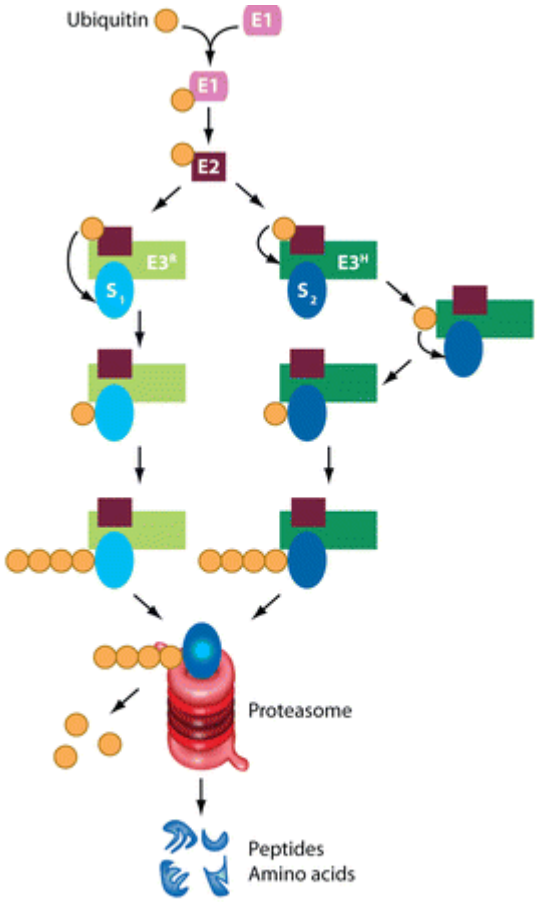

Schwartz AL, Ciechanover A. 2009.
Annu. Rev. Pharmacol. Toxicol. 49:73–96

B

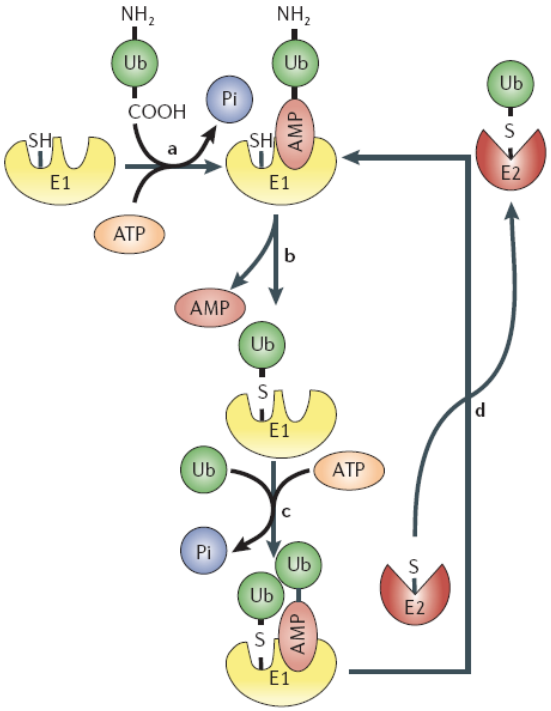

Figure 1: A. Sequence of events in the degradation of a protein via the ubiquitin-proteasome pathway. Activation of ubiquitin by the ubiquitin-activating enzyme, E1. Transfer of the activated ubiquitin from E1 to a ubiquitin-conjugating enzyme, E2. Conjugation of ubiquitin mediated by RING-finger ubiquitin ligases (E3R). Formation of a ternary complex between ubiquitin-charged E2, E3R, and the target substrate (S1), and initiation of synthesis of substrate-bound polyubiquitin chain by direct transfer of the activated ubiquitin moiety from E2 to the substrate. Conjugation of ubiquitin mediated by HECT domain ubiquitin ligases, E3H. Generation of binary complex between the ubiquitin-charged E2 and the E3H, and transfer of activated ubiquitin to the ligase. Transfer of the first ubiquitin moiety from E3H to the substrate (S2). Formation of substrate-bound polyubiquitin chain by the successive conjugation of additional ubiquitin moieties to one another. Binding of the polyubiquitinated substrate to the 26S proteasome and degradation of the ubiquitinated substrate to peptides. Adapted from Schwartz & Ciechanover [1]. B. Biochemistry of the ubiquitin-activation reaction. (a) adenylation of the carboxyl terminus of a ubiquitin molecule by E1; (b) rapid cis transfer of the E1-bound ubiquitin molecule from AMP to the active-site cysteine in E1, with subsequent release of free AMP; (c) adenylation of another free ubiquitin residue by the same Cys~Ub-loaded E1 molecule; and (d) recruitment of E2 followed by transfer of the activated ubiquitin from the active cysteine of E1 to the catalytic cysteine of E2. Adapted from Nalepa et al, 2006 [2].

Introduction

The selective degradation of specific cellular proteins is essential for the cellular metabolism. In eukaryotes, most proteins are degraded via the ubiquitin-proteasome pathway [3]. This mechanism ensures the quality of intracellular proteins by destroying denatured/misfolded or damaged polypeptides [4]. Ubiquitin-mediated proteolysis plays also an important role in the control of numerous cellular processes by regulating the break-down of key regulatory proteins such as cell cycle proteins (e.g. cyclins), transcriptional factors (e.g. IκB) or proto-oncogenes/tumor suppressors (e.g. Jun, p53) [5]. Finally, the ubiquitin-proteasome system is also involved in the immune response, both innate and adaptative [6]. A well known example is the proteasome-dependent processing of many antigenic proteins, whose peptide epitopes are presented by major histocompatibility complex (MHC) class I molecules [7].

Protein degradation via the ubiquitin-proteasome pathway involves two successive steps: the labeling of the substrate by ubiquitin and degradation by the 26S proteasome [8]. Ubiquitin is a highly conserved 76 amino acid-protein; its conjugation to the substrate is mediated by the sequential activities of 3 different enzymes (Fig. 1) [9]. The E1 enzyme (ubiquitin activating enzyme) activates the ubiquitin molecule and transfers it to E2 (ubiquitin conjugating enzyme). E3 (ubiquitin protein ligase) binds to the substrate and recruits Ub-loaded E2 to mediate bond formation between ubiquitin and an internal lysine residue on the substrate. Multiple cycles of conjugation of new ubiquitin moieties to the previous one result in the formation of a polyubiquitin chain. A chain of four or more molecules, formed via lysine 48 of ubiquitin, is recognized by the 26S proteasome [10, 11], which unfolds the substrate and channels the unfolded polypeptide into its catalytic lumen, where a host of protease sites digest the protein into short peptides [12]. The ubiquitin conjugation machinery has a hierarchical structure [13]. In a simplified view, a single E1 activates ubiquitin and interacts with all E2s; each E2 interacts with several E3s and finally each E3 targets several substrates. However, some overlapping interactions may remodel this “pyramid” structure. For instance, specific E3s can interact with more than one E2 and some substrates can be targeted by more than one E3.

The specificity of ubiquitination reaction relies on the many hundreds of E3 enzymes which recognize particular substrates motifs, often referred to as degrons [14]. E3s can be divided into two main groups, based on one of two characteristic protein motifs: the “Homologous E6-associated protein Carboxyl Terminus” (HECT) domain and the “Really Interesting New Gene” (RING) domain [15]. HECT-type E3s transiently accept ubiquitin from E2 via their HECT domain before transferring it onto the substrate (Fig. 1). In contrast RING-type E3s do not catalyze the reaction but assist it by recruiting the ubiquitin loaded-E2 via its RING domain and activating it to discharge its ubiquitin cargo to the substrate [16].

A

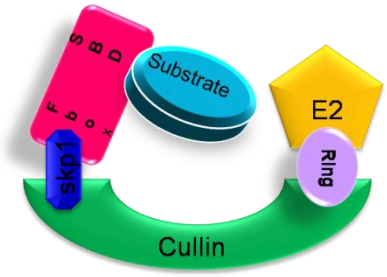

B

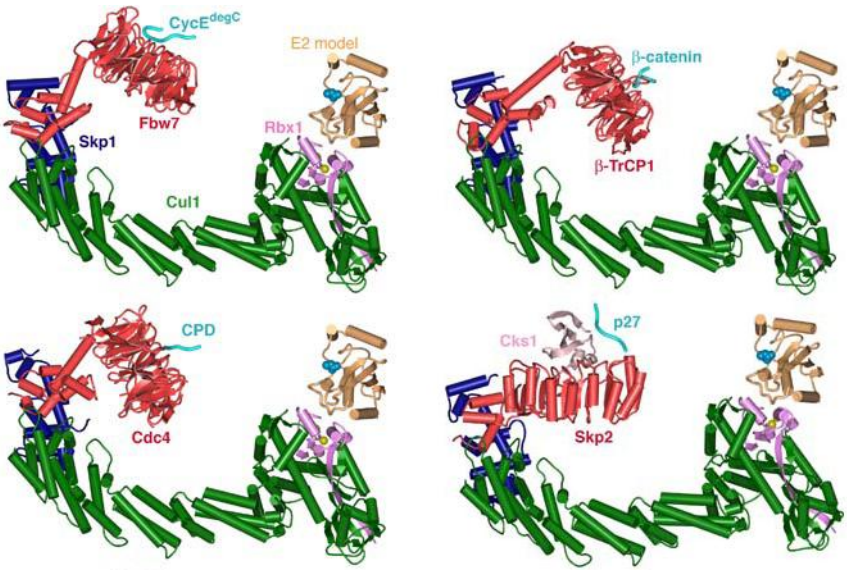

Figure 2: A: Schematic representation of SCF-E2 complex. Cul1, Rbx1, skp1, F-box protein, substrate and E2 are colored in green, purple, dark blue, pink, light blue and orange, respectively. B: Models for the SCF^{Fbw7}-CyclinE-E2 complex, SCF^{Cdc4}-CPD-E2 complex, $SCF^{\beta TrcP1}$ -β catenin-E2 complex and SCF^{skp2}-p27/cks1-E2 complex. Every model was built by superimposing the Skp1-F box portion of the respective Skp1-F box complex structure [17-20] on the corresponding region of the SCF^{Skp2} structure, which had been experimentally determined separately [21]. The UbcH7 E2 (active site cysteine in cyan) was docked on the Rbx1 subunit of the SCF based on the c-Cbl-UbcH7 structure [17, 21]. Proteins were colored as in A. In all SCF-E2 complexes models, the substrate-binding domain points in the general direction of the E2 active site. Adapted from Hao et al., 2007 [20].

SCF (Skp1 - Cullin - F-Box protein) ubiquitin ligases are the archetype for the RING-type E3 enzymes, they are built in a modular format that is conserved from yeast to humans [22] (Fig. 2A). The invariant core complex consists of Cullin, a scaffold subunit with a curved yet rigid and extended structure, at its C-terminus binds the RING-containing protein Rbx1, the E2 docking site, and at its N-terminus binds Skp1, the adaptor subunit. Skp1 connects this core catalytic complex to one of a suite of F-Box proteins, the substrate recognition subunit which recruits a specific pool of substrates [23]. The different SCF complexes are designated according to the variable F-box component (e.g. SCF^{Met30} contains the Met30 F-box protein); 13 F-box proteins were identified in yeast and 68 were found in the human genome [24, 25]. Available structural data show that the SCF complex subunits fit together into a C-shaped conformation and revealed a 50-60 Å gap between the substrate binding domain platform and the location of predicted ubiquitin-thioester bond on docked E2~Ub [17-21] (Fig. 2B). A hypothetical working mechanism of E2 was proposed to bridge this cleft. The ubiquitin-charged Cdc34 (cdc34~Ub) had been observed in dynamic binding equilibrium with SCF [26]. It was then proposed that E2~Ub could bind to the RING domain, dissociate and diffuse across the gap until it finds one of the substrate Lys residues. This "Hit and Run" model is, however, controversial [27]. Other experimental data tend to indicate that the 50-60 Å space is a kind of "hot zone" with a maximal ubiquitination for the substrate lysine residues lying next to the E2 catalytic site [17]. In addition, precise positioning by the F-box protein seemed crucial for certain substrates [18].

Despite the accumulation of biochemical and structural data, little is known about how the SCF-E2 complex mediates the ubiquitination reaction and delivers ubiquitinated substrates to the 26S proteasome. To further unravel the mechanism of ubiquitination by SCF ligases, we used a chimeric F-box protein. F-box proteins contain two essential domains; an N-terminal F-box domain responsible for the interaction with Skp1 and a C-terminal substrate binding domain mostly composed of WD40 repeats or Leucine Rich Repeats [28]. The budding yeast *S. cerevisiae* F-box protein Cdc4 was chosen as scaffold for the design of the chimeric F-box protein. Cdc4 triggers the G1-S phase transition by mediating the degradation of the B-type (Clb)-Cdc28 cyclin-dependent kinase inhibitor Sic1 in a phosphorylation-dependent manner [29]. Sic1 phosphorylation generates several Cdc4 phospho-degrons (CPD) which can be recognized by the WD40 domain of Cdc4 [30]. The crystal structure of a Skp1-Cdc4 complex bound to a high affinity CPD phosphopeptide shed light on phosphodependent substrate selection and enabled modeling of the E2-SCF^{Cdc4} complex to provide visualization of substrate orientation (Fig. 2B) [18]. DARPins, a new binding scaffold based on repeat proteins modular architecture [31], was used to replace the original substrate binding domain of Cdc4. This new artificial substrate binding domain was designed to recognize a model substrate.

In *S. cerevisiae*, the chimeric F-box protein could specifically destabilize a target protein in a SCF- and proteasome-dependent manner. It was then used as tool and the target protein degradation assay as read-out, to investigate how F-box proteins mediate protein degradation. Parameters affecting essential properties of the chimeric F-box protein could be monitored without inducing any toxicity. Information was mostly collected on substrate presentation and delivery to the proteasome. We also propose a model for the F-box protein level regulation mechanism. This new strategy gave further insights into the working mechanism of SCF ubiquitin protein ligases.

Materials & methods

Yeast strains and genetic experiments

Yeast strains are described in Table 1. The genotypes of the yeast strains are:

W303: *ade2-1*, *trp1-1*, *can1-100*, *leu2-3,112*, *his3-11,15*, *ura3-1*, *GAL+*, *psi+*, *ssd1-d2*

S288C: *ade2-101*, *ura3-52*, *lys2-801*, *trp1-Δ1*, *his3Δ200*, *leu2-Δ*

Unless noted otherwise strain K699 was used.

Table 1: Yeast strains

Strain	Relevant genotype	Background	Source
K699	Mat a	W303	M. Peter
Cdc53_1	Cdc53_1	W303	M. Peter
Cdc34_2	Cdc34_2	W303	M. Peter
Erg6	Erg6::KAN	S288C	M. Peter & G. Rabut
MGa	*ura3-1::URA3*-P_{ADH}-MBPGFP	K699	This study
AGa	*ura3-1::URA3*-P_{ADH}-APHGFP	K699	This study
F75Gg	[p415/Gal/cdc4_5GS_off7]	K699	This study
F35Gg	[p415/Gal/cdc4_5GS_3a]	K699	This study
MGaF75Gg	*ura3-1::URA3*-P_{ADH}-MBPGFP [p415/Gal/cdc4_5GS_off7]	K699	This study
AGaF35Gg	*ura3-1::URA3*-P_{ADH}-APHGFP [p415/Gal/cdc4_5GS_3a]	K699	This study
Mg	*ura3-1::URA3*-P_{Gal1}-MBP	K699	This study
MGg	*ura3-1::URA3*-P_{Gal1}-MBPGFP	K699	This study
MgFB5Ga	*ura3-1::URA3*-P_{Gal1}-MBP [p415/ADH/cdc4_5GS_B]	K699	This study
MgF75Ga	*ura3-1::URA3*-P_{Gal1}-MBP [p415/ADH/cdc4_5GS_off7]	K699	This study
eMGgF75Ga	[p415/Gal/MBP-GFP] [p413/ADH/cdc4_5GS_off7]	Erg6	This study
WtMGgF75Ga	[p415/Gal/MBP-GFP] [p413/ADH/cdc4_5GS_off7]	W303	This study
53MGgF75Ga	[p415/Gal/MBP-GFP] [p413/ADH/cdc4_5GS_off7]	Cdc53_1	This study
34MGgF75Ga	[p415/Gal/MBP-GFP] [p413/ADH/cdc4_5GS_off7]	Cdc34_2	This study
MGgF75Ga	*ura3-1::URA3*-P_{Gal1}-MBPGFP [p415/ADH/cdc4_5GS_off7]	K699	This study
MgF710Ga	*ura3-1::URA3*-P_{Gal1}-MBP [p415/ADH/cdc4_10GS_off7]	K699	This study
MgF715Ga	*ura3-1::URA3*-P_{Gal1}-MBP [p415/ADH/cdc4_15GS_off7]	K699	This study
MgF73Aa	*ura3-1::URA3*-P_{Gal1}-MBP [p415/ ADH /cdc4_3ala_off7]	K699	This study
MgF710Aa	*ura3-1::URA3*-P_{Gal1}-MBP [p415/ ADH /cdc4_10ala_off7]	K699	This study
MgF717Aa	*ura3-1::URA3*-P_{Gal1}-MBP [p415/ ADH /cdc4_17ala_off7]	K699	This study

MGgF7'5Ga	*ura3-1::URA3*-P_{Gal1}-MBPGFP [p415/ADH /cdc4_5GS_off7_Y56A]	K699	This study
MGgF7''5Ga	*ura3-1::URA3*-P_{Gal1}-MBPGFP [p415/ADH /cdc4_5GS_off7_Y56AY81A]	K699	This study
MGgF7'''5Ga	*ura3-1::URA3*-P_{Gal1}-MBPGFP [p415/ADH /cdc4_5GS_off7_Y56AY81AY125A]	K699	This study
F75Ga	[p415/ADH/cdc4_5GS_off7]	K699	This study
MGgF75Gaa	*ura3-1::URA3*-P_{Gal1}-MBPGFP [p425/ ADH /cdc4_5GS_off7]	K699	This study
MGgF75Gt	*ura3-1::URA3*-P_{Gal1}-MBPGFP [p415/TEF/cdc4_5GS_off7]	K699	This study
MGgF75Gtt	*ura3-1::URA3*-P_{Gal1}-MBPGFP [p425/TEF/cdc4_5GS_off7]	K699	This study
MgF7Δ5Ga	*ura3-1::URA3*-P_{Gal1}-MBP [p415/ ADH /cdc4_5GS_off7_deltaN]	K699	This study
MgF7Lys5Ga	*ura3-1::URA3*-P_{Gal1}-MBP [p415/ ADH /cdc4_5GS_off7_5Lys]	K699	This study
MLysgF75Ga	*ura3-1::URA3*-P_{Gal1}-MBP_5Lys [p415/ADH/cdc4_5GS_off7]	K699	This study

Standard yeast growth conditions and genetic manipulations were used as described [32]. Yeast cells were cultured in YPD (1% yeast extract, 2% bacto peptone, 2% glucose) or in synthetic media (S) (1.7 g/L yeast nitrogen base, 5 g/L ammonium sulfate) supplemented with a standard amino acid and nucleobases solution (30 mg/L isoleucine, 150 mg/L valine, 40 mg/L adenine, 20 mg/L arginine, 20 mg/L histidine, 100 mg/L leucine, 30 mg/L lysine, 20 mg/L methionine, 50 mg/L phenylalanine, 200 mg/L threonine, 40 mg/L tryptophane, 30 mg/L tyrosine, 20 mg/L uracil, 100 mg/L glutamic acid, 100 mg/L aspartic acid) and 2 % carbon source (glucose (D), raffinose (Raff) or galactose (Gal)). According to the strain and the experiment, a synthetic media prepared without amino acids or nucleobases supplemented with auxotrophic requirements: uracil (-Ura), leucine (-Leu), histidine (-His) and the appropriate carbon source (SD, SRaff or SGal) was used.

Yeast transformations were performed by the lithium acetate procedure [33]. Strains expressing the target protein were created by homologous recombination using StuI linearized plasmid pRS306/ADH/X or pRS306/Gal/X (see below).

DNA manipulations and plasmids

Standard molecular biology procedures were used for recombinant DNA manipulation [34]. Enzymes were from NEB (Ipswich, MA, USA) or Fermentas (Vilnius, Lithuania). PCR reactions were performed with the Phusion ™ High-Fidelity DNA polymerase as recommended by the manufacturer (NEB). Plasmids used as PCR DNA templates and all oligonucleotides are listed in tables 2 and 5.

Chimeric F-box proteins coding sequences cdc4_5GS_off7 (see sequence in annex) and cdc4_5GS_3a were constructed by assembly PCR. The cdc4 (ΔNLS) DNA sequence, encoding residues 1 to 358, and DARPin DNA sequences were amplified by PCR in two separate reactions, and a second PCR step was used to fuse the two sequences. Primers used at the C-terminus of cdc4 part and the N-terminus of DARPins encoded a GSGSG linker. Finally, a third PCR amplified the whole length product with the HA tag at the C terminus, which was then SpeI/XhoI digested and cloned in p415Gal1 [35]. cdc4_5GS_off7 and cdc4_5GS_3a coding sequences were subcloned in p415ADH [35]. The chimeric F-box protein coding sequence cdc4_3ala_off7 (see sequence in annex) was constructed by assembly

PCR, similarly to cdc4_5GS_off7, except that the primers used at the C-terminus of the cdc4 part and the N-terminus of DARPins encoded a AAA linker and that the final product was cloned in p415ADH. p415/ADH/cdc4_10GS_off7 was generated by integrating the annealed double-stranded Gly-Ser encoding oligonucleotides into BamHI/AvaI digested cdc4_5GS_off7 coding sequence and ligating the final product into p415/ADH (see sequence in annex). p415/ADH/cdc4_15GS_off7 was generated by integrating the annealed double-stranded Gly-Ser encoding oligonucleotide into BamHI/AvaI digested cdc4_10GS_off7 and ligating the final product into p415/ADH (see sequence in annex). p415/ADH/cdc4_10ala_off7 and p415/ADH /cdc4_17ala_off7 were produced by adding the double-stranded 10ala or 17ala encoding oligonucleotides into PstI digested p415/ADH/cdc4_3ala_off7 (see sequence in annex). Site-directed mutagenesis was performed by assembly-PCR. Oligos containing the point mutation of choice were used to produce the mutated off7 DNA sequence, which was then used to replace the original off7 sequence in p415/ADH/cdc4_5GS_off7. off7Y56AY81A and off7Y56AY81A DNA sequences were made by using p415/ADH/cdc4_5GS_off7_Y56A and p415/ADH/cdc4_5GS_off7_Y56AY81A as templates, respectively. The chimeric F-box protein genes were cloned between SpeI and Xho I sites of p415Gal, p415ADH or p413 ADH [35]. pQE30/off7_Y56A, pQE30/off7_Y56AY81A and pQE30/off7_Y56AY81AY125A were constructed by amplifying the off7 mutant sequence from p415/ADH/off7_Y56A, p415/ADH/cdc4_5GS_off7_Y56AY81A and p415/ADH/cdc4_5GS_off7_Y56AY81AY125A respectively with primers EWT3 and WTC4 and inserting the digested PCR product at the BamHI and HindIII sites of pQE30 (Qiagen, Chatsworth, CA).

The target protein genes were cloned with a N-terminal RGS$(His)_6$ tag, between SpeI and HindIII or XhoI sites of pRS306/ADH, pRS306/Gal or p415Gal. GFP fused target protein genes were constructed by assembly PCR. The target protein and GFP genes were amplified by PCR in two separate reactions and a final PCR step was used to fuse the two sequences and amplify the whole length product (see sequences in annex). pRS306/ADH and pRS306/Gal were generated by exchanging the original SacI-KpnI fragment of pRS306 [36]with the complete expression cassette (ADH or Gal1 promoter + multiple cloning site+ Cyc1-terminator) originating from p416ADH or p415Gal1, respectively [35]. Their maps are shown in annex.

All constructs were confirmed by sequencing. Plasmids constructed for this study are listed in tables 3 and 4, those marked with an asterisk have their plasmid map shown in annex.

Table 2: Plasmids used as PCR DNA templates for cloning of target proteins and chimeric F-box proteins genes

Plasmids	Templates for	Source
pQEMBP	MBP	Binz, 2004 [37]
pAT223_APH	APH	Amstutz, 2005 [38]
pET28GFP	GFP	Our laboratory, Andreas Ernst
pBM165	cdc4 (K82A, R83A, K85A)	Blondel, 2000 [39]
pQE30_AR_3a	3a	Amstutz, 2005 [38]
pQE30_AR_B	B	Amstutz, 2005 [38]
pQE30_mbpoff7	off7	Binz, 2004 [37]
pQE30_mbp_3_16	mbp16	Binz, 2004 [37]

Table 3: Plasmids constructed for target protein expression

Plasmids for target protein	Relevant characteristics (promoter; gene; resistance; ori)	Source
pRS306/ADH*	ADH; -; URA3 ; -	This study
pRS306/ADH/MBP-GFP*	ADH; MBP-GFP; URA3 ; -	This study
pRS306/ADH/APH-GFP	ADH; APH-GFP; URA3; -	This study
pRS306/Gal	Gal1; -; URA3; -	This study
pRS306/Gal/MBP-GFP	Gal1; MBP-GFP; URA3; -	This study
pRS306/Gal/MBP	Gal1; MBP; URA3; -	This study
pRS306/Gal/APH	Gal1; APH; URA3; -	This study
p415/Gal/MBP-GFP	Gal1; MBP-GFP; LEU2; CEN6	This study
pRS306/Gal/MBP_5Lys	Gal1; MBP_5Lys; URA3; -	This study

Table 4: Plasmids constructed for chimeric F-box proteins expression

Plasmids for chimeric F-box protein	Relevant characteristics (promoter; gene; resistance; ori)	Source
p415/Gal/cdc4_5GS_off7*	Gal1; cdc4_5GS_off7; LEU2; CEN6	This study
p415/Gal/cdc4_5GS_3a	Gal1; cdc4_5GS_3a; LEU2; CEN6	This study
p415/ADH/cdc4_5GS_off7*	ADH; cdc4_5GS_off7; LEU2; CEN6	This study
p415/ADH/cdc4_5GS_mbp16	ADH; cdc4_5GS_mbp16; LEU2; CEN6	This study
p415/ADH/cdc4_5GS_3a	ADH; cdc4_5GS_3a; LEU2; CEN6	This study
p415/ADH/cdc4_5GS_B	ADH; cdc4_5GS_B; LEU2; CEN6	This study
p413/ADH/cdc4_5GS_off7	ADH; cdc4_5GS_off7; HIS3; CEN6	This study
p415/ADH/cdc4_10GS_off7	ADH; cdc4_10GS_off7; LEU2; CEN6	This study
p415/ADH/cdc4_15GS_off7	ADH; cdc4_15GS_off7; LEU2; CEN6	This study
p415/ADH/cdc4_3ala_off7	ADH; cdc4_3ala_off7; LEU2; CEN6	This study
p415/ADH/cdc4_10ala_off7	ADH; cdc4_10ala_off7; LEU2; CEN6	This study
p415/ADH/cdc4_17ala_off7	ADH; cdc4_17ala_off7; LEU2; CEN6	This study
p415/ADH/cdc4_5GS_off7_Y56A	ADH; cdc4_5GS_off7_Y56A; LEU2; CEN6	This study
p415/ADH/cdc4_5GS_off7_Y56AY81A	ADH; cdc4_5GS_off7_Y56AY81A; LEU2; CEN6	This study
p415/ADH/cdc4_5GS_off7_Y56AY81AY125A	ADH;cdc4_5GS_off7_Y56AY81AY125A;LEU2;CEN6	This study
p425/ADH/cdc4_5GS_off7*	ADH; cdc4_5GS_off7; LEU2; 2μ	This study
p415/TEF/cdc4_5GS_off7*	TEF1; cdc4_5GS_off7; LEU2; CEN6	This study
p425/TEF/cdc4_5GS_off7	TEF1; cdc4_5GS_off7; LEU2; 2μ	This study
p415/ADH/cdc4_5GS_off7_deltaN	ADH; cdc4_5GS_off7_deltaN; LEU2; CEN6	This study
p415/ADH/cdc4_5GS_off7_5Lys	ADH; cdc4_5GS_off7_5Lys; LEU2; CEN6	This study
pQE30/ off7_Y56A	T5; RGS$(His)_6$ off7Y56A; Amp; ColE1	This study
pQE30/ off7_Y56AY81A	T5; RGS$(His)_6$ off7Y56AY81A; Amp; ColE1	This study
pQE30/ off7_Y56AY81AY125A	T5; RGS$(His)_6$ off7Y56AY81AY125A; Amp; ColE1	This study

Table 5: Oligonucleotides

Oligonucleotides	Sequence 5'-3' direction	Description (for=forward, rev=reverse)
forSpeI	GTGGTACTAGTATGAGAGGATCGCATCACCATCACCATCACGGA	for target protein with RGS(His)$_6$ tag + SpeI site
revMBPXmaI	GGTGGTCCCGGGAGTCTGCGCGTCTTTCAGGG	rev MBP linker with GFP
revAPHXmaI	GGTGGTCCCGGGAAACAATTCATCCAGTAAAATATAA	rev APH linker with GFP
linkerXmaIGFP	GGTGGTCCCGGGTCCGCTGCTGGTTCTGGCG	for linker GFP
revGFPHindIII	TGGTGGTAAGCTTTTATTTGTAGAGCTCATCCATGC	rev GFP + HindIII site
revAPHXho	GTCTCGAGTTAAAACAATTCATCCAGTAAAATATA	rev APH+ XhoI site
revMBPHindIII	GGTGGTAAGCTTTTAAGTCTGCGCGTCTTTCAGGG	rev MBP + HindIII site
revMBPlys	TTTCTTTTTCTTAGTCTGCGCGTCTTTCAGGG	rev MPB+5Lys (PCR1)
revXhoLys	GTCTCGAGTTACTTTTTCTTTTTCTTAGTCTGCGC	rev MPB+5Lys (PCR2) + XhoI site
forSpeIcdc4	GGT GGT ACT AGT ATG GGG TCG TTT CCC TTA GC	for cdc4 with SpeI site
revcdc45GS	TACCCAGGTCGCCCGAGCCGGATCCATTCTCCAGAAAAGATAATCT	rev 5GS linker
for5GSDARPin	TCTGGAGAATGGATCCGGCTCGGGCGACCTGGGTAAGAAACTGCT	for 5GS linker
revHADARPin	CGTAATCTGGAACATCGTATGGGTATTGCAGGATTTCAGCCAGGT	rev HA tag (25 first bases) + DARPin
revXhoIHA	GTGGTCTCGAGTTAAGCGTAATCTGGAACATCGTATG	rev XhoI site + HA tag (24 last bases)
revcdc43ala	CTTACCCAGGTCGGCTGCAGCATTCTCCAGAAAAGATAATCTAAG	rev 3ala linker
for3alaDARPin	CTTTTCTGGAGAATGCTGCAGCCGACCTGGGTAAGAAACTGCT	For 3ala linker
10alaupstrand	GCGGCAGCTGCCGCAGCTGCA	10 ala linker
10aladownstrand	GCTGCGGCAGCTGCCGCTGCA	10 ala linker
17alaupstrand	GCGGCAGCTGCCGCAGCTGCGGCAGCTGCCGCAGCTGCTGCA	17 ala linker
17aladownstrand	GCAGCTGCGGCAGCTGCCGCAGCTGCGGCAGCTGCCGCTGCA	17 ala linker
Gly-Serupstrand	GATCTGGTTCATCTGGATCCGGC	10 and 15 GS linker
Gly-Ser downstrand	CCGAGCCGGATCCAGATGAACCA	10 and 15 GS linker
foroff7BamHI	AATGGATCCGGCTCGGGCGA	Off7 mutagenesis for primer
Y56Arev	AGATGCAGCAGCCAGGTGCAGCGGAGTAG	Off7 mutant Y56A rev
Y56Afor	CACCTGGCTGCTGCATCTGGTCACCTG	Off7 mutant Y56A for
Y85Yrev	AGTAGCACCAAAAACGTCAGAAGCGTC	Off7 mutant Y81A rev
Y85Afor	TCTGACGTTTTTGGTGCTACTCCGCTG	Off7 mutant Y81A for
Y125Arev	GATTTCCAGGGCACCCCACTTAGCAGC	Off7 mutant Y125A rev
Y125Afor	AAGTGGGGTGCCCTGGAAATCGTTGAAG	Off7 mutant Y125A for
fordeltaNcdc4	GGTACTAGTATGTTAAAGAGGGACCTAATAACGTC	for cdc4 position 808bpb + ATG+ SpeI site
revshortXhoIHA	GGTCTCGAGTTAAGCGTAATCTGG	rev XhoI site + HA tag (15last bases)
revHAlys	TTTTTCTTTTTCTTAGCGTAATCTGGAACATCGTA	rev 3 Lys +HA tag (21 last bases)
revXholIys	GTCTCGAGTTACTTTTTCTTTTTCTTAGCGTAATC	rev 5 Lys + HA tag (9 last bases) + XhoI site
EWT3	TTCCGCGGATCCGACCTGGG	for DARPIn + BamHI site
WTC4	TTTGGGAAGCTTTTGCAGGATTTCAGC	rev DARPIn +HindIII site

Microscopy

MGa and Aga yeast cells (see table 1) were grown to early exponential phase in SD-Ura, and GFP-fused target proteins were visualized on a Zeiss axiophot fluorescence microscope using a Chroma GPII filter. For DAPI staining, cells were fixed 5 min in 70% ethanol and washed twice with water. Cells were then resuspended in a small volume of 50ng/ml DAPI in PBS and observed with a UV filter set.

Degradation assays

Experimental set-up 1: Yeast cells were grown in SD-UL or SGal-UL at 30°C. At OD_{600}=0.6-0.8, cycloheximide was added to a final concentration of 75 µg/ml. At the indicated time points, 2 ml-samples were withdrawn and OD_{600} was measured. Extracts for immunoblotting were immediately prepared as follows: cells were centrifuged for 3 min at 13,000 rpm in a tabletop centrifuge, the pellet was resuspended in 100 µl of 1.85 M NaOH/ 7.6 % v/v 2-mercaptoethanol and incubated for 10 min on ice. After addition of 100 µl of 50 % trichloroacetic acid (TCA), additional 10 min incubation on ice was performed. Precipitated proteins were pelleted at 13,000 rpm for 2 min at 4°C; pellets were washed with acetone, air-dried and resuspended in 3 X Laemmli buffer (63 mM Tris-HCl pH 6.8, 10 % glycerol, 2 % SDS, 50 mM 2-mercaptoethanol, bromophenolblue,). Normalized volumes according to the OD_{600} were loaded on 10 % or 15 % SDS-polyacrylamide gels followed by immunoblotting.

Experimental set-up 2: Yeast cells were grown in SRaff-U or SRaff-UL at 30°C. At OD_{600}=0.6-0.8, 2 % galactose was added. One hour later, 2 % glucose was added, cells were collected by centrifugation for 5 min at 3000 g before being resuspended in SD-U or SD-UL. Cells were further incubated at 30°C and samples of decreasing size were taken at different time points in order to have a relatively constant amount of cells; e.g. : 8 ml at t=0 min, 6.1 ml at t=30 min, 5.3 ml at t=60 min, 4 ml at t=90 min, 3.1 ml at t=120 min and 2 ml at t=180 min. OD_{600} was measured; cells were pelleted for 5 min at 5000 g and immediately stored at -20°C. All samples were then extracted simultaneously as follows. Pellets were thawed and centrifuged for 1 min at maximum speed to remove possible medium traces; they were then resuspended in 200 µl SDS-urea loading buffer (60 mM Tris-HCl, 8 M urea, 5 % glycerol, 3 % SDS, 4 % 2-mercaptoethanol, 5 mM EDTA, bromophenolblue, pH6.8) and transferred in 2 ml-tubes. After 20 min of water-bath sonication, 200 µl of acid-washed 425- to 600-µm glass beads (Sigma-Aldrich, St. Louis, MO) were added. Cells were lysed three times 2 min at 30 Hz in TissueLyser (Qiagen, Chatsworth, CA) and centrifuged at 1000 g. Samples were finally incubated for 5 min at 95°C and centrifuged at 4°C for 5 min at 20000 g. Normalized volumes according to the OD_{600} were loaded on 10 % or 15 % SDS-polyacrylamide gels followed by immunoblotting.

Thermosensitive strains

Yeast cells were grown in SRaff-LH at 25°C. At OD_{600}=0.5, 2 % galactose was added. 2.5 h later, cells were collected by centrifugation for 5 min at 3000 g and resuspended in SD-LH. The t=0 h sample (5.5 ml) was taken and the culture was divided in two halves which were further incubated at 25°C or 37°C. Additional samples of 5 ml, 4.5 ml and 4 ml were taken after 1.5 h, 3 h and 4.5 h, respectively. OD_{600} was measured; cells were pelleted for 5 min at maximum speed in a tabletop centrifuge and immediately stored at -20°C. All samples were then extracted simultaneously according to the protocol described above in the degradation assay experimental set-up 2.

Immunoprecipitations

Yeast cells were grown in the appropriate media (YPD, SRaff-U, SRaff-L or SRaff-UL) at 30°C. At OD_{600}=0.6-0.8, 2 % galactose was added followed by 2 % glucose 1 h 30 min later. OD_{600} was measured. All subsequent steps were performed at 4°C. Cells were collected by centrifugation for 5 min at 3000 g and washed with wash buffer (50 mM Na_2HPO_4 pH 8, 300 mM NaCl, 10 mM N-Ethylmaleimide (NEM)). Pellets were resuspended in ice-cold lysis buffer (50 mM Na_2HPO_4 pH 8, 300 mM NaCl, 10 mM NEM, 50 µM MG132 (Sigma-Aldrich, St. Louis, MO), protease inhibitor cocktail (Sigma-Aldrich, St. Louis, MO)) and cells were mechanically lysed through 4 cycles of a French Press. Cell debris was removed by a 30 min centrifugation step at 18,000 g and cleared lysates were aliquoted in 2ml-tubes, snap-frozen in liquid nitrogen and stored at -80°C. Thawed lysates were centrifuged for 5 min at 20,000 g. Normalized volumes of supernatant (according to OD_{600}) were incubated for 1 h 50 min with 7.5-10 µg anti-HA (product number H 9658) or anti-MBP antibody (product number M6295) (Sigma-Aldrich, St. Louis, MO) pre-captured on 100 ul Dynabeads® ProtG (Invitrogen, San Diego, CA). Beads were washed 4 times with 1 ml wash buffer and resuspended in 80 µl 1 X SDS sample loading buffer (62.5 mM Tris-HCl pH 6.8, 7.5 % glycerol, 2 % SDS, 2.5 % 2-mercaptoethanol, bromophenolblue). After 5 min at 95°C, eluted fractions were resolved by 10 % SDS-PAGE followed by immunoblotting.

Pull-down under denaturing conditions

Yeast cells were grown in the appropriate media (YPD, SRaff-U or SRaff-UL) at 30°C. At OD_{600}=0.6-0.8, 2% galactose was added followed by 2 % glucose 1 h 30 min later. OD_{600} was measured. Cells were collected by centrifugation for 5 min at 3000 g and washed with denaturing buffer (8 M urea, 0.1 M NaH_2PO_4 pH 8, 0.01 M Tric-HCl, 0.05 % Tween 20, 50 mM iodoacetamide). Pellets were resuspended in denaturing buffer and cells were mechanically lysed by 4 cycles of French Press. Cell debris was removed by a 30 min centrifugation step at 18000 g and cleared lysates were aliquoted in 2ml-tubes, snap-frozen in liquid nitrogen and stored at -80°C. Thawed lysates were centrifuged for 5 min at 14000 rpm. Normalized volumes of supernatant (according to OD_{600}) were incubated for 1 h 45 min with 200 µl Ni-NTA magnetic agarose beads (Qiagen, Chatsworth, CA, product number: 36111). Beads were washed 4 times with denaturing buffer and eluted with 80 µl 1X SDS sample loading buffer-EDTA (62.5 mM Tris-HCl pH 6.8, 100 mM EDTA, 7.5% glycerol, 2% SDS, 2.5% 2-mercaptoethanol, bromophenolblue). After 5 min at 95°C, eluted fractions were resolved by 4-12 % SDS-PAGE followed by immunoblotting.

Immunoblotting

Samples were transferred to PVDF membranes and immunoblotted using standard methods. The RGS·His HRP conjugate was used at a 1:10,000 dilution (Qiagen, Chatsworth, CA, product number: 34450). The anti-HA antibody (Sigma-Aldrich, St. Louis, MO, product number H9658) was used at a 1:10,000 dilution, the anti-actin antibody (Millipore, Bedford, MA, product number: MAB1501R) at 1:3000 dilution and they were both detected with anti-horseradish peroxidase (HRP)-coupled anti-mouse antibody 1:10,000 diluted (Thermo Fisher Scientific, Rockford, IL, product number 31438). For immunoprecipitation samples, the RGS·His HRP Conjugate was used at a 1:8000 dilution (Qiagen, Chatsworth, CA, product number: 34450) and the anti-HA peroxydase conjugate at a 1:1000 dilution (Sigma-Aldrich, St. Louis, MO, product number H 6533). The anti-ubiquitin antibody (Abcam, Cambridge, UK, product number: ab19247) was used at a 1:1000 dilution and detected with HRP-coupled anti-rabbit antibody 1:10,000 diluted (Sigma-Aldrich, St. Louis, MO, product number A6154)

Modeling of the rigid linker

PDF files of cdc4 (1NEX) and off7 in complex with MBP (1SVX) were superimposed using the graphics molecular modeling program Insight II. An artificial α-helix made of n alanine residues was aligned to the second helix of cdc4 linker (residues 348-358) and then off7 first helix (residues 12-17). The Skp1 chain was removed from the PDF file in order to visualize only cdc4 and the phosphopeptide chain. Best fits were chosen according to their ability to place MBP on top of cdc4 WD40 domain.

MALDI-MS

Cell lysates were prepared identically as was described for immunoprecipitations. Imidazole and Tween-20 were added to final concentrations of 10 mM and 0.05 %, respectively. All steps were performed at 4°C. 2ml-lysates were incubated for 1 h 45 min with 200 µl Ni-NTA magnetic agarose beads (Qiagen, Chatsworth, CA, product number: 36111). Beads were washed 3 times with 50 mM Na_2HPO_4 pH 8, 300 mM NaCl, 10 mM NEM, 0.05% Tween-20, 20 mM imidazole and eluted with 50 µl of 50 mM Na_2HPO_4 pH 8, 300 mM NaCl, 200 mM imidazole. 15 µl of eluted fraction was precipitated with 75 µl of cold 20% TCA. The precipitate was washed twice with cold acetone. The pellet was diluted in hexafluoroisopropanol/FA 1:3, co-crystallized with CHCA as matrix and measured by MALDI-MS.

Surface Plasmon Resonance (SPR)

Biotinylated MBP was produced in *E. coli* as described [37]. Off7 Y56A, Off7 Y56AY81A and Off7 Y56AY81AY125A cloned in pQE30 were produced on a liter scale and purified as described [37]. SPR was measured using a BIAcore 3000 instrument (GE Healthcare, Waukesha, WI). The running buffer was 20 mM Hepes pH7.4, 150 mM NaCl, 0.005% Tween-20. A streptavidin SA chip was coated with 450 or 900 RU biotinlyated MBP. The interactions were measured at 25°C and a flow of 60 µl/min with 5 min buffer flow, 2 min injection of different concentrations of off7 wt or mutant and an off-rate measurement of 45 min with buffer flow. The signal of an uncoated reference cell was substracted from the measurements. The kinetic data of the interaction were evaluated with a global fit using Biaevaluation 3.0 (GE Healthcare, Waukesha, WI) and Scrubber 2.0 (BioLogic ***Software***, Campbell, Australia).

Results

Target proteins

In order to avoid any interference with the yeast metabolism, heterologous proteins were chosen as target proteins. Maltose Binding Protein (MBP) is a protein expressed in the periplasm of *E. coli*, it plays a key role in the transport of maltose. The aminoglycoside phosphotransferase IIIa (APH) is a bacterial kinase that transfers a phosphate group from ATP to aminoglycoside antibiotics (kanamycin, streptomycin) thereby conferring resistance to this class of antibiotics. APH shares structural homology with eukaryotic protein kinases (EPKs). The coding sequence of MBP and APH was integrated in the genome of *S. cerevisiae* by homologous recombination at the ura locus using the integration vector pRS306/ADH (see material & methods). A RGS(His)$_6$ tag was appended to their N-terminus so that the target proteins could be detected by western blot using an anti-RGS(His)$_4$ antibody. A C-terminal fusion with Green Fluorescent Protein (GFP) showed that both APH and MBP were well expressed and distributed equally through the cytoplasm and nucleus of *S. cerevisiae,* being thus accessible (Fig. 3). The GFP-fused proteins were also used as target proteins, as they were usually easier to detect per western blot than the non-fused ones.

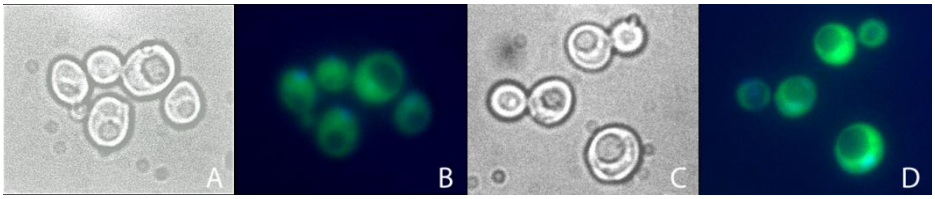

Figure 3: Bright-field image and fluorescence microscopy of AGa (A,B) and MGa cells (C,D) (see material & methods). APH-GFP and MBP-GFP proteins emitted green color while the DNA was DAPI-stained in blue.

Chimeric F-box protein

The yeast F-box protein Cdc4 was chosen as scaffold for the engineering of chimeric F-box proteins. The original coding sequence underwent four major modifications (Fig. 4). First, Cdc4 is normally located in the nucleus, and thus the NLS-mutated variant, Cdc4^{3A} (K82A, R83A and K85A) was used so that it could be distributed everywhere in the cell [39]. Second, the sequence encoding the WD40 domain responsible for substrate binding (residues 367-744), and the following C-terminal residues (residues 745-779), were deleted and replaced with a DARPin coding sequence. Several DARPins, able to bind MBP or APH, were chosen as new substrate binding domains, they differed in their size and affinity (Table 6). Third, the linker between the F-box domain and the WD40 domain, constituted of two α-helices (α1 and α2), was modified. The last few amino-acids of α2, which were interacting with the original WD40 domain (residues 359-366), were deleted and a 5 amino-acid flexible linker (GSGSG) was inserted between the original linker (after residue 358) and the DARPin. Finally, an HA-tag was fused to the C-terminus of the chimeric F-box protein for detection purposes. The designed chimeric F-box proteins were expressed on a plasmid (p415Gal), under control of the Gal 1 promoter and detected by western blot. (Fig. 5)

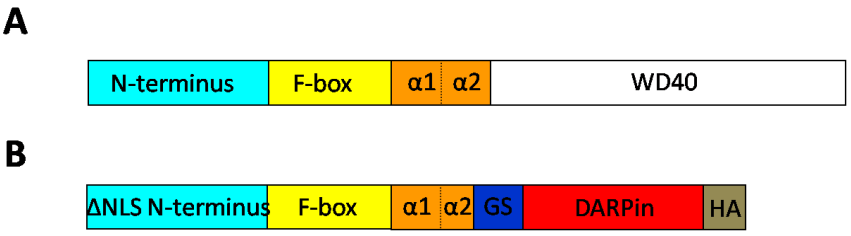

Figure 4: Schematic representation of wt Cdc4 (A) and chimeric Cdc4 (B) domains.

Target	DARPin	Size	k_{on} ($M^{-1} s^{-1}$)	k_{off} (s^{-1})	K_D (M)
APH	3a	N3C (167 aa)	$1.6 \cdot 10^{6}$	$2.7 \cdot 10^{-3}$	$1.8 \cdot 10^{-9}$
	B	N2C (134 aa)	$1.4 \cdot 10^{5}$	$4.1 \cdot 10^{-3}$	$2.85 \cdot 10^{-8}$
MBP	Off7	N3C (167 aa)	$4.2 \cdot 10^{5}$	$1.9 \cdot 10^{-3}$	$4.4 \cdot 10^{-9}$
	mbp16	N2C (134 aa)	$6.0 \cdot 10^{5}$	$1 \cdot 10^{-2}$	$1.7 \cdot 10^{-8}$

Table 6: Characteristics of the different DARPins used as substrate binding domains for the engineering of diverse chimeric Cdc4 proteins. Data from Binz et al, 2004 [37] and Amstutz et al, 2005 [38].

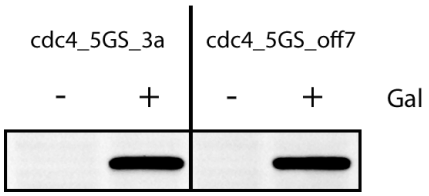

Figure 5: Chimeric F-box proteins expression under the Gal1 promoter and detection. F75Gg and F35Gg cells (see material & methods) were grown in the presence of glucose or galactose to repress or induce the expression of cdc4_5GS_3a or cdc4_5GS_off7. At OD_{600}= 0.6-0.8, total proteins were extracted and samples normalized according to their OD_{600} before being subjected to SDS-PAGE. The chimeric F-box proteins were detected using an anti-HA antibody.

Target protein degradation assay

Experimental set-up 1

In order to test if a chimeric F-box protein could specifically lead a target protein to degradation, a first experimental set-up based on the constitutive expression of the target protein under the ADH promoter (integrated in the genome) and the inducible expression of the chimeric F-box protein under the Gal1 promoter (from plasmid p415Gal) was established. Cells were grown either in presence of glucose, repressing the expression of the F-box protein, or in presence of galactose, activating the expression of the F-box protein. After addition of cycloheximide, a protein translation inhibitor, the stability of the target protein was assessed by monitoring its amount after different time points. Both MBP-GFP and APH-GFP were unstable, but more so in presence of cdc4_5GS_off7 or cdc4_5GS_3a, their respective cognate chimeric F-box proteins (Fig. 6). At time point 0, the amount of both MBP-GFP and APH-GFP was already lower in the presence of the chimeric F-box protein. If the target proteins were indeed constantly degraded, they could only accumulate to a

lower extent before the cycloheximide assay started. The chimeric F-box proteins seemed to be functional as they accelerated the target protein turnover, but they appeared to be also unstable themselves and disappeared quickly after addition of cycloheximide. After 2 to 4h, depending of their sequence, they were almost not present any more in the cells. The target protein degradation process was most likely not optimal under these conditions, since the degradation-adapter was itself degraded and thus removed from the system once its biosynthesis was stopped with cycloheximide.

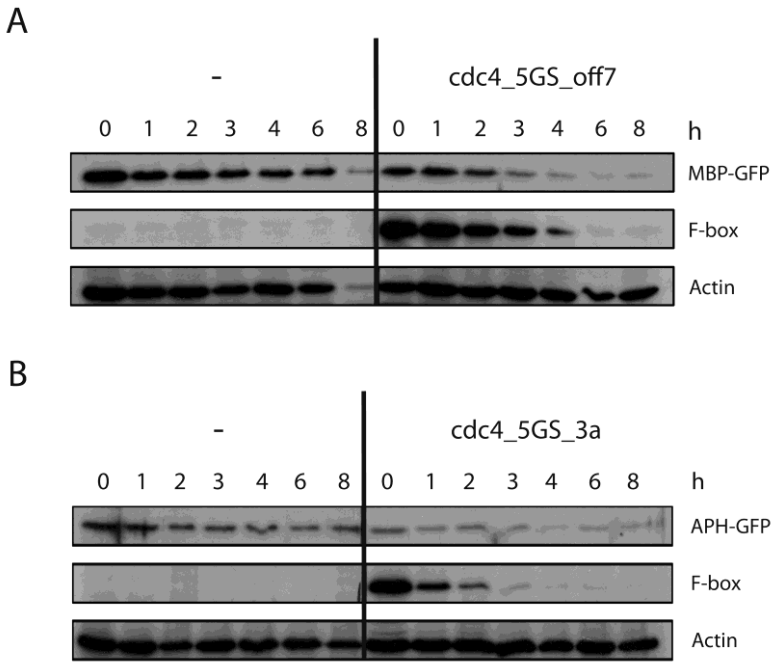

Figure 6: Stability of a target protein in absence or presence of a chimeric F-box protein using the experimental set-up 1. A: MGaF75Gg cells (see material & methods) expressing MBP-GFP were grown in the presence of glucose or galactose to repress or induce the expression of cdc4_5GS_off7. At OD_{600}=0.6-0.8, cycloheximide was added, the t=0 sample was withdrawn followed by other ones at the indicated time points. B: AGaF35Gg cells (see material & methods) expressing APH-GFP were grown in the presence of glucose or galactose to repress or induce the expression of cdc4_5GS_3a. At OD_{600}=0.6-0.8, cycloheximide was added and samples were withdrawn at the indicated time points. A, B: Total proteins were extracted and samples normalized according to their OD_{600} before being subjected to SDS-PAGE. MBP-GFP and APH-GFP were detected with the anti-RGS(His)$_4$ antibody and the chimeric F-box protein cdc4_5GS_off7 and cdc4_5GS_3a with the anti-HA antibody. The actin signal was used as an internal loading control.

Experimental set-up 2

A second experimental set-up was established to circumvent the significant instability of the chimeric F-box protein in the presence of cycloheximide. In this set-up, the target protein was placed under the control of the inducible Gal promoter (integrated in the genome) and the chimeric F-box protein was constitutively expressed under the ADH promoter (from plasmid p415ADH). The target protein was expressed during 1 h in presence of galactose and its stability was followed after promoter shut-off by glucose, in absence or presence of a chimeric F-box protein. No cycloheximide was used. MBP was again more destabilized in presence of cdc4_5GS_off7 than in its absence (Fig. 7). This effect was specific as it was not destabilized in presence of a cdc4_5GS_B bearing an unspecific DARPin, not able to recognize MBP. Identical results were obtained for MBP-GFP (data not shown). On average, the target protein half-life was shortened from around 180 min to 60-90 min in the presence of the chimeric F-box protein. The degradation was thus at least 2-fold accelerated. A similar destabilization was observed for the other target protein previously tested: APH, alone or fused to GFP (data not

shown). In conclusion, all tested chimeric F-box proteins were active and led to an accelerated protein break-down, cdc4_5GS_off7 and cdc4_5GS_mbp16 towards MBP and cdc4_5GS_3a and cdc4_5GS_B towards APH (data not shown). In the active constructs, the DARPin moiety was of different sizes and affinity. This second set-up allowed us to monitor target protein degradation within 3 h. All following degradation assays, unless stated, were then performed using the experimental set-up 2.

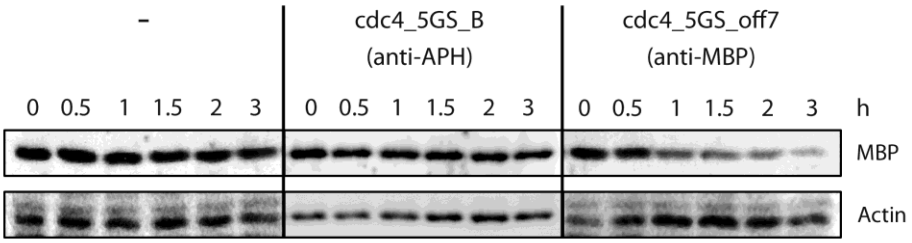

Figure 7: Stability of MBP in the presence of an unspecific or specific chimeric F-box protein using the experimental set-up 2. Cdc4_5GS_B was engineered with a DARPin which was selected against APH and does not recognize MBP. Cdc4_5GS_off7 was engineered with a specific DARPin which was selected against MBP. Mg, MgFB5Ga and MgF75Ga cells (see material & methods) were grown in a synthetic raffinose based medium to an OD_{600} of 0.6-0.8. MBP expression was induced for 1 h with galactose and stopped with glucose. Samples were withdrawn at the indicated time points. Total protein was extracted and samples normalized according to their OD_{600} before being subjected to SDS-PAGE. The levels of MBP were detected by immunoblotting with the anti-RGS(His)$_4$ antibody. The actin signal was used as an internal loading control.

Stability of the target protein in presence of MG132, a proteasome inhibitor

The target protein was destabilized when co-expressed with a specific chimeric F-box protein. To investigate if this unstability was proteasome dependent, the effect of MG132 [40], a reversible proteasome inhibitor was tested. For this assay, a special strain mutated for erg6 [41], a sterol transmethylase involved in the final synthesis of the membrane ergosterol, was used to increase the membrane permeability and allow the compound to pass through the yeast cell wall. Under MG132 treatment, the degradation was slower than in the presence of DMSO (the same amount as used for dissolving MG132) (Fig. 8). MG132, like most proteasome inhibitors, does not inhibit all proteolytic activities but it showed that the target protein was processed by the 26S proteasome, as its degradation was slowed down in the presence of MG132.

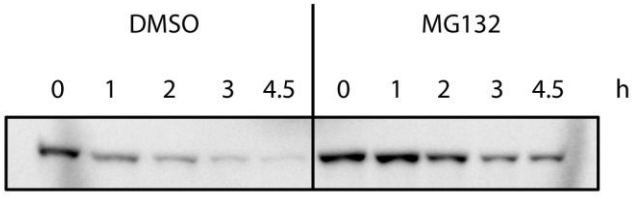

Figure 8: Stability of MBP-GFP co-expressed with cdc4_5GS_off7 in presence of the proteasome inhibitor MG132. eMGgF75Ga cells (see material & methods) were grown in a synthetic raffinose based medium to an OD_{600} of 0.6-0.8. Galactose and DMSO or MG132 were added to the cells. After 1 h, MBP-GFP expression was stopped with glucose. Samples were withdrawn at the indicated time points. Total protein was extracted and samples normalized according to their OD_{600} before being subjected to SDS-PAGE. The levels of MBP-GFP were detected by immunoblotting with an anti-RGS(His)$_4$ antibody.

Stability of the target protein in ubiquitylation mutant strains

In order to make sure that the degradation process not only relied on proteasome activity but also on the SCF ubiquitin ligase (E3) complex which should contain the hybrid cdc4 protein, two plasmids, one containing the MBP-GFP gene and another containing the cdc4_5GS_off7 gene, were co-transformed in two different thermosensitive strains, namely cdc53_1 and cdc34_2 and their wild-type background strain, W303. Cdc53_1 contains a mutation in the cdc53 gene which encodes a deficient cullin 1, another subunit of the SCF ubiquitin ligase (Fig. 2). Cdc34_2 contains a point mutation in the cdc34 gene which encodes the ubiquitin conjugating enzyme (E2) interacting with the SCF complex. A degradation assay was performed for 4.5 h in parallel at 25 and 37°C. In W303, MBP-GFP was quickly degraded, while in cdc53_1, the degradation process was slowed down, but following the same pattern at the permissive and restrictive temperatures (Fig. 9). In cdc34_2, MBP-GFP was also more stable than in the wt strain, but the amount detected at 37°C was lower than at 25°C. These results were not in agreement with the effect of the mutations, meant to be effective at the restrictive temperature only. However when carefully looking at the actin signal, one could see that despite the normalization of the samples, the amount of total protein (represented by actin) present in all samples was not equal. This discrepancy correlated with the differences observed for MBP-GFP signals, especially for the cdc34_2 strain samples. The elongated shape of these mutant cells and the arrest in G1 might explain the difficulty to properly normalize samples while relying on the OD_{600nm} [42]. Thermosensitive strains can partially display their mutant phenotype at the permissive temperature. Thus, despite the lack of reliable sample normalization between the permissive and restrictive temperatures, we could still observe that MBP-GFP was normally degraded in the background strain W303, while it accumulated more in both mutant strains, suggesting that its degradation required both the SCF ubiquitin ligase and the interacting ubiquitin conjugating enzyme.

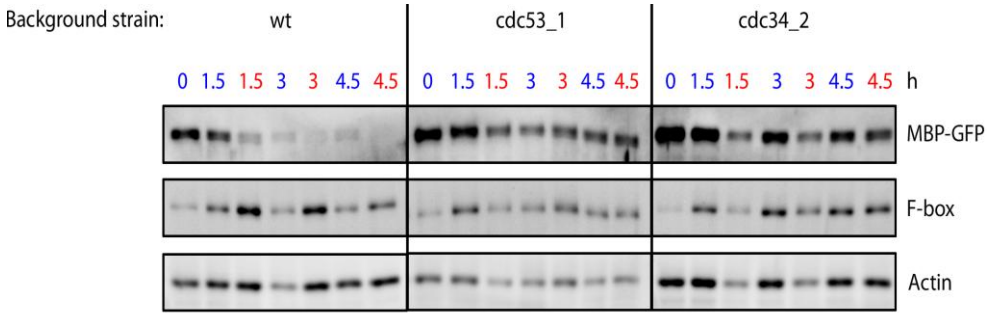

Figure 9: Stability of MBP-GFP co-expressed with cdc4_5GS_off7 in wt, cdc34_2 (deficient in E2) and cd53_1 (deficient in cullin 1) background strains. WtMGgF75Ga, 53MGgF75Ga and 34MGgF75Ga cells (see material & methods) were grown at 25°C in a synthetic raffinose based medium to an OD_{600} of 0.5. MBP-GFP expression was induced for 2.5 h with galactose and stopped with glucose. Halves of cultures were kept at 25°C (blue) and the other halves were switched to 37°C (red). Samples were withdrawn at the indicated time points. Total protein was extracted and samples normalized according to their OD_{600} before being subjected to SDS-PAGE. MBP-GFP and cdc4_5GS_off7 were detected by immunoblotting with anti-RGS(His)$_4$ and anti-HA antibodies, respectively. The actin signal was used as an internal loading control.

Target protein immunoprecipitations and Mass spectrometry analysis

Immunoprecipitations were performed to see if ubiquitinated forms of the target protein could be detected. The MBP could be easily immunoprecipitated using an anti-MBP antibody as bait. An additional band to the one corresponding to the theoretical size of the MBP construct (43 kDa) appeared at 53 kDa, but both in the absence and presence of the chimeric F-box protein cdc4_5GS_off7, ruling out the possibility that it could be an ubiquitinated form of the target protein (Fig. 10A). The anti-ubiquitin antibody did not reveal any specific higher molecular weight species in the presence of the chimeric F-box protein either (Fig. 10B). In order to counteract the general activity of deubiquitinases which can remove ubiquitin molecules and decrease the probability to retrieve ubiquitinated proteins, a pull-down was also performed under denaturing conditions. Ni-NTA magnetic beads were used to pull down MBP via its terminal RGS(His)$_6$ tag in 8 M urea (Fig. 11A). Yet again, no specific higher molecular weight products could be detected (Fig. 11A,B). No ubiquitinated form of the target protein could be detected under the conditions used. Nevertheless, the anti-HA antibody revealed that cdc4_5GS_off7 co-eluted with the target protein showing that they did interact in vivo. (Fig. 10C). cdc4_5GS_off7 was consistantly running at around 70 kDa, which was higher than its theoretical molecular weight of 56.8 kDa.

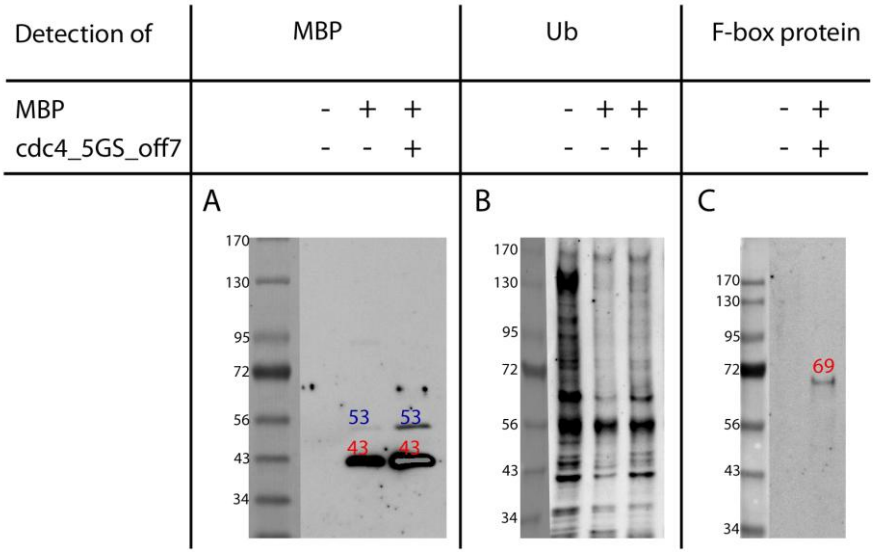

Figure 10: MBP Immunoprecipitation. MBP was expressed alone in Mg cells or with the chimeric F-box protein cdc4_5GS_off7 in MgF75Ga cells (see material & methods). After cell lysis, MBP was immunoprecipitated with an anti-MBP antibody. The eluted fractions were detected with an anti-RGS(His)$_4$ antibody detecting MBP itself (A), an anti-ubiquitin antibody (B) and an anti-HA antibody (C). A: The anti-RGS(His)$_4$ antibody recognized MBP at 43 kDa and a non-identified species at 53 kDa. B: The anti-ubiquitin antibody did not detect ubiquitinated forms of MBP in the presence of the chimeric F-box protein cdc4_5GS_off7. C: The anti-HA antibody detected the chimeric F-box protein cdc4_5GS_off7, running at 69 kDa, which co-immnunoprecipitated with MBP. The size marker is indicated in kDa.

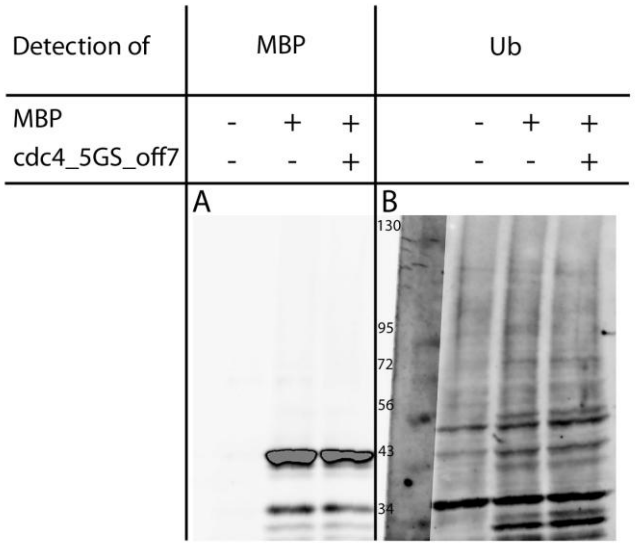

Figure 11: MBP pull-down in denaturing conditions. MBP was expressed alone in Mg cells or with the chimeric F-box protein cdc4_5GS_off7 in MgF75Ga cells (see material & methods). After cell lysis in 8 M urea, MBP was pulled down by Ni-NTA magnetic beads. The eluted fractions were detected with an anti-RGS(His)$_4$ antibody (A) and an anti-ubiquitin antibody (B). A: The anti-RGS(His)$_4$ antibody recognized MBP at around 43 kDa. B: the anti-ubiquitin antibody did not detect ubiquitinated forms of MBP in the presence of the chimeric F-box protein cdc4_5GS_off7. The size marker is indicated in kDa.

Mass spectroscopy was also used to see if any ubiquitinated target protein could be detected. After cells lysis, Ni-NTA magnetic beads were used to pull down MBP-GFP via its terminal RGS(His)$_6$ tag. A sample of the eluted fraction was run on a SDS-PAGE and western-blotted with the anti-RGS(His)$_4$ antibody. The most prominent species in the sample was running at 83 kDa, two other additional proteins were also detected at 62 and 33 kDa while the theoretical size of MBP-GFP was 69964 kDa (Fig. 12A). The eluted sample was subjected to MALDI-MS. The largest species was identified with a molecular weight of 69935 kDa, which corresponded to non-modified MBP-GFP (Fig. 12B). No species of higher molecular weight were revealed in the spectrum but this one was ranging from 8 to 80000 kDa. No species corresponding to the molecular weight of MBP-GFP plus 1,2, 3 or 4 molecules in a doubly charged or triply charged form could be detected, either. It should be noted that MBP-GFP was present in a rather large amount (approximately ≥ 70% of total protein) but did not give a strong signal; it did not fly well under the used conditions. The shift observed in the molecular weight of MBP-GFP per western blot was probably an artifact and did not seem to be due to ubiquitination.

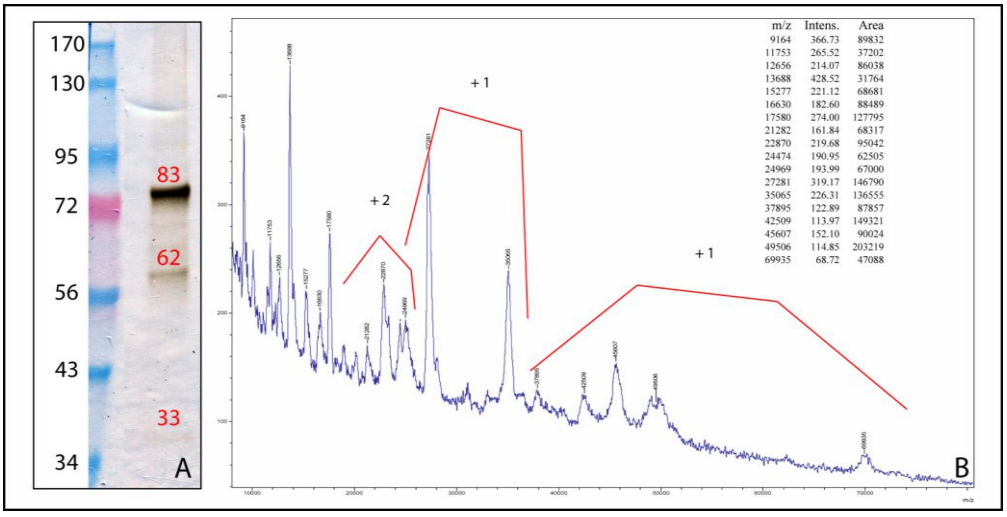

Figure 12: Maldi-MS analysis of MBP-GFP. MBP-GFP was expressed with the chimeric F-box protein cdc4_5GS_off7 in MGgF75Ga cells (see material & methods). After cell lysis, it was pulled down with Ni-NTA magnetic beads. A: A sample of the eluted fraction was subjected to SDS-PAGE and western blot which was performed with the anti-RGS(His)$_4$ antibody. B: Maldi-MS spectrum. The eluted fraction was precipitated with 20% TCA and washed with cold acetone. The pellet was diluted in hexafluoroisopropanol/FA 1:3, co-crystallized with CHCA as matrix and measured by MALDI-MS.

Target protein ubiquitination could then not be demonstrated by immunoprecipitation or mass spectroscopy. However, as target protein degradation relied on the presence of a specific chimeric F-box protein, a functional SCF complex, the activity of the E2 ubiquitin ligase and a proficient 26S proteasome, we assumed that the chimeric F-box protein was functional and was mediating target protein degradation by addressing it to the ubiquitin proteasome pathway. Further experiments were carried out, using the chimeric F-box protein cdc4_5GS_off7 and the target protein MBP to investigate the mechanism of natural F-box proteins.

Linker engineering of the chimeric F-box protein

The linker between the F-box domain and the substrate binding domain seems critical for cdc4 function; it is a stiff helix which is thought to properly position the substrate for subsequent ubiquitination [18]. To probe the importance of orientation and rigidity in this linker domain, it was engineered so that the substrate can be either flexibly or rigidly positioned for an attack by E2 (see Fig. 2). In order to orient the target protein in a similar way to the original WD40 domain, structures of cdc4 and off7 in complex with MBP were superimposed (Fig. 13). An artificial α-helix made of alanine residues was used to extend the second helix of the cdc4 linker into the first helix of DARPin. Using 3, 10 or 17 Ala as a (more or less) rigid linker, MBP, while bound by off7, could be positioned at about the same place as the cdc4 WD40 binding surface, where the substrates are normally bound by the wt cdc4 protein. In addition to the rigid linkers, two additional flexible ones of greater length were made: GSGSSGSGSG (10 GS) and $(GSGSS)_2GSGSG$ (15 GS). These linkers were meant to increase gradually the rotation possibility of the substrate binding domain. MBP (Fig. 14) and MBP-GFP (data not shown) could be both degraded with all kind of linkers. The shortest flexible one made of GSGSG residues (5 GS) was the most efficient one. In general, degradation efficiency was decreasing with linkers of increasing length, for both flexible and rigid ones. The linker rigidity seemed then not to be crucial for the substrate presentation, but rather its length.

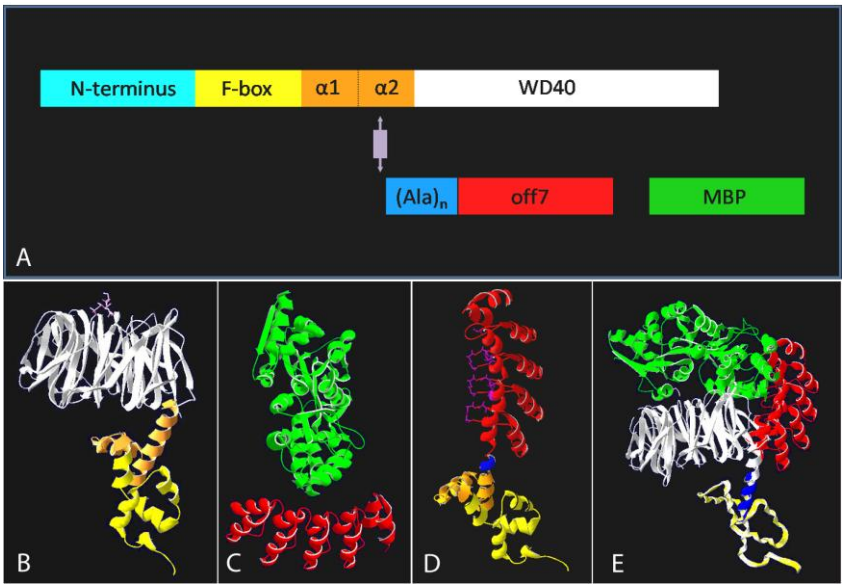

Figure 13: Engineering of a rigid linker in the chimeric F-box protein. A: Schematic representation of the strategy used to engineer a rigid linker between the F-box domain and the DARPins. Structures of cdc4 and off7 in complex with MBP were superimposed. An artificial α-helix made of alanine residues was used to extend the second helix of cdc4 linker into off7 first helix. B: Ribbon representation of cdc4. The F-box domain is colored in yellow, the WD40 domain in white and the linker in-between these domains in orange. The N-terminal domain was not crystallized. C: Ribbon representation of the MBP-Off7 complex. The DARPin Off7 is colored in red and the MBP in green. D: Ribbon representation of cdc4_3ala_off7 model. The F-box domain is colored in yellow, the original linker part in orange, the new linker part in blue and the DARPin Off7 in red. The side chains of residues involved in binding are displayed in purple. E: Superposition of cdc4 and the MBP-Off7 complex. The artificial alanine helix is colored in blue.

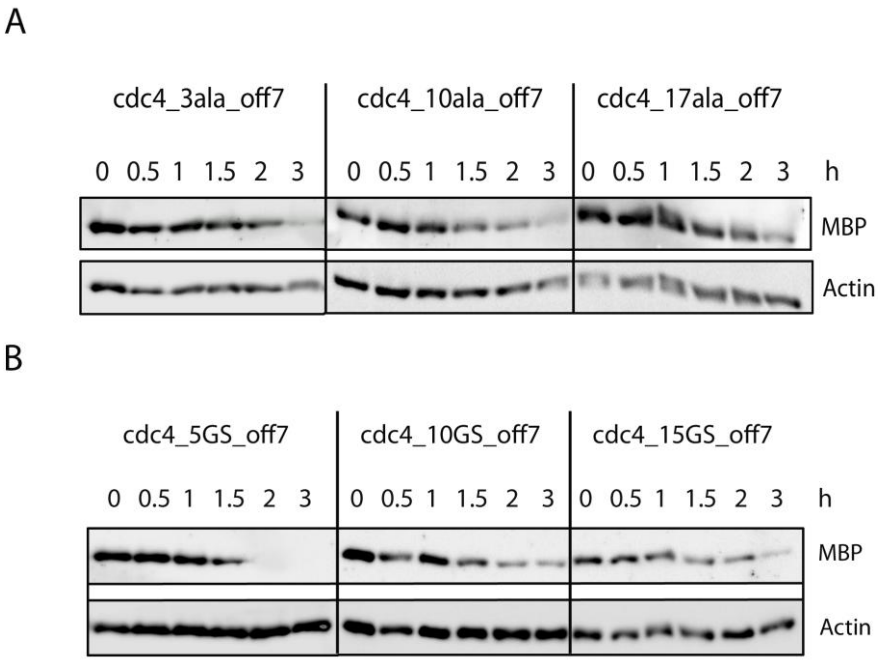

Figure 14: Stability of MBP co-expressed with a chimeric F-box protein engineered with a rigid linker in MgF73Aa, MgF710Aa and MgF717Aa cells (A) or with a flexible linker in MgF75Ga, MgF710Ga and MgF715Ga cells (B). Cells were grown in a synthetic raffinose based medium to an OD_{600} of 0.6-0.8. MBP expression was induced for 1 h with galactose and stopped with glucose. Samples were withdrawn at the indicated time points. Total protein was extracted and samples normalized according to their OD_{600} before being subjected to SDS-PAGE. The levels of MBP were detected by immunoblotting with the anti-RGS(His)$_4$ antibody. The actin signal was used as an internal loading control.

Affinity engineering of the chimeric F-box protein

The exact mechanism of ubiquitinated substrate delivery to the proteasome is not known. One hypothesis is that after ubiquitination, the substrate is released from the SCF complex and goes to the proteasome. The DARPins used for the engineering of the chimeric F-box proteins have a very strong affinity (low nM range), they could be preventing an efficient release of the processed substrate. In order to find the optimal affinity allowing an efficient recruitment and release of the substrate, a series of affinity mutants was generated by site-directed mutagenesis. Using the crystal structure of off7 in complex with MBP [37], three critical residues involved in H-bonds were mutated, leading three single mutants: Y56A; Y81A and Y125A, three double mutants: Y56AY81A; Y56AY125A; Y81AY125A and one triple mutant: Y56AY81AY125A (Fig. 15A). Affinities were determined by SPR for several mutants, the obtained K_D ranged from 11 nM to 2 µM (Fig. 15B). Biophysical properties were analysed by gel filtration, which showed that the mutants had the same running behavior than the wt off7. Chimeric F-box proteins were engineered with the mutated off7, and their effect on target protein stability were compared with the wt one. Whereas MBP-GFP degradation was barely affected by a single mutation in the substrate binding domain, the double and triple mutants partially stabilized the target protein (Fig. 15B). Similar results were obtained with MBP (data not shown). The target protein degradation efficiency gradually decreased as the number of mutations increased. No affinity-engineered mutant improved the degradation rate over wt, which had a K_D of 11nM, a very high affinity down to 2 µM, which is in the typical affinity range for intracellular interactions and had the smallest effect on degradation. With a K_D of 11nM, the substrate was unlikely to be easily released from the F-box subunit. However, it was possible that it did not need to be discharged from the F-box subunit to be degraded, the F-box subunit and the substrate might go to the proteasome as a complex.

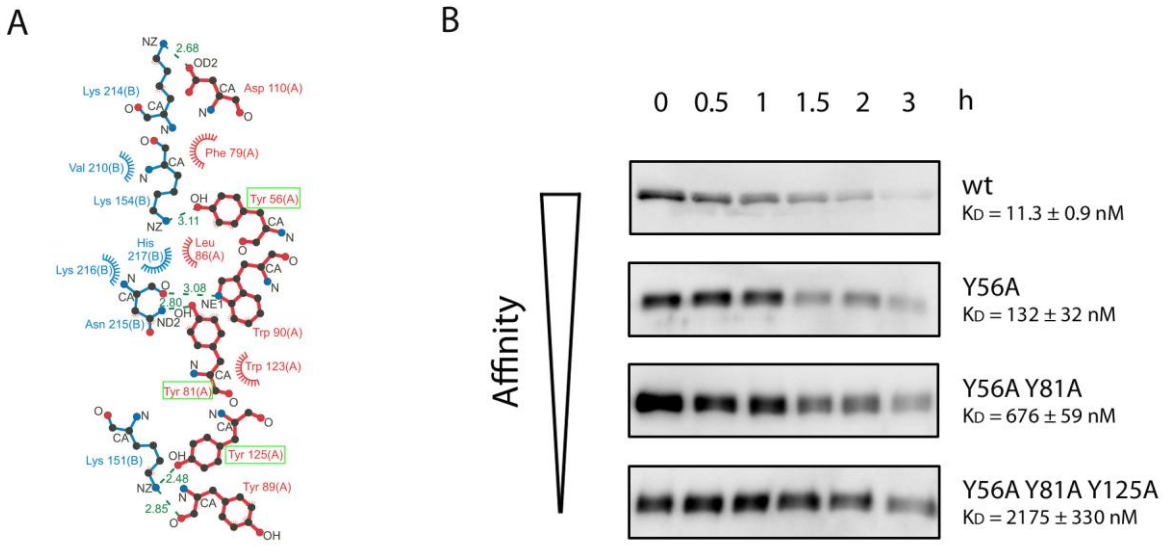

Figure 15: Affinity engineering of the chimeric F-box protein cdc4_5GS_off7. A: Representation of the interaction between MBP (blue) and off7 (red). H bonds are shown in dark green and the mutated residues are boxed in light green. B: MBP-GFP stability in the presence of cdc4_5GS_off7 affinity mutants. MGgF75Ga, MGgF7'5Ga, MGgF7''5Ga and MGgF7'''5Ga cells (see material & methods) were grown in a synthetic raffinose based medium to an OD_{600} of 0.6-0.8. MBP expression was induced for 1 h with galactose and stopped with glucose. Samples were withdrawn at the indicated time points. Total protein was extracted and samples normalized according to their OD_{600} before being subjected to SDS-PAGE. The levels of MBP were detected by immunoblotting with the anti-RGS(His)$_4$ antibody.

Chimeric F-box protein stability

The chimeric F-box protein had already been observed during the first co-expression experiments to be unstable (Fig. 6). To investigate if it was co-degraded with the target protein by the proteasome, its stability was assessed using a modified experimental set-up 1. cdc4_5GS_off7 was expressed on p415Gal for 1 h 30 min, alone or in a strain constitutively expressing MBP-GFP. After Gal1 promoter shut-off, stability of the chimeric F-box protein was followed in the absence or presence of MBP-GFP. In both cases, the chimeric F-box protein was unstable and its half-life was even extended in the presence of the target protein: $t_{½} \leq 60$ min vs. $60 < t_{½} < 120$ min (Fig. 16A). Similar results were obtained for cdc4_5GS_3a whose stability was monitored in the absence or presence of APH-GFP (Fig. 16B).

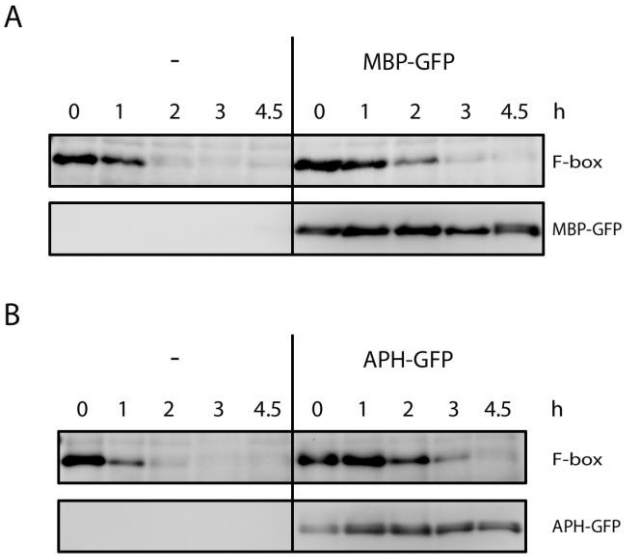

Figure 16: Chimeric F-box protein stability in absence or presence of target protein. A: cdc4_5GS_off7 stability was monitored in F75Gg or MGaF75Gg cells (see material & methods) constitutively expressing MBP-GFP. B: cdc4_5GS_3a stability was monitored in F35Gg or AGaF35Gg cells (see material & methods) constitutively expressing APH-GFP. A, B: Cells were grown in a synthetic raffinose based medium to an OD_{600} of 0.6-0.8. Chimeric F-box protein expression was induced for 1 h 30 min with galactose and stopped with glucose. Samples were withdrawn at the indicated time points. Total protein was extracted and samples normalized according to their OD_{600} before being subjected to SDS-PAGE. Chimeric F-box proteins were detected by immunoblotting with the anti-HA antibody and target proteins (MBP-GFP and APH-GFP) with the anti-RGS(His)$_4$ antibody.

The chimeric F-box protein was observed to be constantly degraded, in absence or presence of the target protein. Cdc4 was reported to be intrisincally unstable; its half-life was estimated according to the study to be 5 or 15 min [43, 44]. Like several other F-box proteins, it was reported to autoubiquitinate itself and be degraded by the proteasome. The chimeric F-box protein might have conserved this characteristic. In order to see if any ubiquitinated form of the chimeric F-box protein could be detected, cdc4_5GS_off7 was immunoprecipitated using an anti-HA antibody. However, no higher molecular weight species were observed when probing the immunoprecipitated samples with the anti-HA or anti-ubiquitin antibodies (Fig. 17A,B). Only the interaction with the target protein in vivo was confirmed a second time, as MBP was co-immunoprecipitated, it ran at 46 kDa. (Fig. 17C). An additional species co-eluting with cdc4_5GS_off7 at 66 kDa also reacted with the anti-RGS(His)$_4$

antibody. However, it did not correspond to any form of ubiquitylated MBP, as it was not detected by the anti-ubiquitin antibody.

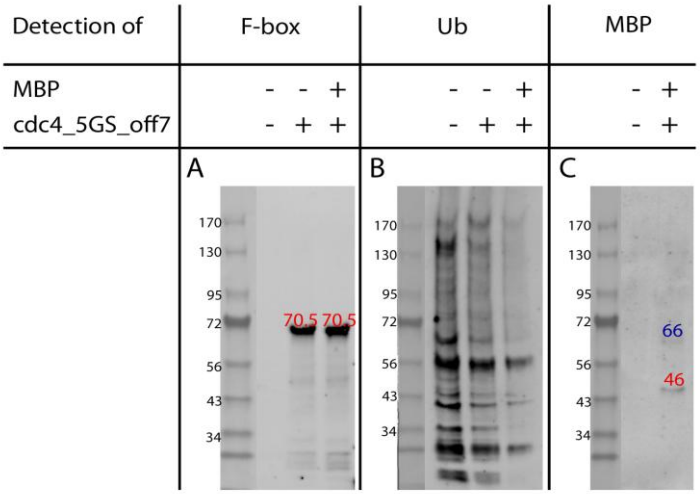

Figure 17: cdc4_5GS_off7 immunoprecipitation. cdc4_5GS_off7 was expressed in F75Ga cells or MgF75Ga cells with the target protein MBP (see material & methods). It was immunoprecipitated with an anti-HA antibody. The eluted fractions were detected with the anti-HA antibody (A), the anti-ubiquitin antibody (B) and the anti-RGS(His)$_4$ antibody (C). A: The anti-HA antibody recognized cdc4_5GS_off7 at 70.5 kDa B: the anti-ubiquitin antibody did not detect specific ubiquitinated forms of cdc4_5GS_off7. C: the anti-RGS(His)$_4$ antibody detected the target protein MBP at 46 kDa and a non-identified species at 66 kDa. The size marker is indicated in kDa.

Chimeric F-box protein overexpression

Since the chimeric F-box protein seems to be constantly degraded, we wondered if it would be possible to improve the degradation of the target protein by increasing the overall amount of available chimeric F-box protein. Three additional increasing levels of expression were tested by placing the cdc4_5GS_off7 coding sequence under the ADH promoter or the stronger TEF promoter in a centromeric (415 plasmid, one copy per cell) or 2 micron (425 plasmid, 10-30 copies per cell) plasmid [35]. Contrary to what might be expected, MBP-GFP degradation efficiency decreased as more and more cdc4_5GS_off7 was expressed (Fig. 18). The chimeric protein, when overexpressed, slowed down the target protein degradation.

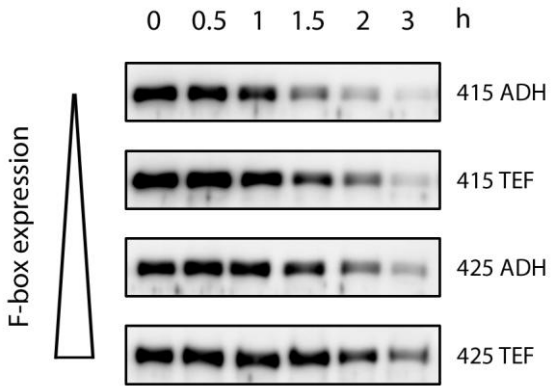

Figure 18: Stability of MBP-GFP co-expressed with increasing amounts of chimeric F-box protein. MGgF75Ga cells, MGgF75Gt cells, MGgF75Gaa cells and MGgF75Gtt cells were grown in a synthetic raffinose based medium to an OD_{600} of 0.6-0.8. MBP-GFP expression was induced for 1 h with galactose and stopped with glucose. Samples were withdrawn at the indicated time points. Total protein was extracted and samples normalized according to their OD_{600} before being subjected to SDS-PAGE. The levels of MBP-GFP were detected by immunoblotting with an anti-RGS(His)$_4$ antibody.

The N-terminal part of the chimeric F-box protein

The N-terminal part of cdc4, upstream of the F-box domain, was left intact for the construction of the chimeric F-box protein, its role being unclear. Cdc4 had been reported to be able to form homomultimers through this region, which also possessed dominant-negative activity [45]. It was unclear, however, if this region was positively or negatively regulating F-box protein activity. In order to estimate the importance of the N terminal part of cdc4 for our chimeric F-box protein, a truncated mutant of cdc4_5GS_off7 was generated by deleting the sequence lying upstream of the F-box domain (ΔN, deletion of aa 1-269). No difference was observed on MBP degradation with cdc4_5GS_off7 or cdc4_5GS_off7 ΔN (Fig. 19). The chimeric F-box, consisting of only the F–box domain, a linker and the substrate binding domain was fully functional to degrade the target protein.

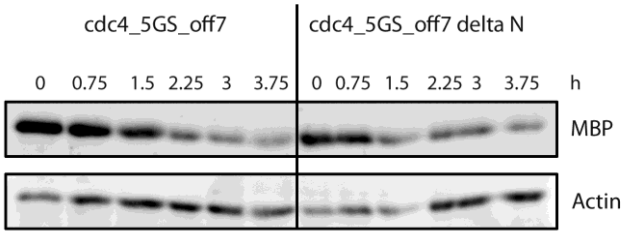

Figure 19: Stability of MBP co-expressed with a N-terminally truncated chimeric F-box protein. MgF75Ga cells and MgF7Δ5Ga cells (see material & methods) were grown in a synthetic raffinose based medium to an OD_{600} of 0.6-0.8. MBP expression was induced for 1 h with galactose and stopped with glucose. Samples were withdrawn at the indicated time points. Total protein was extracted and samples normalized according to their OD_{600} before being subjected to SDS-PAGE. The levels of MBP were detected by immunoblotting with an anti-RGS(His)$_4$ antibody. The actin signal was used as an internal loading control.

Chimeric F-box protein and substrate destabilization

Ubiquitin moieties are attached onto Lys residues. The efficiency of ubiquitylation must then rely on the availability of lysine residues in the target protein sequence. In order to increase the ubiquitylation probability, a tail of 5 lysine residues was fused to the C-terminus of the target protein MBP. Independently, the same lysine tail was also appended to the C-terminus of the chimeric F-box protein, cdc4_5GS_off7. If the F-box protein was degraded in complex with the substrate, increasing its own turnover could potentially help degrading more target protein as well. However, the addition of a lysine tail to the target protein did not improve its degradation, nor did the addition of the lysine tail to the chimeric F-box protein (Fig. 20).

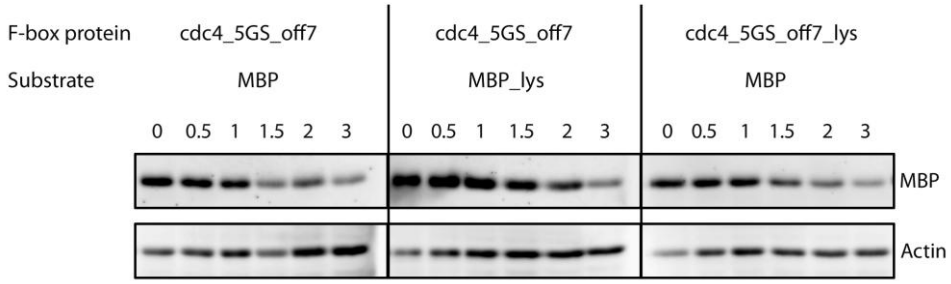

Figure 20: Addition of a lysine tail at the C-terminus of the target protein or the chimeric F-box protein. MgF75Ga cells, MLysgF75Ga cells and MgF7Lys5Ga cells (see material & methods) were grown in a synthetic raffinose based medium to an OD_{600} of 0.6-0.8. MBP or MBP_lys expression was induced for 1 h with galactose and stopped with glucose. Samples were withdrawn at the indicated time points. Total protein was extracted and samples normalized according to their OD_{600} before being subjected to SDS-PAGE. The levels of MBP and MBP_lys were detected by immunoblotting with the anti-RGS$(His)_4$ antibody. The actin signal was used as an internal loading control.

Discussion

S. cerevisiae SCF ^{cdc4} was used as framework for the engineering of an ubiquitin ligase with predefined specificity. A chimeric F-box protein was designed with new artificial substrate specificity using the cdc4 backbone and DARPin, a new binding scaffold, for replacing its original substrate binding domain. In order to investigate if it could function like a normal yeast F-box protein, it was co-expressed with a cognate target protein in *S. cerevisiae*. The target protein was significantly more unstable in the presence of the chimeric F-box protein. Its half-life was only 2- to 3-fold affected but this effect was specific. The target protein was indeed not destabilized by the presence of a chimeric F-box protein engineered with a non-specific DARPin moiety. MG132, a proteasome inhibitor, could partially stabilize it and demonstrated that the target protein was degraded by the 26S proteasome. The degradation process also relied on the SCF activity. The target protein was indeed less destabilized in the cdc53_1 and cdc34_2 thermosensitive strains than in the wt strain. No difference could be observed between the permissive and restrictive temperatures, but the lack of correct sample normalization because of the elongated shape of these mutant cells and the arrest in G1 which might have affected the OD_{600nm} measurements, prevented us to fairly compare the amount of target protein at both temperatures. Immunoprecipitations of the target protein were performed. The chimeric F-box protein was co-immunoprecipitated, proving that they interacted in vivo. However no ubiquitinated forms of the target protein could be revealed. It could be that once ubiquitinated, the target protein was quickly recognized by the proteasome and immediately deubiquitinated before being degraded. The ubiquitin moieties are indeed recycled by deubiquitinating enzymes residing close to or in the proteasome. In *S. cerevisiae*, the metalloprotease Rpn11 is a core structural component of the lid and has been seen to cleave substrate-linked chains at or near their base [46, 47]. This “en bloc“ chain removal resulted in the production of a prominent band of unmodified substrate. A fraction of target protein could also have been deubiquitinated before reaching the proteasome as deubiquitinating enzymes can also be found associated with E3 ligases, directly counteracting their activity [48]. However, even under denaturing conditions, when deubiquitinating enzymes should not have been active any more, no ubiquitinated target protein could be retrieved either. Despite the presence of several lysine residues at its surface, 10 whose surface availaibility was ≥ 40% and 10 whose surface availaibility was ≥ 30%, the exogenous target protein might also have been not very efficiently ubiquitylated (see discussion below). The use of overexpressed tagged ubiquitin instead of endogenous one might help detecting ubiquitinated species.

To summarize, we could not state that our target protein was directly targeted for degradation by ubiquitination, as we could not demonstrate the presence of ubiquitinated target protein by immunoprecipitation or subsequent mass spectroscopy. Nonetheless its degradation relied on its specific recognition by the chimeric F-box protein, a functional SCF complex, the activity of the E2 ubiquitin ligase and a proficient 26S proteasome. Further experiments were carried out, using chimeric F-box proteins as a tool and the target protein degradation assay as a read-out, to investigate the mechanism of natural F-box proteins.

SCF protein subunits fit together into a fairly rigid C-shaped conformation which allows substrate positioning in a 50-60 Å space between the ubiquitin conjugating enzyme (E2) on one end and the F-Box protein on the other end (Fig. 2) [17, 18, 21]. Structural and experimental data make it plausible that this large space is a kind of "hot zone" with a maximal ubiquitin transfer occurring for the substrate lysine residues lying next to the E2 active site. The linker between the F-box domain and the substrate binding domain seemed critical for the native cdc4 function; it is a stiff helix which is conserved throughout evolution as revealed by several F-box proteins structures [17, 18, 20, 21]. It forms a stalk-like structure which projects the WD40 domain away from skp1 and is thought to optimally place the substrate in the vicinity of the E2 active site. To probe the importance of orientation and rigidity in this domain, F-box proteins were designed with either a rigid linker (3, 10 or 17 Alanine residues (ala)) which would position the substrate identically to the original one or a flexible one (5, 10 or 15 total Glycine and Serine residues (GS)). In all cases, the target protein could be degraded, however to a varying extent. In general, short linkers seemed to be more efficient than long ones, the 5GS one being slightly superior to the 3ala one. The longer ones might have positioned the target protein partially outside of the "hot zone". No dramatic difference was observed between the rigid and flexible linker. It is possible that our model for the designed ala helix was not fully accurate and did not position the substrate correctly as it was meant to, or that the rigid linkers were by themselves not as rigid as presumed. Nevertheless, it appeared that the substrate did not need to be presented in a rigid mode and specified orientation to the E2 to be degraded. Orlicky et al. had observed that cdc4 function was sensitive to the insertion of helix-detabilizing residues or additional alanine residues into the stalk [18]. These mutations disrupted the original linker structure, but positioned the substrate in a different orientation from the original one without enabling it to move. In our model, the substrate when bound to the chimeric F-box protein designed with a flexible linker was instead allowed to be in motion in the "hot zone" and probe the vicinity of the E2. Nature might have evolved the chimeric F-box proteins to bind and hold their specific substrates in a defined way to increase the concentration of the substrate lysines at the E2 active site. The ubiquitination rate seems indeed to correlate with the spacing between the substrate Lys and the E2 catalytic site [17]. However for a non-optimally presented substrate, the E2 if functioning according to the "Hit and Run" model, could "sample" the substrate surface and collide with exposed lysines. The working mechanism of E2 is not well understood but the ubiquitin-charged Cdc34 (cdc34~Ub) has been observed in dynamic binding equilibrium with SCF^{cdc4} [26]. It was then proposed that cdc34~Ub could bind to the RING domain, be released in close proximity of the substrate and diffuse in the hot zone until it finds one of its Lys residues. This repetitive "Hit and Run" mechanism could ensure certain flexibility in selection of target lysines, as seen on natural SCF substrates which can be modified on multiple lysines [49], and accommodates the synthesis of multi-ubiquitin chains. Nevertheless, the ubiquitylation efficiency is most likely superior when performed onto optimally pre-positioned lysines, especially as the attachment of the first ubiquitin molecule was shown to be the rate limiting step in the multi-ubiquitin chain assembly [16]. In the case described here, the target protein ubiquitination was most likely not optimal as it did not yield detectable amounts of ubiquitinated products but seemed to be enough to trigger degradation.

After probing the importance of structural integrity of the chimeric F-box protein, we tried to determine its optimal binding strength to the target protein which would achieve a productive substrate recruitment within the SCF complex and a reasonable discharge to interact with the proteasome. Cdc4 has been described to interact with its specific substrate Sic1 with a K_D of 250 nM [50]. A mammalian homolog, the F-box protein β-TrCP 1, binds to its substrates β-catenin and IκBα with similar K_D, in the 500 nM range [17]. It is not known how the substrate, once ubiquitinated, leaves the SCF complex. DARPins have been evolved to high affinity (low nM range) and the target proteins release might be hindered by the binding strength of our artificial substrate binding domain. Site directed mutagenesis was used to gradually decrease the binding affinity of the chimeric F-box protein cdc4_5GS_off7. The degradation efficiency linearly decreased in parallel with the binding affinity. This confirmed the dependence of the degradation process on the specific interaction with the chimeric F-box protein and did not reveal any other binding affinity optimum between 11 nM and 2 μm. The target protein degradation seemed to depend only on the efficiency of the substrate recruitment and not on a fast dissociation rate which would also allow releasing the substrate from the chimeric F-box binding domain. These results led us to think that the substrate was most likely discharged as a complex with the F-box subunit, from the SCF machinery.

Zhou & Howley had previously proposed that F box receptors and their bound substrates were degraded as a unit to ensure a continuous recycling of the SCF holocomplex and permit it to assemble with other F box receptor subunits [43]. The chimeric F-box protein had at the beginning of our study been observed to be unstable when co-expressed with the target protein. If it was co-degraded with the target protein, stabilization might occur in absence of the target protein. However it was not observed. Instead, the chimeric F-box protein was also unstable when expressed alone. The original cdc4 protein, like other F-box protein, is degraded by the proteasome [24, 43, 44]. It gets ubiquitinated within its own SCF complex in an autocatalytic manner. This mechanism may allow rapid switching of F-box protein subunits and dynamically regulate the equilibrium between multiple SCF complexes. We looked for ubiquitinated forms of the chimeric F-box protein but could not detect any. It should be noted that ubiquitinated cdc4 could be readily observed by Galan et al. but Grr1p, another yeast F-box protein shown to autoubiquitinate, could only be accumulated in an ubiquitinated form using a dominant-negative ubiquitin which prevented its degradation [44]. The incapacity to retrieve ubiquitinated form and the longer half-life of our chimeric F-box protein compared to wt cdc4 might suggest a decreased autoubiquitination. Furthermore, some F-box proteins seemed to be more poorly ubiquitinated than others [24]. Noteworthy, the chimeric F-box protein was less unstable when co-expressed with the target protein. A similar observation has been made for HOS, the human homolog of the drosophila Slimb F-box protein, which was protected from autoubiquitination and degradation in presence of its substrate IκBα [51]. Deshaies suggested that a substrate would shield the F-box protein from the core components of the SCF, thus protecting it from autoubiquitination and stabilize it [52]. If a given F-box protein were synthesized in excess, its levels would be quickly pared down to match substrate demand. Our data do not fully agree with this model. In our experimental set-up, the target protein was present in excess amount and it slowed down the degradation process of the chimeric F-box protein but it did not prevent it. In parallel, when the chimeric F-box protein expression level was progressively elevated, it gradually decreased the degradation of the target protein. This effect would speak in favor of inhibition per competition, either at the SCF assembly or proteasomal degradation level. Indeed the F-box protein can assemble with the SCF machinery either alone or bound to the target protein. If the amount of chimeric F-box protein augments and exceeds the target protein one, the pool of free chimeric F-box protein will

increasingly compete for skp1 binding and subsequent SCF assembly and ubiquitination. Another possibility would be that the larger amount of free autoubiquitinated chimeric F-box protein would "jam" the 26S proteasome and reduce the degradation efficiency of other substrates, like the target protein. Either one or both of these models could apply to our experimental data, which show that increasing the amount of F-box protein might not be the solution to enhance substrate degradation. We thus propose a third model for the F-box protein level regulation mechanism. In presence of substrate, the F-box protein binds to it, assembles with the SCF holoenzyme. The substrate is ubiquitinated, the complex of F-box protein and ubiquitinated substrate is released from the SCF machinery and co-degraded. In the absence of substrate, the F-box protein assembles with the SCF holoenzyme. It gets autoubiquitinated, leaves the SCF machinery and is degraded alone. In this model, the F-box protein would be constantly degraded, alone or in complex with its substrate and in all cases travelling to the proteasome with the same rate. We therefore suggest that the stabilization effect of the substrate on the F-box protein half-life would result from the deceleration of the 26S proteasome activity when it processes the F-box protein and the substrate compared to the F-box protein alone. It is indeed plausible that preparation by the 19S and degradation of two polypeptidic chains by the 20S might require more time than for one substrate.

The importance of the N-terminal domain of the F-box protein for its activity was also investigated. The impossibility to crystallize any of the F-box protein unless it was truncated for its N-terminal region prevented us to have insight into its function. Overproduction of polypeptides corresponding to the N-terminal region of cdc4 inhibited SCF^{cdc4} in vivo [45]. cdc4 was shown to homomultimerize through its amino terminus and the dominant negative activity of the N-terminal peptides correlated to their ability to associate with full-length cdc4. A similar observation was made for another F-box protein, Met30. It was thus uncertain if F-box protein multimerization was necessary for their function or could even have an inhibitory effect. The N-terminal region, lying upstream of the F-box protein, was deleted in our chimeric F-box protein. This deletion did not affect its function, as the target protein was degraded at the same rate by both the wt and mutant chimeric F-box proteins. The N-terminal part was thus not needed for the activity of the chimeric F-box protein. Meanwhile, Tang et al further characterized the dimerization domain (D domain) of cdc4 and determined its structure [50]. Their biochemical data suggested that dimerization of cdc4 was required in vivo. In vitro, a monomeric SCF^{cdc4} was deficient in ubiquitin chain initiation and especially elongation of its substrate sic1. SCF^{cdc4} dimerization was, however, not required when sic1 was modified to contain only one high-affinity phosphodegron, binding to the WD40 domain, and was thus bound in only one position. The target protein MBP would be a similar substrate, as it is bound by off7 in a unique configuration. A model of the dimeric holo-SCF^{cdc4} complex based on small-angle X-ray scatter measurements (Fig. 21) revealed that the D domain orients the substrate binding site and E2 binding site of each SCF protomer in a suprafacial configuration, in which cdc4 WD40 domain and E2 catalytic sites lie in the same plane with a separation of 64 Å within and 102 Å between each SCF monomer. The authors suggested that this spatial variability may facilitate lysine acceptor site utilization in both bound substrates and the elongating ubiquitin chain. Similar observations were made for Fbw7, the human homolog of cdc4, which was required to dimerize for the regulation of certain weak interacting substrates [53]. The dimerization ability of the chimeric F-box protein was not tested so it cannot be stated that it could support such a supra-complex but the new substrate binding domain could fit in the structural model of the dimeric holo-SCF^{cdc4} complex.

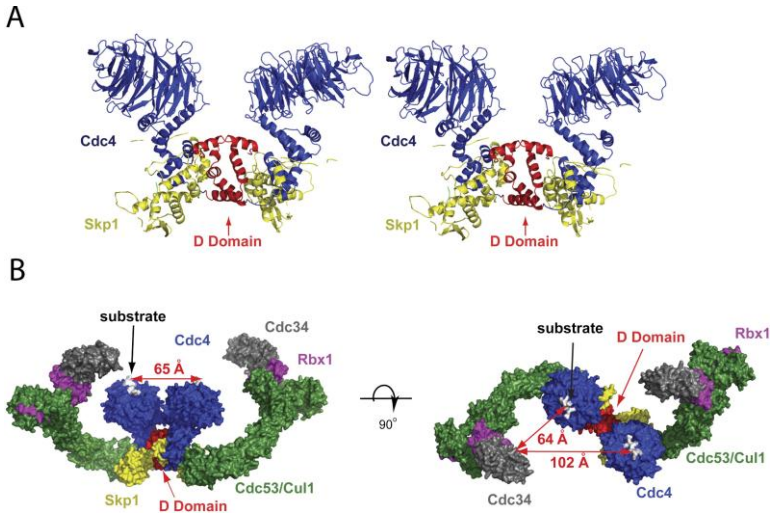

Figure 21: Model of the dimeric SCF cdc4 complex determined by SAXS in solution. A: Stereo ribbons representation of the SAXS solution-based model of the dimeric skp1-cdc4 222-744 subcomplex. B: Space-filling representation of the dimeric SCF cdc4 complex. Calculated distances between substrate-binding sites and catalytic sites are shown. Adapted from Tang et al, 2007 [50].

The use of a chimeric F-box protein allowed us to have better insights into the mechanism of F-box proteins. The availability of a new substrate binding domain which could be stable in vivo enabled us to design chimeric F-box proteins capable of recognizing new substrates. The domains of a chimeric F-box protein could be dissected without interfering with the cell's metabolism and without inducing toxicity. The collected data could, however, not be exploited to dramatically increase the target protein's turnover. As the ubiquitination process seemed most likely to be the limiting step, we also tried to increase lysine availability in our target protein by fusing a lysine residues tail at its C-terminus but this attempt stayed unsuccessful. The presence of additional lysine residues scattered onto the target protein's surface might have been more optimal. However, if the efficiency of the ubiquitination reaction relies on the dynamic interaction of SCF components, the substrate and E2, all assembled in a supra-complex, it is reasonable to think that not all target proteins will be ubiquitinated with the same efficacy. This fine-tuning of supra-complex subunits interplay could be an additional quality control mechanism meant to further regulate the degradation of appropriate substrates only.

The use of tailored F-box proteins is appealing for creating protein knock-out. A similar strategy, based on the fusion of a peptide binding motif to the human F-box protein β-TrCP1 was already successful but has been applied so far to few proteins only [54-59]. This could undoubtedly be due to the lack of known peptide binding motifs or the requirement of other factors inherent to the target proteins. The use of a generalizable binding domain, like DARPins, would broaden the spectrum of targets and enable us to further analyze the characteristics of a proficient SCF substrate.

Annex

Vector maps

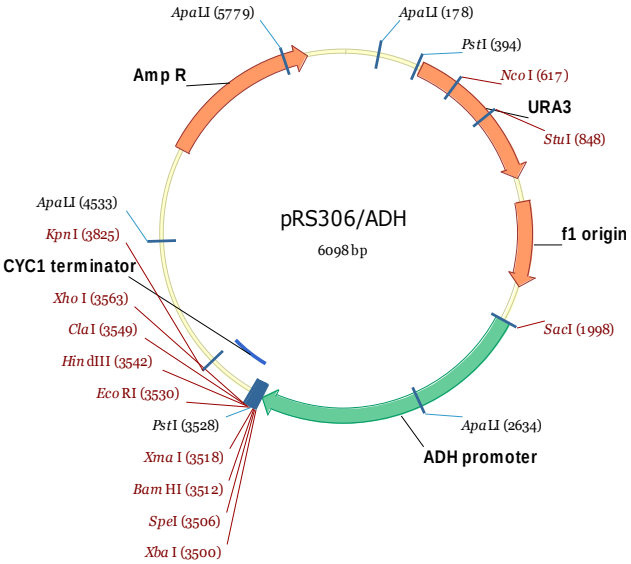

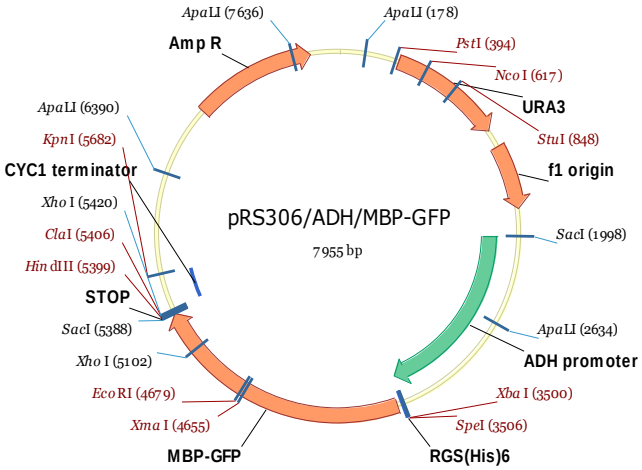

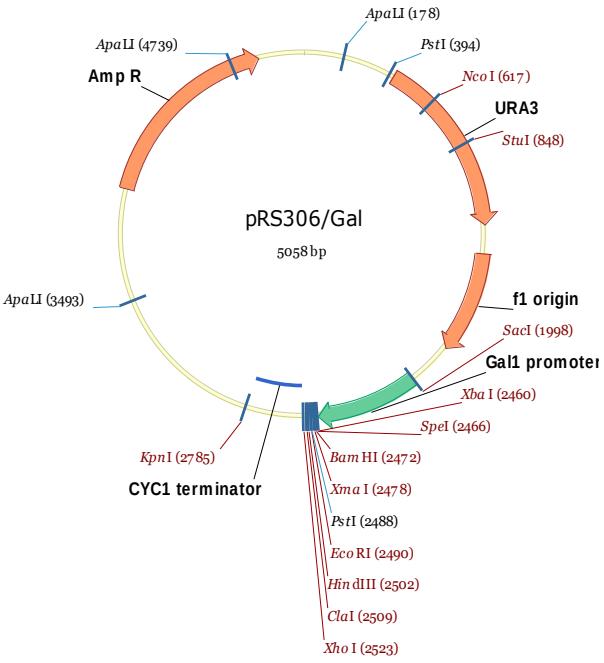

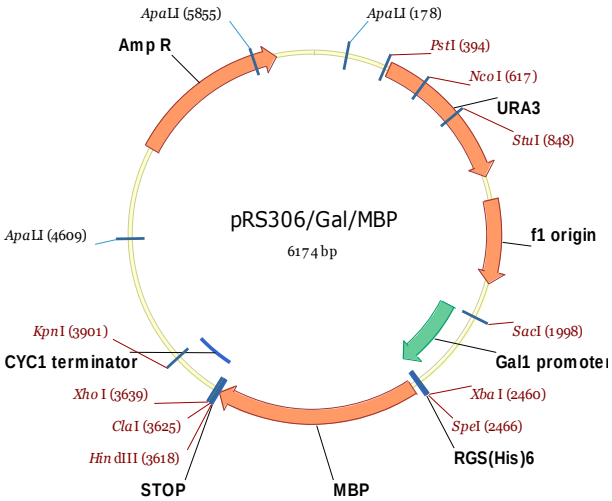

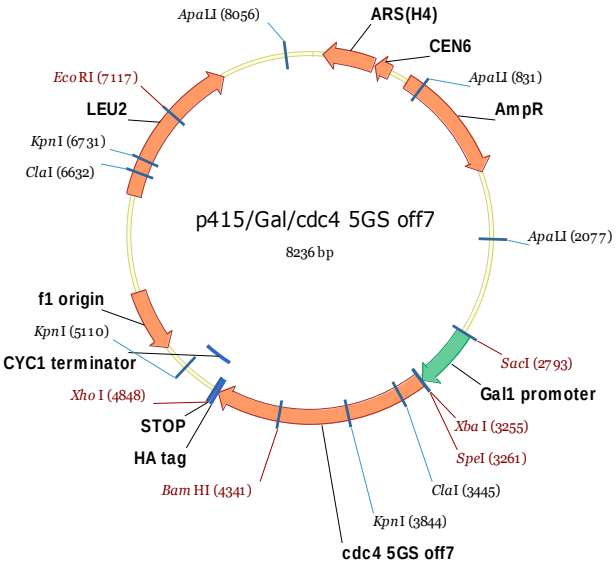
p415/Gal/cdc4 5GS off7
8236 bp
ApaLI (8056)
ARS(H4)
CEN6
ApaLI (831)
AmpR
ApaLI (2077)
SacI (2793)
Gal1 promoter
XbaI (3255)
SpeI (3261)
ClaI (3445)
KpnI (3844)
cdc4 5GS off7
BamHI (4341)
HA tag
STOP
XhoI (4848)
CYC1 terminator
KpnI (5110)
f1 origin
LEU2
EcoRI (7117)
KpnI (6731)
ClaI (6632)

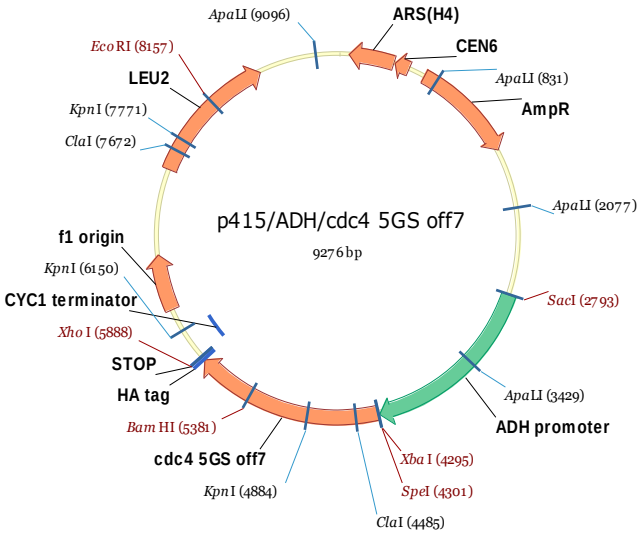
p415/ADH/cdc4 5GS off7
9276 bp
ApaLI (9096)
ARS(H4)
CEN6
ApaLI (831)
AmpR
ApaLI (2077)
SacI (2793)
ApaLI (3429)
ADH promoter
XbaI (4295)
SpeI (4301)
ClaI (4485)
KpnI (4884)
cdc4 5GS off7
BamHI (5381)
HA tag
STOP
XhoI (5888)
CYC1 terminator
KpnI (6150)
f1 origin
LEU2
EcoRI (8157)
KpnI (7771)
ClaI (7672)

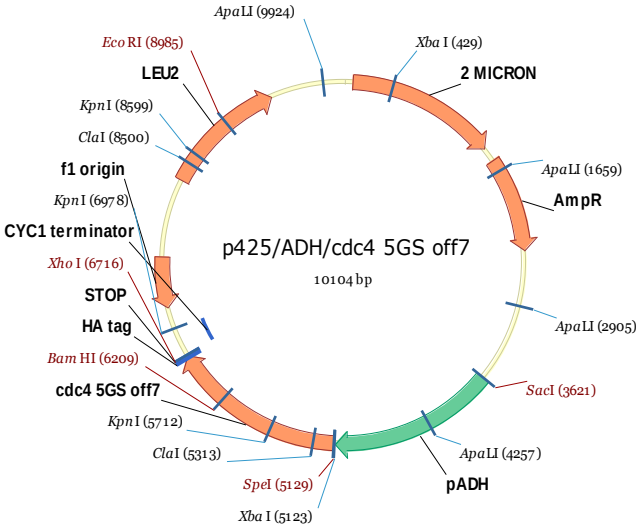
p425/ADH/cdc4 5GS off7
10104 bp
ApaLI (9924)
XbaI (429)
2 MICRON
ApaLI (1659)
AmpR
ApaLI (2905)
SacI (3621)
ApaLI (4257)
pADH
XbaI (5123)
SpeI (5129)
ClaI (5313)
KpnI (5712)
cdc4 5GS off7
BamHI (6209)
HA tag
STOP
XhoI (6716)
CYC1 terminator
KpnI (6978)
f1 origin
LEU2
EcoRI (8985)
KpnI (8599)
ClaI (8500)

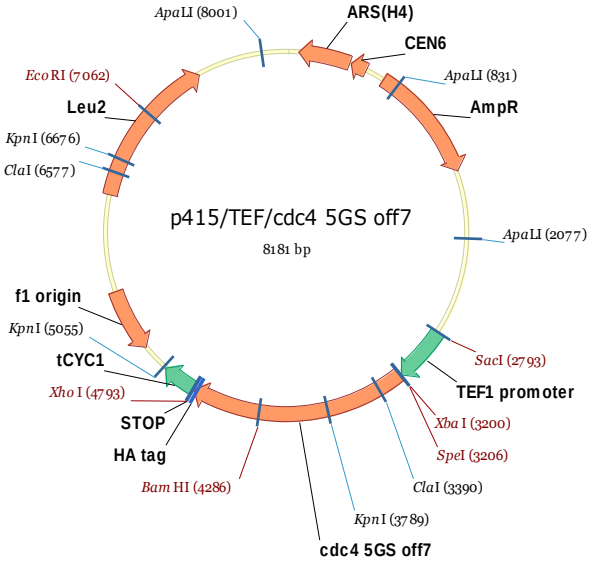
p415/TEF/cdc4 5GS off7
8181 bp
ApaLI (8001)
ARS(H4)
CEN6
ApaLI (831)
AmpR
ApaLI (2077)
SacI (2793)
TEF1 promoter
XbaI (3200)
SpeI (3206)
ClaI (3390)
KpnI (3789)
cdc4 5GS off7
BamHI (4286)
HA tag
STOP
XhoI (4793)
tCYC1
KpnI (5055)
f1 origin
Leu2
EcoRI (7062)
KpnI (6676)
ClaI (6577)

Construct DNA and amino-acid sequences

RGS(His)$_6$MBP-GFP construct DNA sequence

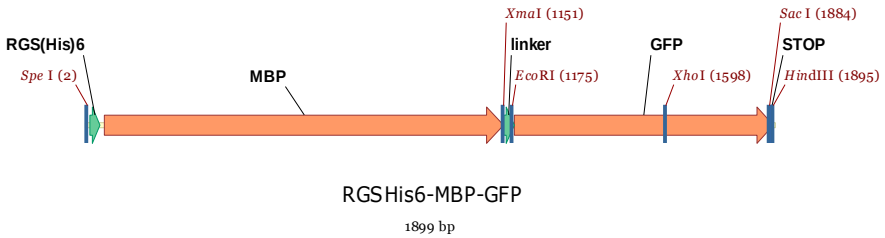

actagtatgagaggatcgcatcaccatcaccatcacggatctggttccatgaaaactgaagaaggtaaactggtaatctggattaacggcgataa
aggctataacggtctcgctgaagtcggtaagaaattcgagaaagataccggaattaaagtcaccgttgagcatccggataaactggaagagaa
attcccacaggttgcggcaactggcgatggccctgacattatcttctgggcacacgaccgctttggtggctacgctcaatctggcctgttggctgaa
atcaccccggacaaagcgttccaggacaagctgtatccgtttacctgggatgccgtacgttacaacggcaagctgattgcttacccgatcgctgtt
gaagcgttatcgctgatttataacaaagatctgctgccgaacccgccaaaaacctgggaagagatcccggcgctggataaagaactgaaagcg
aaaggtaagagcgcgctgatgttcaacctgcaagaaccgtacttcacctggccgctgattgctgctgacgggggttatgcgttcaagtatgaaaa
cggcaagtacgacattaaagacgtgggcgtggataacgctggcgcgaaagcgggtctgaccttcctggttgacctgattaaaaacaaacacatg
aatgcagacaccgattactccatcgcagaagctgcctttaataaaggcgaaacagcgatgaccatcaacggcccgtgggcatggtccaacatcg
acaccagcaaagtgaattatggtgtaacggtactgccgaccttcaagggtcaaccatccaaaccgttcgttggcgtgctgagcgcaggtattaac
gccgccagtccgaacaaagagctggcaaaagagttcctcgaaaactatctgctgactgatgaaggtctggaagcggttaataaagacaaaccg
ctgggtgccgtagcgctgaagtcttacgaggaagagttggcgaaagatccacgtattgccgccactatggaaaacgcccagaaaggtgaaatca
tgccgaacatcccgcagatgtccgctttctggtatgccgtgcgtactgcggtgatcaacgccgccagcggtcgtcagactgtcgatgaagccctga
aagacgcgcagactcccgggtccgctgctggttctggcgaattcagcaaaggagaagaacttttcactggagttgtcccaattcttgttgaattag
atggtgatgttaatgggcacaaattttctgtcagtggagagggtgaaggtgatgctacatacggaaaactcacccttaaatttatttgcactactg
gaaaactacctgttccttggccaacacttgtcactactctgacctatggtgttcaatgcttttcccgttatccggatcacatgaaacggcatgacttt
tcaagagtgccatgcccgaaggttatgtacaggaacgcactatatctttcaaagatgacgggaactacaagacgcgtgctgaagtcaagtttgaa
ggtgataccttgttaatcgtatcgagttaaagggtattgattttaaagaagatggaaacattctcggacacaaactcgagtacaactataactca
cacaatgtatacatcacggcagacaaacaaaagaatggaatcaaagctaacttcaaaattcgccacaacattgaagatggttccgttcaactag
cagaccattatcaacaaaatactccaattggcgatggccctgtccttttaccagacaaccattacctgtcgacacaatctgccctttcgaaagatcc
caacgaaaagcgtgaccacatggtccttcttgagtttgtaactgctgctgggattacacatggcatggatgagctctacaaataaaagctt

RGS(His)$_6$MBP-GFP amino-acid sequence

MRGSHHHHHHGSGSMKTEEGKLVIWINGDKGYNGLAEVGKKFEKDTGIKVTVEHPDKLEEKFPQVAATGDGPDII
FWAHDRFGGYAQSGLLAEITPDKAFQDKLYPFTWDAVRYNGKLIAYPIAVEALSLIYNKDLLPNPPKTWEEIPALDKE
LKAKGKSALMFNLQEPYFTWPLIAADGGYAFKYENGKYDIKDVGVDNAGAKAGLTFLVDLIKNKHMNADTDYSIAE
AAFNKGETAMTINGPWAWSNIDTSKVNYGVTVLPTFKGQPSKPFVGVLSAGINAASPNKELAKEFLENYLLTDEGL
EAVNKDKPLGAVALKSYEEELAKDPRIAATMENAQKGEIMPNIPQMSAFWYAVRTAVINAASGRQTVDEALKDAQ
TPGSAAGSGEFSKGEELFTGVVPILVELDGDVNGHKFSVSGEGEGDATYGKLTLKFICTTGKLPVPWPTLVTTLTYGV
QCFSRYPDHMKRHDFFKSAMPEGYVQERTISFKDDGNYKTRAEVKFEGDTLVNRIELKGIDFKEDGNILGHKLEYNY
NSHNVYITADKQKNGIKANFKIRHNIEDGSVQLADHYQQNTPIGDGPVLLPDNHYLSTQSALSKDPNEKRDHMVLL
EFVTAAGITHGMDELYK

RGS(His)$_6$MBP construct DNA sequence

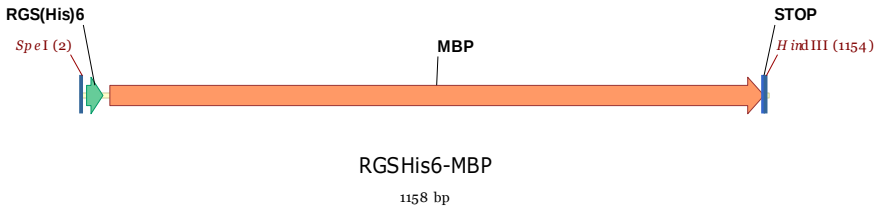

Actagtatgagaggatcgcatcaccatcaccatcacggatctggttccatgaaaactgaagaaggtaaactggtaatctggattaacggcgata
aaggctataacggtctcgctgaagtcggtaagaaattcgagaaagataccggaattaaagtcaccgttgagcatccggataaactggaagaga
aattcccacaggttgcggcaactggcgatggccctgacattatcttctgggcacacgaccgctttggtggctacgctcaatctggcctgttggctga
aatcaccccggacaaagcgttccaggacaagctgtatccgtttacctgggatgccgtacgttacaacggcaagctgattgcttacccgatcgctgt
tgaagcgttatcgctgatttataacaaagatctgctgccgaacccgccaaaaacctgggaagagatcccggcgctggataaagaactgaaagcg
aaaggtaagagcgcgctgatgttcaacctgcaagaaccgtacttcacctggccgctgattgctgctgacggggttatgcgttcaagtatgaaaa
cggcaagtacgacattaaagacgtgggcgtggataacgctggcgcgaaagcgggtctgaccttcctggttgacctgattaaaaacaaacacatg
aatgcagacaccgattactccatcgcagaagctgcctttaataaaggcgaaacagcgatgaccatcaacggcccgtgggcatggtccaacatcg
acaccagcaaagtgaattatggtgtaacggtactgccgaccttcaagggtcaaccatccaaaccgttcgttggcgtgctgagcgcaggtattaac
gccgccagtccgaacaaagagctggcaaaagagttcctcgaaaactatctgctgactgatgaaggtctggaagcggttaataaagacaaaccg
ctgggtgccgtagcgctgaagtcttacgaggaagagttggcgaaagatccacgtattgccgccactatggaaaacgcccagaaaggtgaaatca
tgccgaacatcccgcagatgtccgctttctggtatgccgtgcgtactgcggtgatcaacgccgccagcggtcgtcagactgtcgatgaagccctga
aagacgcgcagacttaaaagctt

RGS(His)$_6$MBP amino-acid sequence

MRGSHHHHHHGSGSMKTEEGKLVIWINGDKGYNGLAEVGKKFEKDTGIKVTVEHPDKLEEKFPQVAATGDGPDII
FWAHDRFGGYAQSGLLAEITPDKAFQDKLYPFTWDAVRYNGKLIAYPIAVEALSLIYNKDLLPNPPKTWEEIPALDKE
LKAKGKSALMFNLQEPYFTWPLIAADGGYAFKYENGKYDIKDVGVDNAGAKAGLTFLVDLIKNKHMNADTDYSIAE
AAFNKGETAMTINGPWAWSNIDTSKVNYGVTVLPTFKGQPSKPFVGVLSAGINAASPNKELAKEFLENYLLTDEGL
EAVNKDKPLGAVALKSYEEELAKDPRIAATMENAQKGEIMPNIPQMSAFWYAVRTAVINAASGRQTVDEALKDAQ
T

Cdc4_5GS_off7 construct DNA sequence

actagtatggggtcgtttcccttagctgagtttccattacgtgatatccctgttccttatagctaccgtgtgtctggcggtatagcttcctcaggtagtg
ttactgcgcttgttactgccgctggcactcatcgaaactcgtccacggctaagacagttgagacagaggacggcgaagaagatatcgatgagtat
cagaggaaaagagcagctggtcctggcgaatccactcctgaacgcagtagtttcgccgcggtagcacatgataatcacaaaaccctccatccag
ttaacttacagaacaccggtgcagcgtctgtggataacgacggtctgcacaatttaacagatatatccaacgatgcagaaaaactttgatgtctg
tggatgatggttctgccgcaccttctacattgagtgtaaacatgggagtggcatctcataatgttgctgctcccactaccgtcaatgcggcaacaat
aactggcagtgatgttagtaacaatgttaatagtgctactattaacaatcctatggaggaaggagcgctgccgttatcacccactgcttcctctcca

ggtaccacaactcctttagctaaaactacgaaaactatcaacaacaataataatatcgccgatttgatagaatccaaagattctataatctcccct
gaataccttttctgatgagattttcagcgcaataaacaataatctccctcacgcatacttcaaaaatttattatttagattagttgccaacatggatag
gagtgaactatccgacttggggactttaatcaaggataatttaaagagggacctaataacgtctttgccttttgaaataagtttgaaaattttcaat
tatttgcaattcgaggatattataaattcccttggggtctcccaaaattggaacaaaataattagaaaatctacatcgttgtggaaaaaacttctga
tatcggaaaattttgtgagcccaaagggttttaattctctcaatctcaaactctcccaaaaatacccaaaactctcacaacaagatcgccttagatt
atcttttctggagaatggatccggctcgggcgacctgggtaagaaactgctggaagctgctcgtgctggtcaggacgacgaagttcgtatcctgat
ggctaacggtgctgacgttaatgctgctgacaatactggtactactccgctgcacctggctgcttattctggtcacctggaaatcgttgaagttctgc
tgaagcacggtgctgacgttgacgcttctgacgtttttggttatactccgctgcacctggctgcttattggggtcacctggaaatcgttgaagttctg
ctgaagaacggtgctgacgttaacgctatggactctgatggtatgactccactgcacctggctgctaagtggggttacctggaaatcgttgaagtt
ctgctgaagcacggtgctgacgttaacgctcaggacaaattcggtaagaccgctttcgacatctccatcgacaacggtaacgaggacctggctga
aatcctgcaatacccatacgatgttccagattacgcttaactcgag

cdc4_5GS_off7 amino-acid sequence (5 GS linker underlined)

MGSFPLAEFPLRDIPVPYSYRVSGGIASSGSVTALVTAAGTHRNSSTAKTVETEDGEEDIDEYQRKRAAGPGESTPER
SSFAAVAHDNHKTLHPVNLQNTGAASVDNDGLHNLTDISNDAEKLLMSVDDGSAAPSTLSVNMGVASHNVAAPT
TVNAATITGSDVSNNVNSATINNPMEEGALPLSPTASSPGTTTPLAKTTKTINNNNNIADLIESKDSIISPEYLSDEIFSA
INNNLPHAYFKNLLFRLVANMDRSELSDLGTLIKDNLKRDLITSLPFEISLKIFNYLQFEDIINSLGVSQNWNKIIRKSTSL
WKKLLISENFVSPKGFNSLNLKLSQKYPKLSQQDRLRLSFLENGSGSGDLGKKLLEAARAGQDDEVRILMANGADVN
AADNTGTTPLHLAAYSGHLEIVEVLLKHGADVDASDVFGYTPLHLAAYWGHLEIVEVLLKNGADVNAMDSDGMTP
LHLAAKWGYLEIVEVLLKHGADVNAQDKFGKTAFDISIDNGNEDLAEILQYPYDVPDYA

cdc4_10GS_off7 amino-acid sequence (10 GS linker underlined)

MGSFPLAEFPLRDIPVPYSYRVSGGIASSGSVTALVTAAGTHRNSSTAKTVETEDGEEDIDEYQRKRAAGPGESTPER
SSFAAVAHDNHKTLHPVNLQNTGAASVDNDGLHNLTDISNDAEKLLMSVDDGSAAPSTLSVNMGVASHNVAAPT
TVNAATITGSDVSNNVNSATINNPMEEGALPLSPTASSPGTTTPLAKTTKTINNNNNIADLIESKDSIISPEYLSDEIFSA
INNNLPHAYFKNLLFRLVANMDRSELSDLGTLIKDNLKRDLITSLPFEISLKIFNYLQFEDIINSLGVSQNWNKIIRKSTSL
WKKLLISENFVSPKGFNSLNLKLSQKYPKLSQQDRLRLSFLENGSGSSGSGSGDLGKKLLEAARAGQDDEVRILMAN
GADVNAADNTGTTPLHLAAYSGHLEIVEVLLKHGADVDASDVFGYTPLHLAAYWGHLEIVEVLLKNGADVNAMDS
DGMTPLHLAAKWGYLEIVEVLLKHGADVNAQDKFGKTAFDISIDNGNEDLAEILQYPYDVPDYA

cdc4_15GS_off7 amino-acid sequence (15 GS linker underlined)

MGSFPLAEFPLRDIPVPYSYRVSGGIASSGSVTALVTAAGTHRNSSTAKTVETEDGEEDIDEYQRKRAAGPGESTPER
SSFAAVAHDNHKTLHPVNLQNTGAASVDNDGLHNLTDISNDAEKLLMSVDDGSAAPSTLSVNMGVASHNVAAPT
TVNAATITGSDVSNNVNSATINNPMEEGALPLSPTASSPGTTTPLAKTTKTINNNNNIADLIESKDSIISPEYLSDEIFSA
INNNLPHAYFKNLLFRLVANMDRSELSDLGTLIKDNLKRDLITSLPFEISLKIFNYLQFEDIINSLGVSQNWNKIIRKSTSL
WKKLLISENFVSPKGFNSLNLKLSQKYPKLSQQDRLRLSFLENGSGSSGSGSSGSGSGDLGKKLLEAARAGQDDEVRI
LMANGADVNAADNTGTTPLHLAAYSGHLEIVEVLLKHGADVDASDVFGYTPLHLAAYWGHLEIVEVLLKNGADVN
AMDSDGMTPLHLAAKWGYLEIVEVLLKHGADVNAQDKFGKTAFDISIDNGNEDLAEILQYPYDVPDYA

Cdc4_3ala_off7 construct DNA sequence

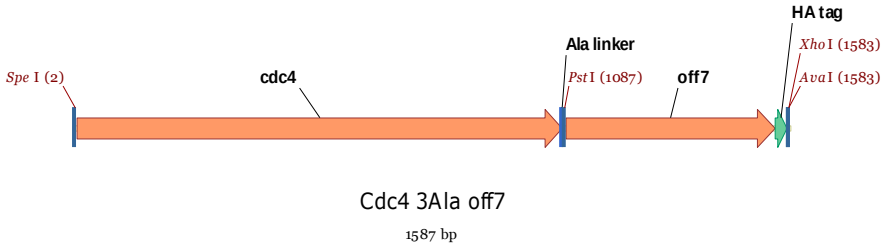

atggggtcgtttcccttagctgagtttccattacgtgatatccctgttccttatagctaccgtgtgtctggcggtatagcttcctcaggtagtgttactg
cgcttgttactgccgctggcactcatcgaaactcgtccacggctaagacagttgagacagaggacggcgaagaagatatcgatgagtatcagag
gaaaagagcagctggtcctggcgaatccactcctgaacgcagtagtttcgccgcggtagcacatgataatcacaaaaccctccatccagttaact
tacagaacaccggtgcagcgtctgtggataacgacggtctgcacaatttaacagatatatccaacgatgcagaaaaacttttgatgtctgtggat
gatggttctgccgcaccttctacattgagtgtaaacatgggagtggcatctcataatgttgctgctcccactaccgtcaatgcggcaacaataactg
gcagtgatgttagtaacaatgttaatagtgctactattaacaatcctatggaggaaggagcgctgccgttatcacccactgcttcctctccaggtac
cacaactcctttagctaaaactacgaaaactatcaacaacaataataatatcgccgatttgatagaatccaaagattctataatctcccctgaata
cctttctgatgagattttcagcgcaataaacaataatctccctcacgcatacttcaaaaatttattatttagattagttgccaacatggataggagtg
aactatccgacttggggactttaatcaaggataatttaaagagggacctaataacgtctttgccttttgaaataagtttgaaaattttcaattatttg
caattcgaggatattataaattcccttggggtctcccaaaattggaacaaaataattagaaaatctacatcgttgtggaaaaaacttctgatatcg
gaaaattttgtgagcccaaagggttttaattctctcaatctcaaactctcccaaaaatacccaaaactctcacaacaagatcgccttagattatctt
ttctggagaatgctgcagccgacctgggtaagaaactgctggaagctgctcgtgctggtcaggacgacgaagttcgtatcctgatggctaacggt
gctgacgttaatgctgctgacaatactggtactactccgctgcacctggctgcttattctggtcacctggaaatcgttgaagttctgctgaagcacg
gtgctgacgttgacgcttctgacgtttttggttatactccgctgcacctggctgcttattggggtcacctggaaatcgttgaagttctgctgaagaac
ggtgctgacgttaacgctatggactctgatggtatgactccactgcacctggctgctaagtggggttacctggaaatcgttgaagttctgctgaagc
acggtgctgacgttaacgctcaggacaaattcggtaagaccgctttcgacatctccatcgacaacggtaacgaggacctggctgaaatcctgcaa
tacccatacgatgttccagattacgcttaa

cdc4_3ala_off7 amino-acid sequence (3 ala linker underlined)

MGSFPLAEFPLRDIPVPYSYRVSGGIASSGSVTALVTAAGTHRNSSTAKTVETEDGEEDIDEYQRKRAAGPGESTPER
SSFAAVAHDNHKTLHPVNLQNTGAASVDNDGLHNLTDISNDAEKLLMSVDDGSAAPSTLSVNMGVASHNVAAPT
TVNAATITGSDVSNNVNSATINNPMEEGALPLSPTASSPGTTTPLAKTTKTINNNNNIADLIESKDSIISPEYLSDEIFSA
INNNLPHAYFKNLLFRLVANMDRSELSDLGTLIKDNLKRDLITSLPFEISLKIFNYLQFEDIINSLGVSQNWNKIIRKSTSL
WKKLLISENFVSPKGFNSLNLKLSQKYPKLSQQDRLRLSFLENAAADLGKKLLEAARAGQDDEVRILMANGADVNA
ADNTGTTPLHLAAYSGHLEIVEVLLKHGADVDASDVFGYTPLHLAAYWGHLEIVEVLLKNGADVNAMDSDGMTPL
HLAAKWGYLEIVEVLLKHGADVNAQDKFGKTAFDISIDNGNEDLAEILQYPYDVPDYA

cdc4_10ala_off7 amino-acid sequence (10 ala linker underlined)

MGSFPLAEFPLRDIPVPYSYRVSGGIASSGSVTALVTAAGTHRNSSTAKTVETEDGEEDIDEYQRKRAAGPGESTPER
SSFAAVAHDNHKTLHPVNLQNTGAASVDNDGLHNLTDISNDAEKLLMSVDDGSAAPSTLSVNMGVASHNVAAPT
TVNAATITGSDVSNNVNSATINNPMEEGALPLSPTASSPGTTTPLAKTTKTINNNNNIADLIESKDSIISPEYLSDEIFSA
INNNLPHAYFKNLLFRLVANMDRSELSDLGTLIKDNLKRDLITSLPFEISLKIFNYLQFEDIINSLGVSQNWNKIIRKSTSL
WKKLLISENFVSPKGFNSLNLKLSQKYPKLSQQDRLRLSFLENAAAAAAAAADLGKKLLEAARAGQDDEVRILMAN
GADVNAADNTGTTPLHLAAYSGHLEIVEVLLKHGADVDASDVFGYTPLHLAAYWGHLEIVEVLLKNGADVNAMDS
DGMTPLHLAAKWGYLEIVEVLLKHGADVNAQDKFGKTAFDISIDNGNEDLAEILQYPYDVPDYA

cdc4_17ala_off7 amino-acid sequence (17 ala linker underlined)

MGSFPLAEFPLRDIPVPYSYRVSGGIASSGSVTALVTAAGTHRNSSTAKTVETEDGEEDIDEYQRKRAAGPGESTPER
SSFAAVAHDNHKTLHPVNLQNTGAASVDNDGLHNLTDISNDAEKLLMSVDDGSAAPSTLSVNMGVASHNVAAPT
TVNAATITGSDVSNNVNSATINNPMEEGALPLSPTASSPGTTTPLAKTTKTINNNNNIADLIESKDSIISPEYLSDEIFSA
INNNLPHAYFKNLLFRLVANMDRSELSDLGTLIKDNLKRDLITSLPFEISLKIFNYLQFEDIINSLGVSQNWNKIIRKSTSL
WKKLLISENFVSPKGFNSLNLKLSQKYPKLSQQDRLRLSFLENAAAAAAAAAAAAAAAADLGKKLLEAARAGQDD
EVRILMANGADVNAADNTGTTPLHLAAYSGHLEIVEVLLKHGADVDASDVFGYTPLHLAAYWGHLEIVEVLLKNGA
DVNAMDSDGMTPLHLAAKWGYLEIVEVLLKHGADVNAQDKFGKTAFDISIDNGNEDLAEILQYPYDVPDYA

References

1. Schwartz, A.L. and A. Ciechanover, *Targeting proteins for destruction by the ubiquitin system: implications for human pathobiology.* Annu Rev Pharmacol Toxicol, 2009. **49**: p. 73-96.
2. Nalepa, G., M. Rolfe, and J.W. Harper, *Drug discovery in the ubiquitin-proteasome system.* Nat Rev Drug Discov, 2006. **5**(7): p. 596-613.
3. Hershko, A. and A. Ciechanover, *The ubiquitin system.* Annu Rev Biochem, 1998. **67**: p. 425-79.
4. Goldberg, A.L., *Protein degradation and protection against misfolded or damaged proteins.* Nature, 2003. **426**(6968): p. 895-9.
5. Mani, A. and E.P. Gelmann, *The ubiquitin-proteasome pathway and its role in cancer.* J Clin Oncol, 2005. **23**(21): p. 4776-89.
6. Liu, Y.C., *Ubiquitin ligases and the immune response.* Annu Rev Immunol, 2004. **22**: p. 81-127.
7. Rock, K.L. and A.L. Goldberg, *Degradation of cell proteins and the generation of MHC class I-presented peptides.* Annu Rev Immunol, 1999. **17**: p. 739-79.
8. Pickart, C.M., *Mechanisms underlying ubiquitination.* Annu Rev Biochem, 2001. **70**: p. 503-33.
9. Pickart, C.M. and M.J. Eddins, *Ubiquitin: structures, functions, mechanisms.* Biochim Biophys Acta, 2004. **1695**(1-3): p. 55-72.
10. Thrower, J.S., et al., *Recognition of the polyubiquitin proteolytic signal.* Embo J, 2000. **19**(1): p. 94-102.
11. Tenno, T., et al., *Structural basis for distinct roles of Lys63- and Lys48-linked polyubiquitin chains.* Genes Cells, 2004. **9**(10): p. 865-75.
12. Hartmann-Petersen, R. and C. Gordon, *Proteins interacting with the 26S proteasome.* Cell Mol Life Sci, 2004. **61**(13): p. 1589-95.
13. Glickman, M.H. and A. Ciechanover, *The ubiquitin-proteasome proteolytic pathway: destruction for the sake of construction.* Physiol Rev, 2002. **82**(2): p. 373-428.
14. Varshavsky, A., *Naming a targeting signal.* Cell, 1991. **64**(1): p. 13-5.
15. Fang, S. and A.M. Weissman, *A field guide to ubiquitylation.* Cell Mol Life Sci, 2004. **61**(13): p. 1546-61.
16. Petroski, M.D. and R.J. Deshaies, *Mechanism of lysine 48-linked ubiquitin-chain synthesis by the cullin-RING ubiquitin-ligase complex SCF-Cdc34.* Cell, 2005. **123**(6): p. 1107-20.
17. Wu, G., et al., *Structure of a beta-TrCP1-Skp1-beta-catenin complex: destruction motif binding and lysine specificity of the SCF(beta-TrCP1) ubiquitin ligase.* Mol Cell, 2003. **11**(6): p. 1445-56.
18. Orlicky, S., et al., *Structural basis for phosphodependent substrate selection and orientation by the SCFCdc4 ubiquitin ligase.* Cell, 2003. **112**(2): p. 243-56.
19. Hao, B., et al., *Structural basis of the Cks1-dependent recognition of p27(Kip1) by the SCF(Skp2) ubiquitin ligase.* Mol Cell, 2005. **20**(1): p. 9-19.
20. Hao, B., et al., *Structure of a Fbw7-Skp1-cyclin E complex: multisite-phosphorylated substrate recognition by SCF ubiquitin ligases.* Mol Cell, 2007. **26**(1): p. 131-43.
21. Zheng, N., et al., *Structure of the Cul1-Rbx1-Skp1-F boxSkp2 SCF ubiquitin ligase complex.* Nature, 2002. **416**(6882): p. 703-9.
22. Willems, A.R., M. Schwab, and M. Tyers, *A hitchhiker's guide to the cullin ubiquitin ligases: SCF and its kin.* Biochim Biophys Acta, 2004. **1695**(1-3): p. 133-70.
23. Cardozo, T. and M. Pagano, *The SCF ubiquitin ligase: insights into a molecular machine.* Nat Rev Mol Cell Biol, 2004. **5**(9): p. 739-51.
24. Kus, B.M., et al., *Functional interaction of 13 yeast SCF complexes with a set of yeast E2 enzymes in vitro.* Proteins, 2004. **54**(3): p. 455-67.
25. Jin, J., et al., *Identification of substrates for F-box proteins.* Methods Enzymol, 2005. **399**: p. 287-309.

26. Deffenbaugh, A.E., et al., *Release of ubiquitin-charged Cdc34-S - Ub from the RING domain is essential for ubiquitination of the SCF(Cdc4)-bound substrate Sic1.* Cell, 2003. **114**(5): p. 611-22.
27. Petroski, M.D., G. Kleiger, and R.J. Deshaies, *Evaluation of a diffusion-driven mechanism for substrate ubiquitination by the SCF-Cdc34 ubiquitin ligase complex.* Mol Cell, 2006. **24**(4): p. 523-34.
28. Petroski, M.D. and R.J. Deshaies, *Function and regulation of cullin-RING ubiquitin ligases.* Nat Rev Mol Cell Biol, 2005. **6**(1): p. 9-20.
29. Verma, R., et al., *Phosphorylation of Sic1p by G1 Cdk required for its degradation and entry into S phase.* Science, 1997. **278**(5337): p. 455-60.
30. Nash, P., et al., *Multisite phosphorylation of a CDK inhibitor sets a threshold for the onset of DNA replication.* Nature, 2001. **414**(6863): p. 514-21.
31. Forrer, P., et al., *A novel strategy to design binding molecules harnessing the modular nature of repeat proteins.* FEBS Lett, 2003. **539**(1-3): p. 2-6.
32. Guthrie, C. and G.R. Fink, eds. *Guide to Yeast Genetics and Molecular Biology*. Methods in enzymology. Vol. 194. 1991, Academic Press: New-York. 3-933.
33. Ito, H., et al., *Transformation of intact yeast cells treated with alkali cations.* J Bacteriol, 1983. **153**(1): p. 163-8.
34. Sambrook, J. and D. Russell, *Molecular Cloning: A Laboratory Manual*. third edition ed. 2001, Cold Spring Harbor: Cold Spring Harbor Laboratory press.
35. Mumberg, D., R. Muller, and M. Funk, *Yeast vectors for the controlled expression of heterologous proteins in different genetic backgrounds.* Gene, 1995. **156**(1): p. 119-22.
36. Sikorski, R.S. and P. Hieter, *A system of shuttle vectors and yeast host strains designed for efficient manipulation of DNA in Saccharomyces cerevisiae.* Genetics, 1989. **122**(1): p. 19-27.
37. Binz, H.K., et al., *High-affinity binders selected from designed ankyrin repeat protein libraries.* Nat Biotechnol, 2004. **22**(5): p. 575-82.
38. Amstutz, P., et al., *Intracellular kinase inhibitors selected from combinatorial libraries of designed ankyrin repeat proteins.* J Biol Chem, 2005. **280**(26): p. 24715-22.
39. Blondel, M., et al., *Nuclear-specific degradation of Far1 is controlled by the localization of the F-box protein Cdc4.* Embo J, 2000. **19**(22): p. 6085-97.
40. Lee, D.H. and A.L. Goldberg, *Selective inhibitors of the proteasome-dependent and vacuolar pathways of protein degradation in Saccharomyces cerevisiae.* J Biol Chem, 1996. **271**(44): p. 27280-4.
41. Graham, T.R., P.A. Scott, and S.D. Emr, *Brefeldin-a Reversibly Blocks Early but Not Late Protein-Transport Steps in the Yeast Secretory Pathway.* Embo Journal, 1993. **12**(3): p. 869-877.
42. Varelas, X., et al., *The Cdc34/SCF ubiquitination complex mediates Saccharomyces cerevisiae cell wall integrity.* Genetics, 2006. **174**(4): p. 1825-39.
43. Zhou, P. and P.M. Howley, *Ubiquitination and degradation of the substrate recognition subunits of SCF ubiquitin-protein ligases.* Mol Cell, 1998. **2**(5): p. 571-80.
44. Galan, J.M. and M. Peter, *Ubiquitin-dependent degradation of multiple F-box proteins by an autocatalytic mechanism.* Proc Natl Acad Sci U S A, 1999. **96**(16): p. 9124-9.
45. Dixon, C., et al., *Overproduction of polypeptides corresponding to the amino terminus of the F-box proteins Cdc4p and Met30p inhibits ubiquitin ligase activities of their SCF complexes.* Eukaryot Cell, 2003. **2**(1): p. 123-33.
46. Yao, T. and R.E. Cohen, *A cryptic protease couples deubiquitination and degradation by the proteasome.* Nature, 2002. **419**(6905): p. 403-7.
47. Verma, R., et al., *Role of Rpn11 metalloprotease in deubiquitination and degradation by the 26S proteasome.* Science, 2002. **298**(5593): p. 611-5.
48. Ventii, K.H. and K.D. Wilkinson, *Protein partners of deubiquitinating enzymes.* Biochem J, 2008. **414**(2): p. 161-75.

49. Petroski, M.D. and R.J. Deshaies, *Context of multiubiquitin chain attachment influences the rate of Sic1 degradation.* Mol Cell, 2003. **11**(6): p. 1435-44.
50. Tang, X., et al., *Suprafacial orientation of the SCFCdc4 dimer accommodates multiple geometries for substrate ubiquitination.* Cell, 2007. **129**(6): p. 1165-76.
51. Li, Y., et al., *Stability of homologue of Slimb F-box protein is regulated by availability of its substrate.* J Biol Chem, 2004. **279**(12): p. 11074-80.
52. Deshaies, R.J., *SCF and Cullin/Ring H2-based ubiquitin ligases.* Annu Rev Cell Dev Biol, 1999. **15**: p. 435-67.
53. Welcker, M. and B.E. Clurman, *Fbw7/hCDC4 dimerization regulates its substrate interactions.* Cell Div, 2007. **2**: p. 7.
54. Zhou, P., et al., *Harnessing the ubiquitination machinery to target the degradation of specific cellular proteins.* Mol Cell, 2000. **6**(3): p. 751-6.
55. Zhang, J., N. Zheng, and P. Zhou, *Exploring the functional complexity of cellular proteins by protein knockout.* Proc Natl Acad Sci U S A, 2003. **100**(24): p. 14127-32.
56. Su, Y., et al., *Eradication of pathogenic beta-catenin by Skp1/Cullin/F box ubiquitination machinery.* Proc Natl Acad Sci U S A, 2003. **100**(22): p. 12729-34.
57. Liu, J., et al., *Targeted degradation of beta-catenin by chimeric F-box fusion proteins.* Biochem Biophys Res Commun, 2004. **313**(4): p. 1023-9.
58. Cohen, J.C., et al., *Transient in utero knockout (TIUKO) of C-MYC affects late lung and intestinal development in the mouse.* BMC Dev Biol, 2004. **4**: p. 4.
59. Chen, W., et al., *Proteasome-mediated destruction of the cyclin a/cyclin-dependent kinase 2 complex suppresses tumor cell growth in vitro and in vivo.* Cancer Res, 2004. **64**(11): p. 3949-57.

An alternative route to the proteasome: ODC and NYV degrons

Chapter 2

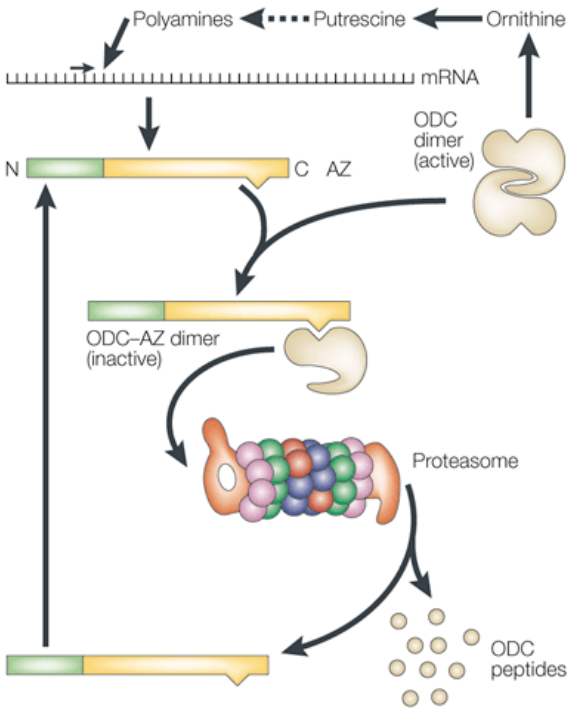

Figure 1: Polyamines regulation. Polyamines increase the production of antizyme (AZ). The carboxy-terminal half of antizyme interacts with ODC, generating AZ:ODC heterodimers at the expense of enzymatically active ODC homodimers. A carboxy-terminal domain of ODC that is occluded within the homodimer is exposed within the heterodimer, and is essential for subsequent degradation. A domain within the amino-terminal portion of antizyme provides a function needed for efficient degradation of ODC by the proteasome. The proteasome processes AZ:ODC, sequestering ODC and then degrading it to peptides but releasing antizyme, which participates in additional rounds of binding and degradation. Antizyme-mediated inhibition and destruction of ODC reduces synthesis of polyamines, the downstream products of the enzyme. Additionally, antizyme inhibits polyamine transport into the cell. Antizyme production is thus reduced, completing the regulatory circuit. Adapted from Coffino, 2001 [1].

Introduction

Selective protein degradation plays a pivotal role in cellular life and function. However, since intracellular proteolysis is a random event regarding which substrate molecule is degraded, cells have elaborated an effective tactic to destroy appropriate substrates and spare other proteins: compartmentalization. This strategy relies on confining proteolytic action to secluded sites that can only be accessed by proteins exhibiting some sort of degradation signals. Such a compartment can be a membrane delimited organelle, such as the lysosome, or the proteolytic chamber of a self-compartmentalizing protease, a structural design that has evolved in prokaryotic cells which are devoid of membrane-bound compartments [2]. The proteasome became the paradigm of this form of regulation [3]. In eukaryotes, the 26S proteasome is the major neutral protease. It is a multicatalytic degradation machinery composed of a barrel-shaped catalytic chamber (20S core particle) flanked by one or two regulatory complexes (19S regulatory particle or PA700) [4]. The 19S regulatory particle interacts with the substrate, unfolds it and opens an axial portal into the 20S chamber to translocate the unfolded polypeptide in the catalytic chamber [5].

The 19S regulatory particle usually identifies its client proteins by the presence of a polyubiquitin tag [6]. A chain of four or more molecules formed via lysine 48 of ubiquitin is normally required [7, 8]. Two subunits were identified as integral ubiquitin receptors: Rpn10 and Rpn13 [9, 10]. They respectively trap their substrates via an Ubiquitin Interacting Motif (UIM) [11] or pleckstrin-like-receptor for ubiquitin (Pru) domain [12]. In addition, a small subset of proteins has been described to be degraded by the proteasome without prior ubiquitination [13, 14]. Some of these evaders seem to be recognized by the proteasome via the presence of a degradation signal, named degron in this study.

The best described ubiquitin-independent proteasome substrate is Ornithine Decarboxylase (ODC) [15]. ODC is the first and rate-limiting enzyme in the biosynthesis of the polyamines spermine and spermidine [16]. Its level is regulated by a polyamine autoregulatory feedback loop maintaining optimal polyamine abundance in eukaryotic cells (Fig. 1). Polyamine accumulation leads to increased expression of Antizyme 1 (AZ1) by promoting ribosomal translational frameshifting [17, 18]. AZ1 disrupts enzymatically active ODC homodimers to form an inactive ODC/AZ1 heterodimeric complex thereby inhibiting its activity [19]. Moreover, AZ1 binding triggers accelerated degradation of ODC by improving its affinity for the 26S proteasome about eightfold [20]. Upon binding AZ1 increases exposure of the C-terminus of ODC [21], a region formerly identified for being responsible for ODC turnover, the ODC degron [22]. Crystal-structural analysis of this region (Fig. 2) had shown conformational disorder [19] but mutational analysis has unveiled the presence of two essential elements in these 37 C-terminal amino-acids [20, 23, 24]. The first one consisted of cysteine 441 which was shown to function as a proteasome association element [23]. In combination with alanine 442, these two adjacent residues must function together as a structural recognition element in which the cysteine thiol must be reduced and the side chain of the next residue must be no larger than a methyl group [24]. The second one was the C-terminus distal to residue 442

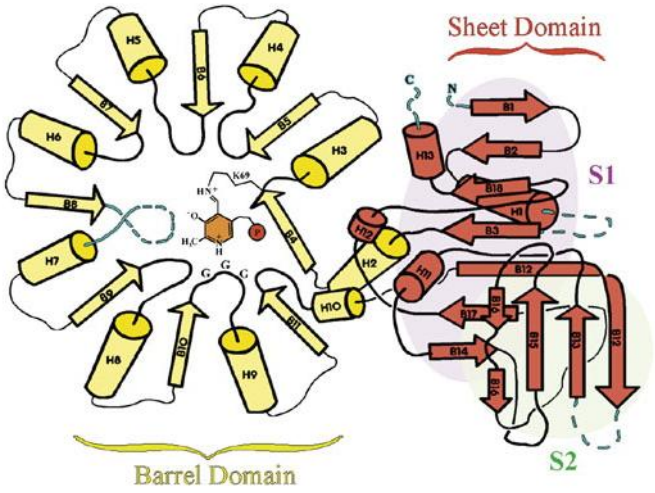

Figure 2: Ornithine Decarboxylase structure. Cartoon drawing of truncated mouse ODC (mODC') (the last 37 residues were omitted), the crystal structure was determined to 1.6 resolution. ODC monomer contains two domains: an α/βbarrel (yellow) which binds the pyridoxal-5'-phosphate (PLP) cofactor and a second domain consisting mostly of β structure which include two sheets, S1 and S2. Disordered segments were colored in cyan. Adapted from Kern & al, 1999 [19].

which engages entry into the proteasome [23, 25]. The C-terminal end had little or no sequence specificity but its span mattered as it was intolerant of long insertions or deletions [24]. The spacing between Cys441-Ala442 and the C-terminal end of the ODC degron seemed then to be crucial for their functional interaction. Despite the absence of similarity, experimental studies had shown that ODC harbor an AZ1-modulated recognition determinant which could be cross-competed by both substrate-linked and free polyubiquitin chains for 26S proteasome association [20]. The authors suggested that the ODC-AZ1 complex and polyubiquitin chain recognition involved a common binding site of the 19S regulatory particle [20]. Yet more recent data were at variance with this model. ODC turnover rate was indeed accelerated in a *rpn10Δ* mutant strain in which the degradation of certain ubiquitinated substrates was impaired [26]. A very recent study also concluded that ODC degradation was not inhibited by ubiquitin chains, indicating that it bound to a different 19S subunit than ubiquitinated substrates [27]. The C-terminal 37 amino-acids of mouse ODC act as a portable ubiquitin-independent degradation signal [22, 28]. When fused to the C-terminus of GFP (Green Fluorescent Protein), the ODC-degron destabilized the fusion protein in vivo in animal cells and in yeast [29, 30].

Another degron was discovered in the cytoplasmic tail of NY-1V hantavirus G1 glycoprotein [31]. Hantaviruses belong to the Bunyaviridae family. While they do not produce disease in the rodent hosts, certain hantaviruses can cause two discrete diseases in humans: hemorrhagic fever with renal syndrome (HFRS) and hantavirus pulmonary syndrome (HPS) [32]. The NY-1 virus (NY-1V) is a pathogenic one which can elicit hantavirus pulmonary syndrome. Hantaviruses are enveloped negative-stranded RNA viruses which encode four proteins: a polymerase, a nucleocapsid protein and two surface glycoproteins G1 and G2. During infection, G1 and G2 form heterodimers that localize to the cis-Golgi compartment. Hantavirus virions are believed to assemble by association of nucleocapsids with glycoproteins embedded in the membranes of the Golgi apparatus, followed by budding into the lumen of the Golgi complex. Virions are then transported in secretory vesicles to the plasma membrane and released by exocytosis. Besides mediating maturation, the NY-1 V G1 glycoprotein has recently been shown to inhibit cellular interferon responses [33]. In addition, the G1 142-residue-long cytoplasmic tail of several pathogenic hantaviruses was observed to be degraded by the proteasome while it was stable in nonpathogenic hantaviruses [31]. A comparison of their sequences revealed a disparity in their C-terminal 30 residues composing a hydrophobic region. Mutational analyses identified residues that selectively directed the proteasomal degradation of pathogenic hantavirus tails. Appending the last 42 residues of the NY-1 V G1 glycoprotein to the C terminus of GFP or RFP (Red Fluorescent Protein) was sufficient to degrade the fusion proteins in mammalian cells [31]. This region seemed then to constitute a degron (NYV-degron) which could autonomously lead a protein to degradation. This cytoplasmic tail of the NY-1 V G1 glycoprotein had previously been observed to be polyubiquitylated [34]. Two lysine residues (K615 and K628) were identified as ubiquitylation sites and thought to be the primary signal responsible for NY-1 V G1 cytoplasmic tail degradation. The degron region contained these two lysine residues but a later study demonstrated that they were not required for the NYV-degron mediated degradation process [31]. Mutation of both lysine residues to alanine had namely no detectable effect on the proteasomal degradation of the fusion protein GAL4-NYV. The exact mechanism by which the NY-1 V G1 cytoplasmic tail is degraded has remained unsolved. It cannot be claimed that the NYV degron

was the only determinant responsible for its proteasomal degradation but it could act as a portable ubiquitin-independent degradation signal.

The ODC-and NYV-degron were used as an ubiquitin free route to evaluate the proteasome processing capacity when fed with different kinds of substrates. It was often debated which minimal characteristics were required from a protein to become a proteasomal substrate and which role was playing a degron in the degradation process. The question of substrate protein intrinsic stability was addressed. We also tried to assess the proteasome ability to degrade a complex formed by a degron-construct and a binding partner. We investigated if a binding partner would affect degradation of the degron-construct. It had been proposed that increasing the local concentration of a substrate at the proteasome site was sufficient for degradation [35]. Finally, we focused our attention on the binding partner's fate to see if it would be processed as collateral damage or else spared by the proteasome.

Materials & methods

Yeast strains and genetic experiments

Yeast strains are described in Table 1. The genotypes of the yeast strains are:

W303: *ade2-1*, *trp1-1*, *can1-100*, *leu2-3,112*, *his3-11,15*, *ura3-1*, *GAL+*, *psi+*, *ssd1-d2*

S288C: *ade2-101*, *ura3-52*, *lys2-801*, *trp1-Δ1*, *his3Δ200*, *leu2-Δ*

Unless noted otherwise strain K699 was used.

Table 1: Yeast strains

Strain	Relevant genotype	Background	Source
K699	Mat a	W303	M. Peter
Erg6	Erg6::KAN	S288C	M. Peter & G. Rabut
K-M	[p416/Gal/MBP]	K699	This study
K-MO	[p416/Gal/MBP-ODC]	K699	This study
K-MN	[p416/Gal/MBP-NYV]	K699	This study
K-G	[p416/Gal/GFP]	K699	This study
K-GO	[p416/Gal/GFP-ODC]	K699	This study
K-GN	[p416/Gal/GFP-NYV]	K699	This study
K-5	[p416/Gal/E3_5]	K699	This study
K-5O	[p416/Gal/ E3_5-ODC]	K699	This study
K-5N	[p416/Gal/ E3_5-NYV]	K699	This study
K-19	[p416/Gal/E3_19]	K699	This study
K-19O	[p416/Gal/ E3_19-ODC]	K699	This study
K-19N	[p416/Gal/ E3_19-NYV]	K699	This study
E-GO	[p416/Gal/GFP-ODC]	Erg6	This study
E-GN	[p416/Gal/GFP-NYV]	Erg6	This study
E-19O	[p416/Gal/ E3_19-ODC]	Erg6	This study
E-19N	[p416/Gal/ E3_19-NYV]	Erg6	This study
KM-7Ot	[p425/ TEF /off7-ODC]	Mg (see chapter 1)	This study
KM-7Nt	[p425/ TEF /off7-NYV]	Mg (see chapter 1)	This study
KM-V	[p425/ ADH]	Mg (see chapter 1)	This study
KM-7Oa	[p425/ ADH /off7-ODC]	Mg (see chapter 1)	This study
KM-7Na	[p425/ ADH /off7-NYV]	Mg (see chapter 1)	This study
K-7	[p416/Gal/off7]	K699	This study
K-7O	[p416/Gal/off7-ODC]	K699	This study
K-7O436	[p416/Gal/off7-ODCT436A]	K699	This study
K-7O438	[p416/Gal/off7-ODCP438A]	K699	This study
KM-7O436a	[p425/ADH/off7-ODCT436A]	Mg (see chapter 1)	This study
KM-7O438a	[p425/ADH/off7-ODCP438A]	Mg (see chapter 1)	This study

Standard yeast growth conditions and genetic manipulations were used as described [36]. Yeast cells were cultured in synthetic media (S) (1.7 g/L yeast nitrogen base, 5 g/L ammonium sulfate) supplemented with a standard amino acid and nucleobases solution (30 mg/L isoleucine, 150 mg/L valine, 40 mg/L adenine, 20 mg/L arginine, 20 mg/L histidine, 100 mg/L leucine, 30 mg/L lysine, 20 mg/L methionine, 50 mg/L phenylalanine, 200 mg/L threonine, 40 mg/L tryptophane, 30 mg/L tyrosine, 20 mg/L uracil, 100 mg/L glutamic acid, 100 mg/L aspartic acid) and 2 % carbon source (glucose (D), raffinose (Raff) or galactose (Gal)). According to the strain and the experiment, a synthetic media prepared without amino acids or nucleobases supplemented with auxotrophic requirements: uracil (-Ura), leucine (-Leu), and the appropriate carbon source (SD, SRaff or SGal) was used.

Yeast transformations were performed by the lithium acetate procedure [37]. The MBP expressing strain was created by homologous recombination using StuI linearized plasmid pRS306/Gal/MBP (see chapter 1).

DNA manipulations and plasmids

Standard molecular biology procedures were used for recombinant DNA manipulation [38]. Enzymes were from NEB (Ipswich, MA, USA) or Fermentas (Vilnius, Lithuania). PCR reactions were performed with the Phusion ™ High-Fidelity DNA polymerase as recommended by the manufacturer (NEB). Plasmids used as templates and all oligonucleotides are listed in Tables 2 and 4.

ODC-, NYV- and stop-constructs ORFs (see schemes below) were constructed in several steps. First a plasmid containing the HA tag and required cloning sites (SpeI, EcoRI, BamHI and XhoI) was constructed by annealing updegron and lowdegron oligonucleotides, amplifying them by PCR using ext for degron and ext rev degron oligonucleotides as primers and introducing the digested PCR product at the SpeI and XhoI sites of p415ADH [39]. Second the low and up mODC/NY1V oligonucleotides were annealed, amplified by PCR using forBamHI and revXhoI ODC/NYV oligonucleotides as primers and the digested PCR product introduced at the BamHI and XhoI sites of the formerly constructed plasmid to yield p415ADH/ODC and p415ADH/NYV respectively. The stop sequence oligonucleotides were designed with BamHI and XhoI sticky ends and were inserted directly after annealing to construct p415/stop.

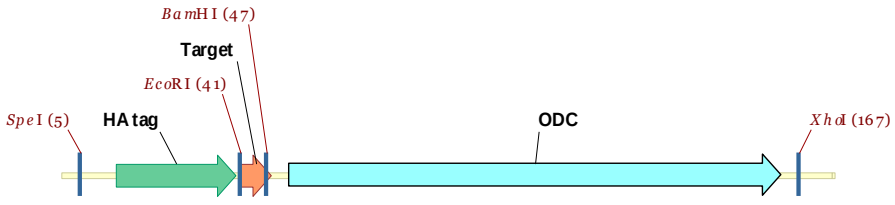

ODC degron construct

174 bp

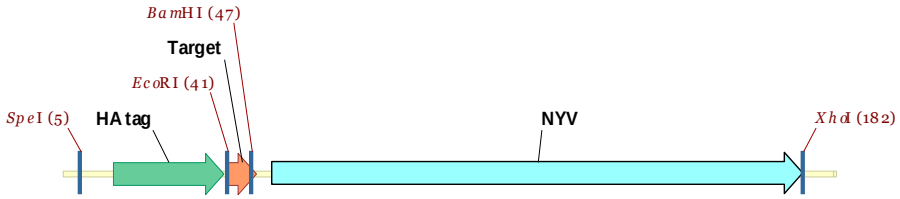

NYV degron construct

189 bp

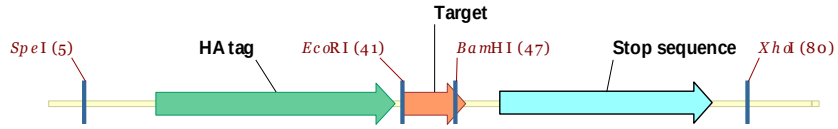

stop degron construct

87 bp

Finally the target protein sequence was amplified by PCR using appropriate for EcoRI and revBamHI oligonucleotides as primers and the digested PCR product was introduced at the EcoRI and BamHI sites of p415/stop, p415ADH/ODC or p415ADH/NYV. The construct genes were subcloned as a SpeI/XhoI fragment in p416Gal, p425ADH or p425TEF [39]. The sequences of E3_5-stop, E3_5-ODC and E3_5-NYV constructs are shown in annex. Site-directed mutagenesis was performed with QuikChange kit (Stratagene, La Jolla, CA) according to the manufacturer's instructions.

pQE30/off7-ODC was constructed by amplifying the ODC degron sequence from p416/Gal/MBP-ODC with HindforODC and HindrevODC oligonucleotides and inserting the digested PCR product at the HindIII site of pQE30_mbpoff7.

All constructs were confirmed by sequencing. Plasmids constructed for this study are listed in Table 3, those marked with an asterisk have their plasmid map and the insert sequences shown in annex.

Table 2: Plasmids used as PCR DNA templates for cloning

Plasmids	Templates for	Source
pQEMBP	MBP	Binz, 2004 [40]
pET28GFP	GFP	Our laboratory, Andreas Ernst
pHKB26E3_5	E3_5	Binz, 2003 [41]
pHKB26E3_19	E3_19	Binz, 2003 [41]
pQE30_mbpoff7	off7	Binz, 2004 [40]

Table 3: Plasmids constructed for this study

Plasmids	Relevant characteristics (promoter; gene; resistance; ori)	Source
p416/Gal/MBP	Gal1; MBP; URA3; CEN6	This study
p416/Gal/GFP	Gal1; GFP; URA3; CEN6	This study
p416/Gal/E3_5*	Gal1; E3_5; URA3; CEN6	This study
p416/Gal/E3_19	Gal1; E3_19; URA3; CEN6	This study
p416/Gal/MBP-ODC	Gal1; MBP-ODC; URA3; CEN6	This study
p416/Gal/GFP-ODC	Gal1; GFP-ODC; URA3; CEN6	This study
p416/Gal/E3_5-ODC*	Gal1; E3_5-ODC; URA3; CEN6	This study
p416/Gal/E3_19-ODC	Gal1; E3_19-ODC; URA3; CEN6	This study
p416/Gal/MBP-NYV	Gal1; MBP-NYV; URA3; CEN6	This study
p416/Gal/GFP-NYV	Gal1; GFP-NYV; URA3; CEN6	This study
p416/Gal/E3_5-NYV*	Gal1; E3_5-NYV; URA3; CEN6	This study
p416/Gal/E3_19-NYV	Gal1; E3_19-NYV; URA3; CEN6	This study
pRS306/Gal/MBP	Gal1; MBP; URA3	Chapter1
p425/ TEF /off7-ODC*	TEF1; off7-ODC; LEU2; 2µ	This study
p425/ ADH /off7-ODC	ADH; off7-ODC; LEU2; 2µ	This study
p425/ TEF /off7-NYV	TEF1; off7-NYV; LEU2; 2µ	This study
p425/ ADH /off7-NYV*	ADH; off7-NYV; LEU2; 2µ	This study
p416/Gal/off7	Gal1; off7; URA3; CEN6	This study
p416/Gal/off7-ODC	Gal1; off7-ODC; URA3; CEN6	This study
p416/Gal/off7-ODCT436A	Gal1; off7-ODCT436A; URA3; CEN6	This study
p416/Gal/off7-ODCP438A	Gal1; off7-ODCP438A; URA3; CEN6	This study
p425/ADH/off7-ODCT436A	ADH; off7-ODCT436A; LEU2; 2µ	This study
p425/ADH/off7-ODCP438A	ADH; off7-ODCP438A; LEU2; 2µ	This study
pQE30/off7-ODC*	T5; RGS$(His)_6$ off7-ODC; Amp; ColE1	This study

Table 4: Oligonucleotides

Oligonucleotides	Sequence 5'-3' direction	Description (for=forward, rev=reverse)
Up degron	GGTACTAGTATGTACCCATACGATGTTCCAGATTACGCTGAATTCG GATCCAAGC	Upper HA tag + cloning sites
Low degron	ACCCTCGAGAGATCTTCCGCCCGAGCCAAGCTTGGATCCGAATTCA GCGTAATC	Lower HA tag + cloning sites
ext for degron	GGT GGT ACT AGT ATG TAC CCA TAC G	For external primer
ext rev degron	ACC ACC CTC GAG AGA TCT TCC G	Rev external primer
Up mODC	GGTAGATCTTTCCCGCCGGAGGTGGAGGAGCAGGATGATGGCAC GCTGCCCATGTCTTGTGCCCAGGAGAGCGGGATGGAC	Upper ODC degron
Low mODC	ACCCTCGAGCACATTGATCCTAGCAGAAGCACAGGCTGCAGGGTG ACGGTCCATCCCGCTCTCCTGGGC	Lower ODC degron
Up NYV	GGTAGATCTCGCCCTGAAGTTAAACAAGGATGCTATAGAACATTG GGTGTTTTTAGATATAAGAGTAGGTGTTATGTTGGTCTTGTGTGG	Upper NYV degron
Low NYV	ACCCTCGAGAGCACTAGCTGCCCAAACTATGAGTTCAGTTGTAAGA AGGACCCCCCACACAAGACCAACATAACACCTAC	Lower NYV degron
forBamHI ODC	GGT GGA TCC TTC CCG CCG GAG GTG GAG G	For ODC + BamHI site
revXhoI ODC	ACC CTC GAG CTA CAC ATT GAT CCT AGC AGA AGC	Rev ODC + XhoI site
forBamHI NYV	GGT GGA TCC CGC CCT GAA GTT AAA CAA GG	For NYV + BamHI site
revXhoI NYV	ACC CTC GAG CTA AGC ACT AGC TGC CCA AAC TAT G	Rev NYV + XhoI site

Up stop	GA TCC TAA TAG TGA AAG CTT TTA GCT GAC C	Upper stop + BamHI/XhoI ends
Low stop	TC GAG GTC AGC TAA AAG CTT TCA CTA TTA G	Lower stop + BamHI/XhoI ends
forEcoRI MBP	GGT GAA TTC ATG AAA ACT GAA GAA GGT AAA CTG G	For MBP + EcoRI site
revBamHI MBP	ACC GGA TCC AGT CTG CGC GTC TTT CAG G	Rev MBP + BamHI site
forEcoRI GFP	GGT GAA TTC AGC AAA GGA GAA GAA CTT TTC AC	For GFP + EcoRI site
revBamHI GFP	ACC GGA TCC TTT GTA GAG CTC ATC CAT GCC	Rev GFP + BamHI site
forEcoRI DARPin	GGT GAA TTC GAC CTG GGT AAG AAA CTG CTG G	For DARPin + EcoRI site
revBamHI DARPin	ACC GGA TCC TTG CAG GAT TTC AGC CAG G	Rev DARPin + BamHI site
for ODC T436A	GCAGGATGATGGCGCGCTGCCCATGTCTTGTGC	For ODC + mutation T436A
Rev ODC T436A	GCACAAGACATGGGCAGCGCGCCATCATCCTGC	Rev ODC + mutation T436A
For ODC P438A	GGATGATGGCACGCTGGCCATGTCTTGTGCCC	For ODC + mutation P438A
Rev ODC P438A	GGGCACAAGACATGGCCAGCGTGCCATCATCC	Rev ODC + mutation P438A
ForHindIII ODC	GGT GGT AAG CTT TTC CCG CCG GAG GTG GAG G	For ODC + HindIII site
RevHindIII ODC	CC ACC AAG CTT CTA CAC ATT GAT CCT AGC AGA AGC	Rev ODC + HindIII site

Determination of steady-state levels of target proteins

Yeast cells were grown in SRaff-U at 30°C. At OD_{600}=0.6-0.8, 2% galactose was added. After 1 h to 4 h, an aliquot was taken, OD_{600} was measured. Cells were collected by centrifugation for 5 min at 5000 g, the pellet was resuspended in 200 µl SDS-urea loading buffer (60 mM Tris-HCl pH 6.8, 8 M urea, 5% glycerol, 3% SDS, 4% 2-mercaptoethanol, 5 mM EDTA, bromophenolblue), transferred in a 2 ml-tube and immediately stored at -20°C. The MG132 experiment was performed similarly; MG132 (Sigma-Aldrich, St. Louis, MO) was added at the same time as galactose to a final concentration of 50 µM (MG132 stock solution was prepared in DMSO with a concentration of 5 mM). An identical volume of DMSO was added to the negative control strains. Aliquots were taken after 1 h, 2 h or 16 h.

Stability assays

By promoter shut-off: Yeast cells were grown in SRaff-U or SRaff-UL at 30°C. At OD_{600}=0.6-0.8, 2 % galactose was added. 1 h to 4 h later, 2 % glucose was added to shut off the Gal1 promoter; cells were collected by centrifugation for 5 min at 3000 g and resuspended in SD-U or SD-UL. Cells were further incubated at 30°C. Samples of decreasing volume were taken at different time points in order to have a relatively constant amount of cells. For each of them, OD_{600} was measured; cells were pelleted for 4 min at 5000 g, resuspended in 200 µl SDS-urea loading buffer and immediately stored at -20°C. For off7-ODC mutants comparison, cells were not resuspended in SD-U, the time-course experiment started immediately after addition of 2 % glucose.

By cycloheximide treatment: Yeast cells were grown in SRaff-UL at 30°C. At OD_{600}=0.6-0.8, 2 % galactose or glucose was added. 90 min later, a first aliquot was removed (t0 sample) before expression was turned off by addition of 75 µg/ml cycloheximide (Sigma-Aldrich, St. Louis, MO) (Cycloheximide stock solution was prepared in water with a concentration of 10 mg/ml). Cells were further incubated at 30°C and samples of decreasing volume were taken at different time points. For each of them, OD_{600} was measured; cells were pelleted for 4 min at 5000 g, resuspended in 200 µl SDS-urea loading buffer and immediately stored at -20°C.

Ni-NTA pull-down assay

Yeast cells were grown in SGal-UL at 30°C. At OD_{600}=0.7-0.8, cells were collected by centrifugation for 5 min at 5000 g and stored at -20°C. Pellets were resuspended in ice-cold lysis buffer (50 mM Na_2HPO_4 pH 8, 300 mM NaCl, 0.05 % Tween-20, 20 mM imidazole) and cells were mechanically lysed through 4 cycles of French press lysis. Cell debris was removed by a 30 min centrifugation step at 18,000 g and cleared lysates were aliquoted in 2ml-tubes, snap-frozen in liquid nitrogen and stored at -80°C. Thawed lysates were incubated for 2 h with 200 µl Ni-NTA magnetic agarose beads (Qiagen, Chatsworth, CA, product number: 36111). Beads were washed 4 times with lysis buffer and eluted with 80 µl 1X SDS sample loading buffer-EDTA (62.5 mM Tris-HCl pH 6.8, 100 mM EDTA, 7.5 % glycerol, 2 % SDS, 2.5 % 2-mercaptoethanol, bromophenolblue). After 5 min at 95°C, eluted fractions were resolved by 15 % SDS-PAGE followed by immunoblotting.

Proteins samples extraction

Samples stored at -20°C were thawed and incubated in a sonicating water bath for 20 min. 200µl of acid-washed 425- to 600-µm glass beads (Sigma-Aldrich, St. Louis, MO) were added and samples were lysed three times 2 min at 30 Hz in TissueLyser (Qiagen, Chatsworth, CA). After a 10 sec spin down at 1000 g, they were finally incubated for 5 min at 95°C and clarified at 10°C for 5 min at 20000 g. Normalized volumes according to the OD_{600} were loaded on 10 % or 15 % SDS-polyacrylamide gels followed by immunoblotting. For E3_5 and E3_19 stability assay samples, SDS-PAGE were run at 60°C.

Immunoblotting

Samples were transferred to PVDF membranes and immunoblotted using standard methods. The anti-HA peroxidase conjugate was used at a 1:1000 dilution (Sigma-Aldrich, St. Louis, MO, product number H 6533) and the RGS·His HRP conjugate (Qiagen, Chatsworth, CA, product number: 34450) at a 1:7000 dilution for detection of $RGS(His)_6$ MBP or 1:8000 dilution for detection of $RGS(His)_6$off7-ODC. The anti-actin antibody (Millipore, Bedford, MA, product number: MAB1501R) was diluted 1:3000 and detected with anti-horseradish peroxidase (HRP)-coupled anti-mouse antibody diluted 1:10000 (Thermo Fisher Scientific, Rockford, IL, product number 31438).

Expression, purification of MBP and off7-ODC and interaction analyses

Biotinylated MBP was produced in *E. coli* as described (Binz, 2004). Off7-ODC was produced on a liter scale and purified as described (Binz, 2004). Interaction analyses were conducted at 25°C and measured on the Octet QK system (ForteBio, Inc., Menlo Park, CA). The running buffer was 50 mM Na_2HPO_4 pH 8, 300 mM NaCl, 0.002 % Tween-20. Streptavidin biosensors were incubated for 5 min in running buffer and coated for 1 min with 100 nM biotinylated MBP. A new baseline was established for 5 min in running buffer. Different concentrations of off7-ODC were allowed to bind MBP-saturated biosensors for 20 min before dissociating for 30 min in running buffer. The kinetic data of the interaction were evaluated with a separate fit using the Octet data analysis software.

In vitro degradation assay

Off7-ODC was first dialyzed against 50 mM Tris pH 7.5, 150 mM NaCl, 0.1 mM EDTA, 10 % glycerol, 1 mM DTT overnight at 4°C. 20 nM Off7-ODC was added to the degradation mix which was kept on ice and contained 50 mM Tris-HCl pH 7.5, 2 mM DTT, 20 nM 26S Proteasome Fraction (Boston Biochem Inc., Cambridge, MA, product number: F-365) and 1X Energy Regeneration Solution (Boston Biochem Inc., Cambridge, MA, product number: B-10). All components were mixed and the t0 sample was immediately taken. The reaction was then incubated at 37°C, aliquots were withdrawn at different time points, mixed to 4 X SDS sample loading buffer (250 mM Tris-HCl pH 6.8, 30% glycerol, 8 % SDS, 10 % 2-mercaptoethanol, bromophenolblue) and immediately stored at -20°C. When the reaction was performed with pre-denatured off7-ODC, a 10 times more concentrated off7-ODC solution was incubated for 5 min at 95°C and centrifuged for 10 sec at 1000 g before an aliquot of the “supernatant” was added to the degradation mix.

Results

Degron constructs design and expression

To test if a target protein could be directly degraded by the proteasome, three kinds of sequences were appended at its C-terminus: the last 37 residues of mouse ornithine decarboxylase (ODC construct), the last 42 residues of the Hantavirus NYV1 G1 protein (NYV construct) or a stop codon only (- construct) as negative control (Fig. 3). Four different protein sequences were used as target proteins: GFP, MBP and the DARPIns E3_5 and E3_19. The final constructs were cloned in p416 Gal with an N-terminal HA tag and transformed in yeast. All target proteins could be detected after a 1 to 4 h galactose induction (Fig. 4, Fig. 5). The steady state amount of constructs not containing a degron-tag (negative control constructs), was always higher than for the ODC- and NYV-containing ones indicating that the degron sequence was destabilizing them. Depending on the target protein, the ratios between the different kinds of constructs varied slightly. MBP seemed to be equally destabilized by the ODC- or NYV-degron, which lowered the steady state level to at least 50%. GFP and the DARPin E3_19 were much more destabilized by the NYV-degron than by the ODC-degron. The DARPin E3_5 was destabilized by both degron sequences, however, their effect could not be compared as the samples were not properly normalized.

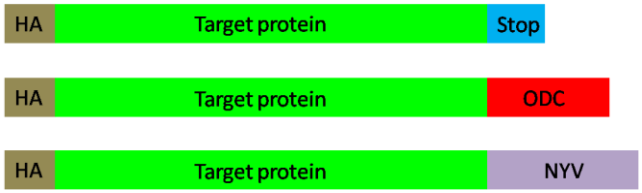

Figure 3: Schematic diagrams of the negative control, ODC- and NYV-constructs. An HA tag was fused to the N-terminus of the target protein. The last 37 residues of mouse ornithine decarboxylase (ODC construct) or the last 42 residues of the Hantavirus NYV1 G1 protein (NYV construct) or a stop codon only (- construct) was appended at its C-terminus.

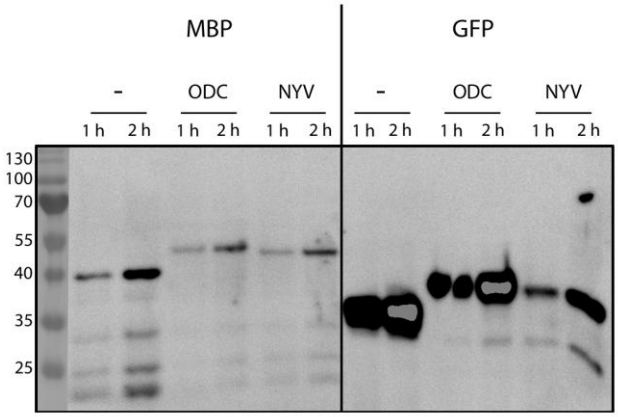

Figure 4: Steady-state levels of MBP and GFP constructs expressed from p416Gal. K-M, K-MO, K-MN, K-G, K-GO and K-GN cells (see material & methods) were grown in a synthetic raffinose-based medium to an OD_{600} of 0.6-0.7. After a 1 h- or 2 h-galactose induction, Total protein was extracted and normalized before being subjected to SDS-PAGE. The levels of MBP and GFP constructs were detected by immunoblotting with the anti-HA antibody. The size marker is indicated in kDa. Theoretical molecular weights: MBP (43 kDa), MBP-ODC (46 kDa), MBP-NYV (47 kDa), GFP (27 kDa), GFP-ODC (32 kDa), GFP-NYV (33 kDa).

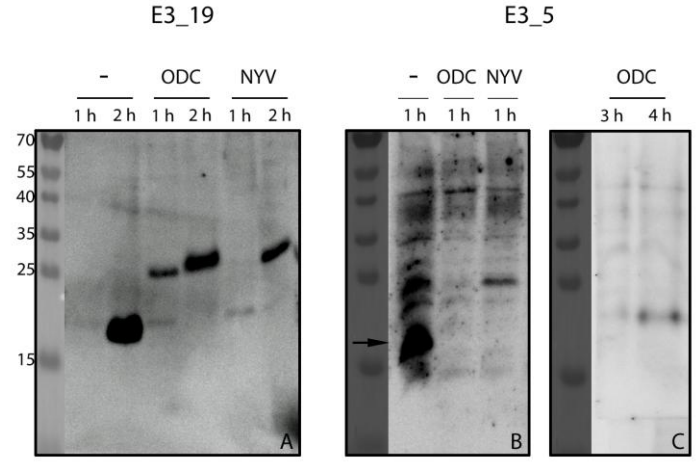

Figure 5: Steady-state expression levels of E3_19 and E3_5 constructs expressed from p416Gal. K-19, K-19O, K-19N, K-5, K-5O and K-5N cells (see material & methods) were grown in a synthetic raffinose-based medium to an OD_{600} of 0.6-0.7. A. After a 1 h- or 2 h-galactose induction, Total protein was extracted and normalized before being subjected to SDS-PAGE. The levels of E3_19 constructs were detected by immunoblotting with the anti-HA antibody. B. After a 1h-galactose induction, proteins were extracted and subjected to SDS-PAGE. The levels of E3_5 constructs were detected by immunoblotting with the anti-HA antibody. E3_5 negative control ran as several bands, this very stable protein was often difficult to denature properly. The completely denatured product is shown with an arrow. E3_5-ODC could not be detected. C. The experiment was repeated for E3_5-ODC with a longer galactose incubation of 3 h or 4 h. The size marker is indicated in kDa. Theoretical molecular weights: E3_5, E3_19 (18 kDa), E3_5-ODC , E3_19-ODC (22 kDa), E3_5-NYV, E3_19-NYV (23 kDa)

Expression of degron constructs under MG132 treatment

In order to investigate if the lower amounts of ODC- and NYV-constructs were really due to proteasomal degradation, their expression was monitored in the presence of MG132, a reversible proteasome inhibitor. For this assay, a special strain mutated for erg6, a sterol transmethylase involved in the biosynthesis of the membrane ergosterol, was used to increase the membrane permeability. E3_19-ODC accumulated quickly under MG132 treatment while E3_19-NYV could do so only after an overnight incubation with the proteasome inhibitor (Fig. 6). Similar results were obtained for the GFP-constructs. The ODC- and NYV-degrons did lead the target proteins to the 26S proteasome. A longer MG132 treatment was required to properly detect the NYV-constructs than the ODC-constructs.

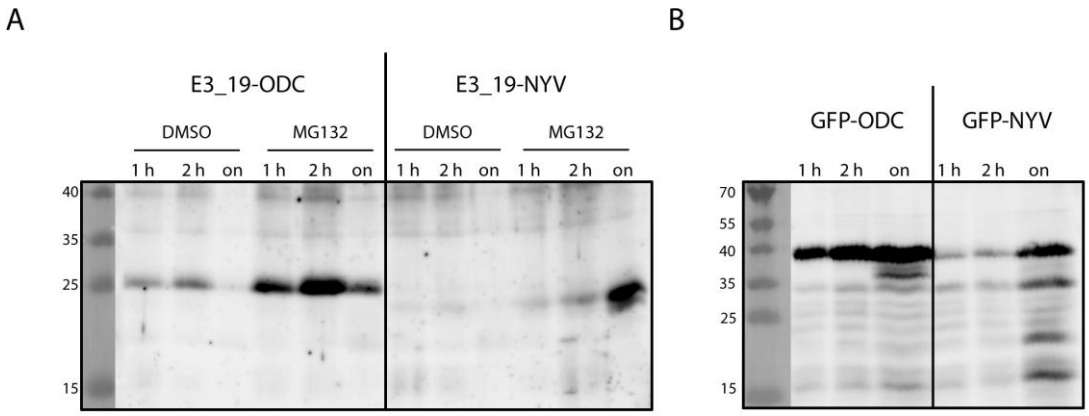

Figure 6: Steady-state expression levels of E3_19 (A) and GFP (B) degron constructs in presence of proteasome inhibitor MG132. A: E-19O and E-19N cells (see material & methods) were grown in a synthetic raffinose-based medium to an OD_{600} of 0.6-0.8. Galactose was then added to the cultures at the same time as DMSO or 50 µM MG132. After 1 h-, 2 h- or an overnight-incubation, total protein was extracted and normalized before being subjected to SDS-PAGE. B: E-GO and E-GN cells (see material & methods) were grown in a synthetic raffinose-based medium to an OD_{600} of 0.6-0.8. Galactose was then added to the cultures at the same time as 50 µM MG132. After 1 h-, 2 h- or an overnight-incubation, total protein was extracted and normalized before being subjected to SDS-PAGE. The levels of E3_19 degron-constructs and GFP degron-constructs were detected by immunoblotting with the anti-HA antibody. The size marker is indicated in kDa.

Comparison of the stabilities of the degron constructs

When fused to a C-terminal degron sequence, target proteins were degraded by the 26S proteasome as concluded from the sensitivity to MG132 treatment. From the steady state and MG132 experiments, it seemed that the NYV-construct levels were lower than the ODC-construct ones. Their half-lives were then compared further. After a 2 to 4 h gal induction, the promoter was shut off by addition of glucose, the cells were shortly centrifuged, resuspended in a glucose-based synthetic medium and the target protein stabilities followed. Among all target proteins, only GFP could be detected at the beginning of the assay, when fused to a degron sequence (Fig. 7, Fig. 8). GFP-ODC had a half-life of less than an hour while GFP-NYV was already barely detectable at the time point 0. Even if their half-lives could not be properly compared as the initial amounts were not identical, this experiment did confirm that the NYV-degron was more efficiently targeting to and/or processed by the 26S proteasome than the ODC-degron. All other target proteins were so quickly degraded that they had already vanished when the stability

assay started, preventing any degradation comparison. It is still unclear why GFP seemed to resist more than the other tested proteins, its higher expression level might help it to counteract its own degradation. Another goal of this experiment was to assess if the substrate intrinsic stability could slow down the degradation process. The DARPins E3_5 and E3_19 differ indeed in their stabilities [41, 42], however they were both extremely quickly degraded when fused to the ODC-or NYV-sequence. Thus, the higher stability of E3_5 was not an issue for the proteasomal degradation. Surprisingly, E3_19 was much better expressed than E3_5 (Fig. 8), whereas only a few residues vary in their amino-acid sequences and the number of rare residues did not significantly differ either. To summarize, all target proteins were of high stability, they could however all be efficiently processed by the 26S proteasome.

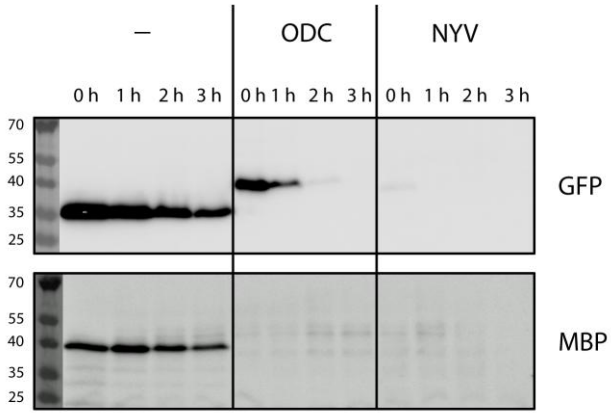

Figure 7: Stabilities of GFP and MBP constructs with and without degron sequences. K-G, K-GO, K-GN, K-M, K-MO and K-MN cells (see material & methods) were grown in a synthetic raffinose-based medium to an OD_{600} of 0.6. After a 2 h-galactose induction, glucose was added; cells were shortly centrifuged and resuspended in a glucose-based medium. Samples were withdrawn every hour. Total protein was extracted and normalized according to their OD_{600} before being subjected to SDS-PAGE. The levels of MBP and GFP constructs were detected by immunoblotting with the anti-HA antibody. The size marker is indicated in kDa.

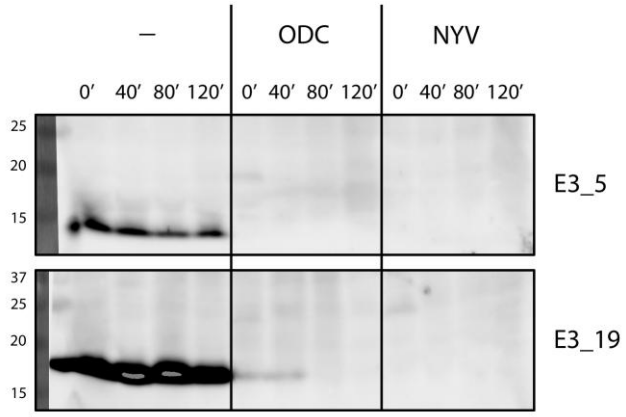

Figure 8: Stabilities of E3_5 and E3_19 constructs with and without degron sequences. K-5, K-5O, K-5N, K-19, K-19O and K-19N cells (see material & methods) were grown in a synthetic raffinose-based medium to an OD_{600} of 0.6. After a 4 h-galactose induction, glucose was added; cells were shortly centrifuged and resuspended in a glucose-based medium. Samples were withdrawn at the indicated time points. Total protein was extracted and normalized according to their OD_{600} before being subjected to SDS-PAGE, ran at 60°C. The levels of E3_5 and E3_19 constructs were detected by immunoblotting with the anti-HA antibody. The size marker is indicated in kDa.

Stabilities of degron constructs in the presence of a binding partner

Appending a degron sequence to the C terminus of a target protein led it to degradation. Would the presence of another protein interacting with the target protein prevent its proteasomal degradation? The influence of a binding partner on the degron construct's stability was studied by performing a co-expression experiment in a different set-up. The ODC- or NYV-degron sequence was fused to the DARPin off7, which recognizes MBP. The off7-degron constructs were designed identically to the E3_5 and E3_19 ones, described above. They were expressed on a plasmid, under the constitutive ADH promoter in a strain for which a RGS(His)$_6$ tagged MBP coding sequence had been integrated in the genome, under the control of a Gal1 promoter. The stabilities of off7-degron constructs were monitored after cycloheximide treatment in the absence or presence of RGS(His)$_6$ MBP in the cells. They were equally unstable in the absence or presence of RGS(His)$_6$ MBP (Fig. 9). off7-ODC could not be detected any more after 30 min. Remarkably, most of off7-NYV had also disappeared after 30 min, but then the degradation slowed down to reach a low level of off7-NYV which remained unchanged from 1 h until the end of the experiment. The starting amount of off7-degron constructs was lower in the presence of MBP but the co-expression of MBP protein might have temporarily decreased the expression level of off7-ODC and off7-NYV. In conclusion, the co-expression of a binding partner did not prevent or slow down off7-ODC or off7-NYV degradation.

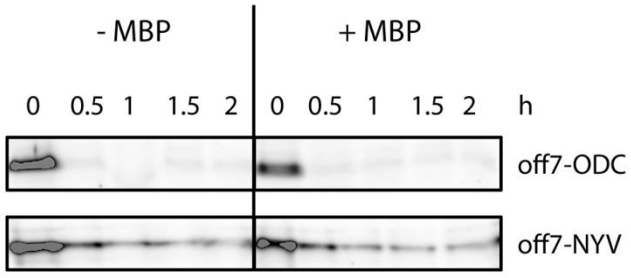

Figure 9: Stabilities of off7-degron constructs in the absence or presence of RGS(His)$_6$MBP. KM-7Ot and KM-7Nt cells (see material & methods) were grown in a synthetic raffinose-based medium to an OD_{600} of 0.6-0.8. The cultures were supplemented with galactose or glucose to induce or repress the expression of RGS(His)$_6$MBP. After 1 h 30 min, cycloheximide was added (t0) and samples were withdrawn every half-hour. Total protein was extracted and normalized according to their OD_{600} before being subjected to SDS-PAGE. The levels of off7-degron constructs were detected by immunoblotting with the anti-HA antibody.

The presence of a binding partner did not influence the degron construct's fate, but could the degron constructs lead the binding partner to the proteasome? To probe if the complex formed by the degron construct bound to its binding partner could be degraded, a second co-expression experiment was carried out. RGS(His)$_6$ MBP was expressed under the galactose promoter and then repressed by addition of glucose. Its stability was monitored in the absence or presence of constitutively expressed off7-ODC or off7-NYV. RGS(His)$_6$MBP remained stable, even when co-expressed with off7-ODC or off7-NYV (Fig. 10). The binding partner was not degraded.

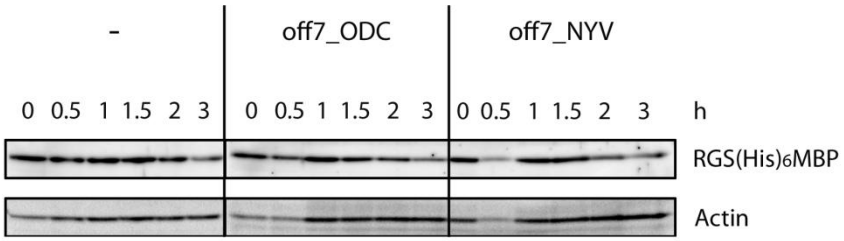

Figure 10: RGS(His)$_6$MBP stability in absence or presence of off7-degron constructs. KM-V, KM-7Oa and KM-7Na cells (see material & methods) were grown in a synthetic raffinose-based medium to an OD$_{600}$ of 0.6-0.8. RGS(His)$_6$MBP expression was induced for 1 h with galactose and stopped with glucose, cells were shortly centrifuged and resuspended in a glucose-based medium. Samples were withdrawn at the indicated time points. Total protein was extracted and normalized according to their OD$_{600}$ before being subjected to SDS-PAGE.. The levels of RGS(His)$_6$MBP were detected by immunoblotting with the anti-RGS(His)$_4$ antibody. The actin signal was used as loading control.

To ensure that off7, when fused to a degron sequence, was able to interact with RGS(His)$_6$MBP in vivo, a pull-down experiment was performed. Cells co-expressing RGS(His)$_6$MBP and off7-ODC or off7-NYV were lysed and magnetic Ni-NTA beads were used to retrieve RGS(His)$_6$MBP. off7-NYV co-eluted with RGS(His)$_6$MBP, showing that they could interact in vivo, but off7-ODC did not (Fig. 11). However, when off7-ODC was expressed and purified from *E. coli,* it could successfully bind RGS(His)$_6$MBP in vitro, identically to off7 (Fig. 16). Both off7-NYV and off7-ODC conserved their excellent binding properties, and thus they should theoretically be able to complex with RGS(His)$_6$MBP. Nevertheless, in vivo the interaction of a degron-construct with its binding partner might be weaker or considerably slower than the one with the 26S proteasome, leading to the degradation of the degron-constructs mostly in free form. The binding partner would in that case not be entering the proteasome if no complex was formed.

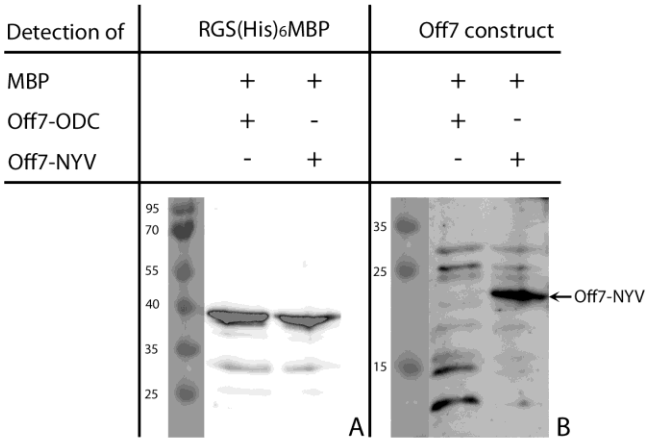

Figure 11: Pull-down of RGS(His)$_6$MBP coexpressed with off7-degron constructs. KM-7Oa and KM-7Na cells (see material & methods) were grown in a synthetic galactose-based medium to an OD_{600} of 0.7-0.8. RGS(His)$_6$MBP was pulled down from cell lysates by magnetic Ni-NTA beads. Eluted fractions were resolved by SDS-PAGE and probed with the anti-RGS(His)$_4$ antibody (A) and the anti-HA antibody (B). The size marker is indicated in kDa.

Off7-ODC degradation mutants

off7-ODC could not be detected in complex with RGS(His)$_6$MBP, it may possibly go too fast to the proteasome and thus not be able to interact with RGS(His)$_6$MBP before being degraded. In order to see if a binding partner could be brought to the proteasome in complex with a degron-construct, one would first need to delay the degron-dependent degradation process. ODC mutants were previously generated by mutating key residues of the mouse ODC PEST sequence (MODC) appended to the C-terminus of eGFP [30]. FACS analysis revealed several mutants with a range of half-lives (Fig. 12, Table 1). The mutations T436A and P438A (residues 436 and 438 of mouse ODC sequence) were shown to gradually diminish eGFP-ODC degradation in CHO cells. These mutations (identically named) were tested with off7-ODC expressed in yeast under the Gal1 promoter. No difference could be observed between the wt off7-ODC and the mutant T436A stabilities, but the degradation was slightly slowed down with the mutant P438A, especially until 15 min after promoter shut-off (Fig. 13)

Figure 12: Schematic map of the PEST sequence of EGFP-MODC-(422-461) and the position of the mutations.
Adapted from Li et al, 1998 [30].

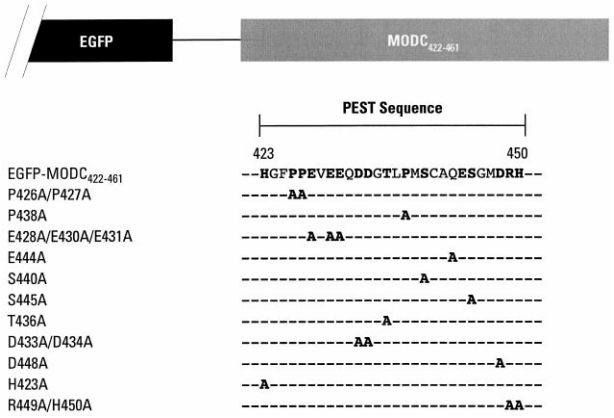

TABLE I
FACS analysis of EGFP, EGFP-MODC-(422–461), and mutations in transfected CHO K1 Tet-off cells

Transfection was performed in CHO/tTA cells using the procedure as described under "Experimental Procedures." After 24 h, cells were treated with CHX for 0, 2, and 4 h and analyzed for fluorescence intensity by FACS caliber (Becton Dickinson). The fluorescent cells at each time point are represented as a percentage of initial.

Constructs	0 h	Initial	2 h	4 h
	%		%	%
EGFP	100	(63.6)	107	92
EGFP-MODC-(422–461)	100	(12.6)	52	29
P426A/P427A	100	(11.5)	39	11
P438A	100	(34.1)	79	60
E428A/E430A/E431A	100	(17.3)	20	15
E444A	100	(12.6)	69	65
S440A	100	(21.6)	78	66
S445A	100	(23.5)	29	20
T436A	100	(46.9)	70	47
D433A/D434A	100	(11.31)	22	6
D448A	100	(32.6)	30	15
H423A	100	(12.2)	50	25
R449A/H450A	100	(27.9)	93	86

Adapted from Li et al, 1998.

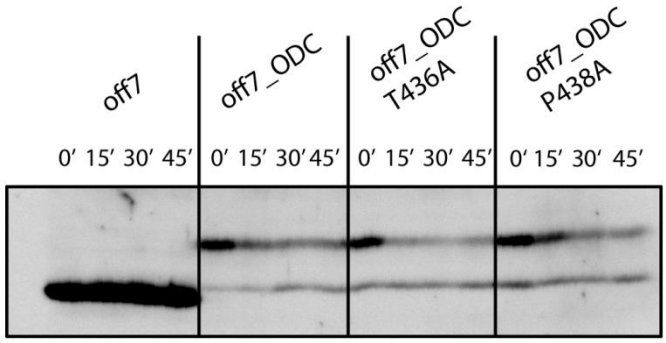

Figure 13: Stabilities of off7-ODC mutant constructs. K-7, K-7O, K-7O436 and K-7O438 cells (see material & methods) were grown in a synthetic raffinose-based medium to an OD_{600} of 0.6-0.8. After a 3 h galactose induction, glucose was added and samples were withdrawn every 15 min. Total protein was extracted and normalized according to the sample's OD_{600} before being subjected to SDS-PAGE. The levels of off7-ODC constructs were detected by immunoblotting with the anti-HA antibody.

These mutants were then assayed in co-expression with RGS(His)$_6$MBP to see if they would allow the binding partner's co-degradation. A regular decrease was observed for the RGS(His)$_6$MBP signal when its stability was monitored in presence of the mutants, while it stayed rather constant when expressed alone or in presence of the wt off7-ODC (Fig. 14A). However, this degradation was observed to a smaller extent when the experiment was repeated and with P438A only (Fig. 14B). By looking at the RGS(His)$_6$MBP and actin amounts, one can see that RGS(His)$_6$MBP level was consistently lower with the off7-ODC P438A than with the wt off7-ODC. The binding partner, when co-expressed with a more slowly degraded ODC-construct, seemed to be degraded as well, though, with a significantly lower degradation efficiency than for the ODC-construct itself.

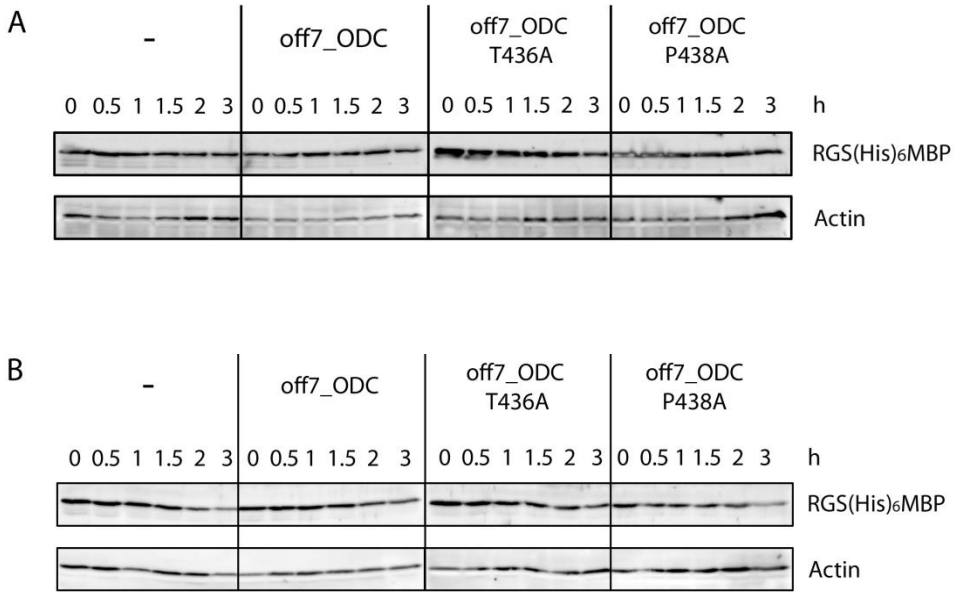

Figure 14: $RGS(His)_6MBP$ stability in the absence or presence of off7-degron mutant constructs. KM-V, KM-7Oa, KM-7O436a and KM-7O438a cells (see material & methods) were grown in a synthetic raffinose-based medium to an OD_{600} of 0.6-0.8. $RGS(His)_6MBP$ expression was induced for 1 h with galactose and stopped with glucose, cells were shortly centrifuged and resuspended in a glucose-based medium. Samples were withdrawn at the indicated time points. Total protein was extracted and normalized according to the sample's OD_{600} before being subjected to SDS-PAGE. The levels of $RGS(His)_6MBP$ were detected by immunoblotting with the anti-$RGS(His)_4$ antibody. The actin signal was used as loading control. A and B were two independent experiments.

In vitro degradation assay

Retarding own degradation of off7-ODC seemed to somewhat allow co-degrading MBP, its binding partner. Nevertheless the degradation efficiencies of both proteins were not comparable, off7-ODC quickly vanished (Fig. 9 & 13) while MBP level only moderately declined over 3 h (Fig. 14). This difference could result from an insufficient complex formation, due to the fast degradation of off7-ODC or by the incomplete processing of a complex by the 26S proteasome. In order to further investigate these hypotheses, an in vitro system was set up using mammalian partially purified 26S proteasomes and an energy regenerating system. Both off7-ODC and MBP were expressed in *E. coli* and purified on IMAC. off7-ODC carried an N-terminal $RGS(His)_6$ tag. MBP was expressed as a fusion protein with an N-terminal AviTag for in vivo biotinylation and a C-terminal $(His)_6$ tag (Fig. 15).

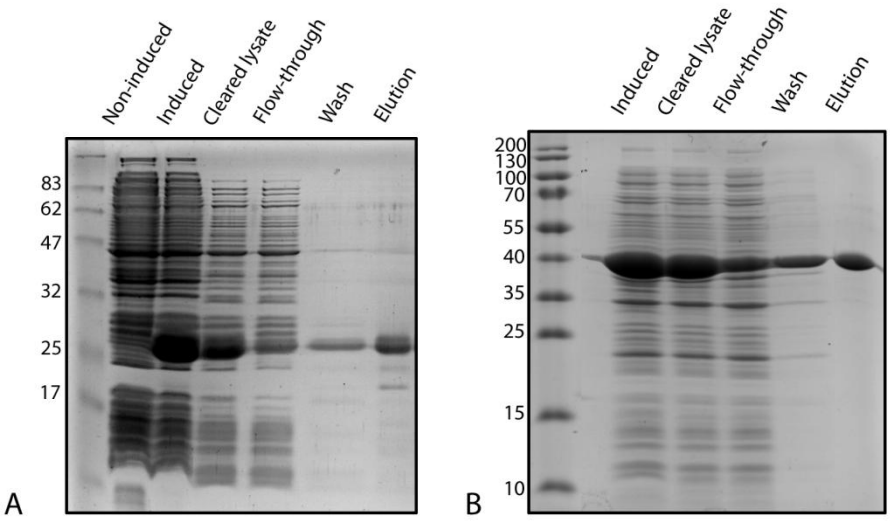

Figure 15: Expression and purification of Off7-ODC (A) and MBP (B). Off7-ODC and MBP were expressed in *E. coli* and purified on a single-step IMAC. The proteins were visualized on a 15% SDS PAGE stained with Coomassie Brilliant Blue. The size marker is indicated in kDa. MBP molecular weight: 43 kDa, Off7-ODC: 22 kDa

The affinity of off7-ODC for MBP was tested in vitro using the octet biosensor platform which enables the analysis of biomolecular interactions. The binding constants were very similar to the wild-type off7 (K_D= 10. 5 nM vs 9.8 nM), proving that the ODC tag did not interfere with off7 binding surface (Fig. 16).

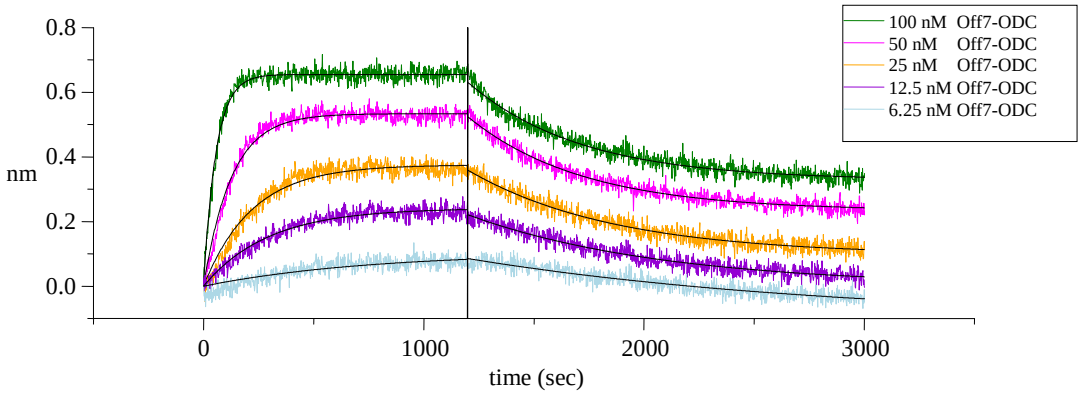

Figure 16: Figure 16: Octet biosensor analysis of Off7-ODC. A MBP-coated biosensor was incubated for 2 min with different concentrations of Off7-ODC (6.25; 12.5; 25; 50; 100 nM) and followed by 30 min with running buffer. Binding curves were separately fitted with a 1:1 model (black lines).

A first experiment was performed to assess if off7-ODC alone could be degraded in our in vitro system. The reaction was performed at 37°C using a 1: 1 molar ratio between off7-ODC and the 26S proteasome. Despite the favorable conditions and an incubation of up to 4h, off7-ODC levels did not decrease, indicating that it was not degraded in vitro. After an overnight incubation, the level was only slightly

reduced. Another protein present in the degradation mixture was recognized as well by the anti-RGS(His)$_4$ Ab (below 70 KDa), it stayed at the same level (Fig. 17). In the in vitro conditions used, off7-ODC degradation was extremely small and not comparable to what was observed in vivo.

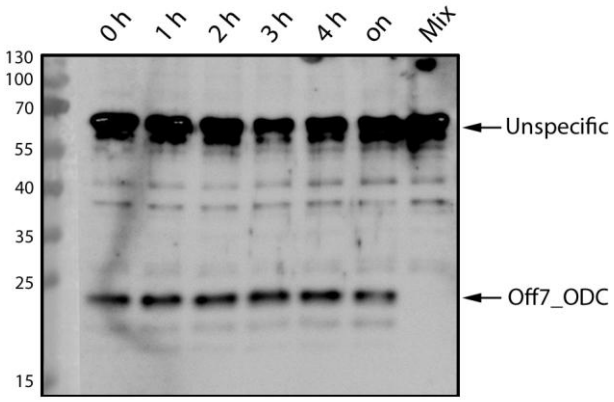

Figure 17: In vitro degradation assay for off7-ODC. The reaction was performed at 37°C. Samples were taken at the indicated time points after addition of off7-ODC to the degradation mix. They were subjected to SDS-PAGE and the levels of off7-ODC were detected by immunoblotting with an anti-RGS(His)$_4$ antibody. The additional band running between 55 and 70 kDa corresponded to another protein present in the degradation mix which was recognized by the anti-RGS(His)$_4$ antibody. The size marker is indicated in kDa.

In order to use an even more accessible substrate, off7-ODC was first denatured 5' at 95°C before being added to the in vitro assay. off7 had indeed been described to fully denature at 95°C (K.Binz, unpublished data). Under these conditions, the amount of off7-ODC did significantly decrease (Fig. 18). Nonetheless, the amount of total protein in the degradation mixture seemed to have also been altered. Indeed the amount of unspecific protein (below 70 KDa) present in the degradation mix and also recognized by the anti-RGS(His)$_4$ Ab, was indeed much lower in samples, for which off7-ODC had been pre-incubated at 95°C than 4°C.

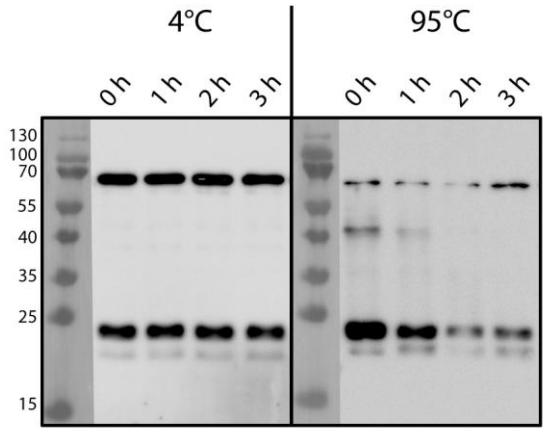

Figure 18: In vitro degradation assay for off7-ODC after partial denaturation. Off7-ODC was first incubated for 5 min at 4°C or 95°C before being shortly centrifuged and added to the degradation mix. The reaction was performed at 37°C. Samples were taken every hour and subjected to SDS-PAGE. The levels of off7-ODC were detected by immunoblotting with an anti-RGS(His)$_4$ antibody. The additional band running between 55 and 70 kDa corresponded to another protein present in the degradation mix which was recognized by the anti-RGS(His)$_4$ antibody (see Fig. 15). The size marker is indicated in kDa.

To make sure that off7-ODC level decrease was due to a degradation process and not an unspecific aggregation, the experiment was repeated. The off7-ODC level was monitored again after a heat denaturation step but this time in the absence or presence of the proteasome. In both cases, the amount of off7-ODC decreased. Therefore the decrease was not proteasome-dependent but rather due to an unspecific heat-induced process (Fig. 19). Curiously, off7-ODC level decreased even faster when the reaction was performed without proteasome. We concluded that off7-ODC alone could not be successfully degraded in our in vitro system. The degradation of a complex could then not be further studied.

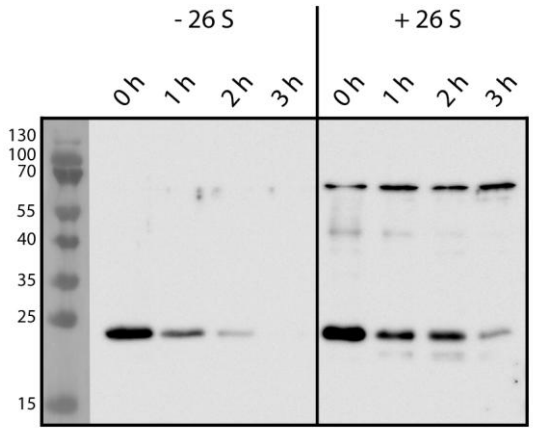

Figure 19: Second in vitro degradation assay for off7-ODC after partial denaturation. Off7-ODC was first incubated for 5 min at 95°C before being shortly centrifuged and added to the degradation mix. The reaction was performed at 37°C in absence or presence of the 26S proteasome. Samples were taken every hour and subjected to SDS-PAGE. The levels of off7-ODC were detected by immunoblotting with the anti-RGS(His)$_4$ antibody. The additional band running between 55 and 70 kDa corresponded to another protein present in the proteasome preparation which was recognized by the anti-RGS(His)$_4$ antibody. The size marker is indicated in kDa.

Discussion

Ornithine Decarboxylase was the first protein described to be degraded in an ubiquitin-independent manner. Its degron sequence has been considerably investigated and previous studies have already proven its efficacy when fused to several target proteins in both yeast and mammalian cells [22, 29, 30]. The NYV-degron which was recently identified in the cytoplasmic tail of the G1 glycoprotein of the NY-1 hantavirus has not been much examined yet [31]. It has been shown to destabilize GFP when expressed as a fusion protein in mammalian cells. In this study, we found that the NYV-degron was also recognized by the yeast proteasome and able to act as a destabilizing element when fused to several proteins. In fact, the NYV-degron seemed even more proficient than the ODC-degron when comparing their effect on the steady-state level of two target proteins, namely GFP and the DARPin E3_19. In contrast, the effects of ODC- and NYV-degrons on MBP steady-state level were similar. The NYV-constructs also required a longer proteasome inhibitor treatment than the ODC ones before accumulating in the cells, while the DARPin fusion E3_19-NYV accumulated only after 24h, the fusion E3_19-ODC was already slowly lost after this time. The degradation efficiencies of the ODC- and NYV-degrons were intended to be further analyzed while monitoring the half-life of the different constructs after promoter shut-off (Fig. 7 and 8). However, the rapidness of the degradation process prevented us to compare the stabilities of most target proteins in our experimental set-up. This assay could eventually only confirm that the GFP-NYV was being faster degraded than GFP-ODC. A radioactive pulse-chase assay would probably be required to compare the relative destabilization induced by the ODC- or NYV-degron at the very low steady-state levels.

It is possible that the ODC- and NYV-degrons differ in their affinity for the proteasome. This would justify their different destabilizing effects observed when they were appended to the same target protein, e.g. GFP. In a similar way, the ODC- and NYV-degrons could not follow the same pathway to the proteasome. Indeed, when their stability was studied after cycloheximide treatment, they did not behave similarly. off7-ODC immediately disappeared while the level of off7-NYV also quickly dropped, before reaching a constant low basal level. These results differed from the previous ones when the target protein stability was followed after promoter shut-off and where the NYV-constructs were completely and more rapidly degraded than the ODC-ones. It is likely that the cycloheximide treatment did also deplete the cell of one of the components involved in the NYV-constructs degradation but not in the ODC-constructs degradation. This could be a short-lived protein, directly or indirectly involved in the recognition of the NYV-degron sequence by the proteasome, e.g. a docking site at the proteasome, or a specific shuttle protein mediating the transport and/or recognition of NYV-substrates.

Different target proteins were tested and the entire set of degron-constructs could be degraded without exception. All chosen target proteins were previously described as relatively stable and well expressed ones [41-45]. MBP is often used as carrier protein for the production of fusion proteins in *E. coli* to improve their yield and facilitate their purification [46]. It also often increases the stability and solubility

of the passenger protein [47]. Structurally, it consists of two strongly interacting globular domains. GFP is exceptional for its structural stability, high expression and fluorescent properties. It is widely used as a reporter to monitor gene expression and localization [48]. Its unique structural motif consists of an 11-stranded ß-barrel which forms a cylinder around the chromophore [44]. Finally, DARPins were designed to possess very favorable biophysical properties. They are soluble, very well expressed (up to 200 mg/L culture) in *E. coli*, show the typical ankyrin repeat domain fold and stable [42]. E3_5 was even described as extremely stable with a melting temperature higher than 85°C while E3_19 was melting at 66°C [41]. Nevertheless no distinction could be observed between the two DARPins, at least in our experimental set-up. In fact, among the different target proteins tested; GFP-ODC seemed to be the "most difficult" substrate. Its measured half-life of less than an hour was close to the previously reported one of 1 to 2 hours when GFP-ODC was expressed in CHO cells [30]. When comparing the resistance of the different target proteins to chemical denaturation and their free energy of unfolding, E3_5 could be expected to be the most challenging substrate (Table 5). However GFP unfolding was described as a slow and stepwise process with a native-like intermediate state [49]. Its high kinetic barrier to unfolding could explain why it appeared to be less rapidly degraded than the other target proteins. It should be noted that GFP was quickly degraded when fused to the NYV degron sequence and a more precise comparison of all NYV-constructs half-lives would be needed to validate this hypothesis. The kinetic studies of several model proteasome substrates have demonstrated that unfolding is a rate-limiting step for their degradation. Methotrexate, a dihydrofolate reductase (DHFR) ligand, has been shown to stabilize the enzyme through binding. This ligand also impaired the proteasomal degradation of DHFR when the enzyme was fused to a Lys48 polyUb chain or the ODC degron [8, 20].

Target protein	Dm, M	Meas. Temp., C	ΔG , kcal/mol	Unfolding model
MBP [1]	1.1	25	12.9	Two-state
GFP [2]	1.7[a] and 4.3[b]	25	10.8	Three-state
E3_5 [3]	5	23	14.8	Two-state
E3_19 [3]	2.9	23	9.6	Two-state

Table 5: Thermodynamic parameters for guanidinium chloride denaturation of target proteins.
The data was gathered from : Fox, et al. (2001) [50] ; Xie and Zhou (2008) [49]; Kohl et al. (2003) [42]. Dm is the midpoint denaturation concentration of guanidinium chloride at the measurement temperature indicated. ΔG is the free energy of unfolding extrapolated to zero denaturant concentration assuming the indicated unfolding model.
midpoint concentration between the native and intermediate state [a]
midpoint concentration between the intermediate and unfoldingstate [b]

The co-expression of a binding partner had no effect on the degron-constructs stabilities and vice-versa. The degron construct was still degraded at the same rate while no destabilization was observed for the binding partner. The presence of the degron sequence did not alter the binding properties of off7 for MBP but it might have prevented an efficient complex formation between the two proteins. Indeed, the degradation process of off7 degron-constructs was remarkably fast. It is then possible that complex formation did not occur for this reason alone. In mammalian cells and yeast, pulse-chase experiments demonstrated that ornithine decarboxylase was mostly degraded before it completed folding [51, 52]. It was thus plausible that the degron-constructs were undergoing degradation immediately after

translation and that they could not completely fold and /or interact with the binding partner before going to the proteasome. To verify this hypothesis, mutations which had been previously identified to slow down the degradation process [30], were introduced in the ODC sequence fused to the DARPin off7. Their effect on off7 stability was less pronounced than what had been observed for GFP-ODC but our experimental data showed that the DARPins were anyhow faster degraded than GFP, so it might have been more problematic to monitor how the degradation kinetic was affected in this context as all of them remained to be degraded too fast to be accurately measured. These off7-ODC mutants were co-expressed with a cognate binding partner, RGS(His)$_6$MBP which seemed to be partially degraded, but only to a very low extent compared to the degradation of the cognate DARPin-degron fusion. Either the mutated off7-ODC constructs were still degraded too fast and only a small fraction of RGS(His)$_6$MBP could bind to them and be brought to the proteasome, or the entire complex was going to the proteasome, but RGS(His)$_6$MBP was not degraded along. It could be that the 19S subunit was interacting with the degron-construct solely and that RGS(His)$_6$MBP could not penetrate the proteasome. Alternatively, the whole complex might enter the proteasome but upon unfolding of the degron-construct in the 19S particle, the binding partner could dissociate and escape if not trapped by a specific recognition element.

In yeast and mammals, when the ornithine decarboxylase is bound to the antizyme 1 (AZ1), it can be better recognized and processed by the proteasome, but AZ1 is apparently not degraded along with the ornithine decarboxylase [18]. In ornithine decarboxylase overproducing 653-1 mouse myeloma cells, ODC and AZ1 differed in their rate of degradation and AZ1 degradation relied on a functional ubiquitin system [53]. In yeast, ubiquitinated forms of AZ1 were also detected, suggesting that AZ1 degradation occurs mostly if not only independently of ornithine decarboxylase [18]. A protein might not solely need to interact with the proteasome to be processed as a substrate. The presence of a degradation signal might be required, and/or only a moderate structural stability might be tolerated to enable an efficient and rapid unfolding. Even if we have observed that MBP, when fused to the ODC- or NYV- degron could be well processed by the proteasome, it cannot be excluded that the degron sequence not only directed MBP to the proteasome but also promoted its unfolding in the 19S subunit. This unstructured peptide stretch at the C-terminus of the substrate could function as an initiation site, engaging the proteasome unfolding machinery [23, 54]. It was indeed observed that the proteasome initiated degradation of mouse ornithine decarboxylase at its C-terminus where its degron sequence is located [25]. Unfused MBP would, in that case, not constitute an identical substrate to MBP-ODC or MBP-NYV, and its unfolding might have been more problematic.

In vitro degradation experiments would have been very beneficial to observe the potential degradation of a complex. It would have been more appropriate to monitor the stability of a degradation-prone protein and a non degradation-prone binding partner. We tried to set-up such an in vitro assay, but unfortunately, off7-ODC, which was very unstable in vivo, was not degraded in vitro. Similar results have been reported for other studies, e.g. GFP-ODC was not destabilized in an in vitro system either [20]. In the same way, when produced in *E. coli*, mouse ornithine decarboxylase could only be degraded to 10-15% by purified yeast or rat 26S proteasomes [29], while up to 70% of in vitro translated protein could be deprived in a reticulocyte lysate fraction II [15]. Important co-factors, normally associated with the proteasome could have then been missing in our in vitro experimental set-up. Chaperone proteins

extrinsic to the proteasome might participate in unfolding the substrate. To test this hypothesis, off7-ODC was first shortly heat-denatured before being added to the in vitro assay, but this substrate was not degraded, either. It is nevertheless possible that once denatured, the off7 structure was altered and its ODC degron sequence not exposed anymore, or that off7 aggregated to the bottom of the assay tube and was not available anymore for degradation. Its decreasing amount, even in the absence of 26S proteasomes in the assay, could favor this last explanation, but part of it was still in solution until the end of the experiment and should have been an appropriate substrate. Shuttle proteins which would help mediating off7-ODC interaction with the proteasome could have also been missing in the in vitro system. However, previous results have shown that even if GFP-ODC could not be processed in vitro, it was still able to interact with the proteasome by inhibiting the degradation of mouse ornithine decarboxylase [20]. This could be consistent with the observation that, when denatured off7-ODC was used as a substrate, its level decreased faster in absence of proteasome. off7-ODC was most likely interacting with the proteasome which could keep it longer in solution but not degrade it.

Overall, our data showed that in vivo the yeast 26S proteasome could process all tested substrates in spite of their intrinsic stability or slow unfolding properties, as long as they were fused to the ODC- or NYV-degron sequence. It is reasonable to assume that this degradation did mostly take place shortly after the translation. The 26S proteasome might be able to efficiently process these proteins only before they reach their folded state. It has been demonstrated that ornithine decarboxylase was mostly degraded before it completed folding and that mature proteins could still turnover, but to a lower extent [51, 52]. This could explain why a purified degron-fusion could not be degraded in vitro. It is still unclear if a co-expressed binding partner could be led to the 26S proteasome and co-degraded as we found so far no clear evidence for this reaction. Another set-up allowing the exposure of the degron-sequence upon induction would allow controlling degradation in a time-manner and better comprehending how the degron-constructs and possibly binding partners are processed by the proteasome. If a complex could indeed be degraded, further investigating the prerequisites of the binding partner making it eligible for degradation would also help understanding how the proteasome selects its substrates and degrades them.

Annex

Vector maps

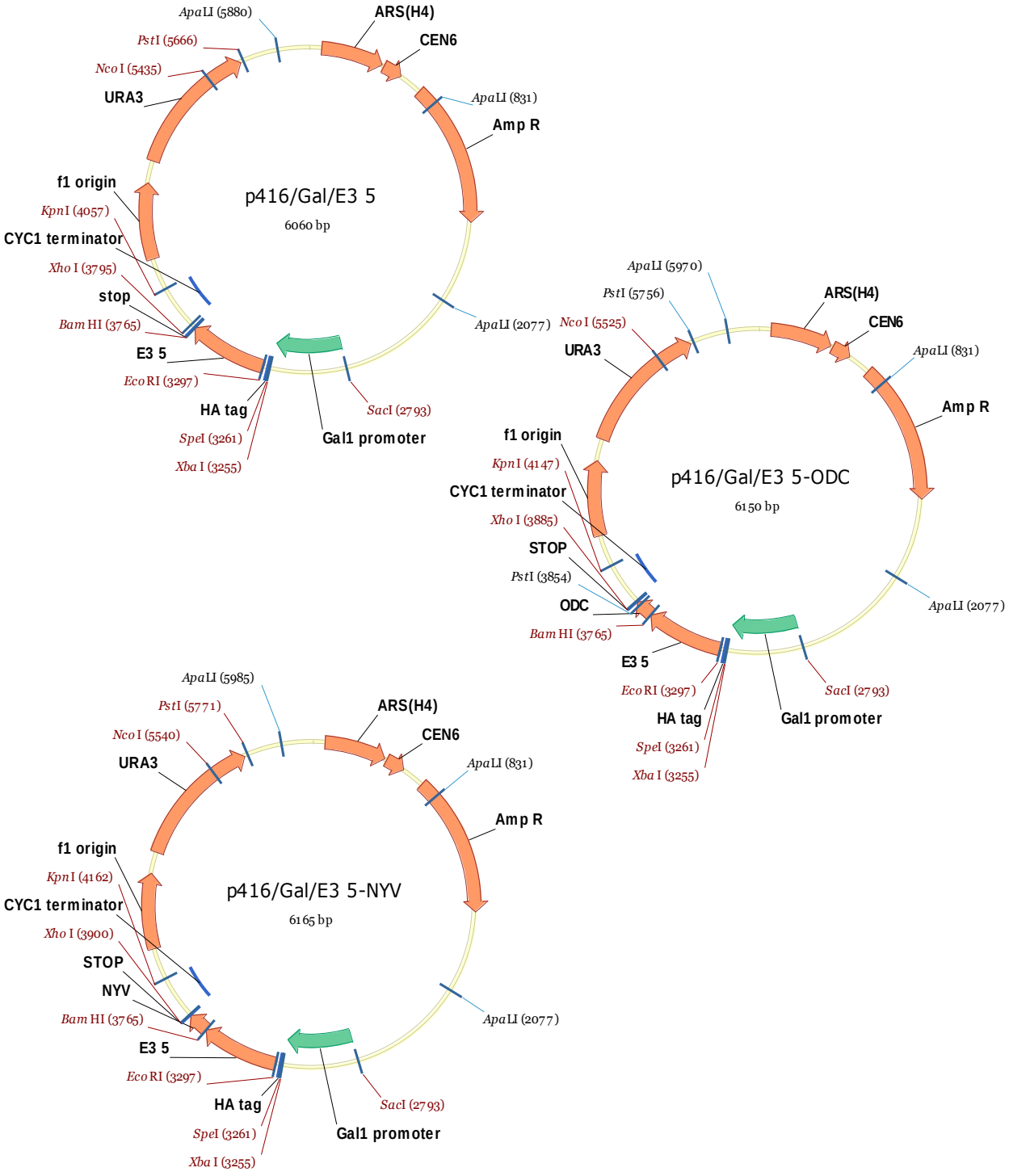

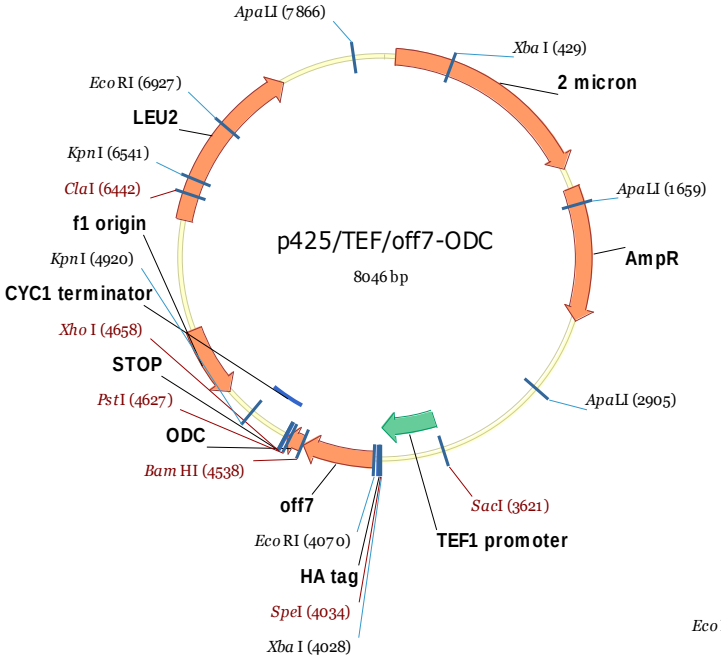
ApaLI (7866)
Xba I (429)
2 micron
EcoRI (6927)
LEU2
KpnI (6541)
ClaI (6442)
ApaLI (1659)
f1 origin
AmpR
p425/TEF/off7-ODC
8046 bp
KpnI (4920)
CYC1 terminator
Xho I (4658)
STOP
ApaLI (2905)
PstI (4627)
ODC
Bam HI (4538)
off7
SacI (3621)
EcoRI (4070)
TEF1 promoter
HA tag
SpeI (4034)
Xba I (4028)

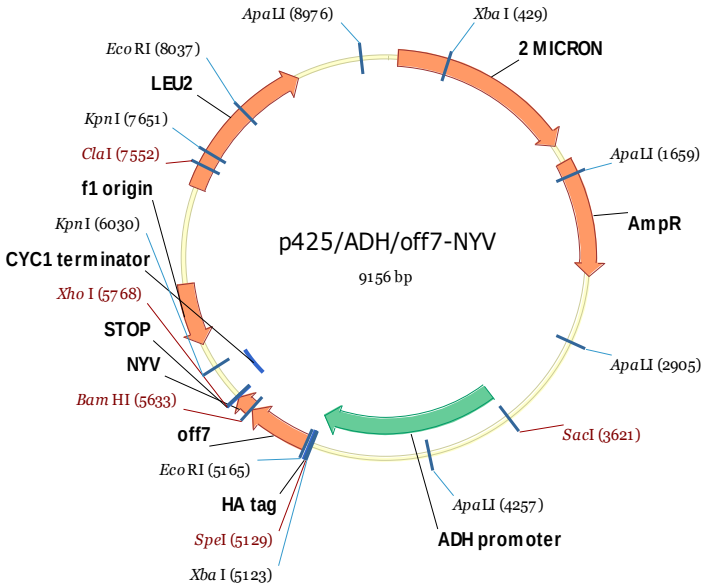
ApaLI (8976)
Xba I (429)
2 MICRON
EcoRI (8037)
LEU2
KpnI (7651)
ClaI (7552)
ApaLI (1659)
f1 origin
AmpR
KpnI (6030)
p425/ADH/off7-NYV
9156 bp
CYC1 terminator
Xho I (5768)
STOP
ApaLI (2905)
NYV
Bam HI (5633)
SacI (3621)
off7
EcoRI (5165)
HA tag
ApaLI (4257)
SpeI (5129)
ADH promoter
Xba I (5123)

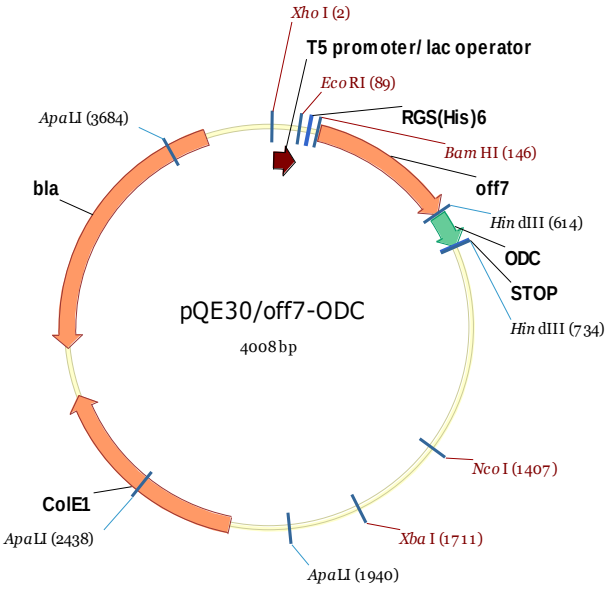
Xho I (2)
T5 promoter/ lac operator
EcoRI (89)
ApaLI (3684)
RGS(His)6
Bam HI (146)
bla
off7
Hin dIII (614)
ODC
STOP
pQE30/off7-ODC
4008 bp
Hin dIII (734)
NcoI (1407)
ColE1
Xba I (1711)
ApaLI (2438)
ApaLI (1940)

Construct DNA and amino-acid sequences

E3_5-stop construct DNA sequence

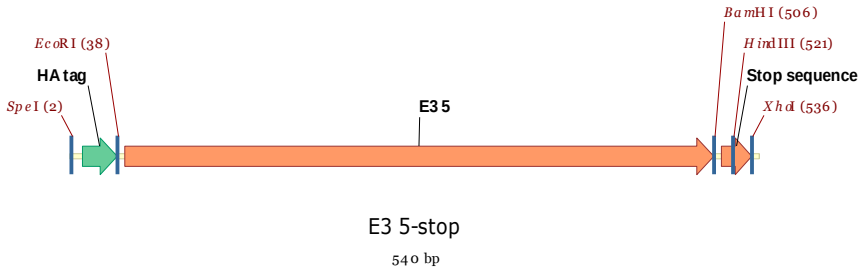

actagtatgtacccatacgatgttccagattacgctgaattcgacctgggtaagaaactgctggaagctgctcgtgctggtcaggacgacgaagttcgt
atcctgatggctaacggtgctgacgttaacgctactgacaatgatggttatactccgctgcacctggctgcttctaatggtcacctggaaatcgttgaagt
tctgctgaagaacggtgctgacgttaacgcttctgaccttactggtattactccgctgcacctggctgctgctactggtcacctggaaatcgttgaagttct
gctgaagcacggtgctgacgttaacgcttatgacaatgatggtcatactccgctgcacctggctgctaagtatggtcacctggaaatcgttgaagttctg
ctgaagcacggtgctgacgttaacgctcaggacaaattcggtaagaccgctttcgacatctccatcgacaacggtaacgaggacctggctgaaatcct
gcaaggatcctaatagtgaaagcttttagctgacctcgag

E3_5-stop amino-acid sequence

MYPYDVPDYAEFDLGKKLLEAARAGQDDEVRILMANGADVNATDNDGYTPLHLAASNGHLEIVEVLLKNGADVNASD
LTGITPLHLAAATGHLEIVEVLLKHGADVNAYDNDGHTPLHLAAKYGHLEIVEVLLKHGADVNAQDKFGKTAFDISIDNG
NEDLAEILQGS

E3_5-ODC construct DNA sequence

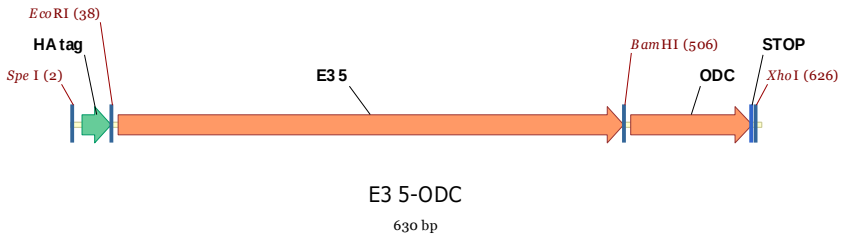

actagtatgtacccatacgatgttccagattacgctgaattcgacctgggtaagaaactgctggaagctgctcgtgctggtcaggacgacgaagttcgt
atcctgatggctaacggtgctgacgttaacgctactgacaatgatggttatactccgctgcacctggctgcttctaatggtcacctggaaatcgttgaagt
tctgctgaagaacggtgctgacgttaacgcttctgaccttactggtattactccgctgcacctggctgctgctactggtcacctggaaatcgttgaagttct
gctgaagcacggtgctgacgttaacgcttatgacaatgatggtcatactccgctgcacctggctgctaagtatggtcacctggaaatcgttgaagttctg
ctgaagcacggtgctgacgttaacgctcaggacaaattcggtaagaccgctttcgacatctccatcgacaacggtaacgaggacctggctgaaatcct
gcaaggatccttcccgccggaggtggaggagcaggatgatggcacgctgcccatgtcttgtgcccaggagagcgggatggaccgtcaccctgcagcct
gtgcttctgctaggatcaatgtgtagctcgag

E3_5-ODC amino-acid sequence

MYPYDVPDYAEFDLGKKLLEAARAGQDDEVRILMANGADVNATDNDGYTPLHLAASNGHLEIVEVLLKNGADVNASD
LTGITPLHLAAATGHLEIVEVLLKHGADVNAYDNDGHTPLHLAAKYGHLEIVEVLLKHGADVNAQDKFGKTAFDISIDNG
NEDLAEILQGSFPPEVEEQDDGTLPMSCAQESGMDRHPAACASARINV

E3_5-NYV construct DNA sequence

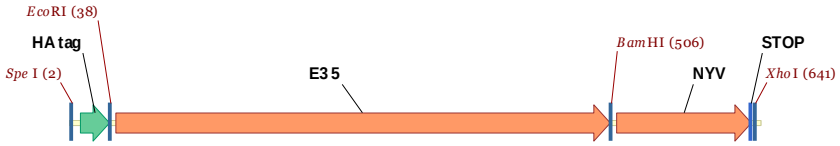

E3 5-NYV

645 bp

actagtatgtacccatacgatgttccagattacgctgaattcgacctgggtaagaaactgctggaagctgctcgtgctggtcaggacgacgaagttcgt
atcctgatggctaacggtgctgacgttaacgctactgacaatgatggttatactccgctgcacctggctgcttctaatggtcacctggaaatcgttgaagt
tctgctgaagaacggtgctgacgttaacgcttctgaccttactggtattactccgctgcacctggctgctgctactggtcacctggaaatcgttgaagttct
gctgaagcacggtgctgacgttaacgcttatgacaatgatggtcatactccgctgcacctggctgctaagtatggtcacctggaaatcgttgaagttctg
ctgaagcacggtgctgacgttaacgctcaggacaaattcggtaagaccgctttcgacatctccatcgacaacggtaacgaggacctggctgaaatcct
gcaaggatcccgccctgaagttaaacaaggatgctatagaacattgggtgtttttagatataagagtaggtgttatgttggtcttgtgtgggggtccttc
ttacaactgaactcatagtttgggcagctagtgcttagctcgag

E3_5-NYV amino-acid sequence

MYPYDVPDYAEFDLGKKLLEAARAGQDDEVRILMANGADVNATDNDGYTPLHLAASNGHLEIVEVLLKNGADVNASD
LTGITPLHLAAATGHLEIVEVLLKHGADVNAYDNDGHTPLHLAAKYGHLEIVEVLLKHGADVNAQDKFGKTAFDISIDNG
NEDLAEILQGSRPEVKQGCYRTLGVFRYKSRCYVGLVWGVLLTTELIVWAASA

Off7-ODC construct DNA sequence

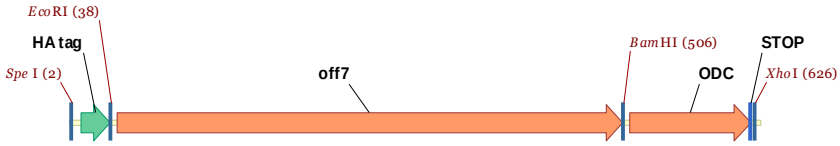

0ff7-ODC

630 bp

Actagtatgtacccatacgatgttccagattacgctgaattcgacctgggtaagaaactgctggaagctgctcgtgctggtcaggacgacgaagttcgt
atcctgatggctaacggtgctgacgttaatgctgctgacaatactggtactactccgctgcacctggctgcttattctggtcacctggaaatcgttgaagt
tctgctgaagcacggtgctgacgttgacgcttctgacgtttttggttatactccgctgcacctggctgcttattggggtcacctggaaatcgttgaagttct
gctgaagaacggtgctgacgttaacgctatggactctgatggtatgactccactgcacctggctgctaagtggggttacctggaaatcgttgaagttctg
ctgaagcacggtgctgacgttaacgctcaggacaaattcggtaagaccgctttcgacatctccatcgacaacggtaacgaggacctggctgaaatcct
gcaaggatccttcccgccggaggtggaggagcaggatgatggcacgctgcccatgtcttgtgcccaggagagcgggatggaccgtcaccctgcagcct
gtgcttctgctaggatcaatgtgtagctcgag

Off7-ODC amino-acid sequence

MYPYDVPDYAEFDLGKKLLEAARAGQDDEVRILMANGADVNAADNTGTTPLHLAAYSGHLEIVEVLLKHGADVDASD
VFGYTPLHLAAYWGHLEIVEVLLKNGADVNAMDSDGMTPLHLAAKWGYLEIVEVLLKHGADVNAQDKFGKTAFDISID
NGNEDLAEILQGSFPPEVEEQDDGTLPMSCAQESGMDRHPAACASARINV

Off7-NYV construct DNA sequence

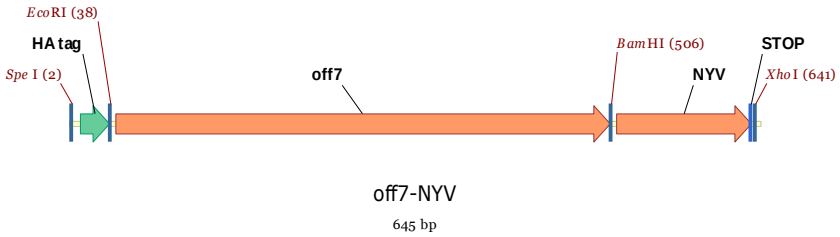

actagtatgtacccatacgatgttccagattacgctgaattcgacctgggtaagaaactgctggaagctgctcgtgctggtcaggacgacgaagttcgt
atcctgatggctaacggtgctgacgttaatgctgctgacaatactggtactactccgctgcacctggctgcttattctggtcacctggaaatcgttgaagt
tctgctgaagcacggtgctgacgttgacgcttctgacgtttttggttatactccgctgcacctggctgcttattggggtcacctggaaatcgttgaagttct
gctgaagaacggtgctgacgttaacgctatggactctgatggtatgactccactgcacctggctgctaagtggggttacctggaaatcgttgaagttctg
ctgaagcacggtgctgacgttaacgctcaggacaaattcggtaagaccgctttcgacatctccatcgacaacggtaacgaggacctggctgaaatcct
gcaaggatcccgccctgaagttaaacaaggatgctatagaacattgggtgtttttagatataagagtaggtgttatgttggtcttgtgtgggggtccttc
ttacaactgaactcatagtttgggcagctagtgcttagctcgag

Off7-NYV amino-acid sequence

MYPYDVPDYAEFDLGKKLLEAARAGQDDEVRILMANGADVNAADNTGTTPLHLAAYSGHLEIVEVLLKHGADVDASD
VFGYTPLHLAAYWGHLEIVEVLLKNGADVNAMDSDGMTPLHLAAKWGYLEIVEVLLKHGADVNAQDKFGKTAFDISID
NGNEDLAEILQGSRPEVKQGCYRTLGVFRYKSRCYVGLVWGVLLTTELIVWAASA

RGS(His)$_6$off7-ODC construct DNA sequence

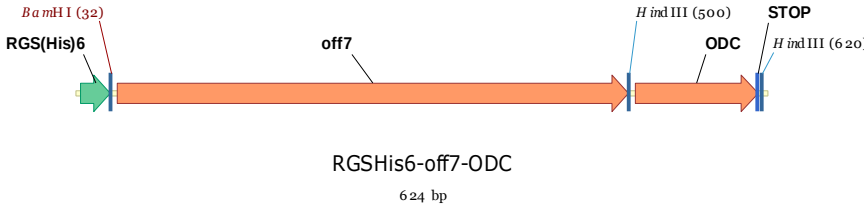

Atgagaggatcgcatcaccatcaccatcacggatccgacctgggtaagaaactgctggaagctgctcgtgctggtcaggacgacgaagttcgtatcct
gatggctaacggtgctgacgttaatgctgctgacaatactggtactactccgctgcacctggctgcttattctggtcacctggaaatcgttgaagttctgc
tgaagcacggtgctgacgttgacgcttctgacgtttttggttatactccgctgcacctggctgcttattggggtcacctggaaatcgttgaagttctgctga
agaacggtgctgacgttaacgctatggactctgatggtatgactccactgcacctggctgctaagtggggttacctggaaatcgttgaagttctgctgaa
gcacggtgctgacgttaacgctcaggacaaattcggtaagaccgctttcgacatctccatcgacaacggtaacgaggacctggctgaaatcctgcaaa
agcttttcccgccggaggtggaggagcaggatgatggcacgctgcccatgtcttgtgcccaggagagcgggatggaccgtcaccctgcagcctgtgctt
ctgctaggatcaatgtgtagaagctt

RGS(His)$_6$off7-ODC amino-acid sequence

MRGSHHHHHHGSDLGKKLLEAARAGQDDEVRILMANGADVNAADNTGTTPLHLAAYSGHLEIVEVLLKHGADVDAS
DVFGYTPLHLAAYWGHLEIVEVLLKNGADVNAMDSDGMTPLHLAAKWGYLEIVEVLLKHGADVNAQDKFGKTAFDISI
DNGNEDLAEILQKLFPPEVEEQDDGTLPMSCAQESGMDRHPAACASARINV

References

1. Coffino, P., *Regulation of cellular polyamines by antizyme.* Nat Rev Mol Cell Biol, 2001. **2**(3): p. 188-94.
2. Lupas, A., et al., *Self-compartmentalizing proteases.* Trends Biochem Sci, 1997. **22**(10): p. 399-404.
3. Baumeister, W., et al., *The proteasome: paradigm of a self-compartmentalizing protease.* Cell, 1998. **92**(3): p. 367-80.
4. Voges, D., P. Zwickl, and W. Baumeister, *The 26S proteasome: a molecular machine designed for controlled proteolysis.* Annu Rev Biochem, 1999. **68**: p. 1015-68.
5. Bajorek, M. and M.H. Glickman, *Keepers at the final gates: regulatory complexes and gating of the proteasome channel.* Cell Mol Life Sci, 2004. **61**(13): p. 1579-88.
6. Pickart, C.M., *Mechanisms underlying ubiquitination.* Annu Rev Biochem, 2001. **70**: p. 503-33.
7. Tenno, T., et al., *Structural basis for distinct roles of Lys63- and Lys48-linked polyubiquitin chains.* Genes Cells, 2004. **9**(10): p. 865-75.
8. Thrower, J.S., et al., *Recognition of the polyubiquitin proteolytic signal.* Embo J, 2000. **19**(1): p. 94-102.
9. Deveraux, Q., et al., *A 26 S protease subunit that binds ubiquitin conjugates.* J Biol Chem, 1994. **269**(10): p. 7059-61.
10. Husnjak, K., et al., *Proteasome subunit Rpn13 is a novel ubiquitin receptor.* Nature, 2008. **453**(7194): p. 481-8.
11. Fujiwara, K., et al., *Structure of the ubiquitin-interacting motif of S5a bound to the ubiquitin-like domain of HR23B.* J Biol Chem, 2004. **279**(6): p. 4760-7.
12. Schreiner, P., et al., *Ubiquitin docking at the proteasome through a novel pleckstrin-homology domain interaction.* Nature, 2008. **453**(7194): p. 548-52.
13. Hoyt, M.A. and P. Coffino, *Ubiquitin-free routes into the proteasome.* Cell Mol Life Sci, 2004. **61**(13): p. 1596-600.
14. Orlowski, M. and S. Wilk, *Ubiquitin-independent proteolytic functions of the proteasome.* Arch Biochem Biophys, 2003. **415**(1): p. 1-5.
15. Bercovich, Z., et al., *Degradation of ornithine decarboxylase in reticulocyte lysate is ATP-dependent but ubiquitin-independent.* J Biol Chem, 1989. **264**(27): p. 15949-52.
16. Pegg, A.E., *Recent advances in the biochemistry of polyamines in eukaryotes.* Biochem J, 1986. **234**(2): p. 249-62.
17. Matsufuji, S., et al., *Autoregulatory frameshifting in decoding mammalian ornithine decarboxylase antizyme.* Cell, 1995. **80**(1): p. 51-60.
18. Palanimurugan, R., et al., *Polyamines regulate their synthesis by inducing expression and blocking degradation of ODC antizyme.* Embo J, 2004. **23**(24): p. 4857-67.
19. Kern, A.D., et al., *Structure of mammalian ornithine decarboxylase at 1.6 A resolution: stereochemical implications of PLP-dependent amino acid decarboxylases.* Structure, 1999. **7**(5): p. 567-81.
20. Zhang, M., C.M. Pickart, and P. Coffino, *Determinants of proteasome recognition of ornithine decarboxylase, a ubiquitin-independent substrate.* Embo J, 2003. **22**(7): p. 1488-96.
21. Li, X. and P. Coffino, *Degradation of ornithine decarboxylase: exposure of the C-terminal target by a polyamine-inducible inhibitory protein.* Mol Cell Biol, 1993. **13**(4): p. 2377-83.

22. Ghoda, L., et al., *Trypanosome ornithine decarboxylase is stable because it lacks sequences found in the carboxyl terminus of the mouse enzyme which target the latter for intracellular degradation.* J Biol Chem, 1990. **265**(20): p. 11823-6.
23. Takeuchi, J., H. Chen, and P. Coffino, *Proteasome substrate degradation requires association plus extended peptide.* Embo J, 2007. **26**(1): p. 123-31.
24. Takeuchi, J., et al., *Structural elements of the ubiquitin-independent proteasome degron of ornithine decarboxylase.* Biochem J, 2008. **410**(2): p. 401-7.
25. Zhang, M., et al., *Proteasomes begin ornithine decarboxylase digestion at the C terminus.* J Biol Chem, 2004. **279**(20): p. 20959-65.
26. Hoyt, M.A., et al., *A genetic screen for Saccharomyces cerevisiae mutants affecting proteasome function, using a ubiquitin-independent substrate.* Yeast, 2008. **25**(3): p. 199-217.
27. Shabek, N., Y. Herman-Bachinsky, and A. Ciechanover, *Ubiquitin degradation with its substrate, or as a monomer in a ubiquitination-independent mode, provides clues to proteasome regulation.* Proc Natl Acad Sci U S A, 2009. **106**(29): p. 11907-12.
28. Loetscher, P., G. Pratt, and M. Rechsteiner, *The C terminus of mouse ornithine decarboxylase confers rapid degradation on dihydrofolate reductase. Support for the pest hypothesis.* J Biol Chem, 1991. **266**(17): p. 11213-20.
29. Hoyt, M.A., M. Zhang, and P. Coffino, *Ubiquitin-independent mechanisms of mouse ornithine decarboxylase degradation are conserved between mammalian and fungal cells.* J Biol Chem, 2003. **278**(14): p. 12135-43.
30. Li, X., et al., *Generation of destabilized green fluorescent protein as a transcription reporter.* J Biol Chem, 1998. **273**(52): p. 34970-5.
31. Sen, N., A. Sen, and E.R. Mackow, *Degrons at the C terminus of the pathogenic but not the nonpathogenic hantavirus G1 tail direct proteasomal degradation.* J Virol, 2007. **81**(8): p. 4323-30.
32. Schmaljohn, C. and B. Hjelle, *Hantaviruses: a global disease problem.* Emerg Infect Dis, 1997. **3**(2): p. 95-104.
33. Alff, P.J., et al., *The NY-1 hantavirus Gn cytoplasmic tail coprecipitates TRAF3 and inhibits cellular interferon responses by disrupting TBK1-TRAF3 complex formation.* J Virol, 2008. **82**(18): p. 9115-22.
34. Geimonen, E., et al., *Tyrosine residues direct the ubiquitination and degradation of the NY-1 hantavirus G1 cytoplasmic tail.* J Virol, 2003. **77**(20): p. 10760-868.
35. Janse, D.M., et al., *Localization to the proteasome is sufficient for degradation.* J Biol Chem, 2004. **279**(20): p. 21415-20.
36. Guthrie, C. and G.R. Fink, eds. *Guide to Yeast Genetics and Molecular Biology*. Methods in enzymology. Vol. 194. 1991, Academic Press: New-York. 3-933.
37. Ito, H., et al., *Transformation of intact yeast cells treated with alkali cations.* J Bacteriol, 1983. **153**(1): p. 163-8.
38. Sambrook, J. and D. Russell, *Molecular Cloning: A Laboratory Manual*. third edition ed. 2001, Cold Spring Harbor: Cold Spring Harbor Laboratory press.
39. Mumberg, D., R. Muller, and M. Funk, *Yeast vectors for the controlled expression of heterologous proteins in different genetic backgrounds.* Gene, 1995. **156**(1): p. 119-22.
40. Binz, H.K., et al., *High-affinity binders selected from designed ankyrin repeat protein libraries.* Nat Biotechnol, 2004. **22**(5): p. 575-82.
41. Binz, H.K., et al., *Designing repeat proteins: well-expressed, soluble and stable proteins from combinatorial libraries of consensus ankyrin repeat proteins.* J Mol Biol, 2003. **332**(2): p. 489-503.
42. Kohl, A., et al., *Designed to be stable: crystal structure of a consensus ankyrin repeat protein.* Proc Natl Acad Sci U S A, 2003. **100**(4): p. 1700-5.

43. Novokhatny, V. and K. Ingham, *Thermodynamics of maltose binding protein unfolding.* Protein Sci, 1997. **6**(1): p. 141-6.
44. Ormo, M., et al., *Crystal structure of the Aequorea victoria green fluorescent protein.* Science, 1996. **273**(5280): p. 1392-5.
45. Ward, W.W. and S.H. Bokman, *Reversible denaturation of Aequorea green-fluorescent protein: physical separation and characterization of the renatured protein.* Biochemistry, 1982. **21**(19): p. 4535-40.
46. Riggs, P., *Expression and purification of recombinant proteins by fusion to maltose-binding protein.* Mol Biotechnol, 2000. **15**(1): p. 51-63.
47. Kapust, R.B. and D.S. Waugh, *Escherichia coli maltose-binding protein is uncommonly effective at promoting the solubility of polypeptides to which it is fused.* Protein Sci, 1999. **8**(8): p. 1668-74.
48. Ward, T.H. and J. Lippincott-Schwartz, *The uses of green fluorescent protein in mammalian cells.* Methods Biochem Anal, 2006. **47**: p. 305-37.
49. Xie, J.B. and J.M. Zhou, *Trigger factor assisted folding of green fluorescent protein.* Biochemistry, 2008. **47**(1): p. 348-57.
50. Fox, J.D., R.B. Kapust, and D.S. Waugh, *Single amino acid substitutions on the surface of Escherichia coli maltose-binding protein can have a profound impact on the solubility of fusion proteins.* Protein Sci, 2001. **10**(3): p. 622-30.
51. Toth, C. and P. Coffino, *Regulated degradation of yeast ornithine decarboxylase.* J Biol Chem, 1999. **274**(36): p. 25921-6.
52. van Daalen Wetters, T., et al., *Polyamine-mediated regulation of mouse ornithine decarboxylase is posttranslational.* Mol Cell Biol, 1989. **9**(12): p. 5484-90.
53. Gandre, S., Z. Bercovich, and C. Kahana, *Ornithine decarboxylase-antizyme is rapidly degraded through a mechanism that requires functional ubiquitin-dependent proteolytic activity.* Eur J Biochem, 2002. **269**(4): p. 1316-22.
54. Prakash, S., et al., *An unstructured initiation site is required for efficient proteasome-mediated degradation.* Nat Struct Mol Biol, 2004. **11**(9): p. 830-7.

Target protein degradation experiments in mammalian cells

Chapter 3

Introduction

The selective depletion of intracellular proteins can be a powerful tool for protein function analysis and, in the long run, therapeutic applications. Reduction of a protein steady-state level often results in biochemical and/or phenotypic alterations; analysis of these physiological effects does usually give good leads on its function. Gene disruption at the DNA level has markedly advanced biological research. However, deletion of certain genes led to developmental arrest and/or lethality, and limitation in temporal and spatial specificities prevented a complete study of associated phenotypes. Moreover, developmental compensational effects could mask some loss-of-function-phenotypes. Nowadays, siRNA (short interfering RNA) and antisense oligonucleotides are preferred over traditional genetics and elicit a great deal of interest; they can easily prevent the expression of a given protein by mRNA destruction and/or inhibition of mRNA translation by physical blockade of ribosomes. While being popular, this gene silencing technique may not be absolutely specific and can trigger "off targets" effects in addition to knockdown of the targeted gene [1, 2]. Furthermore, in some cases siRNAs can act as agonists of Toll-like receptors [3] and specific sequence motifs can induce cellular immune responses [4, 5]. Last but not least, functional assessment of knockdown or knockout phenotype depends also on the intrinsic stability of the targeted protein.

Instead of maneuvering at the biosynthesis stage, other methods were developed to operate post-translationally. Most of them relied on the exploitation of the ubiquitin proteasome pathway, the major path for regulated degradation of intracellular proteins in eukaryotes [6]. Protein degradation via the ubiquitin-proteasome pathway requires first the labeling of the substrate by ubiquitin and then degradation by the 26S proteasome. Several strategies tried to take advantage of the ubiquitination machinery or hijack it to degrade specific target proteins. The first described one aimed at mimicking the mode of action of the human papillomavirus (HPV) oncoprotein E6. Scheffner and colleagues had discovered that this protein could bind to the tumor suppressor p53 and stimulate in vitro its degradation via the "ubiquitin-dependent proteolysis system" [7]. Without having fully deciphered the mechanism of HPV E6 action yet (targeting p53 to the E6AP ubiquitin ligase), they investigated if it could induce degradation of other proteins brought into complex with itself. The domain of HPV E7, which contains the binding domain for the tumor suppressor retinoblastoma protein (pRB) was N-terminally fused to HPV E6; this chimeric fusion protein promoted pRB degradation in a rabbit reticulocyte lysate [8]. The authors envisioned that "E6 fusion proteins might therefore be useful tools in the study of protein-protein interactions in vitro and in vivo". However, the in vivo efficacy has not been demonstrated due to the instability of E6-E7 fusion inside the cells [9]. Gosink and Viestra modified the C-terminus of ubiquitin conjugating enzymes (E2) with protein-binding domains, to induce ubiquitination of new target proteins [10]. Several natural or artificial ligands were fused to the C-terminus of two plant E2s: UBC1 from *Aradopsis thaliana* and UBC4 from wheat. A variety of ligand protein interactions, including protein A-antibody, epitope-antibody, peptide hormone-receptor and protein subdomains,

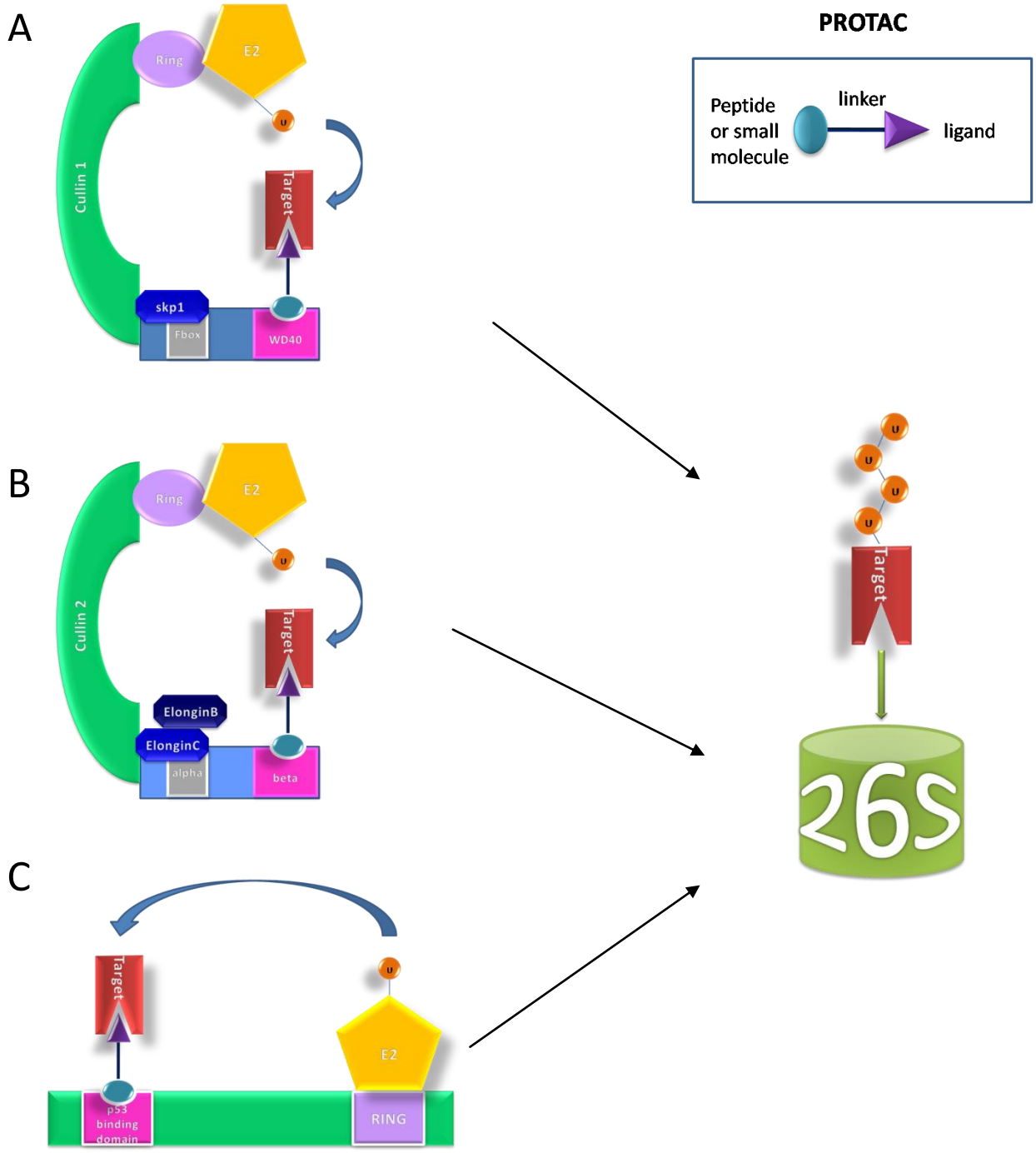

Figure 1: Overview of the PROTAC strategy meant to achieve chemical protein knock out. A PROTAC molecule is an adapter which, brings a target protein into contact with a multi-subunit E3 RING ubiquitin ligase (A: $SCF^{\beta\text{-}TrCP}$ ubiquitin ligase, B: VBC ubiquitin ligase, C: Mdm2 ubiquitin ligase) prompting transfer of ubiquitin (Ub) from an E2 ubiquitin conjugating enzyme, leading to polyubiquitination of the target protein and degradation by the 26S proteasome. A PROTAC molecule consists of a ligand or small molecule which is recognized by the E3 substrate binding domain (A: WD40 domain of β-TrCP, B: beta domain of VHL, C: p53 binding domain of Mdm2) and a ligand which binds the target protein. As it is added from the outside, the PROTAC molecule must be cell-permeable.

were tested. In vitro modified E2s could in presence of E1 and ATP ubiquitinate the protein recognized by the fused ligand. One of the target proteins was also partially degraded in a reticulocyte lysate. This was the only attempt to engineer E2, the following strategies took advantage of ubiquitin ligases (E3) domains or activity; the last enzyme of the ubiquitination cascade, in charge of substrate recruitment.

A new ubiquitin ligase was created by fusing the catalytic HECT domain of yeast ubiquitin ligase Rsp5 to the C-terminus of a peptide aptamer [11]. The HECT domain is a highly conserved domain, invariably located at the carboxyl-terminal region of HECT ubiquitin ligases; it accepts ubiquitin from bound E2 and subsequently transfers it to the substrate [12]. Peptide aptamers are engineered binding proteins, consisting of a variable peptide loop attached at both ends to a protein scaffold, in this case *E. coli* thioredoxin-A. Using a peptide aptamer selected against Cdk2 fused to the catalytic HECT domain, a LexA-Cdk2 fusion protein could be ubiquitinated in *S. cerevisiae* but was not degraded, even in presence of additional lysine residues and increased ubiquitination efficiency.

While the three former strategies were not followed up, two other approaches could successfully and repeatedly harness multisubunit RING E3s ubiquitination machineries. They led to the development of “chemical knockout” and “protein knockout” techniques.

Chemical knockout relies on the use of adapter molecules which have been termed PROteolysis Targeting Chimeric MoleculeS (PROTACS). PROTACS are bifunctional molecules comprising a ligand for the target protein, chemically linked to an ubiquitin ligase binding moiety (peptide). They were designed with the aim of bringing a target protein to the E3, in close enough proximity to allow multiubiquitin attachement and subsequent degradation. In a proof-of-principle experiment, methionine aminopeptidase 2 (MetAP-2), a stable protein which cleaves N-terminal methionine residues from nascent polypeptides, could when pre-bound to PROTAC-1, be degraded in Xenopus egg extracts [13]. PROTAC-1 consisted of a known covalent inhibitor of MetAP-2, ovalicin, joined to the 10-amino-acid phosphopeptide of IκBα sequence which is normally recognized by the mammalian F-box protein β-TrCP, the substrate binding subunit of ubiquitin ligase $SCF^{\beta\text{-}TrCP}$. By exchanging the substrate binding moiety with Estradiol or dihydroxytestosterone, PROTAC-2 and PROTAC-3 were generated to target two cancer-promoting proteins: the estrogen receptor α (ER α) and androgen receptors (AR), respectively [14]. PROTAC-3 could, upon microinjection in HEK293 cells stably expressing AR-GFP ($HEK293^{AR\text{-}GFP}$), activate the fusion protein turnover using the cellular degradation machinery. PROTAC-5 was designed to be cell permeable; IKBα phosphopeptide was replaced with a 7-amino acid peptide, recognized by the von-Hippel-Lindau tumor suppressor protein (VHL), the substrate recruiting unit of the VBC (VHL-elongin C/elongin B) ubiquitin ligase [15]. The VHL subunit, contrary to β-TrCP, does not recognize its substrate upon phosphorylation but upon hydroxylation [16]. Additionally, a polyarginine tag was fused to the C-terminus of the PROTAC 5 to mimic HIV Tat protein translocation mechanism into cells. PROTAC-5 could upon addition to $HEK293^{AR\text{-}GFP}$ induce degradation of AR-GFP. Subsequently the 7-amino acid VHL recognition sequence was simplified to a pentapeptide [17]. Finally, an anti-ERα PROTAC designed in a fully genetic manipulation-free way (containing Estradiol, a linker and VHL pentapeptide), was able to potently inhibit endothelial cell differentiation in a three-dimensional angiogenic sprouting assay and inhibited proliferation of ERα-dependent breast cancer cells [18, 19]. Addition of a polyarginine tag allowed decreasing the effective concentration of PROTAC in the low μM range [18].

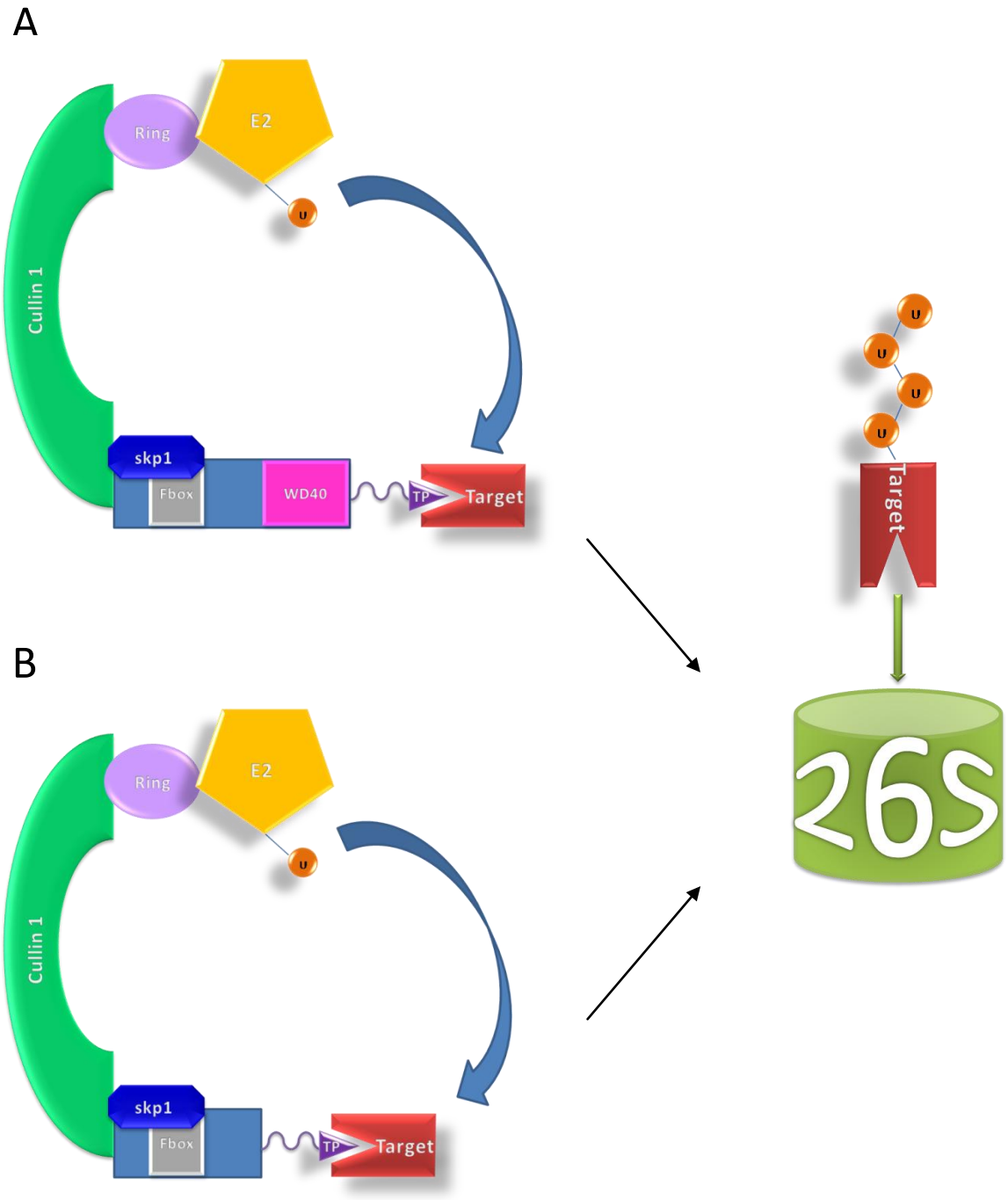

Figure 2: Protein knock out strategy using chimeric F-box proteins. The target protein is recruited to the core SCF machinery by either fusing a targeting peptide (TP) to the C-terminus of the F-box protein (A), or directly replacing the F-box protein original substrate binding domain (in this case, WD40 domain) by a targeting peptide (TP). The target protein is ubiquitinated and subsequently degraded by the 26S proteasome.

A dihydroxytestosterone-based PROTAC inhibited proliferation of androgen-dependent prostate cancer cells [18, 20]. Later on, a new target, the Aryl Hydrocarbon Receptor (AHR) could also be degraded in epithelial cells; the AHR pathway, involved in tumor promotion was inhibited (Puppala, 2008). Recently, another example of PROTAC was developed where the E3-recognizing peptide was replaced with a small molecule [21]. An "all-small molecule PROTAC" was constructed with a non-steroidal androgen receptor ligand (SARM) and nutlin, a ligand of the ubiquitin ligase MDM2, connected by a PEG-based linker. MDM2 normally regulates the intracellular levels of p53 [22] and nutlin is an imidazoline derivative which has been shown to disrupt the binding of MDM2 to its target p53. This new PROTAC was capable of promoting degradation of AR transiently expressed in HeLa cells. Small molecule PROTAC libraries could be envisioned, leading to chemical proteomics and/or therapeutic applications. However, cell permeability issues have to be completely circumvented. The high concentrations needed to observe an effect (between 3.8 μM and 50 μM) might limit the application of PROTACS for therapeutic applications.

The second strategy did not rely on bridging molecules but on the direct engineering of F-Box proteins, the substrate recruiting subunits of SCF ubiquitin ligases. Zhou and Howley constructed chimeric F-box proteins by fusing them to a targeting peptide (TP), capable of binding a target protein [23]. Their pioneering work consisted of selectively degrading pRb in yeast by co-expressing it with the F-box protein cdc4 to which they had C-terminally fused the N-terminal 35 residues of HPV E7, which contain a pRb binding motif. A similar engineering study was conducted on the mammalian F-box protein β-TrCP [23]. Transient expression of this chimeric F-box protein (βTrCP-E7N) in the human osteosarcoma SAOS-2 cells decreased pRb levels and inhibited Rb-induced growth arrest. The properties of this protein knockout system were then further evaluated. It appeared that the formerly engineered βTrCP-E7N could also be used to degrade another member of the Rb proteins family; p107 levels could be reduced upon its expression in C33A cervical carcinoma cells [23]. Moreover, this proteolysis could be controlled by adjusting the amount of recombinant βTrCP-E7N adenoviruses used to infect C33A cells [24]. In addition to fine-tuning intracellular protein levels, the degradation could be confined to a post-translationally modified subpopulation. HPV E7 was found to selectively bind to the hypophosphorylated form of pRB. When present in U2OS osteosarcoma cells, expressing both hypo- and hyperphosphorylated forms of pRB, βTrCP-E7N was only eliminating hypophosphorylated pRB [24]. To reduce risk of unspecific interaction of the chimeric F-box protein, a minimal binding domain of HPV E7 was used (9 instead of 35 residues) and interference with native βTrCP substrates was prevented by mutating βTrCP substrate binding sites [24]. Another chimeric F-box protein was designed by fusing β-catenin binding domain of E-cadherin to βTrCP, it was successfully employed to degrade β-catenin in HEK293 cells [25]. It seemed to preferentially target soluble nuclear/cytosolic β-catenin (involved in Wnt signaling) for degradation, sparing the membrane-associated one. Its expression inhibited tumorigenicity of DLD1 colon cancer cells grown in vitro and in vivo, in mice. The design of chimeric F-box proteins was further refined; instead of hitchhiking for a ride with βTrCP, β-catenin was allowed to carjack it. The targeting peptide was not fused any more to the C-terminus of the full-length β-TrCP but used to replace its entire original substrate binding domain [26, 27]. Finally, a minimal chimeric F-box protein was constructed by deleting both the N-terminal domain upstream of the F-box motif and the WD40 substrate binding domain, this truncated molecule was linked via a 10-amino acid serine-glycine peptide

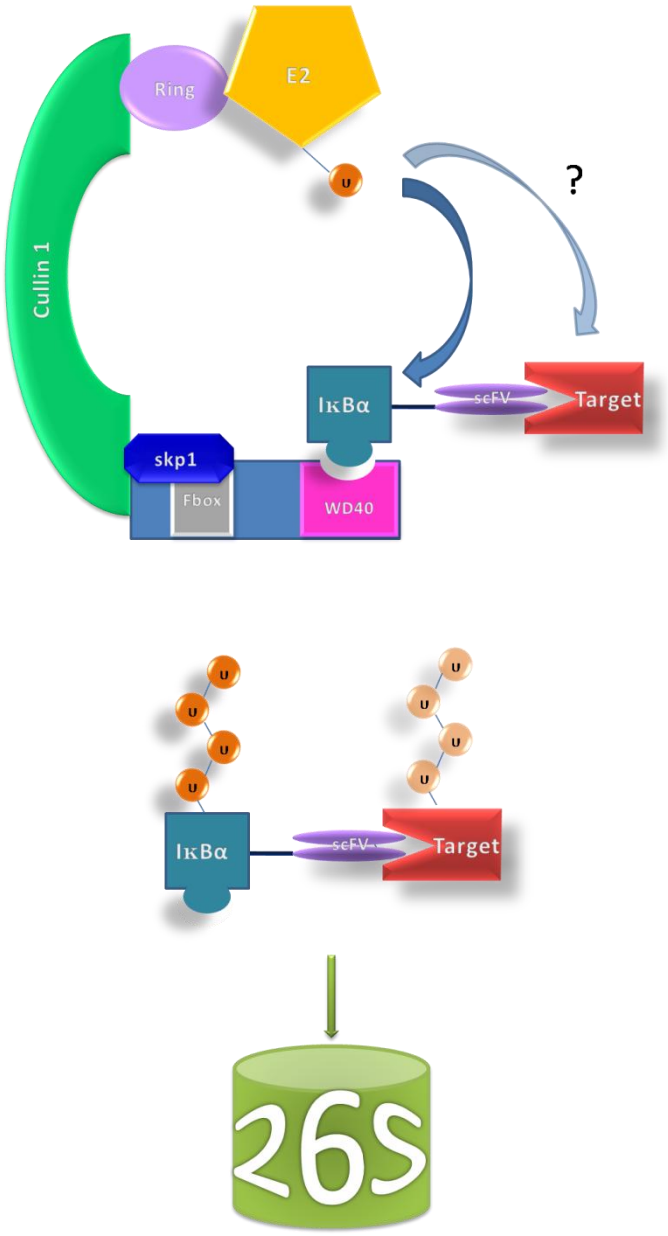

Figure 3: Strategy of SIT assisted degradation of a target protein. IKBα, a known substrate of the F-box protein βTrCP is fused to the intrabody (here depicted as a scFv), thereby creating a chimeric bifunctional protein. The intrabody domain carries out the target protein recruiting function while IKBα serves as a bridging molecule with the ubiquitination complex and acts as a degradation domain. The faded ubiquitin chain appended to the target protein highlights the possible ubiquitination that the target undergoes before being degraded.

to four copies of a 15 residue-β-catenin binding motif found in the adenomatous polyposis coli (APC). This new molecule could induce colorectal cancer cell death in vitro and in vivo [26]. In addition to pRB proteins family and β-catenin, c-myc and cyclin A could be targeted for degradation. Cohen and colleagues fused c-myc interacting domain of the protein Max to the C-terminus of βTrCP [28]. Using in utero gene transfer, they revealed a role for c-myc in murine lung and intestine development. The therapeutic potential of the protein knockout strategy was further demonstrated with the degradation of Cyclin A/Cyclin-Dependent Kinase 2 (cdk2) complex [29]. An 8 residue peptide named LFG, originally found in the transcription factor E2F1, and able to bind Cyclin A, was C-terminally fused to βTrCP. Degradation of cyclin A in complex with cdk2 induced apoptosis for several tumor cell lines in vitro and also had antitumor effects in vivo, when tested in subcutaneous or intracranial tumor models.

"Chemical knockout" and "protein knockout" technologies open new possibilities for proteomics, drug target validation and therapeutic applications. Both technologies are nevertheless limited in the range of targets, as they rely on the availability of a tight-binding "adapter", i.e. a ligand or a known naturally occurring binding motif. Recently, another strategy emerged which would allow not a case-by-case but a more general applicability. Melchionna and Cattaeno developed the Suicide (or silencing) Intrabody Technology (SIT) [30]. SIT relies on the use of an intrabody C-terminally fused to IκBα, a βTrCP substrate. IκBα is only recognized by the ubiquitin ligase upon phosphorylation which results from NF-kB signaling pathway activation. This stimulus-induced degradation could be exploited to turn the fusion protein into a switchable suicide intrabody. Two constructs made with an anti-Tau and an anti-β-galactosidase intrabody were transiently expressed in Hela cells. Upon addition of Tumor Necrosis Factor alpha (TNFα), both suicide antibodies were undergoing degradation. When co-expressed with the C-terminal domain of Tau (τ) protein or whole length β-galactosidase, they could respectively induce their degradation. The steady-state level of endogenous τ was also highly decreased when the specific suicide antibody was expressed in TNFα-stimulated human neuroblastoma cells. The suicide intrabody seemed to act in a catalytic way as its steady-state level was always lower than the target protein's one. It was suggested that the suicide antibody could escort the target protein to the proteasome but escape degradation and be recycled for a new round of action. The intrabody-based knock-out technology seems promising but does rely on the expression and degradation of an intrinsic player (IκBα) via activation of a signaling cascade. The use of biologically inactive compounds for both interaction with the ubiquitin ligase and activation of the degradation cascade would lower the risk of side-effects. The precise mechanism by which suicide antibodies induce *trans*-degradation of their target protein remains to be investigated and the general applicability of the system to be further proven. If sufficient functional intracellular antibodies should be readily available to target a large spectrum of proteins, the in-trans mode of action may restrict it. The degradation of target protein necessitates namely two additional actors: IκBα and the intrabody which might eventually be degraded too. In other words, the proteasome needs to process between two and three substrates at each round; this overloading approach may lower its overall processing efficiency and function properly for easy degradable target proteins only. It should be noted that the degradation efficiency differed greatly, from 70-90 % for the C-terminal domain of τ protein (30 kDa) to only 15-20% for β-galactosidase (120 kDa).

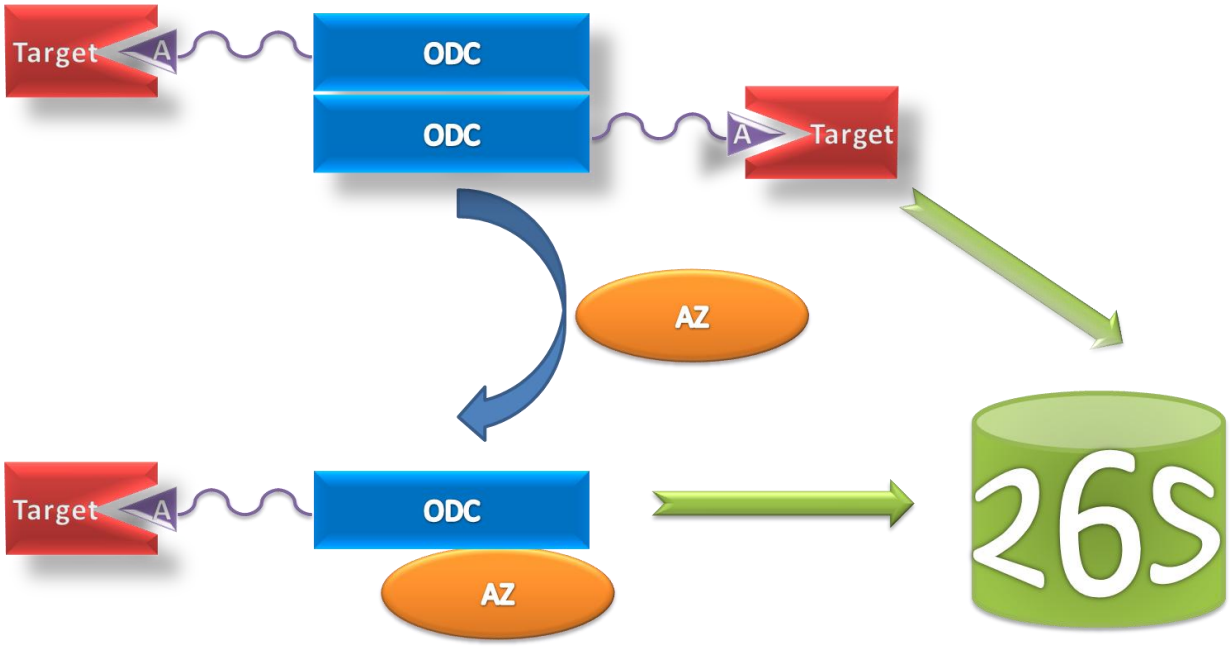

Figure 4: Strategy for AZ-assisted degradation of target proteins by ODC chimeric fusion proteins. A protein interaction domain (adapter= A) is expressed with ODC attached to its C-terminus with a flexible linker sequence. The ODC fusion protein binds the target protein and dimerizes. AZ dissociates the ODC fusion proteins dimer, induces a conformational change which enhances degradation of one ODC fusion protein with the target protein along by the 26S proteasome**.** In certain cases ODC fusion protein can be efficiently recognized by the proteasome and be degraded along with the target protein, without previous interaction with AZ.

To summarize, a strategy which could harness the ubiquitination machinery without interfering with the cell homeostasis and be readily adapted to a large range of target proteins would be optimal for achieving specific protein breakdown in the cell. Our chimeric F-box protein, described in chapter 1, does respond to these expectations. They are extremely specific and continuously degraded so they should not disturb the cell metabolism and DARPins, the solid scaffold used as substrate binding moiety can be selected against virtually any target.

Selectively targeting a protein for ubiquitination and subsequent degradation opens another avenue for protein knock-out, but bypassing the target protein labeling step may be more powerful for "high-throughput degradation". Avoiding the use of an additional intracellular machinery may simplify and accelerate the degradation process. What's more, it is very likely that some substrates are more prone to ubiquitination than others, based on their primary and tertiary structures. Matsuzawa and colleagues elaborated an alternative strategy for degrading selected proteins in an ubiquitin-independent way [31]. Their method was based on the use of ornithine decarboxylase (OZ), an enzyme which can naturally bind to the 26S proteasome thanks to its C-terminal sequence, called ODC-degron. Upon association with antizyme (AZ), ODC undergoes a conformational change which increases exposure of the ODC degron and accelerates its turnover rate 50- to 100-fold. Matsuzawa & al. fused a binding moiety (whole protein, protein domain or peptide ligand) via a flexible linker to the N-terminus of ODC and co-expressed these ODC fusion proteins with their respective binding partner in HEK293 cells, in absence or presence of overexpressed AZ [31]. 12 pairs of interacting proteins were tested, 5 of them resulted in specific reduction of the target protein. For two of them, degradation was strictly AZ-dependent while for another case, it was only enhanced by AZ and the last two ODC fusion proteins were functional independently of AZ. The system could increase target protein turn-over rate from at least two fold, reducing overexpressed TRAF-6 half-life from about 2 h to less than an hour. Endogenous TRAF-6 and pRB could also successfully be targeted, significantly affecting their intracellular activities. While having the advantage of being more straightforward, this method suffers from the same drawback than most of the previously described methods, namely the need of a known adapter. Furthermore, the use of active ODC and AZ molecules might alter cellular polyamines levels or other intracellular proteins, leading to several artifacts resulting in other phenotypes or toxicity. To prevent interference with the cellular metabolism, the authors proposed to use a mutant ODC which would be enzymatically non-active or unable to bind endogenous ODC, but have not demonstrated such molecules.

With our DARPIn-degron strategy, described in chapter 2, we went two steps ahead. A general adaptable binding protein was used and side-effects were circumvented by using not the entire ODC molecule but only its degron sequence. Another degron sequence identified in the NYV G1 glycoprotein was also tested. When expressed in *S. cerevisiae*, all DARPIn-degrons were extremely rapidly degraded but failed to efficiently induce destruction of their binding partner. We envisioned that our molecules were disappearing too fast in the yeast system to function as carriers to the 26S proteasome. Inspired by the formerly described strategy elaborated in mammalian cells, we tested the DARPIn-degrons in a mammalian system. In parallel, we also examined the potential of our chimeric F-box protein (described in chapter 1) in mammalian cells. The F-box protein we used was designed on a yeast scaffold, but SCF ligases are well conserved throughout evolution as witnessed by their preserved structure [32-36]. Fbxw7, a homolog of cdc4 was identified in mammals, but its F-box domain does not display significant

similarity. However when a blast search was carried out against the human proteome database, cdc4 F-box domain showed 42%, 38%, 36% and 34% identity with other F-box domain contained in human F-box proteins named Fbxl5, Fbxl21, Fbxw8 and Fbxw2, respectively.

Materials & methods

Plasmids and oligonucleotides

Standard molecular biology procedures were used for recombinant DNA manipulation [37]. Enzymes were from NEB (Ipswich, MA, USA) or Fermentas (Vilnius, Lithuania). PCR reactions were performed with the Phusion ™ High-Fidelity DNA polymerase as recommended by the manufacturer (NEB). All oligonucleotides are listed in Table 1.

E3-5, Off7, Off7-ODC, Off7-NYV and cdc4-off7 constructs were described in chapter 2. The Off7 construct was subcloned in pcDNA3.1(+) (Invitrogen, San Diego, CA) at the SpeI and XhoI sites of the multiple cloning site. pcDNA3.1(+) also contained a SpeI site at the beginning of the CMV promoter. The ligation proceeded in two steps; SpeI/XhoI digested off7 construct was first ligated with the SpeI CMV promoter part before the rest of pcDNA3.1(+) backbone was added to the ligation mixture. The Off7 construct was subcloned as a HindIII fragment from pcDNA3+_Off7 in pcDNA5/FRT/TO (Invitrogen, San Diego, CA). For fluorescence microscopy, off7 was subcloned from pQE30_mbpoff7 (Binz, 2004, see chapter 1) in BamHI/HindIII sites of pTAG-RFP-DARPin (plasmid provided by Anja Mohr). For production of biotinylated off7, the off7 DNA sequence was amplified from pQE30_mbpoff7 (Binz, 2004, see chapter 1) by PCR using pQE_for and Avi_NcoI_G3_B oligonucleotides as primers and the digested PCR product was introduced at the BamHI and HindIII sites of pBD001 (plasmid provided by Brigit Dreier) to yield pBDoff7.E3-5, Off7-ODC and Off7-NYV constructs coding sequences were subcloned in EcorI and XhoI sites of pcDNA3+_Off7.

pcDNA3+_cdc4-off7 was constructed by subcloning cdc4-off7 in pcDNA3.1(+) at the SpeI and XhoI sites of the multiple cloning site in a three-step process. The cdc4-off7 coding sequence was first ligated to SpeI/XhoI digested pcDNA3.1(+) lacking the SpeI CMV promoter part, which was added in a second cloning step. Finally, the cdc4-off7 coding sequence was subcloned as a HindIII/XhoI fragment in a fresh pcDNA3.1(+) backbone. The cdc4-off7 coding sequence was subcloned from pcDNA3+_cdc4-off7 as a HindIII/XhoI fragment in pcDNA5/FRT/TO. The cdc4-E3_5 coding sequence was constructed by assembly PCR as described in chapter 1 with the exception that the oligonucleotide forHindcdc4 was used instead of forSpeIcdc4 (see chapter 1). The cdc4-E3_5 coding sequence was cloned at the HindIII/XhoI sites of pcDNA5/FRT/TO.

The MBP DNA sequence was amplified from pQEMBP [38] by PCR using MBPforHind and MBPrevBamHI oligonucleotides as primers and the digested PCR product was introduced at the HindIII and BamHI sites of pcDNA3.1(+). For fluorescence microscopy, the MBP-GFP DNA sequence was amplified from pRS306/Gal/MBP-GFP (see chapter 1) by PCR using MBPforHind and revGFPHindIII oligonucleotides as primers and the digested PCR product was introduced at the HindIII site of pcDNA3.1(+). MBP-ODC and MBP-NYV constructs are similar to those described in chapter 2, except that they do not contain the N-terminal HA tag. Their coding sequences were subcloned from p416/Gal/GFP-ODC and p416/Gal/GFP-NYV as EcoRI/ XhoI fragments in pcDNA3.1(+) (see chapter 2). MBP coding sequence was subcloned from pcDNA3+_MBP as a HindIII/XhoI fragment in pcDNA5/FRT/TO.

All constructs were confirmed by sequencing. Plasmids constructed for this study are listed in Table 2, those marked with an asterisk have their plasmid map and the insert sequences shown in annex.

Table 1: Oligonucleotides

Oligonucleotides	Sequence 5'-3' direction	Description (for=forward, rev=reverse)
forHindcdc4	GGT GGT AAG CTT ATG GGG TCG TTT CCC TTA GC	for cdc4 with HindIII site
revcdc45GS	TACCCAGGTCGCCCGAGCCGGATCCATTCTCCAGAAAAGATAATCT	rev 5GS linker
for5GSDARPin	TCTGGAGAATGGATCCGGCTCGGGCGACCTGGGTAAGAAACTGCT	for 5GS linker
revHADARPin	CGTAATCTGGAACATCGTATGGGTATTGCAGGATTTCAGCCAGGT	rev HA tag (25 first bases) with DARPin
revXhoIHA	GTGGTCTCGAGTTAAGCGTAATCTGGAACATCGTATG	rev XhoI site with HA tag (24 last bases)
MBPforHind	GT GGT AAG CTT ATG AAA ACT GAA GAA GGT AAA CTG	for MBP with HindIII site
MBPrevBamHI	GT GGT GGA TCC CTA AGT CTG CGC GTC TTT CAG G	rev MBP with BamHI site
revGFPHindIII	TGGTGGTAAGCTTTTATTTGTAGAGCTCATCCATGC	rev GFP with HindIII site
pQE_for	CTTTCGTCTTCACCTCGAG	for pQEMBP
Avi_NcoI_G3_B	GGCGAAGCTTGTTGCAGGATTTCAGCCAGGTCCTC	rev off7 with HindIII site

Table 2: Plasmids constructed for this study

Plasmids	Relevant characteristics (promoter; gene; ori)	Source
pcDNA3+_Off7*	CMV; Off7; SV40	This study
pcDNA3+_Off7-ODC*	CMV; Off7-ODC; SV40	This study
pcDNA3+_Off7-NYV*	CMV; Off7-NYV; SV40	This study
pcDNA3+_cdc4-off7	CMV; cdc4-off7; SV40	This study
pcDNA5/FRT/TO_emptyV	CMV/$TetO_2$; -; -	This study
pcDNA5/FRT/TO_MBP*	CMV/$TetO_2$; MBP; -	This study
pcDNA3+_MBP-GFP	CMV; MBP-GFP; SV40	This study
pTAG-RFP-off7	CMV; off7-RFP; SV40	This study
pBDoff7	T5; AviTag-off7; colE1	This study
pcDNA3+_E3_5	CMV; E3_5; SV40	This study
pcDNA3+_MBP	CMV; MBP; SV40	This study
pcDNA3+_MBP-ODC*	CMV; MBP-ODC; SV40	This study
pcDNA3+_MBP-NYV*	CMV; MBP-NYV; SV40	This study
pcDNA5/FRT/TO_Off7	CMV/$TetO_2$; Off7; -	This study
pcDNA5/FRT/TO_cdc4-off7*	CMV/$TetO_2$; cdc4-off7; -	This study
pcDNA5/FRT/TO_cdc4-E3_5*	CMV/$TetO_2$; cdc4-E3_5; -	This study

Cell culture

HEK293T and Flp-In T-REx cells were grown in DMEM (Sigma-Aldrich, St. Louis, MO) supplemented with 10% (v/v) heat-inactivated Foetal Bovine Serum (PAA Laboratories GmbH, Pasching, Austria) and 1 % Penicillin-Streptomycin (Sigma-Aldrich, St. Louis, MO) at 37°C with 5 % CO_2 in a humified incubator. For Flp-In T-REx cells, 15 µg/ml µg/ml Blasticidin (Invitrogen, San Diego, CA) was added to the medium in combination with 100 µg/ml Zeocin (Invitrogen, San Diego, CA) for wt cells or 150 µg/ml Hygromycin (PAA Laboratories GmbH, Pasching, Austria) for established stable Flp-In T-REx cell lines. When tetracycline induction was performed, tetracycline was first added at a final concentration of 1 µg/ml to fresh medium which was then added to the cells.

Transfections

Cells were transiently transfected at 90-95 % confluency with Lipofectamine 2000 (Invitrogen, San Diego, CA) or 70-80 % confluency with Fugene HD (Roche Applied Science, Penzberg, Germany) following the manufacturer's instructions. The equivalent of 1.5 µg DNA and 3.75 µl Lipofectamine reagent or 1 µg DNA with 3 µl Fugene HD reagent were used to transfect cells grown in a well of a 12-well culture plate. Alternatively lipofectamine transfection experiments were also performed with cells in solution; the transfection mix was added to the well (untreated or pre-coated with 0.1 % fibronectin (Sigma-Aldrich, St. Louis, MO) for 2 h at 37°C) shortly before cells were seeded. For co-transfection experiments, the same amount of total DNA was used. Cells were also transiently transfected using DNA-calcium-phosphate co-precipitates. At 60-70 % confluency, 1 to 2 µg DNA was diluted in 40 µl 250 mM $CaCl_2$ and 40 µl of HEPES solution (50 mM HEPES, pH 7.05, 1.5 mM Na_2HPO_4, 140 mM NaCl) was added, the final solution was quickly mixed and added onto the cells after 1 min standing time. The medium was changed 6 h after transfection.

Stable transfections of Flp-In T-REx cells were performed according to the manufacturer's instructions. Cells grown to 90% confluency in a 6 cm dish were transfected with 20 µl Lipofectamine 2000 and 1 µg pcDNA5/FRT/TO/X plus 7 µg pOG44. 48 h later, cells were split to reach 25% confluency the next day at which stage 150 µg/ml Hygromycin was added to the medium. 15 µg/ml Blasticidin was added as well the following day. Two weeks after transfection, colonies were picked using cloning disks (Sigma-Aldrich, St. Louis, MO) and expanded. Positive clones were confirmed by sensitivity to 100 µg/ml Zeocin and expression of the protein of interest.

Determination of steady-state levels and stability assays

One day before transfection, cells were counted with the CASY cell counter TT (Schärfe System GmbH, Reutlingen, Switzerland) and seeded at the same density in several 12-well plates. At the indicated time points after transfection, samples (cells contained in one well) were extracted for steady-state level determination or further treated with MG132 (Sigma-Aldrich, St. Louis, MO) or cycloheximide (Sigma-Aldrich, St. Louis, MO). MG132 was added in each well at a final concentration of 30 µM (stock solution prepared in DMSO with a concentration of 10 mM). An identical volume of DMSO was added to the negative control strains. For stability assays, cycloheximide was added in each well at a final concentration of 20 µg/ml (stock solution was prepared in water with a concentration of 2 mg/ml). In both cases, cells were further incubated at 37°C and samples extracted at the indicated time points.

Proteins extracts

The procedure is described for one sample, meaning cells contained in one well of a 12-well culture plate. Cells were washed with 500 µl PBS, 200 µl cold ***ProteoJET™*** Mammalian Cell Lysis reagent (Fermentas, Vilnius, Lithuania) was added and the plate was agitated at 1200 rpm for 10 min at RT. The lysate was transferred in a 1.5 ml-tube and centrifuged for 15 min at 18,000 g at 10°C. 100 µl of the supernatant was stored at -20 °C. Total protein was quantified using the bicinchoninic acid (BCA) kit (Sigma-Aldrich, St. Louis, MO). The assay was performed in a 96-well plate format with 200 µl BCA working reagent and 10 µl of BSA standards (prepared in ***ProteoJET™*** Mammalian Cell Lysis reagent) or 5 µl sample complemented with 5 µl ***ProteoJET™*** Mammalian Cell Lysis reagent. OD was measured at 540 nm. Normalized volumes were loaded on 10 % or 15 % SDS-Polyacrylamide gels followed by immunoblotting.

Pull-down experiments

Lysate preparation: 20 h after induction with 1 µg/ml Tc, about 1.10^7 FlpIn Trex MBP cells were washed with PBS, trypsinized and resuspended in 6 ml PBS. Cells were pelleted 5 min at 3000 g and resuspended in 2.4 ml RIPA buffer (50 mM Tris-HCl pH 7.5, 150 mM NaCl, 1% NP40, 0.25 % sodium-deoxycholate, 0.5 mM EDTA, complete protease inhibitor cocktail EDTA-free (Roche Applied Science, Penzberg, Germany)), shortly vortexed and incubated 5 min on ice. Cell debris was removed by a 2 min centrifugation step at 5000 g, 1 ml-aliquots of cleared lysates were snap-frozen in liquid nitrogen and stored at -80°C.

Off7 pull-down: RGS$(His)_6$off7 was produced in *E. coli* as described (Binz, 2004). All subsequent steps were performed at 4°C. 50 µl Ni-NTA magnetic agarose beads (Qiagen, Chatsworth, CA, product number: 36111) were incubated for 90 min with 30 µg off7 protein diluted in PBST buffer (PBS, 0.05 % Tween 20) or only PBST buffer. Beads were washed 3 times with 0.5 ml PBST buffer and incubated for 1 h 45 min with cell lysates which had been centrifuged for 10 min at 8000 g after thawing. Beads were washed 4 times with PBST buffer and eluted with 60 µl 1 x SDS sample loading buffer-EDTA (62.5 mM Tris-HCl pH 6.8, 100 mM EDTA, 7.5% glycerol, 2% SDS, 2.5% 2-mercaptoethanol, bromophenolblue). After 5 min at 95°C, eluted fractions were resolved by 15 % SDS-PAGE followed by immunoblotting.

Biotinylated off7 pull-down: Biotinylated off7 was produced in *E. coli* using the plasmid pBDoff7. Expression and purification of the biotinylated protein were performed as described (Binz, 2004). The protocol was identical to the one used for Off7 pull-down, except that 30 µg biotinylated off7 was bound to 50 µl magnetic Dynabeads MyOne Streptavidin T1 beads (Invitrogen, San Diego, CA) and the elution was performed with SDS sample loading buffer (62.5 mM Tris-HCl pH 6.8, 7.5% glycerol, 2 % SDS, 2.5 % 2-mercaptoethanol, bromophenolblue).

Immunoprecipitations

Lysate preparation: FlpIn Trex emptyV and FlpIn Trex cdc4-off7 cells were grown in three 6 cm-dishes for 16 h in presence of 1 µg/ml Tc. Two dishes FlpIn Trex cdc4-off7 cells and one dish FlpIn Trex emptyV cells were transfected with pcDNA3+_MBP-NYV. 26 h after transfection, MG132 was added at a final concentration of 30 µM. 6 h later, cells were washed with PBS and lysed by addition of 1 ml cold ***ProteoJET™*** Mammalian Cell Lysis reagent complemented with 10 mM NEM, 50 µM iodoacetamide and complete protease inhibitor cocktail EDTA-free (Roche Applied Science, Penzberg, Germany) per dish and

a 10 min agitation at 1200 rpm. Lysates were transferred in 1.5 ml-tubes and centrifuged for 15 min at 18,000 g at 10°C. 900 µl aliquots of cleared lysates were snap-frozen in liquid nitrogen and stored at -80°C. Total protein was quantified using the BCA assay as described above.

Immunoprecipitations: All subsequent steps were performed at 4°C. Thawed lysates were centrifuged for 5 min at 8000 g. Normalized volumes of supernatant corresponding to approximately 1.9 mg and 1.6 mg total protein were incubated for 2 h 30 min with 25 µg anti-HA (Sigma-Aldrich, St. Louis, MO, product number H 9658) or 10 µg anti-MBP antibody (NEB, Ipswich, MA, product number E8032) pre-captured on 80 µl Dynabeads® ProtG (Invitrogen, San Diego, CA), respectively. Beads were washed 4 times with 1 ml wash buffer (PBS, 10 mM NEM, 50 µM iodoacetamide, complete protease inhibitor cocktail EDTA-free, 0.05 % Tween 20) and resuspended in 100 µl 1 x SDS sample loading buffer (62.5 mM Tris-HCl pH 6.8, 7.5 % glycerol, 2 % SDS, 2.5 % 2-mercaptoethanol, bromophenolblue). After 5 min at 95°C, eluted fractions were resolved by 10 % and 15 % SDS-PAGE followed by immunoblotting.

Immunoblotting

Samples were transferred to PVDF membranes and immunoblotted using standard methods. The anti-HA peroxydase conjugate was used at a 1:1000 dilution (Sigma-Aldrich, St. Louis, MO, product number H 6533) and the anti-MBP HRP Conjugated (NEB, Ipswich, MA, product number E8038) at a 1:2000 dilution. The anti-β-actin peroxidase antibody (Sigma-Aldrich, St. Louis, MO, product number A3854) was diluted 1:15000. The HRP conjugated anti-mono-and polyubiquitinylated conjugates antibody (Enzo Life Sciences Inc, Farmingdale, NY, product number: PW0150) was used at a 1:1000 dilution. The anti-skp1 antibody (Abcam, Cambridge, UK, product number: ab76502) was diluted 1:1000 and detected with anti-alkaline phosphatase-coupled anti-rabbit antibody diluted 1:10,000 (Sigma-Aldrich, St. Louis, MO, product number A3687)

Fluorescence microscopy

HEK293T cells were seeded on poly-L-lysine-coated glass coverslips (18*18 mm) contained in a 6-well culture plate. The next day, cells were transfected with pcDNA3_MBPGFP, pTAG-RFP-off7 or both plasmids. The following day, cells were fixed with 4% (w/v) paraformaldehyde and DAPI stained. Cover slides were mounted using Fluoromont G (Brunschwig chemie, B.V., Amsterdam) and sealed after an overnight incubation at 4°C. Fluorescence images were acquired using a Lecia Leitz DMXRE microscope equipped with a DFC350FX camera. Colors, contrast and brightness were adjusted in Adobe Photoshop CS2 (Adobe systems, San Jose, CA).

ELISA

Lysate preparation: FlpIn Trex emptyV, FlpIn Trex off7 and FlpIn Trex cdc4-off7 cells were grown in a 10 cm-dishes for 24 h in presence of 1 µg/ml Tc. MG132 was added at a final concentration of 10 µM. 14 h later, cells were washed with PBS, trypsinized and resuspended in PBS. Cells were transferred to 1.5 ml-tubes and pelleted 5 min at 300 g and resuspended in 800 µl cold ***ProteoJET™*** Mammalian Cell Lysis reagent complemented with 10 mM NEM, 50 µM iodoacetamide and complete protease inhibitor cocktail EDTA-free (Roche Applied Science, Penzberg, Germany). Tubes were agitated for 10 min and

centrifuged for 10 min at 20,000 g at 10°C. 750 µl of cleared lysates were snap-frozen in liquid nitrogen and stored at -80°C. Total protein was quantified using the BCA assay as described above.

ELISA: Biotinylated MBP was produced in *E. coli* and immobilized on neutravidin-coated Maxisorp plates (Nunc, Rochester, NY) as described (Binz, 2004). 300 µg, 150 µg or 75 µg total proteins were applied to the wells and incubated for 1 h 30 min at 37°C in a final volume of 200 µl using ELISA buffer (50 mM Tris-HCl pH 7.4, 150 mM NaCl, 0.2 % BSA, 0.05 % Tween 20). After extensive washing with ELISA buffer, binding was detected with the anti-HA antibody (Sigma-Aldrich, St. Louis, MO, product number H 9658) diluted 1:3000, followed by the anti-mouse IgG alkaline phosphatase conjugate (Sigma-Aldrich, St. Louis, MO, product number A3562) diluted 1:7500. 50 nM off7 protein, purified as described (Binz, 2004), was used as positive control. Its binding was detected with the RGS-His antibody (Qiagen, Chatsworth, CA, product number: 34610) diluted 1:5000 instead of the anti-HA antibody. Absorbance was read at 405 nm at different time points after addition of p-nitrophenylphosphate and incubation at room temperature. Each sample was assayed in duplicates.

Results

Degradation of a target protein with different effector proteins

Effector proteins expression and stability

Three different effector proteins were designed using the DARPin off7 (Fig. 5). Two kinds of ubiquitin independent degradation degron sequences, the last 37 residues of mouse ornithine decarboxylase (Off7-ODC) or the last 42 residues of the Hantavirus NYV1 G1 protein (Off7-NYV) were appended at its C-terminus. Alternatively, the yeast F-box protein cdc4 was chosen as scaffold for the engineering of the third effector protein meant to exploit the ubiquitin proteasome pathway. off7 was used to replace its original substrate binding domain yielding a chimeric F-box protein, named cdc4-off7 which could function like a normal F-box protein in *S. cerevisiae* (see chapter 1). Finally, naked off7 was used as negative control (Off7). For detection purposes, an HA tag was added to the N-terminus of all effector proteins, except for cdc4-off7 where it was fused to its C-terminus. The effector proteins were cloned in pcDNA3(+) under the CMV promoter and their expression in mammalian cells was tested after transient transfection in HEK293T cells. All of them were expressed and could be detected 24 to 48h after transfection (Fig. 6). Significant differences could be observed in their steady-state levels. To our surprise, naked off7 level was low while it was reported to be very well expressed in *E. coli* (Fig. 6A) [38]. Off7-ODC level decreased from 24 h to 72 h, suggesting that it was most likely unstable, while Off7-NYV level stayed rather constant. Finally, cdc4-off7 was present in small amounts and was the most difficult species to detect, an additional band running right below it was also revealed by the anti-HA antibody, indicating that cd4-off7 might be degraded (Fig. 6B).

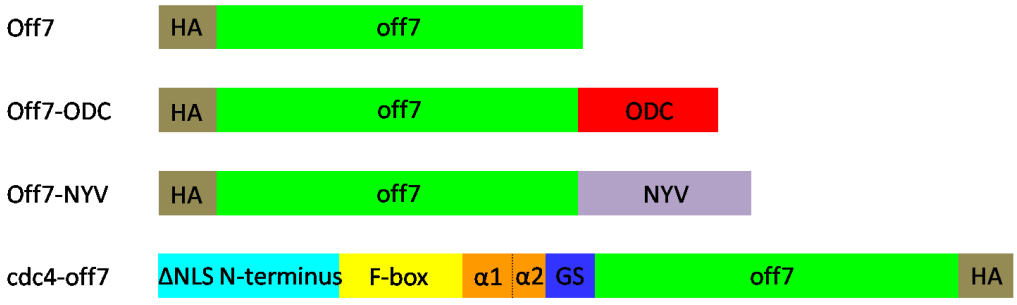

Figure 5: Schematic diagrams of the effector proteins. Off7-ODC was built by fusing the last 37 residues of mouse ornithine decarboxylase (red) to off7 (green) and Off7-NYV by fusing the last 42 residues of the Hantavirus NYV1 G1 protein (purple) to off7 (green), these constructs are explained in more detail in chapter 2. Cdc4-off7 was designed on the yeast cdc4 scaffold. Its NLS sequence present in the N-terminal part (light blue) was mutated. Its F-box domain was conserved (yellow). The linker made of two helices α1 and α2 (orange) was reengineered; part of α2 was replaced with a gly-ser linker (dark blue). Its substrate binding domain was deleted and replaced with off7 (green). An HA tag was fused to each effector protein (light brown). Cdc4-off7 construct is explained in more detail in chapter 1.

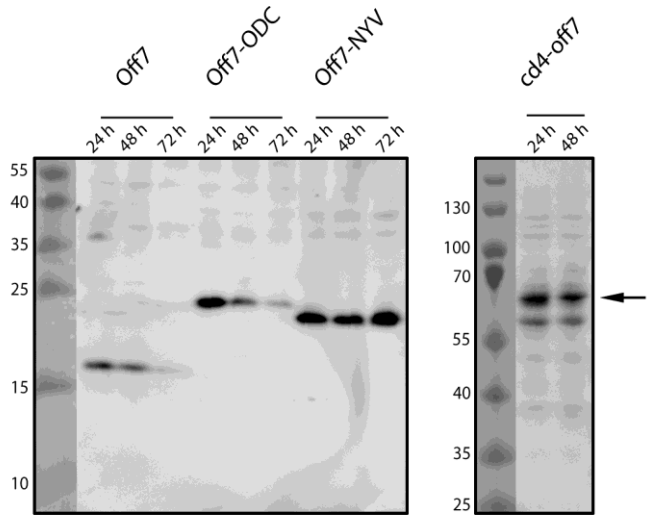

Figure 6: Expression of the effector proteins. HEK293T cells were transfected with pcDNA3+_Off7, pcDNA3+_Off7-ODC, pcDNA3+_Off7-NYV or pcDNA3+_cdc4-off7. 24, 48h or 72h later, total protein was extracted and samples were subjected to SDS-PAGE. Off7 (18 kDa), Off7-ODC (22 kDa), Off7-NYV (23 kDa) and cdc4-off7 (57 kDa) were detected by immunoblotting with the anti-HA antibody. The size marker is indicated in kDa.

The stability of the various effector proteins was then compared under cycloheximide treatment. All species were unstable, but to a different degree (Fig. 7A). Off7 and Off7-ODC disappeared rather quickly with a half-life roughly estimated between 30' and 60' while off7-NYV turnover was much slower with a half-life of 1 to 2 h. Again, cdc4-off7 levels were extremely difficult to monitor and its half-life was also evaluated between 30' and 60'. In presence of the proteasome inhibitor MG132, all effector proteins accumulated, demonstrating that they were processed by the 26S proteasome (Fig. 7A). Off7-ODC and Off7-NYV had been both observed to be rapidly degraded in *S. cerevisiae,* but Off7-NYV unexpectedly behaved differently in mammalian cells, it was much more stable. Surprisingly as well, off7 was degraded by the proteasome, while it did not bear any specific known degradation signal. In order to confirm these results, a second cycloheximide experiment was performed to better compare the stabilities of Off7 and Off7-ODC. Off7-ODC appeared to be slightly more unstable than Off7 with respective half-lives estimated to 45' and 60' (Fig. 7B). Off7 was then not further considered as a negative control, but rather as a fourth effector protein, potentially able to lead a target protein to the proteasome. Off7, Off7-ODC and Off7-NYV were all going to the proteasome with a different rate. cdc4-off7 was unstable as well like in *S. cerevisiae* where it had a half-life close from 1 h and degraded via the proteasome. F-box proteins are normally unstable and degraded via autoubiquitination which occurs within the E3 ligase complex [39]. We hypothesized that the yeast based chimeric F-box protein was likely to be degraded via the same process. If it was indeed recognized by the human SCF machinery, it could potentially work as an endogenous F-box protein.

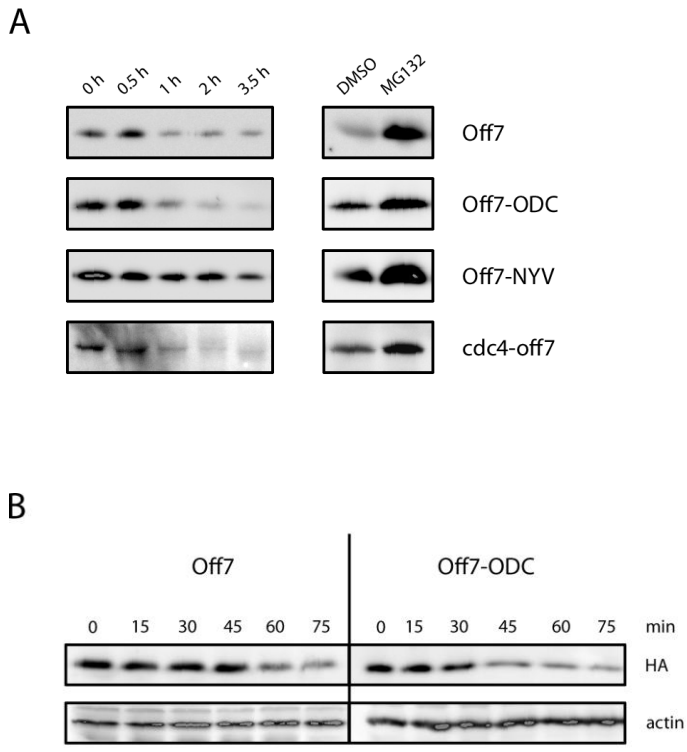

Figure 7: Stability of the effector proteins in presence of cycloheximide or MG132. A: HEK293T cells were transfected with pcDNA3+_Off7, pcDNA3+_Off7-ODC, pcDNA3+_Off7-NYV or pcDNA3+_cdc4-off7. 24 h later, 20 µg/ml cycloheximide was added to the cells and samples were withdrawn at the indicated time points. Independently, cells were treated with DMSO or 30 uM MG132 for 4 h. Total protein was extracted and samples were subjected to SDS-PAGE. The effector proteins were detected by immunoblotting with the anti-HA antibody. B: HEK293T cells were transfected with pcDNA3+_Off7 or pcDNA3+_Off7-ODC. 24 h later, 20 µg/ml cycloheximide was added to the cells and samples were withdrawn at the indicated time points. Total protein was extracted and samples were subjected to SDS-PAGE. The effector proteins were detected by immunoblotting with the anti-HA antibody. The actin signal was used as an internal loading control.

Establishment of MBP stable cell line: FLp-In T-Rex MBP

In order to investigate the effect of different effector proteins on their target protein, a stable cell line expressing MBP under tetracycline control was generated using the Flp-In T-REx system (Invitrogen, San Diego, CA). A plasmid containing a FRT site and MBP coding sequence under the control of the tetracycline-regulated CMV/TetO_2 promoter was integrated at a single FRT site in Flp-In T-Rex 293 cells via the action of Flp recombinase (Fig. 8). An identical plasmid missing the MBP coding sequence was also used to generate a negative control strain (emptyV). The Flp-In T-REx cell line also stably expressed the Tet repressor so that addition of tetracycline (Tc) to the medium would derepress the expression of the protein of interest. The recombination event should confer hygromycin resistance and zeocin sensitivity to the cells and lead to a loss of their ß-galactosidase activity. Antibiotic resistance and sensitivity enabled screening of the correctly transfected clones (Fig. 9A) which were then further tested for expression of MBP in absence or presence of Tc (Fig. 9B). All tested hygromycin-resistant clones were also sensitive to zeocin and expressed under Tc only MBP, which could be detected slightly below 40 kDa. Several additional bands running between 55 and 130 kDa were also recognized by the anti-MBP antibody. These species were not MBP-related as they were present in both the empty vector and MBP

strains, with and without Tc. As the clones expressed the protein of interest and showed the right antibiotic resistance, their ß-galactosidase activity was not tested.

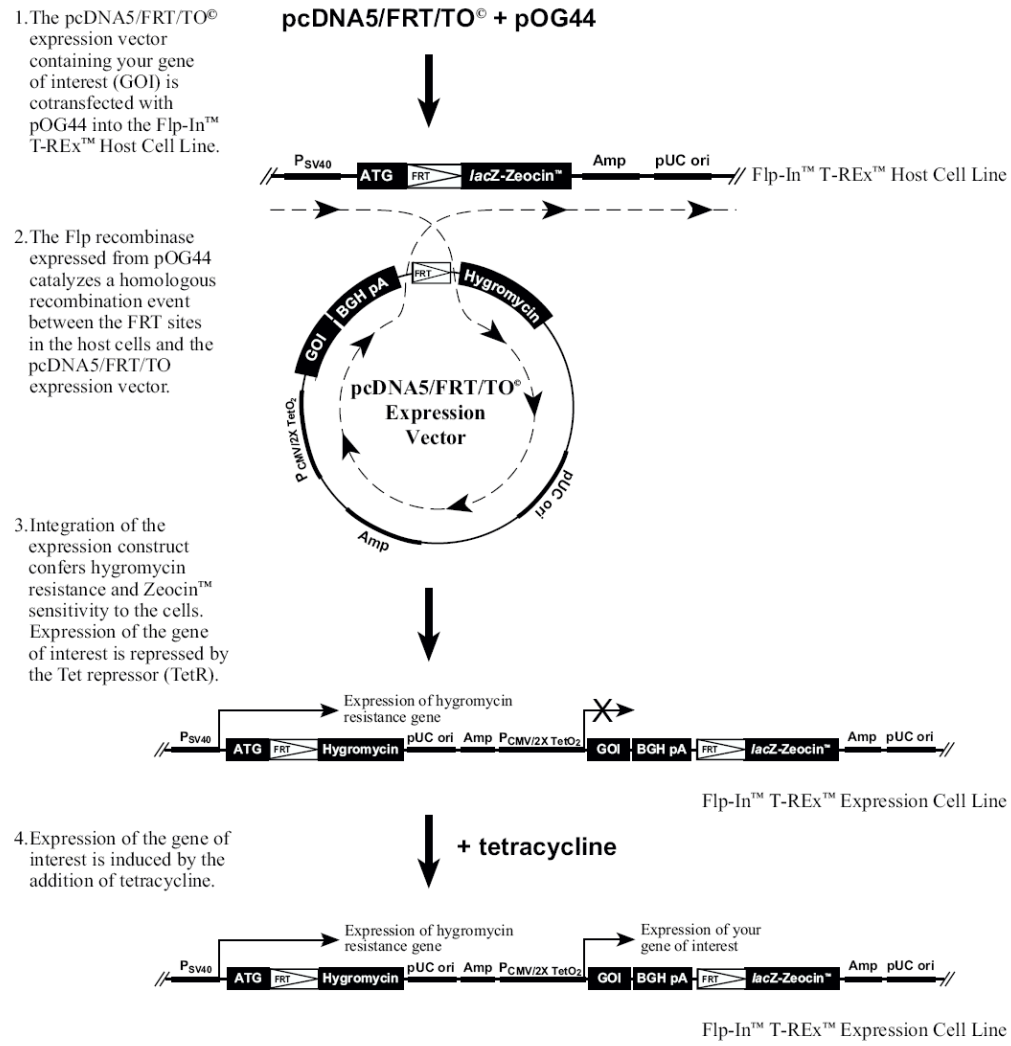

Figure 8: Diagram of the Flp-In TREx system. Adapted from Invitrogen's manual.

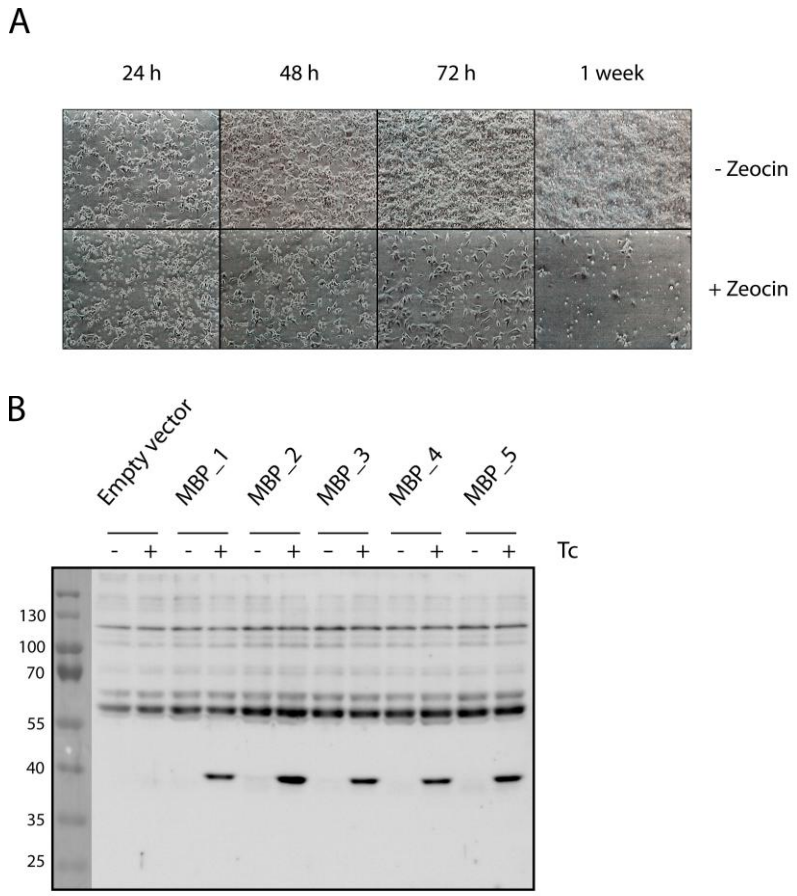

Figure 9: Selection of FLp-In T-Rex MBP cell lines. After recombination and growth in the presence of hygromycin, 5 positive clones (1,2,3,4 and 5) were tested for their zeocin sensitivity (A) and expression of MBP (B). A: Zeocin sensitivity was assessed by looking at the cell viability after 24, 48, 72 h or 1 week in presence of 100 µg/ml zeocin. Example of an isolated clone. B: Expression of MBP was induced with 1 µg/ml Tc. After 24 h, total protein was extracted and samples were subjected to SDS-PAGE. MBP (43 kDa) was detected by immunoblotting with an anti-MBP antibody. The size marker is indicated in kDa.

Off7 and MBP localization and interaction

Off7 was described to bind MBP in vitro with a strong affinity (K_D= 4.4 nM). To make sure that the constructs studied here would also be able to interact in vivo, their localization in HEK293T cells was monitored by fluorescence microscopy. Off7 was fused to RFP (Fig. 10A) and MBP was fused to GFP(Fig. 10B). They were both distributed equally throughout the cell and were shown to colocalize (Fig. 10C). Off7, Off7-ODC and Off7-NYV only differed at their C terminus and the degron sequence was not expected to have any influence on localization. Cdc4, the scaffold F-box protein used for the engineering of cdc4-off7, contained a non-functional NLS sequence. This mutated NLS was previously shown to result in cdc4 expression in the nucleus and cytoplasm of *S.cerevisiae* [40], it was expected to behave similarly when expressed in mammalian cells. All effector proteins and MBP, the target protein, were predicted to be located in the cytoplasm.

To test if off7 was still able to recognize MBP expressed in mammalian cells, a pull-down assay was performed. RGS(His)$_6$off7 was produced in *E. coli* and bound to Ni-NTA magnetic beads. In parallel, it was in vivo biotinylated and bound to magnetic streptavidin beads. Pre-loaded beads were incubated with FLp-In T-Rex MBP cell lysates; in both cases, part of MBP could be specifically pulled down (Fig. 10D,E). Two contaminating proteins migrating between 55 and 70 kDa interacted with the Ni-NTA beads but not the streptavidin beads. All effector proteins were desiged, so that off7 binding properties would not be affected by the presence of a degron or F-box motif, so the effector proteins were predicted to be able to interact with MBP as well. Off7-ODC was the only protein which could be easily expressed and purified in *E. coli*, it was observed to bind MBP with a similar affinity to the wt (see chapter 2).

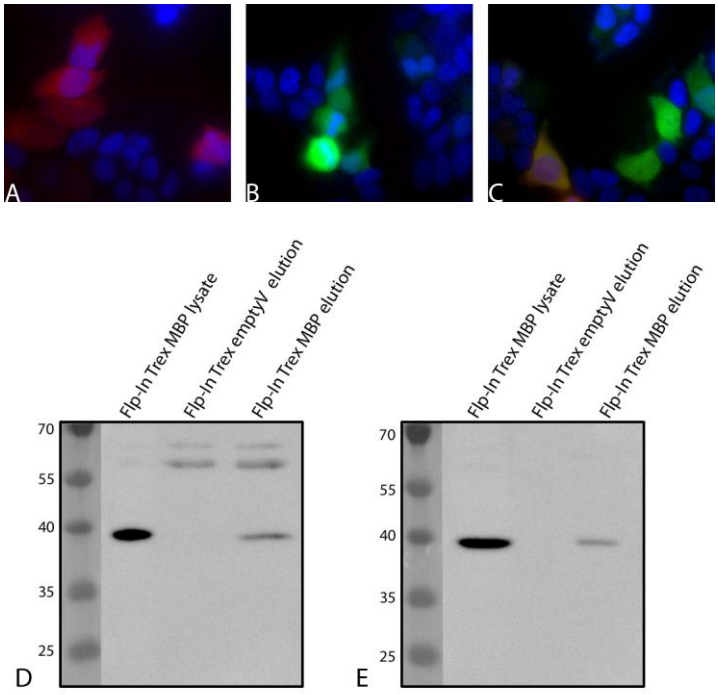

Figure 10: Off7 and MBP localization and interaction. A: Fluorescence microscopy of HEK293T cells expressing off7-RFP. B: Fluorescence microscopy of HEK293T cells expressing MBP-GFP. C: HEK293T cells expressing off7-RFP and MBP-GFP. D: Pull-down experiment of MBP with off7 bound to Ni-NTA beads. E: Pull-down experiment of MBP with biotinylated off7 bound to streptavidin beads. D,E: FlpIn Trex emptyV or FlpIn Trex MBP cells were lysed 24 h after induction with 1 µg/ml Tc. Lysates were incubated with Ni-NTA beads preloaded with *E. coli*-produced off7 (D) or streptavidin beads preloaded with *E. coli*-produced biotinylated off7 (E). Samples of FlpIn Trex MBP lysates, FlpIn Trex emptyV eluates and FlpIn Trex MBP eluates were subjected to SDS-PAGE and immunoblotted with an anti-MBP antibody. The size marker is indicated in kDa.

Steady-state level of MBP in presence of effector proteins

To test if one or several of the effector proteins could lead a target protein to degradation, identical amounts of FLp-In T-Rex cells stably expressing MBP, were transiently transfected with a plasmid encoding under the CMV promoter, Off7, Off7-ODC, Off7-NYV or cdc4-off7. MBP steady-state levels were compared by western blot. Several strategies were investigated to test different conditions regarding the timing of MBP induction and transient transfection. A first experiment was performed

where MBP expression was induced before or after the effector protein transfection. MBP was either induced 24 h before and stopped 6 h after transfection (30 h MBP expression) or induced 6 h after transfection (18 h MBP expression). 24 h after transfection, MBP steady-state levels were assessed. There was no significant difference between the non-transfected cells and the transfected ones but a small decrease could be observed when MBP was induced for 18 h only in presence of cdc4-off7 (Fig. 11).

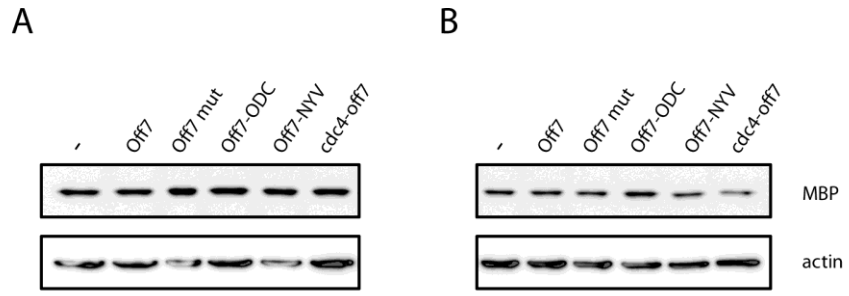

Figure 11: Steady state level of MBP, expressed under Tet promoter and stably integrated into the chromosome, after transient transfection with the effector proteins. A: FLp-In T-Rex MBP cells were induced with 1 µg/ml Tc. 24 h later, they were transiently transfected with pcDNA3+_Off7, pcDNA3+_Off7-ODC, pcDNA3+_Off7-NYV or pcDNA3+_cdc4-off7. 6 h later after transfection, a medium without Tc was added to the cells to stop inducing MBP expression. Untransfected cells were used as negative control (-). B: FLp-In T-Rex MBP cells were transfected with pcDNA3+_Off7, pcDNA3+_Off7-ODC, pcDNA3+_Off7-NYV or pcDNA3+_cdc4-off7. 6 h later, MBP expression was induced with 1 µg/ml Tc. Untransfected cells were used as negative control (-) A, B: 24 h after transfection, total protein was extracted and samples normalized before being subjected to SDS-PAGE. The levels of MBP were detected by immunoblotting with an anti-MBP antibody. The actin signal was used as an internal loading control.

MBP was well expressed and seemed rather stable, and thus a second experiment was conducted on a longer time scale. MBP expression was first induced for 24 h, stopped and 6 h later, the cells were transfected. 24 h, 39 h and 48 h after transfection, MBP steady-state levels were compared. Despite the longer time range, no dramatic difference could be observed except a slight decrease 39 h after transfection with cdc4-off7 (Fig. 12).

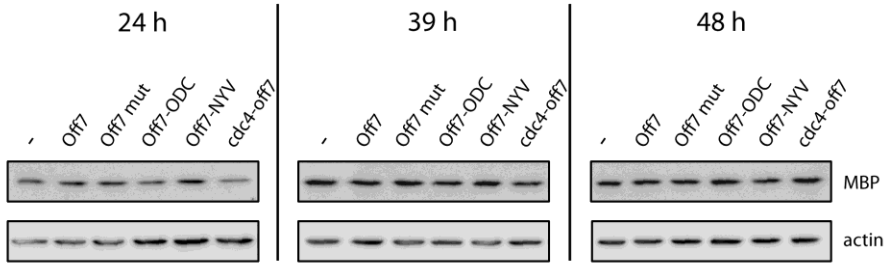

Figure 12: Steady state level of MBP after transient transfection with the effector proteins. FLp-In T-Rex MBP cells were treated with 1 µg/ml Tc for 24 h. 6 h later, they were transiently transfected with pcDNA3+_Off7, pcDNA3+_Off7-ODC, pcDNA3+_Off7-NYV or pcDNA3+_cdc4-off7. Untransfected cells were used as negative control (-). 24 h, 39 h and 48 h after transfection, total protein was extracted and samples normalized before being subjected to SDS-PAGE. The levels of MBP were detected by immunoblotting with an anti-MBP antibody. The actin signal was used as an internal loading control.

Finally, the second experiment was repeated with a slightly modified protocol. MBP expression was induced for 19 h only and stopped; the transfection was performed 4.5 h later. The non-specific DARPin E3_5 (does not recognize MBP) was used as negative control in case the transient transfection would have an impact on MBP level. Similarly to the previous results, MBP level was fainter 24 h after transfection with cdc4-off7, but not after 30 h (Fig. 13). To conclude, MBP steady-state level was not affected by the presence of Off7, Off7-ODC or Off7-NYV. Even if these effector proteins might efficiently go to the proteasome, they did not seem to induce MBP degradation. A faint effect was observed with cdc4-off7, but not on a regular basis.

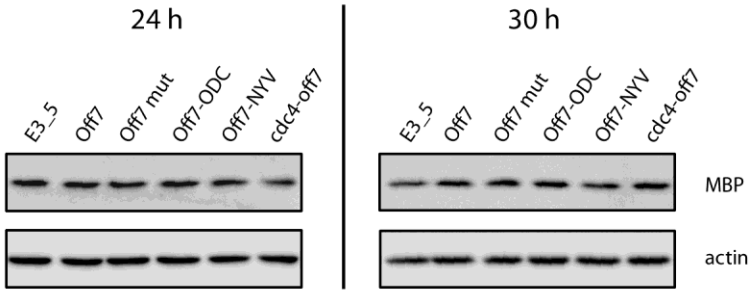

Figure 13: Steady state level of MBP after transient transfection with the effector proteins. FLp-In T-Rex MBP cells were treated with 1 µg/ml Tc for 19 h. 4 h 30 min later, they were transiently transfected with pcDNA3+_E3_5, pcDNA3+_Off7, pcDNA3+_Off7-ODC, pcDNA3+_Off7-NYV or pcDNA3+_cdc4-off7. 24 h and 30 h after transfection, total protein was extracted and samples normalized before being subjected to SDS-PAGE. The levels of MBP were detected by immunoblotting with an anti-MBP antibody. The actin signal was used as an internal loading control.

MBP-ODC and MBP-NYV, potential alternative substrates to MBP

In yeast, MBP had already been used as target protein and could be degraded by cdc4-off7 (see chapter 1). In mammalian cells, its steady-state level was at most slightly affected, and only under certain experimental conditions. MBP was perhaps not an appropriate proteasomal substrate when expressed in mammalian cells. Its behavior was examined after cycloheximide treatment and it appeared indeed to be extremely stable with a half-life superior to 8 h (Fig. 14). It was not degraded by the proteasome, as the addition of MG132 did not increase its level. This highly stable molecule was probably reluctant to any degradation strategy.

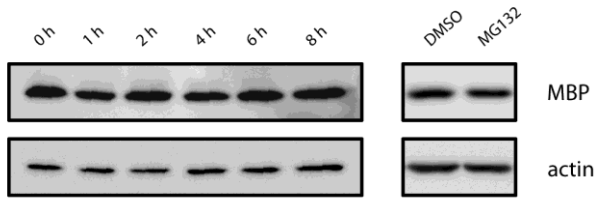

Figure 14: MBP stability in the presence of cycloheximide or MG132. HEK293T cells were transfected with pcDNA3(+)_MBP. 24 h after transfection, 20 µg/ml cycloheximide was added to the cells and samples were taken at the indicated time points. Independently, cells were treated with DMSO or 30 uM MG132 for 5 h. Total protein was extracted and normalized samples were subjected to SDS-PAGE. MBP levels were detected by immunoblotting with an anti-MBP antibody. The actin signal was used as an internal loading control.

We therefore sought to use another target protein which could still be recognized by off7 but which could also be degraded by the proteasome. The ODC and NYV degrons which were previously used to construct Off7-ODC and Off7-NYV, were fused to the C-terminus of MBP, yielding MBP-ODC and MBP-NYV (no HA tag at N-terminus). Their effect on MBP stability was inspected after addition of cycloheximide. MBP-ODC was also very stable, with a half-life higher than 8 h, while MBP-NYV had a half-life close to 2 h and was the only one to accumulate in presence of MG132 (Fig. 15). Similarly to their effect on off7, ODC and NYV degron sequences did not result in the same destabilization of MBP and remarkably, their effect seemed to be also dependent on the target protein. Indeed, Off7 was more destabilized by the ODC degron for which no effect could be observed on MBP. Instead, MBP was more destabilized by the NYV degron which had less an effect on Off7.

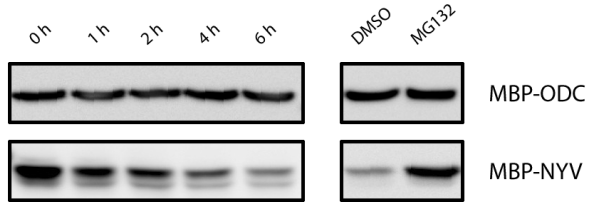

Figure 15: MBP-ODC and MBP-NYV stability in the presence of cycloheximide or MG132. HEK293T cells were transfected with pcDNA3(+)_MBP-ODC or pcDNA3(+)_MBP-NYV. 24 h after transfection, 20 µg/ml cycloheximide was added to the cells and samples were taken at the indicated time points. Independently, cells were treated with DMSO or 30 uM MG132 for 5 h. Total protein was extracted and normalized samples were subjected to SDS-PAGE. MBP-ODC and MBP-NYV levels were detected by immunoblotting with an anti-MBP antibody.

Co-transfection experiments with MBP-NYV

MBP-NYV seemed to be an appropriate proteasomal substrate, and therefore was used as target protein instead of MBP. We aimed to look at its stability in the absence or presence of a specific effector protein. No stable cell line was generated with MBP-NYV, but a plasmid encoding MBP-NYV was co-transfected with a plasmid encoding E3_5, Off7, Off7-ODC, Off7-NYV or cdc4-off7 in HEK293T cells. 24 h after co-transfection, cells were treated with cycloheximide and different behaviors were observed. In the

presence of E3_5 (which does not recognize MBP), the negative control, MBP-NYV level rapidly dropped within 1 h before reaching a basal level (Fig. 16). This behavior differed somewhat from what had been witnessed previously when MBP-NYV was expressed alone and slowly and regularly degraded (Fig. 15). With Off7-ODC and Off7, a similar trend to what was described with E3_5, was observed but the reaction seemed to be slower and reached a constant level which was higher than the basal one observed wit E3_5 (Fig. 16). Both effects were more pronounced for Off7 than Off7-ODC. With Off7-NYV, MBP-NYV did not seem to be degraded or very slightly only (Fig. 16). Finally, when MBP-NYV was co-expressed with cdc4-off7, a slow regular decrease was observed reaching a final level lower than the basal one observed with E3_5 (Fig. 16). It seemed then that different processes were taking place, interfering with MBP-NYV own degradation pathway. The effector proteins Off7-ODC and Off7 especially were hampering MBP-NYV degradation as they were slowing it down and Off7-NYV even inhibited it. In parallel, the chimeric F-box did not inhibit the degradation of MBP-NYV, in fact when comparing with the effect of E3_5, cdc4-off7 seemed to bring it to completion. After 4 h 30 min, MBP-NYV level in the presence of cdc4-off7 was indeed lower than in the presence of E3_5. MBP-NYV stability pattern was also different when it was co-expressed with cdc4-off7. This slow regular decrease was very close to what could be observed in yeast when MBP was degraded by the action of cdc4-off7 and the ubiquitin proteasome pathway (see chapter 1).

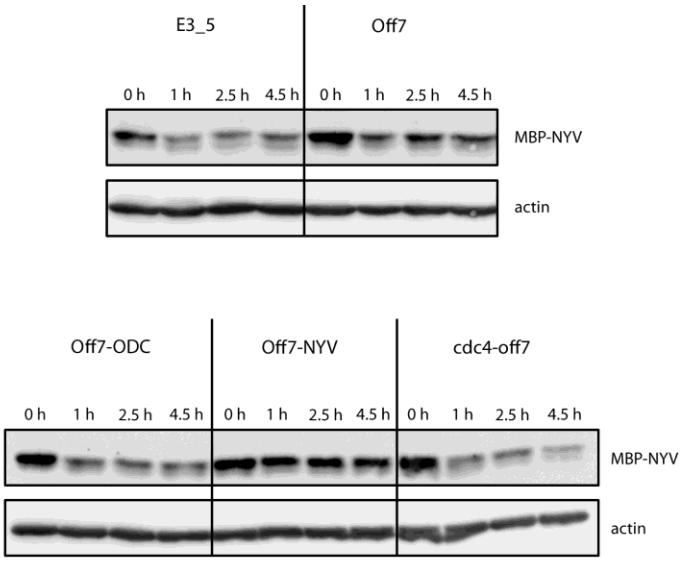

Figure 16: Stability of MBP-NYV in the presence of all effector proteins. HEK293T cells were co-transfected with a 1:2 ratio of pcDNA3(+)_MBP-NYV and pcDNA3+_E3_5, pcDNA3+_Off7, pcDNA3+_Off7-ODC, pcDNA3+_Off7-NYV or pcDNA3+_cdc4-off7. 24 h after transfection, 20 µg/ml cycloheximide was added to the cells and samples were taken at the indicated time points. Total protein was extracted and normalized samples were subjected to SDS-PAGE. MBP-NYV levels were detected by immunoblotting with an anti-MBP antibody. The actin signal was used as an internal loading control.

A second experiment was conducted but with E3_5, Off7 and cdc4-off7 only. MBP-NYV stability could not be nicely followed like in the first co-transfection experiment, but similar results were obtained (Fig. 17). With E3_5, the negative control, MBP-NYV stayed at a constant low level. With off7, it was slowly decreasing and with cdc4-off7, it was so quickly disappearing that it was almost impossible to monitor. These co-transfection experiments results led us to think that cdc4-off7 was not inhibiting the degron-dependent degradation pathway but more importantly, could be mediating MBP-NYV degradation via another mechanism, possibly the ubiquitin proteasome pathway.

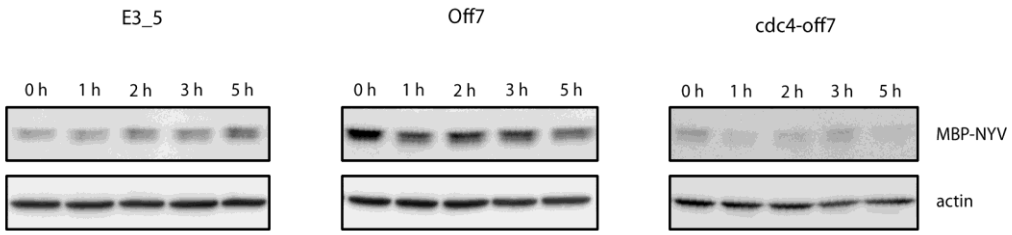

Figure 17: Stability of MBP-NYV in presence of E3_5, off7 or cdc4-off7. HEK293T cells were co-transfected with a 1:2 ratio of pcDNA3(+)_MBP-NYV and pcDNA3+_E3_5, pcDNA3+_Off7 or pcDNA3+_cdc4-off7. 24 h after transfection, 20 µg/ml cycloheximide was added to the cells and samples were taken at the indicated time points. Total protein was extracted and normalized samples were subjected to SDS-PAGE. MBP-NYV levels were detected by immunoblotting with an anti-MBP antibody. The actin signal was used as an internal loading control.

Degradation of a target protein with a chimeric F-box protein

Establishment of chimeric F-box proteins stable cell lines

In order to better assess if chimeric F-box proteins could really degrade a target protein via the ubiquitin proteasome pathwayin mammalian cells, stable cell lines expressing the chimeric F-box protein cdc4-off7 or cdc4-E3_5 were generated using the Flp-In T-REx system (Fig. 18). Cdc4-E3_5 was designed identically to cdc4-off7, the non-selected DARPin E3_5 was used instead of off7, to replace cdc4 original substrate binding domain. cdc4-off7 and cdc4-E3_5 coding sequences were integrated in the genome of the Flp-In T-Rex cells, yielding the FLp-In T-Rex cdc4-off7 and FLp-In T-Rex cdc4-E3_5 cells, respectively. In addition to the non-specific chimeric F–box protein cell line, two other ones were generated as negative controls. The first one contains off7, the naked DARPin, which cannot interact with the SCF machinery without any F-box domain (FLp-In T-Rex off7) (Fig. 18). The second one was constructed with the same plasmid as for the other ones but without any coding sequence (FLp-In T-Rex EmptyV). Selected clones which were hygromycin resistant, zeocin sensitive and lacking their ß–galactosidase activity, were induced with Tc. All tested clones expressed the protein of interest (Fig. 19). Different expression levels were observed depending on the construct, cdc4-E3_5 was relatively well expressed, closely followed by cdc4-off7 while off7 was barely detectable. The low level of off7 expression was consistently observed. Remarkably, FLp-In T-Rex off7 grew also more slowly than the other stable cell lines. Phenotypically, FLp-In T-Rex cdc4-

off7, FLp-In T-Rex cdc4-E3_5 and FLp-In T-Rex off7 were not spreading on the surface as homogeneously as the FLp-In T-Rex EmptyV cells and they tended to stack on the top of each other. This observation was made in the absence or presence of Tc.

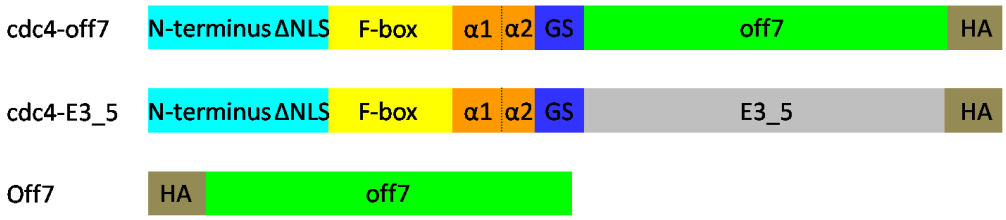

Figure 18: Schematic diagrams of the chimeric F-box proteins used to generate stable cell lines. cdc4-off7 and cdc4-E3_5 were designed on the cdc4 scaffold. Its NLS sequence present in the N-terminal part (light blue) was mutated. Its F-box domain was conserved (yellow). The linker made of two helices α1 and α2 (orange) was reengineered; part of α2 was replaced with a gly-ser linker (dark blue). Its substrate binding domain was deleted and replaced with off7 or E3_5. An HA tag was fused to their C-terminus (brown). Off7 with an HA tag at its N-terminus was used to generate the control FLp-In T-Rex off7 cell line.

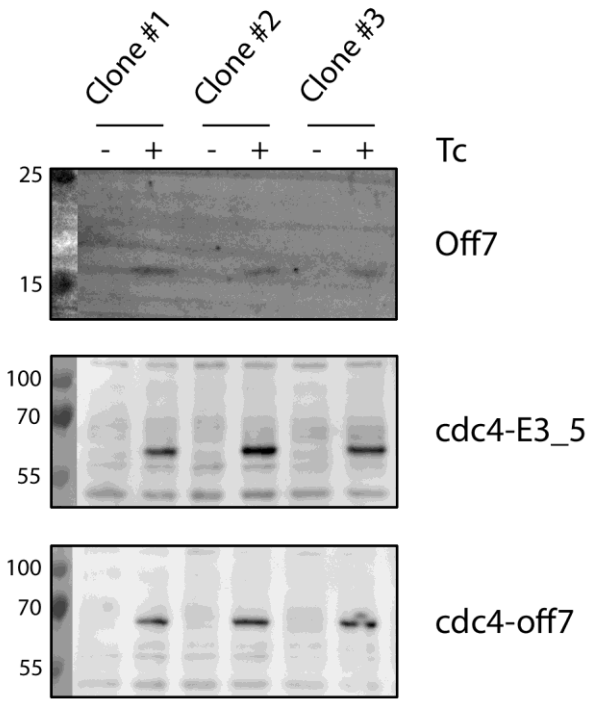

Figure 19: Expression test for the stable cell lines FLp-In T-Rex off7, FLp-In T-Rex cdc4-E3_5 and FLp-In T-Rex cdc4-off7. Expression was induced with 1 µg/ml Tc. After 24 h, total protein was extracted and normalized samples were subjected to SDS-PAGE. Off7 (18.2 kDa), cdc4-E3_5 (56.6 kDa) and cdc4-off7 (56.8 kDa) were detected by immunoblotting with the anti-HA antibody. The size marker is indicated in kDa.

MBP steady-state level and stability in chimeric F-box proteins stable cell lines

MBP was cloned, without any additional tag, in pcDNA3(+) under the CMV promoter and transiently transfected in FLp-In T-Rex cdc4-off7, FLp-In T-Rex cdc4-E3_5, FLp-In T-Rex off7 and FLp-In T-Rex emptyV cells. 15 to 22 h after transfection, Tc was added to the cells to induce the expression of cdc4-off7, cdc4-E3_5 or off7. MBP steady state levels were monitored after 24 h and 32 h of Tc treatment. The relative amount of MBP varied from strain to strain, resulting from different transfection efficiencies (Fig. 20). All cell lines could not be transfected using the same conditions as they grew differently. FLp-In T-Rex cdc4-E3_5 and FLp-In T-Rex cdc4-off7 cells were transfected with Lipofectamine and 1.5 µg DNA while FLp-In T-Rex off7 and FLp-In T-Rex emptyV cells were transfected 7 h later with Fugene and 1 µg DNA. For each assay, the optimal transfection method was chosen according to the cells confluency and was always constant within a group of samples: emptyV and Off7 cell lines formed one group and cdc4-E3_5 and cdc4-off7 the second one. A comparison of MBP steady-state levels in between different cell lines was then not possible but only within each cell line, in absence or presence of Tc. No distinction could be made in absence or presence of Tc in any of the cell lines. MBP steady-state level was not affected by the co-expression of the chimeric F-box protein cdc4-off7.

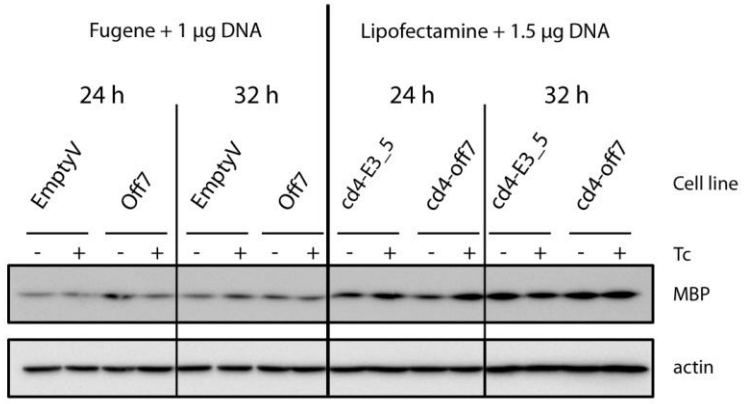

Figure 20: Steady state level of MBP, expressed under CMV promoter on pcDNA 3(+), after transient transfection in FLp-In T-Rex emptyV, FLp-In T-Rex off7, FLp-In T-Rex cdc4-E3_5 or FLp-In T-Rex cdc4-off7 stable cell lines. FLp-In T-Rex cdc4-E3_5 and FLp-In T-Rex cdc4-off7 cells were transfected with lipofectamine and 1.5 µg pcDNA3(+)_MBP. 7h later, FLp-In T-Rex emptyV and FLp-In T-Rex off7 cells were transfected with Fugene and 1 µg pcDNA3(+)_MBP. 15 h later, Tc was added to all cells to induce expression of Off7, cdc4-E3_5 and cdc4-off7. After 24 h or 32 h of Tc treatment, total protein was extracted and samples normalized before being subjected to SDS-PAGE. The levels of MBP were detected by immunoblotting with an anti-MBP antibody. The actin signal was used as an internal loading control. N.B: Tc concentration in the medium was readjusted to a final concentration of 1 µg/ml after 24 h for samples which were withdrawn after 32 h.

MBP stability was then examined in in FLp-In T-Rex cdc4-off7, FLp-In T-Rex cdc4-E3_5, FLp-In T-Rex off7 and FLp-In T-Rex emptyV cells. 16 h after transient transfection, Tc was added to the cells to induce the expression of cdc4-off7, cdc4-E3_5 or Off7. After a 24 h Tc treatment, cells were subjected to cycloheximide and MBP levels followed. In all cases, MBP level stayed constant during the whole experiment (Fig. 21). MBP half-life was higher than 8 h in every cell line. Similar to the previous experiment, relative amounts of MBP varied from strain to strain as different transfection methods were

used. Only cdc4-off7 cells were transfected with another method. They received 1.5 µg DNA while 1 µg was transfected in the other cell lines. This might explain why the amount of MBP was higher in these cells. In this second experimental set-up, MBP was not destabilized by cdc4-off7, either.

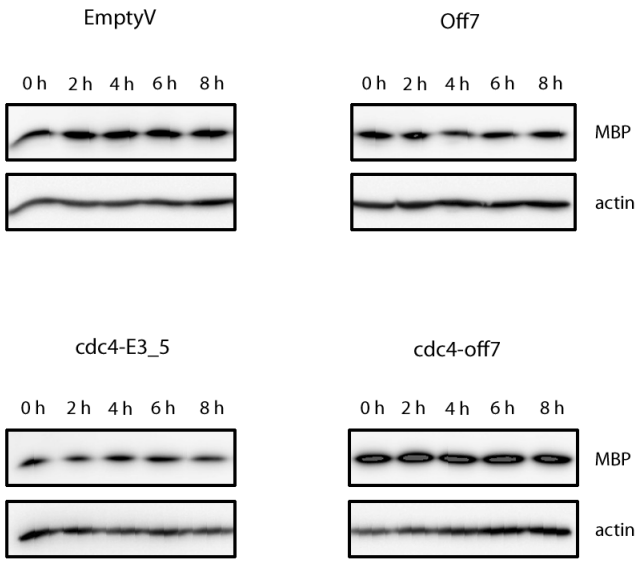

Figure 21: MBP stability in FLp-In T-Rex emptyV, FLp-In T-Rex off7, FLp-In T-Rex cdc4-E3_5 or FLp-In T-Rex cdc4-off7 cells. FLp-In T-Rex cdc4-off7 cells were transfected with lipofectamine and 1.5 µg pcDNA3(+)_MBP. 6 h later, FLp-In T-Rex emptyV , FLp-In T-Rex off7 and FLp-In T-Rex cdc4-E3_5 were transfected with Fugene and 1 µg pcDNA3(+)_MBP. 16 h later, 1 µg/ml Tc was added to all cells to induce expression of Off7, cdc4-E3_5 and cdc4-off7. After 24 h of Tc treatment, 20 µg/ml cycloheximide was added to the cells and samples were taken at the indicated time points. Total protein was extracted and normalized samples were subjected to SDS-PAGE. MBP levels were detected by immunoblotting with an anti-MBP antibody. The actin signal was used as an internal loading control.

MBP-NYV steady-state level in stable cell lines expressing chimeric F-box proteins

When MBP-NYV was co-transfected with cdc4-off7, it seemed to be degraded via another process (Fig. 16). To double check this observation and compare with the observations made above with MBP, additional experiments were conducted in the established chimeric F-box proteins stable cell lines, using MBP-NYV as substrate. First, the MBP-NYV steady-state level was compared after transient transfection, under the same experimental conditions than for MBP. Within each strain, no difference was observed in the absence or presence of Tc. Surprisingly, MBP-NYV steady-state level did not seem to be affected by the co-expression of the chimeric F-box protein cdc4-off7 (Fig. 22).

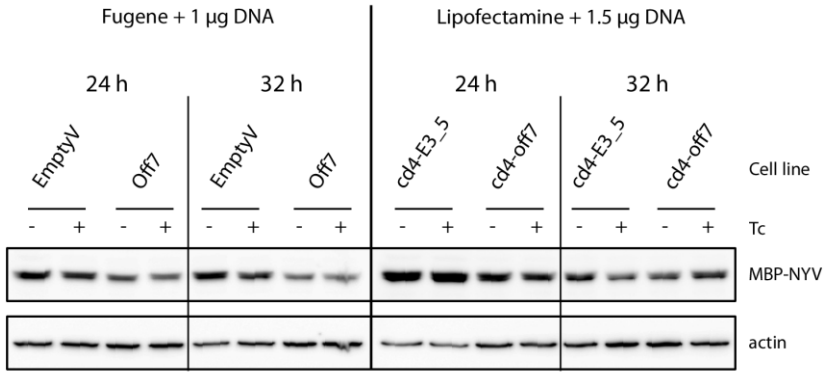

Figure 22: Steady state level of MBP-NYV after transient transfection in FLp-In T-Rex emptyV, FLp-In T-Rex off7, FLp-In T-Rex cdc4-E3_5 or FLp-In T-Rex cdc4-off7 cell lines. FLp-In T-Rex cdc4-E3_5 and FLp-In T-Rex cdc4-off7 were transfected with lipofectamine and 1.5 µg pcDNA3(+)_MBP-NYV. 7 h later, FLp-In T-Rex emptyV and FLp-In T-Rex off7 were transfected with Fugene and 1 µg pcDNA3(+)_MBP_NYV. 15 h later, Tc was added to all cells to induce expression of Off7, cdc4-E3_5 and cdc4-off7. After 24 h and 32 h of Tc treatment, total protein was extracted and samples normalized before being subjected to SDS-PAGE. The levels of MBP-NYV were detected by immunoblotting with an anti-MBP antibody. The actin signal was used as an internal loading control. N.B: Tc concentration in the medium was readjusted to a final concentration of 1 µg/ml after 24 h for samples which were withdrawn after 32 h.

Different transfection protocols were then tested to check if cdc4-off7 could have an effect on MBP-NYV steady-state levels under different conditions. First, FLp-In T-Rex cdc4-off7 and FLp-In T-Rex cdc4-E3_5 cells were calcium phosphate-transfected with a varying amount of pcDNA3(+)_MBP-NYV, 1, 1.5 or 2 µg DNA. 6 h after transfection, a fresh medium containing Tc was added to the cells. MBP-NYV steady-state levels were monitored after 24 h, 41 h or 48 h of Tc treatment. Despite lowering the amount of MBP-NYV, no differences could be seen in the steady-state levels between the absence or presence of Tc (Fig. 23).

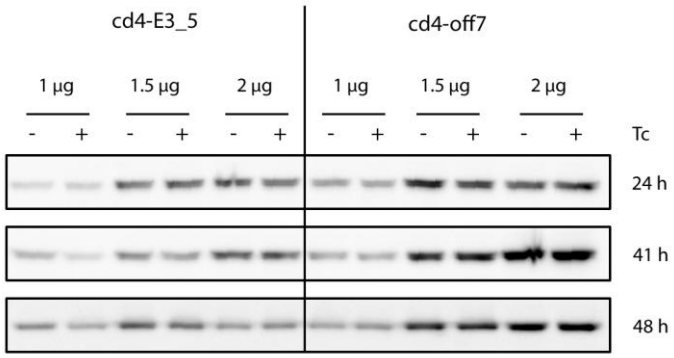

Figure 23: Steady state level of MBP-NYV after calcium phosphate transient transfection in FLp-In T-Rex cdc4-E3_5 or FLp-In T-Rex cdc4-off7 cells with varying amount of DNA. Cells were transfected with 1, 1.5 or 2 µg pcDNA3(+)_MBP-NYV. 6 h after transfection, Tc was added to the cells to induce expression of cdc4-E3_5 and cdc4-off7. After 24 h, 41 h or 48 h of Tc treatment, total protein was extracted and samples normalized before being subjected to SDS-PAGE. The levels of MBP-NYV were detected by immunoblotting with an anti-MBP antibody. The actin signal was used as an internal loading control. N.B: Tc concentration in the medium was readjusted to a final concentration of 1 µg/ml after 24 h for samples which were withdrawn after 41 h and 48 h.

Another protocol consisted of performing the transfection with cells in solution instead of immobilized on a cell culture plate. The different cell lines were not growing at the same speed and not spreading properly on the surface, and therefore it was difficult to carry out transfections under the same conditions and even sometimes within the same cell line. To limit variability, the same number of FLp-In T-Rex cdc4-off7 and FLp-In T-Rex cdc4-E3_5 cells were simultaneously transfected and seeded on a cell culture plate. 16 h later, Tc was added and 24 h after induction of chimeric F-box proteins expression, the MBP-NYV steady-state level was monitored (Fig. 24A). No difference was detected between the absence or presence of Tc for both cell lines. In spite of carrying out the transfection with the same number of cells, MBP level was still not identical in both FLp-In T-Rex cdc4-off7 and FLp-In T-Rex cdc4-E3_5 cells. A better normalization of the cell number used for transfection was achieved with this protocol, but cells did not adhere very well, they were probably disturbed by the transfection process. A second transfection experiment was performed similarly but using 0.1 % Fibronectin pre-coated cell culture plates. Cells did easily adhere after seeding and were better distributed on the surface. Again, the MBP-NYV steady-state level was unaltered in the presence of Tc and despite all efforts; the level of MBP-NYV was still not identical between the two strains (Fig. 24B).

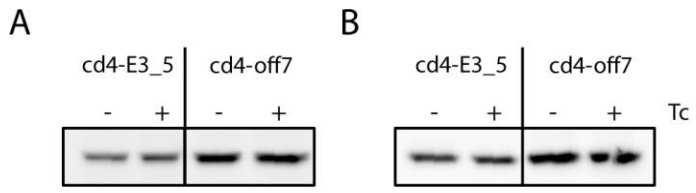

Figure 24: Steady state level of MBP-NYV in FLp-In T-Rex cdc4-E3_5 or FLp-In T-Rex cdc4-off7 cells after transient transfection in solution. Cells were simultaneously seeded and transfected with lipofectamine and 1.5 µg pcDNA3(+)_MBP-NYV. 16 h later, Tc was added to the cells to induce expression of cdc4-E3_5 and cdc4-off7. After 24 h of Tc treatment, total protein was extracted and samples normalized before being subjected to SDS-PAGE. The levels of MBP-NYV were detected by immunoblotting with an anti-MBP antibody. The actin signal was used as an internal loading control. A: Cells were seeded on normal culture plates. B: Culture plates were first pre-coated with 0.1 % fibronectin for 2 h at 37°C.

MBP-NYV stability in stable cell lines expressing chimeric F-box proteins

Several conditions were tested and MBP-NYV steady-state was definitely not affected by the presence of cdc4-off7, but could its turnover be altered? MBP-NYV stability was examined in FLp-In T-Rex cdc4-off7, FLp-In T-Rex cdc4-E3_5, FLp-In T-Rex off7 and FLp-In T-Rex emptyV cells in the absence or presence of Tc. 12 h to 17 h after transient transfection with pcDNA3(+)_MBP-NYV, Tc was added to the cells. After 24 h Tc treatment, cells were treated with cycloheximide and MBP-NYV levels were followed. In FLp-In T-Rex emptyV and FLp-In T-Rex cdc4-E3_5 cells, no difference could be observed between the absence and the presence of Tc (Fig. 25). In FLp-In T-Rex off7 and FLp-In T-Rex cdc4-off7 cells, MBP-NYV degradation was slowed down and barely taking place in the presence of Tc. These results correlated with what had been previously seen for off7 in the co-transfection experiments but not with what had been observed for cdc4-off7 (Fig. 16 & 17). In the co-transfection experiments, MBP-NYV was still turned over in the presence of cdc4-off7, at a lower rate, but it was degraded within the same experimental time frame. In

the latter experiment, cdc4-off7 had the same effect than off7. The second experimental set-up proved that cdc4-off7 was interfering with MBP-NYV own degradation pathway but did not reveal how.

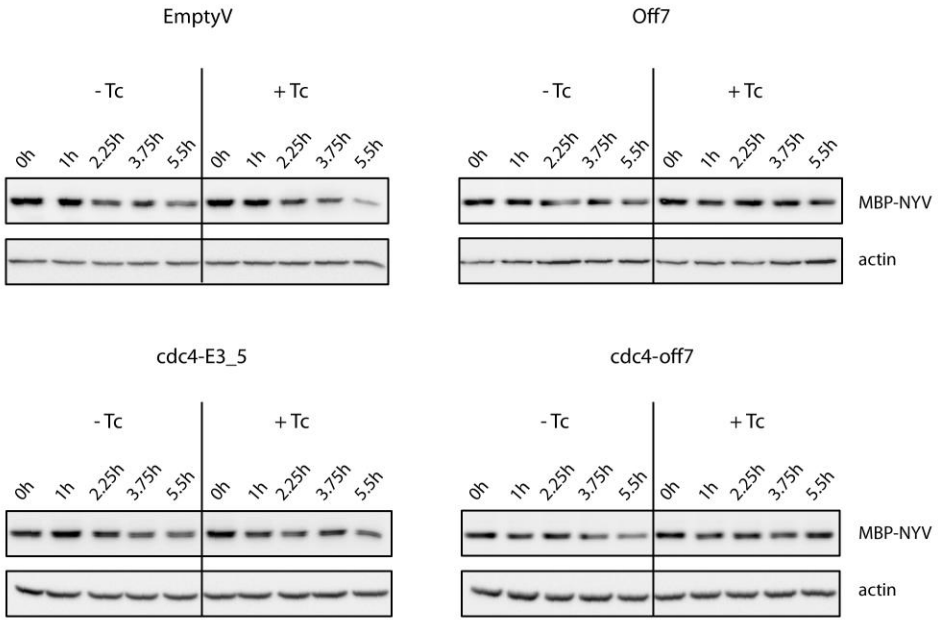

Figure 25: MBP-NYV stability in FLp-In T-Rex emptyV, FLp-In T-Rex off7, FLp-In T-Rex cdc4-E3_5 or FLp-In T-Rex cdc4-off7 cells. FLp-In T-Rex emptyV and FLp-In T-Rex off7 cells were transfected with Fugene and 1 µg pcDNA3(+)_MBP_NYV. 5 h later, FLp-In T-Rex cdc4-E3_5 and FLp-In T-Rex cdc4-off7 were transfected with calcium phosphate and 1.8 µg pcDNA3(+)_MBP_NYV. 12 h later, 1 µg/ml Tc was added to all cells to induce expression of Off7, cdc4-E3_5 and cdc4-off7. After 24 h Tc treatment, 20 µg/ml cycloheximide was added to the cells and samples were taken at the indicated time points. Total protein was extracted and normalized samples were subjected to SDS-PAGE. MBP-NYV levels were detected by immunoblotting with an anti-MBP antibody. The actin signal was used as an internal loading control.

Immunoprecipitation of cdc4-off7 and MBP-NYV

To investigate if cdc4-off7 was redirecting MBP-NYV to the ubiquitin proteasome pathway, we looked for ubiquitylated forms of it. MBP-NYV was transfected in FLp-In T-Rex cdc4-off7 and FLp-In T-Rex emptyV cells, it was immunoprecipitated using the anti-MBP antibody. No additional species of higher molecular weight could be detected (Fig. 26A). When the eluates were probed with the anti-ubiquitin antibody, a smear appeared but both in absence and presence of cdc4-off7, and therefore it did not correspond to ubiquityled forms of MBP-NYV, but probably to other ubiquitylated proteins, possibly interacting with MBP-NYV (Fig. 26C). The experiment was repeated with cell lysates containing MBP instead of MBP-NYV, but ubiquitylated species were not detected either and the smear observed with MBP-NYV was not present any more (data not shown). The chimeric F-box protein (56.8 kDa), running below 70 kDa, co-eluted with MBP-NYV (47 kDa), proving that they were interacting in vivo (Fig. 26B). Strangely, when cdc4-off7 was immunoprecipitated with the anti-HA antibody, it did not co-precipitate MBP-NYV (Fig. 26B). When the experiment was repeated with cell lysates containing MBP instead of MBP-NYV, identical results were obtained (data not shown). Cdc4-off7 was present in MBP immunoprecipitation eluate but

MBP was not detected in cdc4-off7 immunoprecipitation samples. F-box proteins are normally autoubiquitinated but no ubiquitylated forms of cdc4-off7 could be detected with the anti-HA or anti-ubiquitin antibodies (Fig. 26B,C).

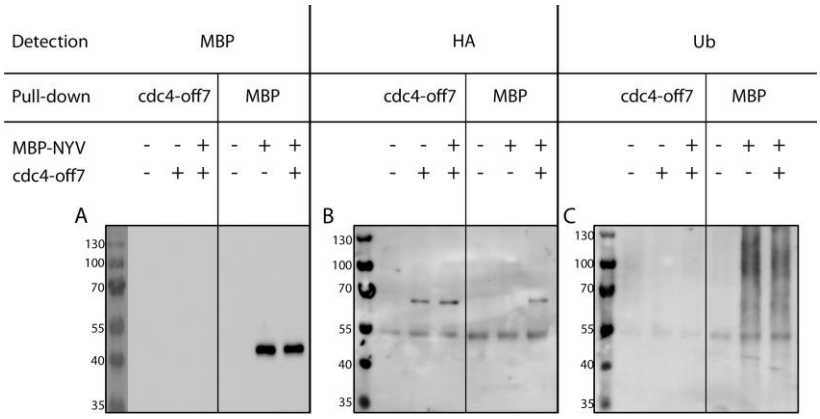

Figure 5. Immunoprecipitations of MBP-NYV and cdc4-off7. MBP-NYV was transfected in FLp-In T-Rex emptyV and FLp-In T-Rex cdc4-off7 cells which were cultured in the presence of 1 µg/ml Tc. 24 h after transfection, cells were treated with 30 uM MG132 for 6 h. After cell lysis, MBP-NYV (47 kDa) was immunoprecipitated with an anti-MBP antibody and cdc4-off7 (56 kDa) with an anti-HA antibody. The eluted fractions were detected with an anti-MBP antibody (A), the anti-HA antibody (B) and the anti-ubiquitin antibody (C). The size marker is indicated in kDa.

Remarkably, the in vivo interaction of MBP-NYV and cdc4-off7 could be observed in only one direction by immunoprecipitation. Cdc4-off7 co-eluted with MBP-NYV, but when cdc4-off7 was pulled down, MBP-NYV could not be detected. Identical results were obtained with MBP. To make sure that cdc4-off7 was not unspecifically pulled-down with MBP-NYV (or MBP) which was present in higher amount, its binding properties were checked by ELISA. MBP was produced in *E. coli* and immobilized. Lysates from FLp-In T-Rex off7, FLp-In T-Rex cdc4-off7 and FLp-In T-Rex emptyV cells were incubated for 1 h 30 min at 37°C. FLp-In T-Rex off7 lysate gave a huge signal, which was quickly saturated, confirming that off7 could readily bind to MBP (Fig. 27). FLp-In T-Rex cdc4-off7 lysate gave a more moderate but constantly increasing signal; after 90 min of development, it was 5-fold higher than the one obtained with FLp-In T-Rex emptyV cells. cdc4-off7 could thus, when produced in FLp-In T-Rex HEK293 cells, bind to *E. coli* produced MBP. Its binding strength seemed lower than off7's one but it might have been more affected by the incubation at 37°C than off7 alone which is very stable in vitro. In addition, cdc4-off7 structural integrity and/or binding capacities were also altered by the buffer used for cell lysis as 100 µl lysate sample mixed with 100 µl ELISA buffer or 50 µl lysate sample mixed with 150 µl ELISA buffer gave a stronger signal than a 200 µl lysate sample. The effect was not so pronounced for off7. ELISA results confirmed that cdc4-off7 had the capacity to bind MBP and led us to think that an experimental artifact was preventing us to detect their in vivo interaction by cdc4-off7 immunoprecipitation.

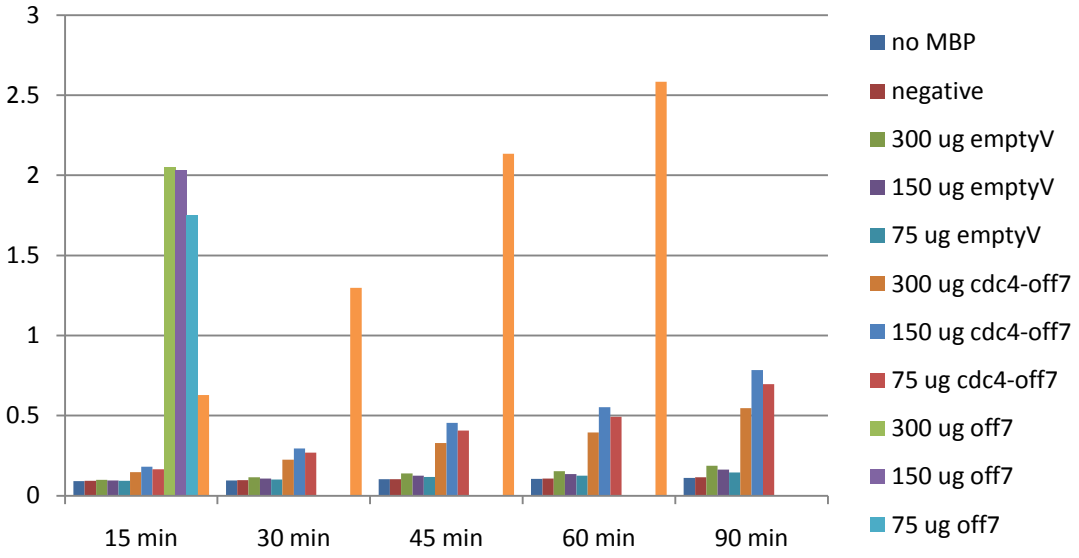

Figure 27: ELISA with FLp-In T-Rex emptyV, FLp-In T-Rex off7 and FLp-In T-Rex cdc4-off7 crude cells lysates. Biotinylated MBP was immobilized on neutravidin pre-coated plates. 300 µg (200 µl crude cell lysate), 150 µg (100 µl crude cell lysate) or 75 µg (50 µl crude cell lysate) total protein was incubated for 1 h 30 min at 37°C in a final volume of 200 µl using TBS + 0.2 % BSA + 0.05 % Tween-20. The anti-HA antibody was used for detection followed by an alkaline phosphatase conjugated anti-mouse antibody. Each sample was assayed in duplicates. 50 nM purified off7 was used as positive control with the antiRGSHis$_4$ Ab instead of the anti-HA one.

In vivo interaction of cdc4-off7 and SCF E3 ligase

According to the immunoprecipitations results, cdc4-off7 was interacting with the target protein but none of them could be detected in an ubiquitylated form. Its interaction with human skp1, the adaptor subunit of the SCF complex, was tested by a second immunoprecipitation assay. MBP was transfected in FLp-In T-Rex emptyV and FLp-In T-Rex cdc4-off7 cells. MBP and cdc4-off7 were pulled down using the anti-MBP and the anti-HA antibodies as respective baits and their eluates were probed with an anti-skp1 antibody. While skp1 (18 kDa) was easily detected in Flp-In T-Rex cdc4-off7 crude cells lysate, it was not present after immunoprecipitation of cdc4-off7 or MBP (Fig. 28). The only visible protein in the elution samples was the light chain of the antibody used for immunoprecipitation, which cross-reacted with the secondary Ab used for detection. No physical interaction could thus be observed in vivo between cdc4-off7 and skp1. According to these results, the chimeric F-box protein, containing a yeast F-box motif, was not recognized by the mammalian SCF machinery. However, co-immunoprecipitation seemed to be problematic under these conditions with cdc4-off7, e.g. it could not co-immunoprecipitate MBP, a highly expressed binding partner. Therefore the pull-down of endogenous skp1 could have been even more problematic. The ELISA also showed that the lysis buffer used for immunoprecipitation was probably not optimal for looking at cdc4-off7 interactions. Under these conditions, it was difficult to exclude the possibility that cdc4-off7 might still associate with the mammalian SCF complex. Nonetheless, we have found no direct evidence for it.

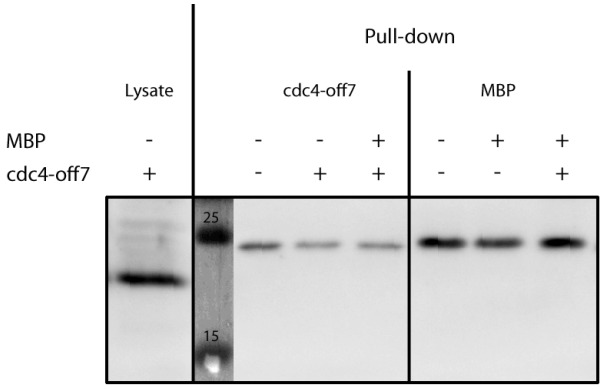

Figure 28: Skp1 interaction. MBP was transfected in FLp-In T-Rex emptyV and FLp-In T-Rex cdc4-off7 cells which were cultured in the presence of 1 µg/ml Tc. 24 h after transfection, cells were treated with 10 uM MG132 for 6 h. After cell lysis, MBP was immunoprecipitated with an anti-MBP antibody and cdc4-off7 with an anti-HA antibody. FLp-In T-Rex cdc4-off7 crude lysate and all eluted fractions were detected with the anti-skp1 antibody. The size marker is indicated in kDa. Skp1 MW= 18 kDa.

Chimeric F-box protein stability in presence of MBP or MBP-NYV

F-box proteins were described as short-lived proteins which can catalyze their own degradation by autoubiquitylation [39]. cdc4-off7 was indeed very unstable in yeast and it behaved similarly in mammalian cells (Fig. 7). We considered the possibility that this chimeric F-box protein, engineered from a yeast F-box protein scaffold, might be functional as a F-box protein and interact with the host SCF ubiquitin ligase. We could not verify this hypothesis by detecting ubiquitylated forms of cdc4-off7, nor by verifying an interaction with skp1. We used a last approach to test if cdc4-off7 was protected from degradation by the presence of MBP or MBP-NYV. When cdc4-off7 was expressed in yeast as a functional F-box protein, the presence of the target protein MBP protected it from degradation and extended its half-life. cdc4-off7 was interacting with MBP-NYV and MBP in yeast and most likely in mammalian cells as well, even though the pull-down experiments worked only in one direction. Therefore we looked at the effect of MBP and MBP-NYV on cdc4-off7 stability. FLp-In T-Rex cdc4-off7 cells were grown in the presence of Tc and transiently transfected with pcDNA3+_MBP or pcDNA3+_MBPNYV. 24 h later, cycloheximide was added to the cultures and cdc4-off7 levels were monitored. In all cases, the chimeric F-box protein was very unstable with a half-life higher than 1 h (Fig. 29). The presence of MBP-NYV did not alter cdc4-off7 stability, nor did the more stable MBP. If cdc4-off7 had functionally recruited MBP or MBP-NYV as substrate, they would have interfered with its own degradation, but this was not the case. These results indicated that cdc4-off7 degradation process was not affected by the presence of a stable binding partner and was very likely independent of the SCF machinery.

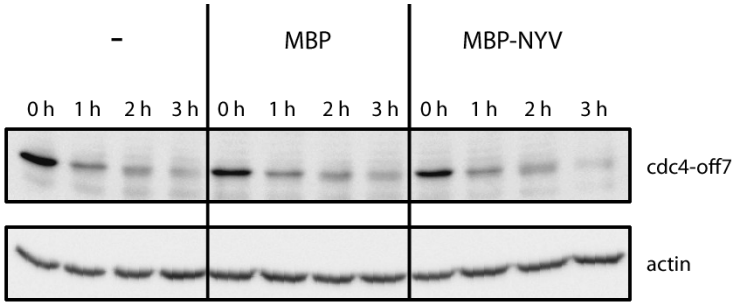

Figure 29: Stability of cdc4-off7 in the absence or presence of MBP and MBP-NYV. FLp-In T-Rex cdc4-off7 cells were cultured in presence of 1 µg/ml Tc. 24 h after transefction with pcDNA3(+)_MBP_NYV or pcDNA3(+)_MBP, 20 µg/ml cycloheximide was added to the cells and samples were taken at the indicated time points. Total protein was extracted and normalized samples were subjected to SDS-PAGE. cdc4-off7 levels were detected by immunoblotting with the anti-HA antibody. The actin signal was used as an internal loading control.

Discussion

Two different strategies were tested to lead a specific target protein for degradation by the 26S proteasome. One relied on the ubiquitin-free route which is employed by the mammalian ornithine decarboxylase and the G1 glycoprotein of the NY-1 hantavirus. The other one was chosen to exploit the ubiquitin proteasome pathway using a chimeric F-box protein. The DARPin off7 was used as scaffold for the engineering of all effector proteins meant to mediate the degradation of its binding partner: Maltose Binding Protein (MBP), in an ubiquitin-independent or -dependent way.

Mouse ornithine decarboxylase and G1 glycoprotein of the NY-1 hantavirus harbor each a specific sequence, which is recognized by the 26S proteasome, that we, respectively, named the ODC- and NYV-degron in our study [41, 42]. When any of these degrons was appended to the C-terminus of several proteins expressed in *S. cerevisiae*, they provoked their fast degradation by the yeast proteasome (see Chapter 2). These degron sequences had however variable effects when fused to proteins expressed in mammalian cells. Off7-ODC was unstable with a half-life of 45 min which was longer compared to the 15 min observed in yeast. MBP-ODC was as stable as MBP, for at least 8 h while it was wholly degraded in yeast. Off7-NYV and MBP-NYV were both degraded with a similar half-life between 1 and 2 h. The ODC- and NYV-degron did not similarly affect proteins stabilities, depending on the protein sequence they were appended to and depending on the expression system. In general, both degrons were less proficient in mammalian cells. Degron-fused proteins were so rapidly degraded when expressed in yeast that their half-life could be barely determined. In HEK293T cells, the ODC degron could not even destabilize MBP anymore. It should be noted that an additional HA tag was present for both MBP-ODC and MBP-NYV expressed in yeast but it was fused at their N-terminus and it should not have promoted or enhanced degradation. It was indeed observed that the proteasome initiated degradation of mouse ornithine decarboxylase at its C-terminus, where its degron sequence is located, and it is likely that it did so for our ODC-degron constructs too [43]. It is difficult to speculate what could explain the differences observed between yeast and mammalian cells. It could be that the degron sequences were not handled identically in both systems; they could be differently recognized by the yeast and human proteasomes and/or associated factors. Additional checkpoints could exist in mammalian cells for these degron sequences which were identified in proteins normally expressed in mouse (mouse ornithine decarboxylase) or in all rodents and occasionally humans (NY-1 hantavirus hosts). Alternatively, degron recognition could take place at different time points after their synthesis, depending on the host system. It has indeed been demonstrated that ornithine decarboxylase is mostly degraded before it completes folding and that “mature proteins” could still turnover but to a lower extent [44, 45]. It is possible than in yeast, degron sequences were mostly recognized while or shortly after the proteins were synthesized and they could be efficiently degraded before they terminated folding and that in mammalian cells, the degron sequences were recognized at a later stage when proteins were more and more or completely folded and had become more strenuous substrates for the proteasome. Another striking difference was

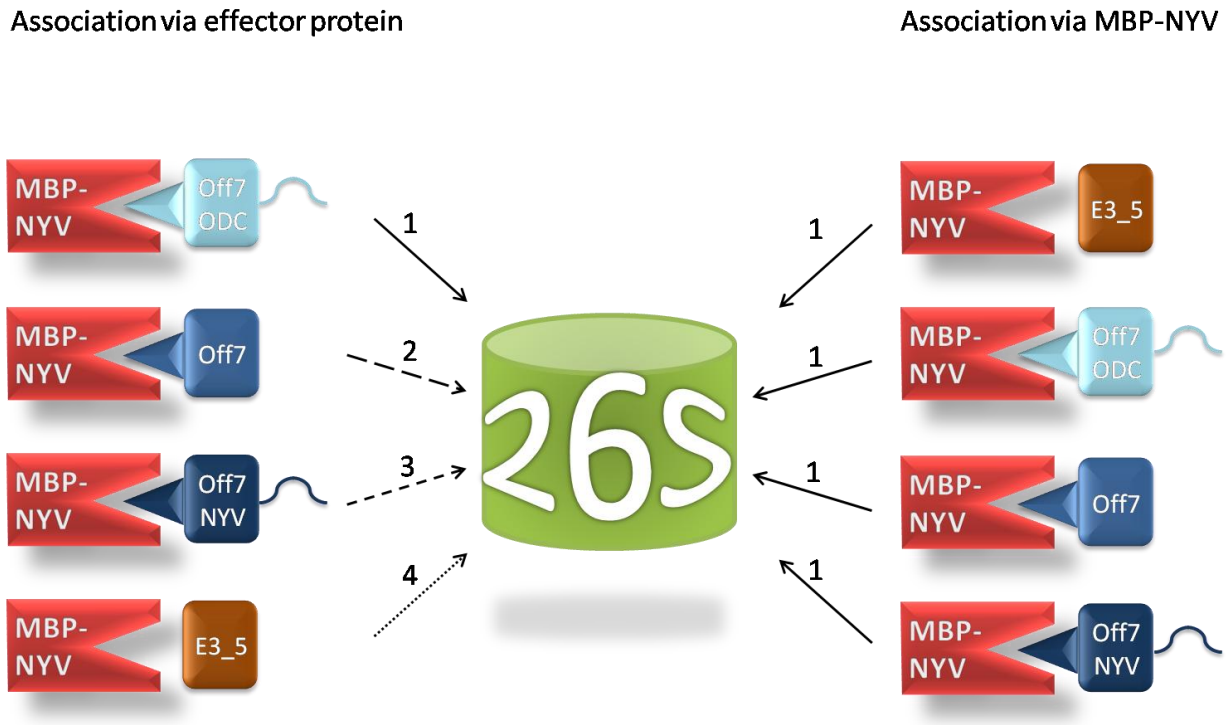

Figure 30: Schematic representation of model 1. Model 1 assumes that the effector proteins Off7-ODC, Off7 and Off7-NYV have decreasing affinity for the proteasome, respectively and considers that there is only the rate by which the complex is going to the proteasome, which matters. If MBP-NYV was brought to the proteasome via the action of the co-expressed effector protein (left side), the degradation rate would decrease in this order 1, 2, 3 and 4. If the complex was brought to the proteasome at MBP-NYV normal own rate (right side), no difference would be seen and MBP-NYV degradation rate would be identical between all combinations.

observed between the yeast and mammalian systems. The DARPin off7 was described as a highly expressed and stable protein when produced in *E. coli* [38]. A similar behavior was observed when it was expressed in *S. cerevisiae* (see chapter 2) but in HEK293T cells, its steady-state level was low, as it appeared to be degraded by the proteasome. In spite of the absence of any degron sequence, it was only slightly more stable than off7-ODC ($t_{1/2}$ ~ 1h). An incorrect folding of off7 in mammalian cells was unlikely and could be excluded, as its binding properties were conserved when an ELISA was performed with crude cell lysates. Upon multiple molecular dynamics simulation, the C-terminal cap of DARPins was observed to denature first [46]. Several mutations aiming at increasing the stability of the C-cap were predicted in silico and validated experimentally in vitro. The mutated C-cap also enhanced off7 steady-state level in HEK293T cells and increased its stability (data not shown). In addition, the non-selected full consensus DARPin N3C, whose stability was far exceeding that of the most favorable selected DARPins [46], was highly expressed in HEK293T cells and stable (data not shown). It seemed thus that in mammalian cells, there was an active recognition of a detachable C-terminal sequence, independent of the overall high stability of a protein. It is possible that the sequence features recognized differ between mammalian cells and yeast.

Off7, Off7-ODC and Off7-NYV were all proteasomally degraded but at different rates so we sought to investigate if these constructs could induce the degradation of a cognate target protein. When MBP was co-expressed with any of them, its steady-state level was not affected. However, MBP appeared to be extremely stable in HEK293T cells, with a half-life higher than 8 h, while a half-life of about 3 h was observed in *S. cerevisiae* (see Chapter 1). This difference correlated with the observation that MBP-ODC could be readily degraded in yeast but not in HEK293T cells. MBP could however be partially destabilized by the NYV-degron. As MBP-NYV was witnessed as a functional proteasome substrate and had a half-life higher than those of the effector proteins (Off7, Off7-ODC and Off7-NYV), it was used as an alternative target protein. Upon co-transfection experiments, MBP-NYV stability was monitored in the presence of each effector protein (Fig. 16). With Off7 and Off7-ODC turnover being faster than that of MBP-NYV, it was postulated that, if MBP-NYV was recruited to the proteasome, it would be degraded more rapidly than normally. However, none of them accelerated the degradation of MBP-NYV, instead they slowed it down. The effect was even more pronounced with Off7-NYV, which almost prevented MBP-NYV degradation.

Off7, Off7-ODC and Off7-NYV were apparently interfering with the MBP-NYV degradation pathway. Several alternative models can be formulated, assuming that a complex could be formed between the effector protein and MBP-NYV, as none of them was extremely quickly degraded by the proteasome when expressed alone.

Model 1 assumes that the different effector proteins (Off7, Off7-ODC and Off7-NYV) degradation rates are due to differences in their affinity for the proteasome, and considers that the only matter is the rate by which the complex is going to the proteasome (Fig. 30). If MBP-NYV was brought to the proteasome via the action of the co-expressed effector protein, it would be expected to turnover at a similar rate than the effector protein itself and thus faster than alone. It would be in agreement with the continuous

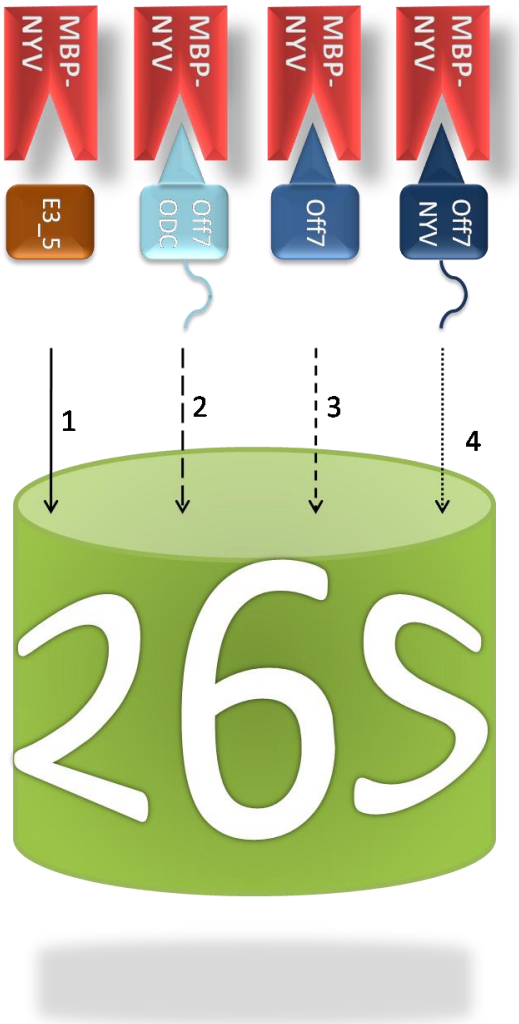

Figure 31: Schematic representation of model 2. Model 2 assumes that all effector proteins, Off7-ODC, Off7and Off7-NYV have the same affinity for the proteasome and that their degradation rates (Off7-ODC ≥ Off7 ≥ Off7-NYV) are due to differences in their unfolding efficiency by the proteasome. Model 2 considers that the proteasome degrades the complex, formed by the effector protein and the bound MBP-NYV, but that the unfolding of the effector protein slows down MBP-NYV processing. In this case, MBP-NYV degradation rate would decrease in presence of an effector protein, following the order 1, 2, 3 and 4.

decreasing degradation rates of MBP-NYV, observed in presence of off7-ODC, off7 and off7-NYV, respectively. However MBP-NYV was degraded faster when it was co-expressed with the negative control: E3_5, the non-specific DARPin. In this case, the degradation was not accelerated by the presence of a specific effector protein. If the complex was brought to the proteasome at MBP-NYV normal own rate, no difference would be seen between all combinations and this was not the case either.

Model 2 assumes that the different effector proteins (Off7, Off7-ODC and Off7-NYV) have the same affinity for the proteasome and that their degradation rates are due to differences in their unfolding efficiency by the proteasome (Fig. 31). Model 2 considers that the proteasome degrades the complex, formed by the effector protein and the bound partner (MBP-NYV), but that the unfolding and digestion of the effector proteins might hamper or disrupt MBP-NYV processing. Model 2 would be in agreement with the faster degradation of MBP-NYV in presence of E3_5, the non-specific DARPin and the continuous decreasing degradation rates observed in presence of off7-ODC, off7 and off7-NYV, respectively.

Finally model 3 takes into account that the complex, formed by the effector protein (Off7, Off7-ODC and Off7-NYV) bound to MBP-NYV, might associate with the proteasome at different rates, and that the presence of the effector protein might impede MBP-NYV degradation (Fig. 32). The effector protein could simply compete with MBP-NYV for degradation, its unfolding and digestion could slow down the processing of MBP-NYV (like in model 2). Another possibility would be that MBP-NYV, when bound to the effector protein, could become structurally more stable and not be efficiently degraded any more by the proteasome. Methotrexate, a dihydrofolate reductase (DHFR) ligand, has been shown to stabilize the enzyme through binding and impaired the proteasomal degradation of DHFR when this one was fused the ODC degron [41]. If the complexe associated with the proteasome via MBP-NYV, MBP-NYV turn over would be gradually slowed down as the intrinsic stability of the effector protein increased. If the complex associated with the proteasome via the effector protein, it would be hard to predict if MBP-NYV would be faster degraded alone or in complex with off7-ODC or off7. In other words we cannot know if a faster association step could compensate a slower digestion step. Both models 2 and 3 could fit with the experimental data, but are questionable. off7-NYV for e.g. could have been rivaling MBP-NYV. As both proteins were bearing the same degradation signal, they could have been competing for interaction with key actors of the NYV degron degradation pathway. The non-specific DARPin E3-5 was used as negative control, but it was not optimal, as E3_5, like off7, was seen to be unstable and degraded by the proteasome, although at a lower rate. This did not seem to interfere too much with MBP-NYV degradation but it might explain why MBP-NYV degradation only reached a final basal level and did not fully complete (Fig. 16). A protein which could neither bind the target protein nor interact with the proteasome would be a better negative control. Finally a destabilized version of MBP, which could be degraded by the proteasome but could not associate with it, would be a better substrate than MBP-NYV to test the net effect of Off7, Off7-ODC and Off7-NYV on their binding partner stability.

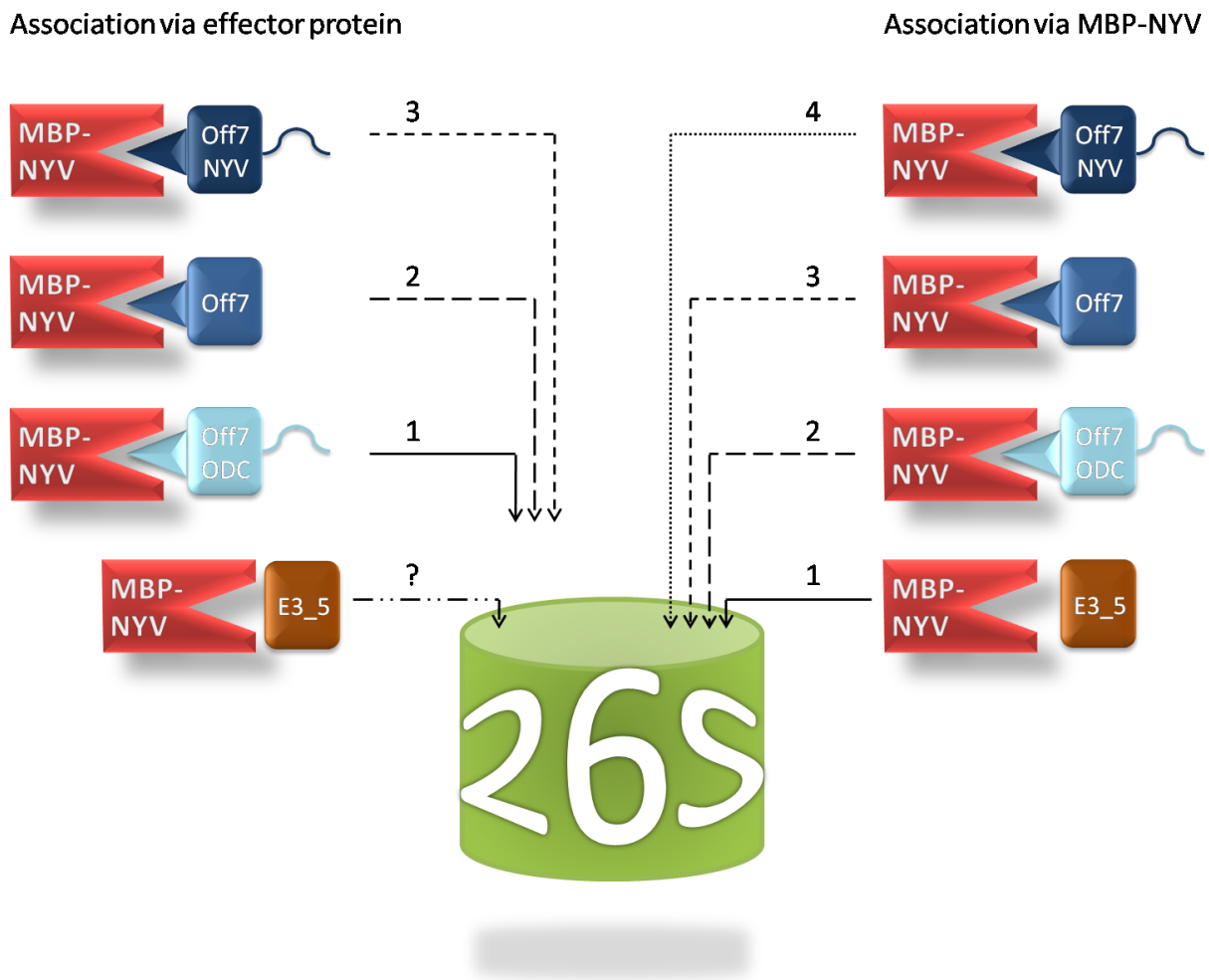

Figure 32: Schematic representation of model 3. Model 3 takes into account the different association rate of the complex, formed by the effector protein (Off7-ODC, Off7 and Off7-NYV) bound to MBP-NYV, with the proteasome, and the presence of the effector protein, which might impede MBP-NYV degradation. The effector protein could slow down MBP-NYV degradation, simply by competing for proteasomal processing (like in model 2) or by increasing MBP-NYV stability and resistance to unfolding. If the complex associates with the proteasome via the effector protein (left side), MBP-NYV degradation rate would decrease following the order 1, 2 and 3. It cannot be predicted if MBP-NYV would be faster degraded alone or in complex with off7-ODC or off7, which might bring it faster to the proteasome but might also slow down its proteasomal processing. If all complexes associated with the proteasome via MBP-NYV, MBP-NYV turn over would be gradually slowed down, following the order 1, 2, 3 and 4, as the intrinsic stability of the effector protein increased.

Our experimental data seemed to indicate that a target protein, in spite of interacting with a protein prone for proteasomal destruction, was not necessarily co-degraded by the mammalian proteasome. When Matsuzawa et al. employed a similar set-up, by expressing protein-interaction domains as chimeric fusions with the whole ornithine decarboxylase and surveying the antizyme 1-dependent degradation of the interacting binding partners, only five out of twelve protein pairs could be degraded [31]. The authors hypothesized that for their negative cases, the affinity interaction was insufficient or that these proteins were recalcitrant to degradation. Interacting with the proteasome and achieving a high local concentration might not be enough for becoming an eligible substrate. In yeast and mammals, when the ornithine decarboxylase is bound to the antizyme 1 (AZ1), it can be better recognized and processed by the proteasome, but AZ1 is not degraded along [47]. AZ1 degradation occurs mostly, if not only, independently of ornithine decarboxylase, via the ubiquitin proteasome pathway [47]. The 26S proteasome has also been observed for selectively degrading single subunits of multimeric complexes. When ubiquitylated Sic1 was embedded within S phase cyclin-Cdk complexes, it could be specifically extracted by the 26S proteasome and degraded while bound partners were released untouched [48]. This subunit-selective degradation, often exploited as a regulatory switch for the cell's metabolism, might tell us that in order to degrade a target protein, a clear degradation signal should be appended to it.

Proteasomes usually require a polyubiquitin tag as the price of admission. The second tested degradation strategy was aiming to exploit the ubiquitin proteasome pathway. The E3 ligase SCF was chosen to label new target proteins. In order to harness this ubiquitination machinery, a chimeric F-box protein, cdc4-off7 was employed. It was based on the yeast cdc4 F-box protein, but whose substrate binding domain has been replaced with off7. cdc4-off7 had been observed in yeast to specifically induce the degradation of the target protein MBP (see Chapter 1). Several SCF ligases, whose structural and functional details had been deciphered, showed that they had been well conserved [32-36]. cdc4 and Fbxw7, its human homolog, displayed very high similarities [34, 36], cdc4-off7 was thus tested in mammalian cells. Like in yeast, the chimeric F-box protein was unstable and degraded by the proteasome. We thus hypothesized that it was recognized by the mammalian SCF complex. Furthermore, upon transient transfection in a cell line stably expressing MBP, it seemed to slightly decrease MBP steady-state level. To investigate if cdc4-off7 could induce MBP degradation by the ubiquitin proteasome pathway, a second experimental set-up was established. A stable cell line expressing cdc4-off7 was created, but under these conditions, the chimeric F-box protein had no effect on transfected MBP steady-state levels. In spite of playing with the transfection methods and several parameters, the results observed in the first experimental set-up could not be reproduced. The main difference between the two experimental set-ups was the ratio between cdc4-off7 and MBP. The relative amount of chimeric F-box protein and target protein seems to be crucial for operating degradation [49]. cdc4-off7 was probably present in a higher amount in the first set-up, as it was expressed from transfected plasmid(s) while in the stable cell line, it was expressed from a single locus at a lower level than MBP, which was expressed from transfected plasmid(s). Considering that cdc4-off7 had, in addition, a short half-life, it is possible that under these conditions, it could not reach a sufficient amount to efficiently degrade MBP, which was furthermore well expressed and highly stable. In other studies, recombinant adenoviruses and

retroviruses were used for the high-level delivery and expression of chimeric F-box proteins, targeting more challenging substrates like endogenous proteins [24, 29].

A destabilized version of MBP fused to the NYV degron, MBP-NYV was tested in co-transfection experiments with cdc4-off7. The chimeric F-box protein somehow shifted MBP-NYV normal degradation pattern towards a slower one very similar to what had been previously observed for MBP when it was co-expressed with cdc4-off7 in yeast. We first thought that cdc4-off7 could be using MBP-NYV as substrate too and redirect it towards the ubiquitin proteasome pathway, and potentially increase its degradation rate. However, MBP-NYV degradation was slowed down and barely taking place when it was monitored in Flp-In TRex cdc4-off7 cells. The second experimental set-up confirmed that cdc4-off7 was impeding MBP-NYV's own degradation pathway. The lack of acceleration of degradation led us to test the authenticity of the working hypothesis: was cdc4-off7 really a functional F-box protein in mammalian cells? Immunoprecipitation experiments could not detect any interaction with skp1, indicating that cdc4-off7 could most likely not associate with the mammalian SCF complex. This result was confirmed by cdc4-off7 stability, which stayed unaffected by the presence of a target protein previously observed to extend half-life in yeast. Most likely, cdc4-off7 was therefore, not a functional F-box protein and could in that case not induce MBP or MBP-NYV degradation. Human skp1 protein might not be able to recognize and/or bind to the cdc4 F-box motif with enough affinity even if its F-box binding domain was highly conserved (68% identity with yeast). skp1 binds to various F-box sequences, but the use of a homologous F-box domain might be decisive. Zhou and colleagues constructed their chimeric F-box proteins using β-TrCP as scaffold, a mammalian F-box protein [23, 24, 26]. The effect of cdc4-off7 on MBP steady-state level, which was monitored several times in the first experimental set-up, was very likely not specific, these results could namely not be repeated. We cannot explain how cdc4-off7 was interfering with MBP-NYV degradation. Since a similar effect was observed with Off7, it is possible that both Off7 and cdc4-off7 were hampering MBP-NYV degradation simply upon binding and their "unstable" C-terminus might be directly interfering with NYV-degron interaction with the proteasome. cdc4-off7 was most likely not degraded by the SCF complex. The pathway leading it to the proteasome stays unknown, it could be upon direct binding with the proteasome, but we can only conclude that the presence of a stable binding partner did not affect it.

Our chimeric F-box protein cdc4-off7 failed to induce the degradation of a cognate specific protein in mammalian cells. However, the strategy relying on the use of the ubiquitin proteasome pathway should not be condemned. The scaffold of a homologous F-box protein might be crucial for designing an effective chimeric F-box protein, as demonstrated by previous successful protein knock-out attempts [23, 24, 26-29]. These chimeric F-box proteins based on the in-frame fusion of a known "adapter" (ligand or a known naturally occurring binding motif), are nevertheless limited in the range of targets. The use of a generalizable binding domain like DARPins would broaden the spectrum of targets. A second generation of chimeric F-box protein, based on a homologous F-box protein scaffold and DARPIns, might lead to a general strategy to engineer specific protein breakdown in the cell.

Annex

Vector maps

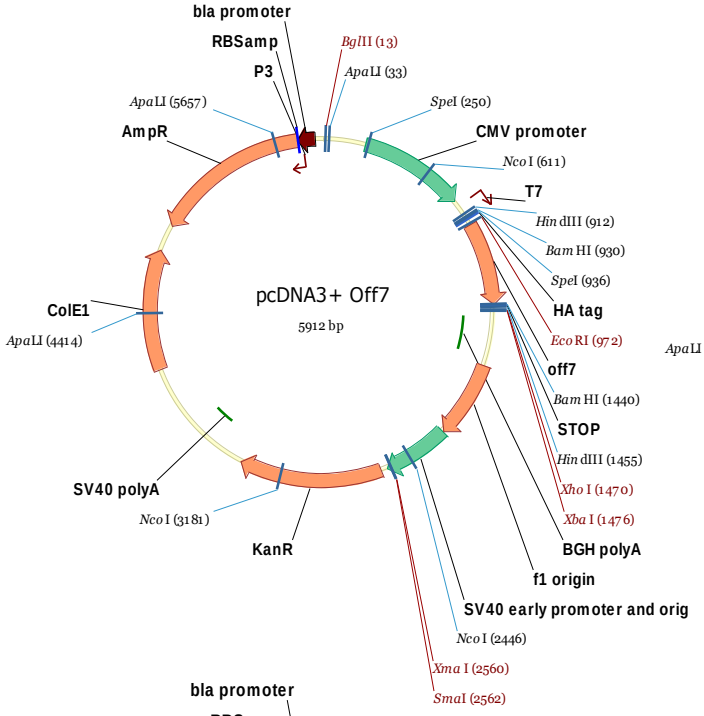

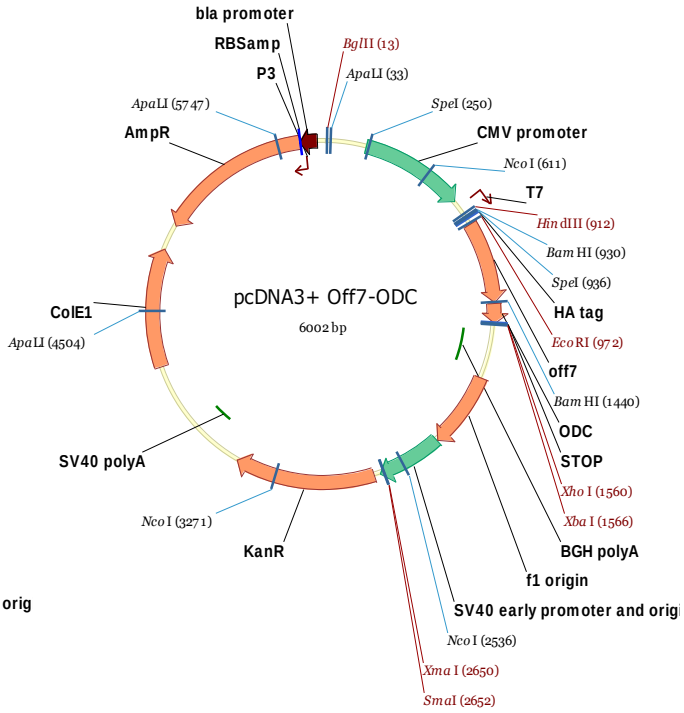

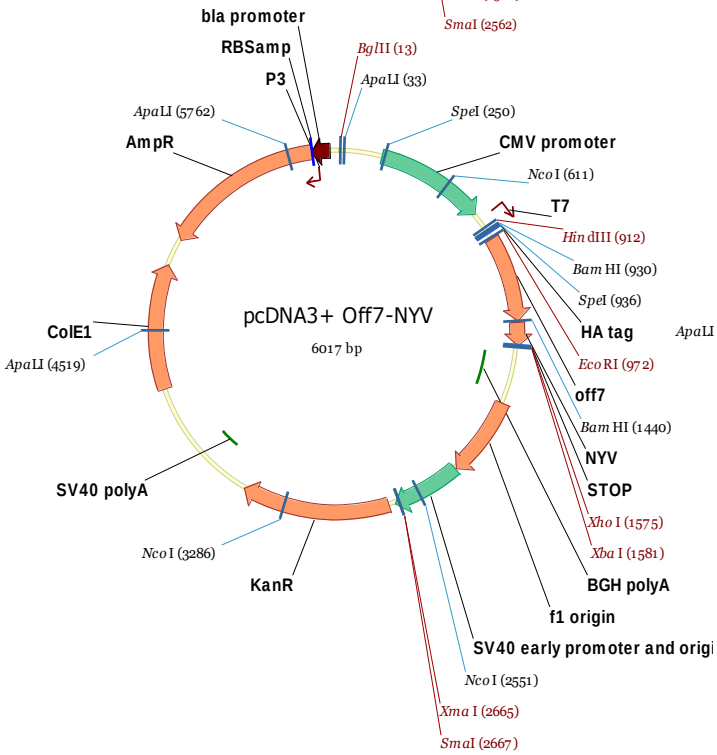

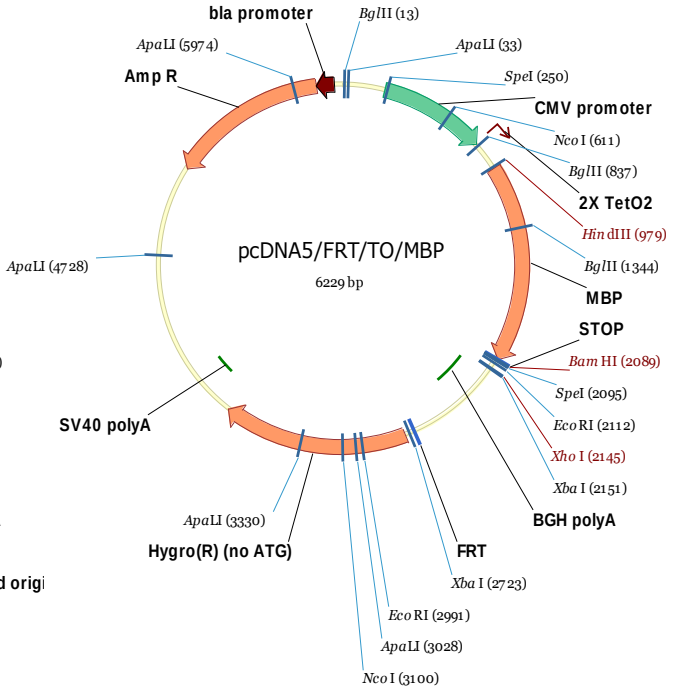

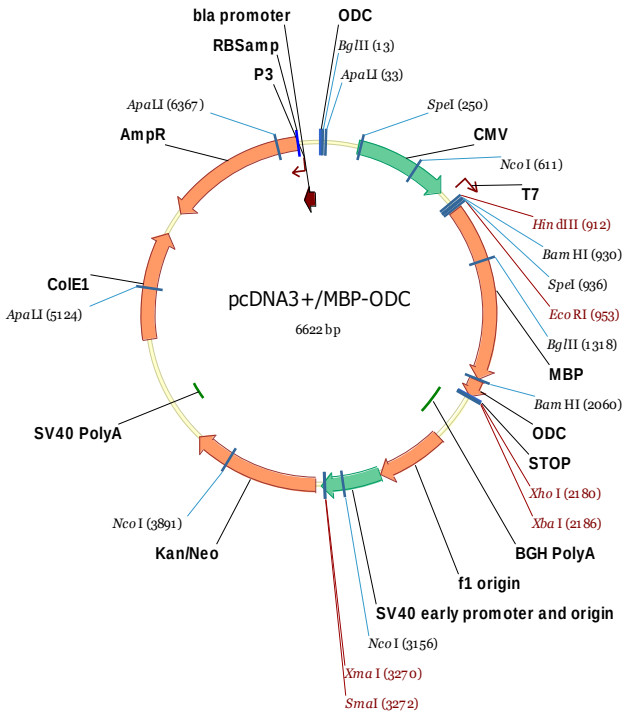
pcDNA3+/MBP-ODC
6622 bp
bla promoter
ODC
RBSamp
P3
AmpR
CMV
T7
MBP
ODC
STOP
BGH PolyA
f1 origin
SV40 early promoter and origin
SV40 PolyA
ColE1
Kan/Neo
BglII (13)
ApaLI (33)
SpeI (250)
NcoI (611)
HindIII (912)
BamHI (930)
SpeI (936)
EcoRI (953)
BglII (1318)
BamHI (2060)
XhoI (2180)
XbaI (2186)
NcoI (3156)
XmaI (3270)
SmaI (3272)
NcoI (3891)
ApaLI (5124)
ApaLI (6367)

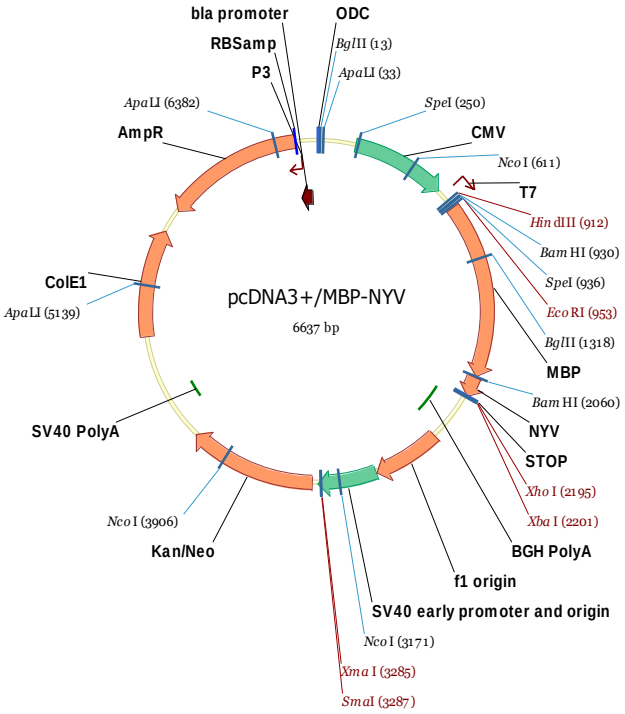
pcDNA3+/MBP-NYV
6637 bp
bla promoter
ODC
RBSamp
P3
AmpR
CMV
T7
MBP
NYV
STOP
BGH PolyA
f1 origin
SV40 early promoter and origin
SV40 PolyA
ColE1
Kan/Neo
BglII (13)
ApaLI (33)
SpeI (250)
NcoI (611)
HindIII (912)
BamHI (930)
SpeI (936)
EcoRI (953)
BglII (1318)
BamHI (2060)
XhoI (2195)
XbaI (2201)
NcoI (3171)
XmaI (3285)
SmaI (3287)
NcoI (3906)
ApaLI (5139)
ApaLI (6382)

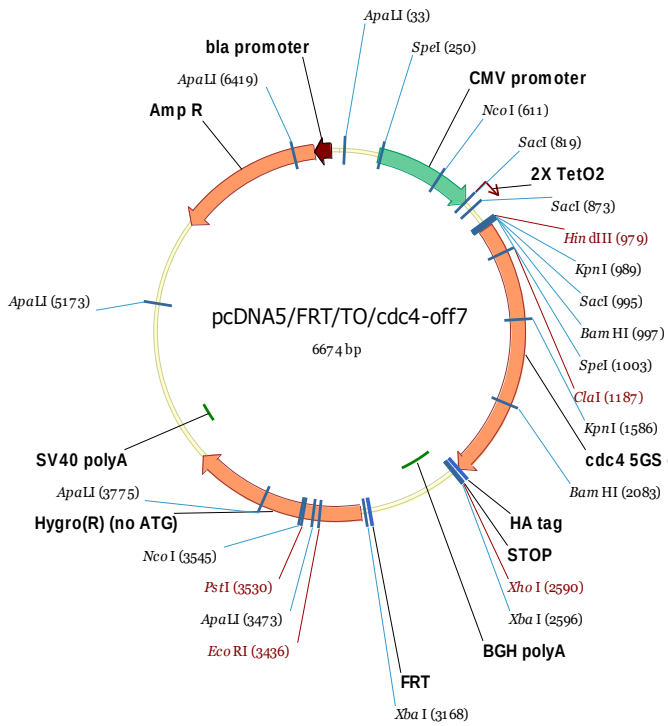
pcDNA5/FRT/TO/cdc4-off7
6674 bp
bla promoter
Amp R
CMV promoter
2X TetO2
cdc4 5GS off7
HA tag
STOP
BGH polyA
FRT
SV40 polyA
Hygro(R) (no ATG)
ApaLI (33)
SpeI (250)
NcoI (611)
SacI (819)
SacI (873)
HindIII (979)
KpnI (989)
SacI (995)
BamHI (997)
SpeI (1003)
ClaI (1187)
KpnI (1586)
BamHI (2083)
XhoI (2590)
XbaI (2596)
XbaI (3168)
EcoRI (3436)
ApaLI (3473)
PstI (3530)
NcoI (3545)
ApaLI (3775)
ApaLI (5173)
ApaLI (6419)

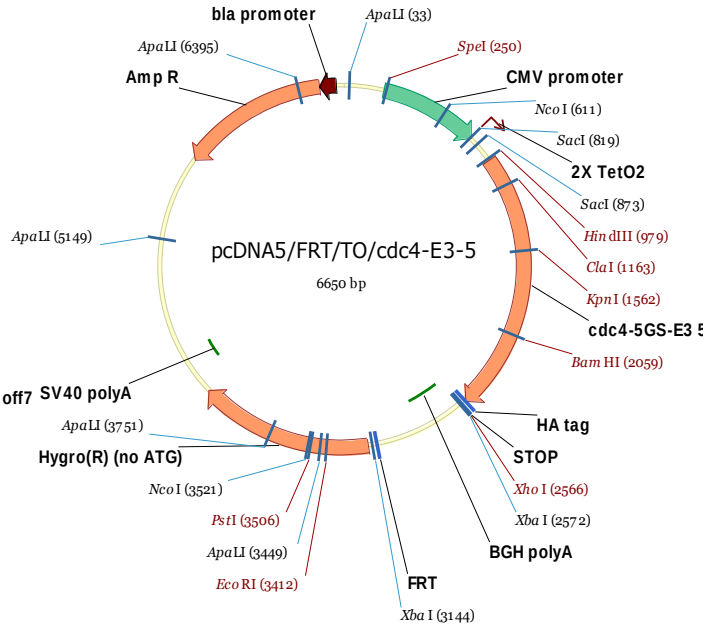
pcDNA5/FRT/TO/cdc4-E3-5
6650 bp
bla promoter
Amp R
CMV promoter
2X TetO2
HA tag
STOP
BGH polyA
FRT
SV40 polyA
Hygro(R) (no ATG)
ApaLI (33)
SpeI (250)
NcoI (611)
SacI (819)
SacI (873)
HindIII (979)
ClaI (1163)
KpnI (1562)
BamHI (2059)
XhoI (2566)
XbaI (2572)
XbaI (3144)
EcoRI (3412)
ApaLI (3449)
PstI (3506)
NcoI (3521)
ApaLI (3751)
ApaLI (5149)
ApaLI (6395)

Construct DNA and amino-acid sequences

Off7 construct DNA sequence

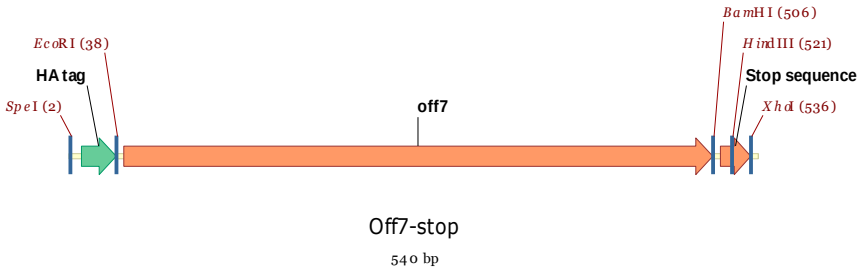

Tctgctgaagcacggtgctgacgttgacgcttctgacgtttttggttatactccgctgcacctggctgcttattggggtcacctggaaatcgttgaagttct
gctgaagaacggtgctgacgttaacgctatggactctgatggtatgactccactgcacctggctgctaagtggggttacctggaaatcgttgaagttctg
ctgaagcacggtgctgacgttaacgctcaggacaaattcggtaagaccgctttcgacatctccatcgacaacggtaacgaggacctggctgaaatcct
gcaaggatcctaatagtgaaagcttttagctgacctcgagactagtatgtacccatacgatgttccagattacgctgaattcgacctgggtaggaaact
gctggaagctgctcgtgctggtcaggacgacgaagttcgtatcctgatggctaacggtgctgacgttaatgctgctgacaatactggtactactccgctg
cacctggctgcttattctggtcacctggaaatcgttgaagt

Of7 amino-acid sequence

MYPYDVPDYAEFDLGRKLLEAARAGQDDEVRILMANGADVNAADNTGTTPLHLAAYSGHLEIVEVLLKHGADVDASD
VFGYTPLHLAAYWGHLEIVEVLLKNGADVNAMDSDGMTPLHLAAKWGYLEIVEVLLKHGADVNAQDKFGKTAFDISID
NGNEDLAEILQGS

Off7-ODC and Off7-NYV constructs:

see in annex from chapter 2

MBP construct DNA sequence

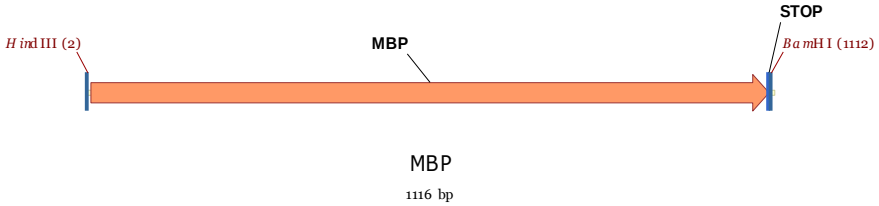

Aagcttatgaaaactgaagaaggtaaactggtaatctggattaacggcgataaaggctataacggtctcgctgaagtcggtaagaaattcgagaaag
ataccggaattaaagtcaccgttgagcatccggataaactggaagagaaattcccacaggttgcggcaactggcgatggccctgacattatcttctggg
cacacgaccgctttggtggctacgctcaatctggcctgttggctgaaatcaccccggacaaagcgttccaggacaagctgtatccgtttacctgggatgc
cgtacgttacaacggcaagctgattgcttacccgatcgctgttgaagcgttatcgctgatttataacaaagatctgctgccgaacccgccaaaaacctgg
gaagagatcccggcgctggataaagaactgaaagcgaaaggtaagagcgcgctgatgttcaacctgcaagaaccgtacttcacctggccgctgattg
ctgctgacgggggttatgcgttcaagtatgaaaacggcaagtacgacattaaagacgtgggcgtggataacgctggcgcgaaagcgggtctgaccttc
ctggttgacctgattaaaaacaaacacatgaatgcagacaccgattactccatcgcagaagctgcctttaataaaggcgaaacagcgatgaccatcaa
cggcccgtgggcatggtccaacatcgacaccagcaaagtgaattatggtgtaacggtactgccgaccttcaagggtcaaccatccaaaccgttcgttg
gcgtgctgagcgcaggtattaacgccgccagtccgaacaaagagctggcaaaagagttcctcgaaaactatctgctgactgatgaaggtctggaagc
ggttaataaagacaaaccgctgggtgccgtagcgctgaagtcttacgaggaagagttggcgaaagatccacgtattgccgccactatggaaaacgcc
cagaaaggtgaaatcatgccgaacatcccgcagatgtccgctttctggtatgccgtgcgtactgcggtgatcaacgccgccagcggtcgtcagactgtc
gatgaagccctgaaagacgcgcagacttagggatcc

MBP amino-acid sequence

MKTEEGKLVIWINGDKGYNGLAEVGKKFEKDTGIKVTVEHPDKLEEKFPQVAATGDGPDIIFWAHDRFGGYAQSGLLAE
ITPDKAFQDKLYPFTWDAVRYNGKLIAYPIAVEALSLIYNKDLLPNPPKTWEEIPALDKELKAKGKSALMFNLQEPYFTWP
LIAADGGYAFKYENGKYDIKDVGVDNAGAKAGLTFLVDLIKNKHMNADTDYSIAEAAFNKGETAMTINGPWAWSNIDT
SKVNYGVTVLPTFKGQPSKPFVGVLSAGINAASPNKELAKEFLENYLLTDEGLEAVNKDKPLGAVALKSYEEELAKDPRIA
ATMENAQKGEIMPNIPQMSAFWYAVRTAVINAASGRQTVDEALKDAQT

MBP-ODC construct DNA sequence

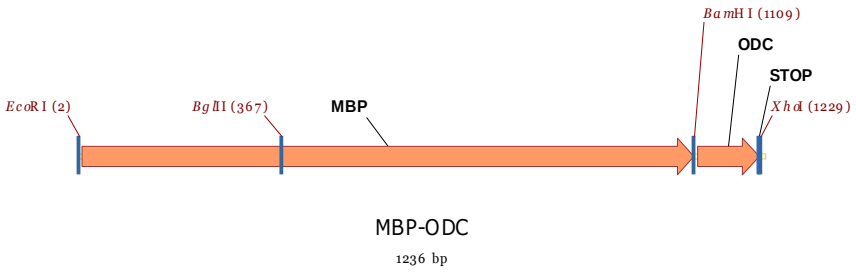

gaattcatgaaaactgaagaaggtaaactggtaatctggattaacggcgataaaggctataacggtctcgctgaagtcggtaagaaattcgagaaag
ataccggaattaaagtcaccgttgagcatccggataaactggaagagaaattcccacaggttgcggcaactggcgatggccctgacattatcttctggg
cacacgaccgctttggtggctacgctcaatctggcctgttggctgaaatcaccccggacaaagcgttccaggacaagctgtatccgtttacctgggatgc
cgtacgttacaacggcaagctgattgcttacccgatcgctgttgaagcgttatcgctgatttataacaaagatctgctgccgaacccgccaaaaacctgg
gaagagatcccggcgctggataaagaactgaaagcgaaaggtaagagcgcgctgatgttcaacctgcaagaaccgtacttcacctggccgctgattg
ctgctgacgggggttatgcgttcaagtatgaaaacggcaagtacgacattaaagacgtgggcgtggataacgctggcgcgaaagcgggtctgaccttc
ctggttgacctgattaaaaacaaacacatgaatgcagacaccgattactccatcgcagaagctgcctttaataaaggcgaaacagcgatgaccatcaa
cggcccgtgggcatggtccaacatcgacaccagcaaagtgaattatggtgtaacggtactgccgaccttcaagggtcaaccatccaaaccgttcgttg
gcgtgctgagcgcaggtattaacgccgccagtccgaacaaagagctggcaaaagagttcctcgaaaactatctgctgactgatgaaggtctggaagc
ggttaataaagacaaaccgctgggtgccgtagcgctgaagtcttacgaggaagagttggcgaaagatccacgtattgccgccactatggaaaacgcc
cagaaaggtgaaatcatgccgaacatcccgcagatgtccgctttctggtatgccgtgcgtactgcggtgatcaacgccgccagcggtcgtcagactgtc

gatgaagccctgaaagacgcgcagactggatccttcccgccggaggtggaggagcaggatgatggcacgctgcccatgtcttgtgcccaggagagcg
ggatggaccgtcaccctgcagcctgtgcttctgctaggatcaatgtgtagctcgag

MBP-ODC amino-acid sequence

MKTEEGKLVIWINGDKGYNGLAEVGKKFEKDTGIKVTVEHPDKLEEKFPQVAATGDGPDIIFWAHDRFGGYAQSGLLAE
ITPDKAFQDKLYPFTWDAVRYNGKLIAYPIAVEALSLIYNKDLLPNPPKTWEEIPALDKELKAKGKSALMFNLQEPYFTWP
LIAADGGYAFKYENGKYDIKDVGVDNAGAKAGLTFLVDLIKNKHMNADTDYSIAEAAFNKGETAMTINGPWAWSNIDT
SKVNYGVTVLPTFKGQPSKPFVGVLSAGINAASPNKELAKEFLENYLLTDEGLEAVNKDKPLGAVALKSYEEELAKDPRIA
ATMENAQKGEIMPNIPQMSAFWYAVRTAVINAASGRQTVDEALKDAQTGSFPPEVEEQDDGTLPMSCAQESGMDR
HPAACASARINV

MBP-NYV construct DNA sequence

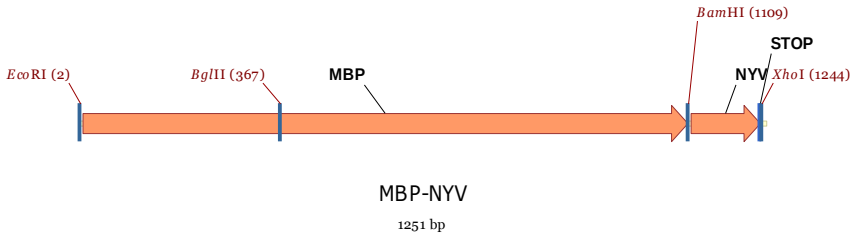

gaattcatgaaaactgaagaaggtaaactggtaatctggattaacggcgataaaggctataacggtctcgctgaagtcggtaagaaattcgagaaag
ataccggaattaaagtcaccgttgagcatccggataaactggaagagaaattcccacaggttgcggcaactggcgatggccctgacattatcttctggg
cacacgaccgctttggtggctacgctcaatctggcctgttggctgaaatcaccccggacaaagcgttccaggacaagctgtatccgtttacctgggatgc
cgtacgttacaacggcaagctgattgcttacccgatcgctgttgaagcgttatcgctgatttataacaaagatctgctgccgaacccgccaaaaacctgg
gaagagatcccggcgctggataaagaactgaaagcgaaaggtaagagcgcgctgatgttcaacctgcaagaaccgtacttcacctggccgctgattg
ctgctgacgggggttatgcgttcaagtatgaaaacggcaagtacgacattaaagacgtgggcgtggataacgctggcgcgaaagcgggtctgaccttc
ctggttgacctgattaaaaacaaacacatgaatgcagacaccgattactccatcgcagaagctgcctttaataaaggcgaaacagcgatgaccatcaa
cggcccgtgggcatggtccaacatcgacaccagcaaagtgaattatggtgtaacggtactgccgaccttcaagggtcaaccatccaaaccgttcgttg
gcgtgctgagcgcaggtattaacgccgccagtccgaacaaagagctggcaaaagagttcctcgaaaactatctgctgactgatgaaggtctggaagc
ggttaataaagacaaaccgctgggtgccgtagcgctgaagtcttacgaggaagagttggcgaaagatccacgtattgccgccactatggaaaacgcc
cagaaaggtgaaatcatgccgaacatcccgcagatgtccgctttctggtatgccgtgcgtactgcggtgatcaacgccgccagcggtcgtcagactgtc
gatgaagccctgaaagacgcgcagactggatcccgccctgaagttaaacaaggatgctatagaacattgggtgtttttagatataagagtaggtgttat
gttggtcttgtgtgggggtccttcttacaactgaactcatagtttgggcagctagtgcttagctcgag

MBP-NYV amino-acid sequence

MKTEEGKLVIWINGDKGYNGLAEVGKKFEKDTGIKVTVEHPDKLEEKFPQVAATGDGPDIIFWAHDRFGGYAQSGLLAE
ITPDKAFQDKLYPFTWDAVRYNGKLIAYPIAVEALSLIYNKDLLPNPPKTWEEIPALDKELKAKGKSALMFNLQEPYFTWP
LIAADGGYAFKYENGKYDIKDVGVDNAGAKAGLTFLVDLIKNKHMNADTDYSIAEAAFNKGETAMTINGPWAWSNIDT
SKVNYGVTVLPTFKGQPSKPFVGVLSAGINAASPNKELAKEFLENYLLTDEGLEAVNKDKPLGAVALKSYEEELAKDPRIA
ATMENAQKGEIMPNIPQMSAFWYAVRTAVINAASGRQTVDEALKDAQTGSRPEVKQGCYRTLGVFRYKSRCYVGLV
WGVLLTTELIVWAASA

Cdc4-off7 construct

see cdc4_5GS_off7 in annex from chapter 1

Cdc4-E3_5 construct DNA sequence

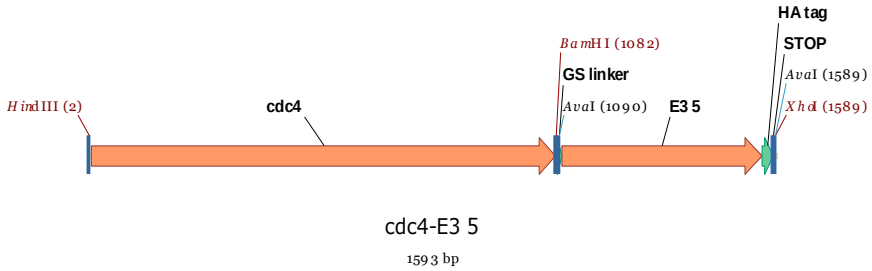

aagcttatggggtcgtttcccttagctgagtttccattacgtgatatccctgttccttatagctaccgtgtgtctggcggtatagcttcctcaggtagtgtta
ctgcgcttgttactgccgctggcactcatcgaaactcgtccacggctaagacagttgagacagaagacggcgaagaagatatcgatgagtatcagagg
aaaagagcagctggttctggcgaatccactcctgaacgcagtagtttcgcagcggtagcacatgataatcacaaaaccctccatccagttaacttacag
aacaccggtgcagcgtctgtggataatgacggtctgcacaatttaacagatatatccaacgatgcagaaaaacttttgatgtctgtggatgatggttctg
ccgcaccttctacattgagtgtaaacatgggagtggcatctcataatgttgctgctcccactaccgtcaatgcggcaacaataactggcagtgatgttag
taacaatgttaatagtgctactattaacaatcctatggaggaaggagcgctgccgttatcacccactgcttcctctccaggtaccacaactcctttagcta
aaactacgaaaactatcaacaacaataataatatcgccgatttgatagaatccaaagattctataatctcccctgaataccttttctgatgagattttcag
cgcaataaacaataatctccctcacgcatacttcaaaaatttattatttagattagttgccaacatggataggagtgaactatccgacttggggacttta
atcaaggataatttaaagagggacctaataacgtctttgccttttgaaataagtttgaaaattttcaattatttgcaattcgaggatattataaattcccctt
ggggtctcccaaaattggaacaaaataattagaaaatctacatcgttgtggaaaaaacttctgatatcggaaaattttgtgagcccaaagggttttaat
tctctcaatctcaaactctcccaaaaatacccaaaactctcacaacaagatcgccttagattatcttttctggagaatggatccggctcgggcgacctgg
gtaagaaactgctggaagctgctcgtgctggtcaggacgacgaagttcgtatcctgatggctaacggtgctgacgttaacgctactgacaatgatggtt
atactccgctgcacctggctgcttctaatggtcacctggaaatcgttgaagttctgctgaagaacggtgctgacgttaacgcttctgaccttactggtatt
actccgctgcacctggctgctgctactggtcacctggaaatcgttgaagttctgctgaagcacggtgctgacgttaacgcttatgacaatgatggtcata
ctccgctgcacctggctgctaagtatggtcacctggaaatcgttgaagttctgctgaagcacggtgctgacgttaacgctcaggacaaattcggtaaga
ccgctttcgacatctccatcgacaacggtaacgaggacctggctgaaatcctgcaatacccatacgatgttccagattacgcttaactcgag

cdc4-E3_5 amino-acid sequence

MGSFPLAEFPLRDIPVPYSYRVSGGIASSGSVTALVTAAGTHRNSSTAKTVETEDGEEDIDEYQRKRAAGSGESTPERSSF
AAVAHDNHKTLHPVNLQNTGAASVDNDGLHNLTDISNDAEKLLMSVDDGSAAPSTLSVNMGVASHNVAAPTTVNAA
TITGSDVSNNVNSATINNPMEEGALPLSPTASSPGTTTPLAKTTKTINNNNNIADLIESKDSIISPEYLSDEIFSAINNNLPHA
YFKNLLFRLVANMDRSELSDLGTLIKDNLKRDLITSLPFEISLKIFNYLQFEDIINSLGVSQNWNKIIRKSTSLWKKLLISENFV
SPKGFNSLNLKLSQKYPKLSQQDRLRLSFLENGSGSGDLGKKLLEAARAGQDDEVRILMANGADVNATDNDGYTPLHLA
ASNGHLEIVEVLLKNGADVNASDLTGITPLHLAAATGHLEIVEVLLKHGADVNAYDNDGHTPLHLAAKYGHLEIVEVLLK
HGADVNAQDKFGKTAFDISIDNGNEDLAEILQYPYDVPDYA

References

1. Scacheri, P.C., et al., *Short interfering RNAs can induce unexpected and divergent changes in the levels of untargeted proteins in mammalian cells.* Proc Natl Acad Sci U S A, 2004. **101**(7): p. 1892-7.
2. Jackson, A.L., et al., *Expression profiling reveals off-target gene regulation by RNAi.* Nat Biotechnol, 2003. **21**(6): p. 635-7.
3. Agrawal, S. and E.R. Kandimalla, *Role of Toll-like receptors in antisense and siRNA [corrected].* Nat Biotechnol, 2004. **22**(12): p. 1533-7.
4. Judge, A.D., et al., *Sequence-dependent stimulation of the mammalian innate immune response by synthetic siRNA.* Nat Biotechnol, 2005. **23**(4): p. 457-62.
5. Castanotto, D. and J.J. Rossi, *The promises and pitfalls of RNA-interference-based therapeutics.* Nature, 2009. **457**(7228): p. 426-33.
6. Hershko, A. and A. Ciechanover, *The ubiquitin system.* Annu Rev Biochem, 1998. **67**: p. 425-79.
7. Scheffner, M., et al., *The E6 oncoprotein encoded by human papillomavirus types 16 and 18 promotes the degradation of p53.* Cell, 1990. **63**(6): p. 1129-36.
8. Scheffner, M., et al., *Targeted degradation of the retinoblastoma protein by human papillomavirus E7-E6 fusion proteins.* Embo J, 1992. **11**(7): p. 2425-31.
9. Zhou, P., *Targeted protein degradation.* Curr Opin Chem Biol, 2005. **9**(1): p. 51-5.
10. Gosink, M.M. and R.D. Vierstra, *Redirecting the specificity of ubiquitination by modifying ubiquitin-conjugating enzymes.* Proc Natl Acad Sci U S A, 1995. **92**(20): p. 9117-21.
11. Colas, P., et al., *Targeted modification and transportation of cellular proteins.* Proc Natl Acad Sci U S A, 2000. **97**(25): p. 13720-5.
12. Fang, S. and A.M. Weissman, *A field guide to ubiquitylation.* Cell Mol Life Sci, 2004. **61**(13): p. 1546-61.
13. Sakamoto, K.M., et al., *Protacs: chimeric molecules that target proteins to the Skp1-Cullin-F box complex for ubiquitination and degradation.* Proc Natl Acad Sci U S A, 2001. **98**(15): p. 8554-9.
14. Sakamoto, K.M., et al., *Development of Protacs to target cancer-promoting proteins for ubiquitination and degradation.* Mol Cell Proteomics, 2003. **2**(12): p. 1350-8.
15. Schneekloth, J.S., Jr., et al., *Chemical genetic control of protein levels: selective in vivo targeted degradation.* J Am Chem Soc, 2004. **126**(12): p. 3748-54.
16. Liu, Y.C., *Ubiquitin ligases and the immune response.* Annu Rev Immunol, 2004. **22**: p. 81-127.
17. Zhang, D., et al., *Targeted degradation of proteins by small molecules: a novel tool for functional proteomics.* Comb Chem High Throughput Screen, 2004. **7**(7): p. 689-97.
18. Rodriguez-Gonzalez, A., et al., *Targeting steroid hormone receptors for ubiquitination and degradation in breast and prostate cancer.* Oncogene, 2008. **27**(57): p. 7201-11.
19. Bargagna-Mohan, P., et al., *Use of PROTACS as molecular probes of angiogenesis.* Bioorg Med Chem Lett, 2005. **15**(11): p. 2724-7.
20. Tang, Y.Q., et al., *Chimeric molecules facilitate the degradation of androgen receptors and repress the growth of LNCaP cells.* Asian J Androl, 2009. **11**(1): p. 119-26.
21. Schneekloth, A.R., et al., *Targeted intracellular protein degradation induced by a small molecule: En route to chemical proteomics.* Bioorg Med Chem Lett, 2008. **18**(22): p. 5904-8.
22. Lim, M.S. and K.S. Elenitoba-Johnson, *Ubiquitin ligases in malignant lymphoma.* Leuk Lymphoma, 2004. **45**(7): p. 1329-39.
23. Zhou, P., et al., *Harnessing the ubiquitination machinery to target the degradation of specific cellular proteins.* Mol Cell, 2000. **6**(3): p. 751-6.

24. Zhang, J., N. Zheng, and P. Zhou, *Exploring the functional complexity of cellular proteins by protein knockout.* Proc Natl Acad Sci U S A, 2003. **100**(24): p. 14127-32.
25. Cong, F., et al., *A protein knockdown strategy to study the function of beta-catenin in tumorigenesis.* BMC Mol Biol, 2003. **4**: p. 10.
26. Su, Y., et al., *Eradication of pathogenic beta-catenin by Skp1/Cullin/F box ubiquitination machinery.* Proc Natl Acad Sci U S A, 2003. **100**(22): p. 12729-34.
27. Liu, J., et al., *Targeted degradation of beta-catenin by chimeric F-box fusion proteins.* Biochem Biophys Res Commun, 2004. **313**(4): p. 1023-9.
28. Cohen, J.C., et al., *Transient in utero knockout (TIUKO) of C-MYC affects late lung and intestinal development in the mouse.* BMC Dev Biol, 2004. **4**: p. 4.
29. Chen, W., et al., *Proteasome-mediated destruction of the cyclin a/cyclin-dependent kinase 2 complex suppresses tumor cell growth in vitro and in vivo.* Cancer Res, 2004. **64**(11): p. 3949-57.
30. Melchionna, T. and A. Cattaneo, *A protein silencing switch by ligand-induced proteasome-targeting intrabodies.* J Mol Biol, 2007. **374**(3): p. 641-54.
31. Matsuzawa, S., et al., *Method for targeting protein destruction by using a ubiquitin-independent, proteasome-mediated degradation pathway.* Proc Natl Acad Sci U S A, 2005. **102**(42): p. 14982-7.
32. Zheng, N., et al., *Structure of the Cul1-Rbx1-Skp1-F boxSkp2 SCF ubiquitin ligase complex.* Nature, 2002. **416**(6882): p. 703-9.
33. Wu, G., et al., *Structure of a beta-TrCP1-Skp1-beta-catenin complex: destruction motif binding and lysine specificity of the SCF(beta-TrCP1) ubiquitin ligase.* Mol Cell, 2003. **11**(6): p. 1445-56.
34. Orlicky, S., et al., *Structural basis for phosphodependent substrate selection and orientation by the SCFCdc4 ubiquitin ligase.* Cell, 2003. **112**(2): p. 243-56.
35. Hao, B., et al., *Structural basis of the Cks1-dependent recognition of p27(Kip1) by the SCF(Skp2) ubiquitin ligase.* Mol Cell, 2005. **20**(1): p. 9-19.
36. Hao, B., et al., *Structure of a Fbw7-Skp1-cyclin E complex: multisite-phosphorylated substrate recognition by SCF ubiquitin ligases.* Mol Cell, 2007. **26**(1): p. 131-43.
37. Sambrook, J. and D. Russell, *Molecular Cloning: A Laboratory Manual*. third edition ed. 2001, Cold Spring Harbor: Cold Spring Harbor Laboratory press.
38. Binz, H.K., et al., *High-affinity binders selected from designed ankyrin repeat protein libraries.* Nat Biotechnol, 2004. **22**(5): p. 575-82.
39. Galan, J.M. and M. Peter, *Ubiquitin-dependent degradation of multiple F-box proteins by an autocatalytic mechanism.* Proc Natl Acad Sci U S A, 1999. **96**(16): p. 9124-9.
40. Blondel, M., et al., *Nuclear-specific degradation of Far1 is controlled by the localization of the F-box protein Cdc4.* Embo J, 2000. **19**(22): p. 6085-97.
41. Zhang, M., C.M. Pickart, and P. Coffino, *Determinants of proteasome recognition of ornithine decarboxylase, a ubiquitin-independent substrate.* Embo J, 2003. **22**(7): p. 1488-96.
42. Sen, N., A. Sen, and E.R. Mackow, *Degrons at the C terminus of the pathogenic but not the nonpathogenic hantavirus G1 tail direct proteasomal degradation.* J Virol, 2007. **81**(8): p. 4323-30.
43. Zhang, M., et al., *Proteasomes begin ornithine decarboxylase digestion at the C terminus.* J Biol Chem, 2004. **279**(20): p. 20959-65.
44. van Daalen Wetters, T., et al., *Polyamine-mediated regulation of mouse ornithine decarboxylase is posttranslational.* Mol Cell Biol, 1989. **9**(12): p. 5484-90.
45. Toth, C. and P. Coffino, *Regulated degradation of yeast ornithine decarboxylase.* J Biol Chem, 1999. **274**(36): p. 25921-6.
46. Interlandi, G., et al., *Characterization and further stabilization of designed ankyrin repeat proteins by combining molecular dynamics simulations and experiments.* J Mol Biol, 2008. **375**(3): p. 837-54.

47. Palanimurugan, R., et al., *Polyamines regulate their synthesis by inducing expression and blocking degradation of ODC antizyme.* Embo J, 2004. **23**(24): p. 4857-67.
48. Verma, R., et al., *Selective degradation of ubiquitinated Sic1 by purified 26S proteasome yields active S phase cyclin-Cdk.* Mol Cell, 2001. **8**(2): p. 439-48.
49. Zhang, J. and P. Zhou, *Ectopic targeting of substrates to the ubiquitin pathway.* Methods Enzymol, 2005. **399**: p. 823-33.

Conclusions and outlook

Table 1. The table summarizes diseases where proteasomes are known to be implicated

Diseases	Defects/symptoms	Proteasome activity
Cancers		
Colon cancer	Mutation in the adenomatous polyposis coli, a regulator of beta-catenin, substrate of the UPS	Increased activity
Breast cancer	Mutation in BRCA1, an E3 enzyme	Increased activity
Ovarian Cancer	Mutation in BRCA1, an E3 enzyme	Increased activity
Multiple myeloma	Suppression of apoptosis,induction of proliferation	Increased activity, depressed expression
Renal carcinoma	Suppression of apoptosis,induction of proliferation	Increased activity, depressed expression
Uterine cervical cancer	HPV-mediated accelerated degradation of p53 by the UPS	Decreased expression, inhibition
Kaposi's sarcoma and KSHV	KSHV virus mediated accelerated degradation	—
Neurodegenerative disorders		
Alzheimer's disease	β-amyloid plaques/tau tangles, neuronal loss	Decreased activity
Parkinson's disease	Lewy bodies, neuronal loss	Decreased activity
Huntington's disease	Poly-glutamine inclusions, neuronal dysfunction/loss	Decreased activity
Polyglutamine disease	Ubiquitinated nuclear inclusions (NI)	Inhibition
Amyotrophic lateral neuron loss	SOD1 aggregates, motor sclerosis	Decreased activity
Prion Disease	Mutant prion protein	Inhibition
Angelman syndrome	Mutation in E6-AP, an E3 enzyme	—
Lafora disease	Accumulation of starch-like polyglucosans, or Lafora bodies	Decreased activity
Viral infections		
HIV/adenovirus	—	—
Hepatitis B	Hepatitis	Inhibition
HTLV	—	—
Cardiac dysfunction		
Transient ischemia/Reperfusion	—	—
Pressure overload	—	—
Inclusion body myositis	—	—
Autoimmune/rheumatoid Diseases		
Sjogren's syndrome	Tissue destruction	Decreased expression
Other Disorders		
The Liddle Syndrome	Mutation in the β/γ subunit of a renal sodium channel, a substrate of the UPS	Inhibition
Cystic fibrosis (CF)	Mutation in CFTR, DF508	Increased activity
α_1-antitrypsin deficiency	Mutation in α_1-antitrypsin (Z)	Accelerated degradation
Wilson's disease	Mutation in Wilson protein	Accelerated degradation
Fanconi anemia	Mutation in the FANCD2 protein, a substrate UPS	—

Table 1: The table was adapted from [1].

A wide variety of human diseases, including neurodegenerative disorders, cancer, inflammatory diseases, hypoxia, genetic diseases and muscle wasting disorder, involve the ubiquitin proteasome pathway [1, 2]. An overview of different aberrations in the ubiquitin proteasome system (UPS), which have been implicated in the pathogenesis of many inherited and acquired pathologies is given in Table 1.

Alterations in the expression of the UPS genes can result in uncontrolled and/or accelerated degradation of a substrate (loss of function). Enhanced removal of tumor suppressors, such as p53 and p27, are involved in the pathogenesis of malignancies. Levels of p53, the "guardian of the genome", are mostly controlled by the ubiquitin ligase MDM2. A subset of human tumors has been shown to contain amplifications of the *mdm2* gene, leading to over-expression of Mdm2 [3]. Also, a naturally occurring polymorphism within the *mdm2* promoter, leading to increased Mdm2 protein in human populations, may account for variations in some individuals' susceptibility to cancer and accelerated tumor formation [4, 5]. p27 is, like p53, a negative cell-cycle regulator, its degradation by the ubiquitin ligase SCF^{skp2} regulates progression into mitosis. p27 level is markedly reduced in a wide range of human cancers where skp2 is overexpressed [6].

Other pathologies are due to the stabilization of a substrate that can result from mutational inactivation of the ubiquitination machinery involved in its degradation, or mutation of the substrate itself, which prevents its recognition and/or proteasomal degradation (gain of function). Autosomal-recessive juvenile Parkinson disease (PD) is in 50% of the patients associated to mutations and deletions in the Parkin gene [7]. Parkin encodes a RING-finger protein with E3 ligase activity. Recently, it was witnessed to form a complex with two other proteins, also linked to early onset familial form of PD, pten-induced putative kinase 1 (*PINK1*) and *DJ-1* [8], which enhanced its ubiquitin ligase activity. This PPD complex could constitute a novel kind of E3 ligase complex, which seemed to play an important role in promoting degradation of un-/misfolded Parkin substrates. Relevant substrates of Parkin are not known, but Parkin can protect dopaminergic cells from neurotoxicity, probably by degrading yet unknown proteins [9]. VHL ubiquitin ligase is mutated in all renal cell carcinomas and in von Hippel-Lindau syndrome, which is characterized by highly vascularized tumors. Its principal substrate, HIF1α, the hypoxia inducible transcription factor, is stabilized and leads to activation of hypoxia-responsive genes, in the presence of oxygen, such as the vascular endothelial growth factor (VEGF), which stimulates angiogenesis [2, 9]. Huntington disease is caused by a mutation, leading to an abnormal expansion of CAG trinucleotides in the gene encoding the huntingtin, a protein which may be involved in gene transcription [10]. This mutation confers a toxic gain-of-function on the mutant protein, as the polyglutamine tract can form amyloid-like fibrils, which can form aggregates in the cytoplasm and/or nucleus, a hallmark of the disease. Several data suggest that Huntingtin may be a proteasome substrate and that eukaryotic proteasomes cleave proteins with expanded polyglutamine sequences very slowly, if at all [11]. It was then proposed that these polyglutamine proteins would impair the UPS, but this model is controversial as several conflicting sets of data have been reported [10].

Now that several components of the UPS could be linked to the initiation and/or progression of specific human pathologies, their potential as targets for therapeutic strategies are being investigated (Fig. 2). The proteasome itself was first successfully targeted by the proteasome inhibitor Bortezomib (Velcade)

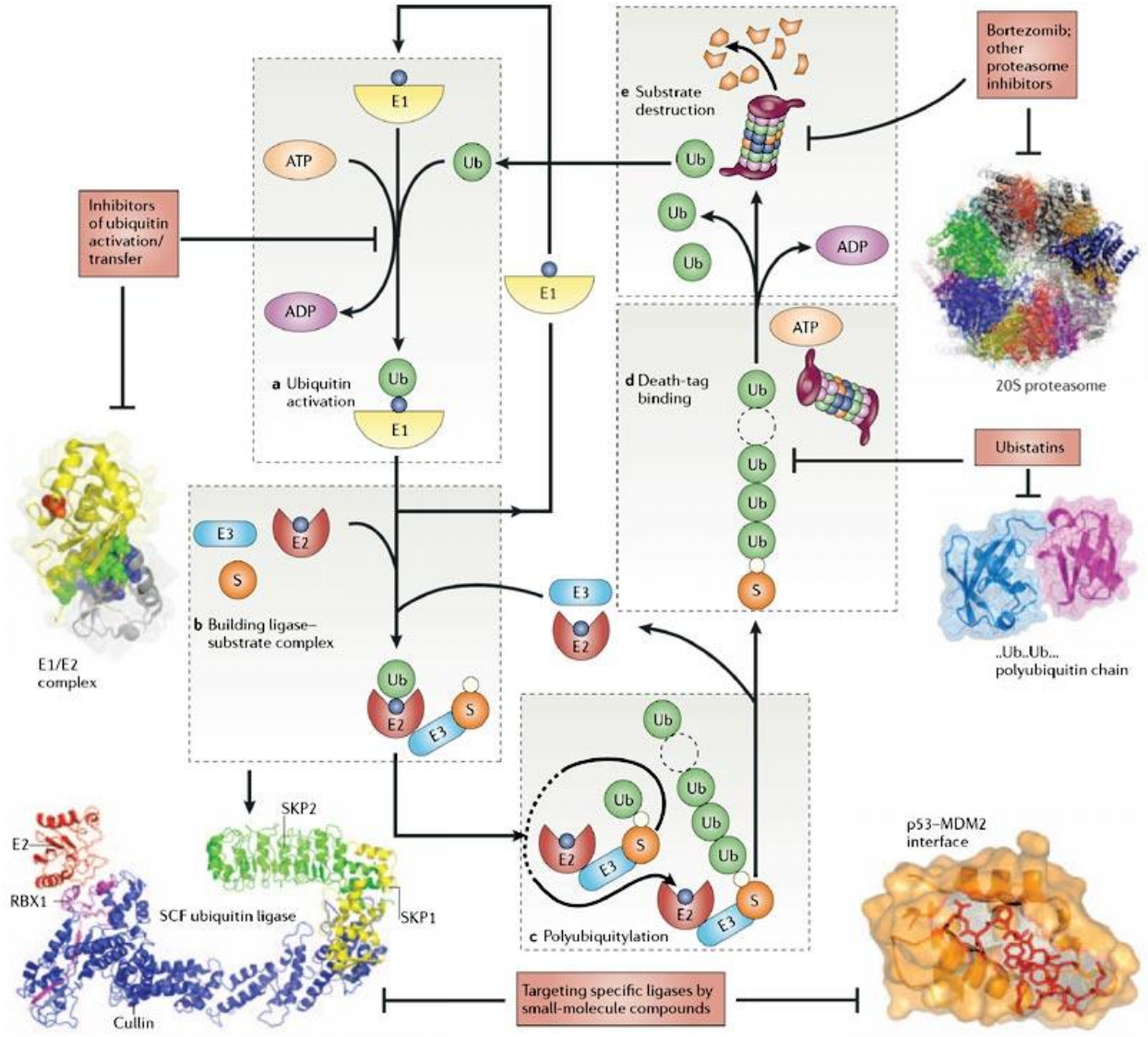

Figure 1: Overview of the ubiquitin proteasome system (UPS) and potential sites for drug development. Protein degradation through the UPS is a highly regulated process, involving several steps. The first step in the cascade is ubiquitin activation by E1 (ubiquitin-activating enzyme) followed by ubiquitin delivery to E2 (ubiquitin-conjugating enzyme) (a). The second step involves complex formation by E2-Cys ~ Ub, E3 (ubiquitin ligase) and the substrate (b). The third step (c) comprises transfer of ubiquitins to the substrate lysine(s) to earmark the substrate with a polyubiquitin chain. In the fourth step of the pathway (d), a polyubiquitylated substrate is released from E3. Proteasomes recognize the polyubiquitin chain as a signal to de-ubiquitylate and destroy the substrate. The fifth step seals the fate of a doomed protein (e). The proteasome removes the ubiquitin chain, and threads the unfolded protein into the proteasome chamber, where the protease active sites are located. The ubiquitin molecules are recycled, and the peptides generated are used in major histocompatibility class I-coupled antigen presentation or degraded to amino acids that are recycled for new protein synthesis. Potential sites for drug development are shown in red colored boxes. MDM2, double minute 2; SCF, SKP1–Cullin–F-box; SKP, S-phase kinase-associated protein; RBX, RING-box protein. Adapted from [9].

(Millenium Pharmaceuticals, Cambridge, MA) [9]. This tripeptide boronic acid (PS341) was the first UPS targeting drug approved by the FDA, for the treatment of multiple myeloma patients, as a second line therapy. Surprisingly, this reversible proteasome inhibitor showed specificity towards cancer cells, it seemed to downregulate the pro-oncogenic NF-κB pathway [12]. Additionally, it is thought that proteasome inhibition might lead to accumulation of misfolded proteins in the ER, inducing unfolded protein response, and cell death. Alternatively, interfering with polyubiquitin chain recognition at the proteasome site is another approach for inhibition of the UPS. Small-molecule inhibitors, called ubistatins, identified by a chemical genetic screen performed in Xenopus extracts, bind to the hydrophobic interface of the Lys48-linked polyubiquitin chains, and prevent recognition of ubiquitinated substrates by ubiquitin-chain receptors of the proteasome [13].

Targeting other compounds of the UPS may open the door to other therapeutic interventions. Inhibitors of E1, the ubiquitin activating enzyme, through blocking access of ATP, could prevent ubiquitin activation, the first step of the ubiquitination cascade [9]. Otherwise, inhibiting the interaction transfer at the E1/E2 level could put a stop to the transfer of the activated ubiquitin molecule onto the ubiquitin conjugating enzyme (E2) [9]. According to previous studies, E1 inhibitors might provoke cell-cycle arrest and thus counteract hyperproliferative pathologies, but they might also have side-effects on other pathways [9].

Regulating the activity of certain proteins via attacking E3 ligases, the specificity module for the ubiquitination reaction, would increase the specificity of the therapy and eliminate side-effects. In the past decade, the biotech and pharmaceutical industries have sought to target specific E3 ligases by developing inhibitors and agonists [14]. Small molecule inhibitors, called nutlins, were identified in a chemical library screen, to inhibit the interaction between mdm2 and p53 [9]. Nutlins could activate p53-dependent cell-cycle arrest and apoptosis. However, these anti-mdm2 compounds are not specific for p53 and may compete with other mdm2 substrates [12]. Alternatively, another hit originating from a chemical library screen, called RITA, was identified to bind the N-terminus of p53 and prevent its interaction with mdm2. However, RITA does also affect p53 interaction with other binding partners. SCF^{skp2} is also a highly interesting pharmacological target. Preventing the interaction of the F-box subunit skp2 with its substrate p27 is likely to be beneficial to slow down proliferation of cancer cells [9]. On the other hand, promoting the activity of certain E3 enzymes could also be beneficial. SCF^{Fbxw7} degrades oncoproteins, such as c-Myc or cyclin E. The binding pocket of F-box protein Fbxw7 is mutated in several types of cancers, leading to a high expression level of its substrates. Identifying an agonist of Fbxw7 would be challenging, even if not as much as reactivating a mutant allele. Restoring the activity of the VHL ubiquitin ligase, which fails to degrade HIF1α, which in turn promotes angiogenesis, could be of interest as well, to reduce tumor vascularization. The advantages in inhibiting or activating certain E3 ligases are numerous but the strategies do need to be highly specific.

Targeted degradation of a specific protein would offer a new strategy for the removal of oncoproteins, and other proteins, which the UPS fails to degrade, and can ultimately be toxic for the cell, e.g. stabilized substrates in neurodegenerative diseases or viral proteins. Moreover, the degradation of a key viral protein should not only prevent the virus multiplication but also increase the host immune response, as proteasome-processed viral peptides are presented onto MHC I molecules.

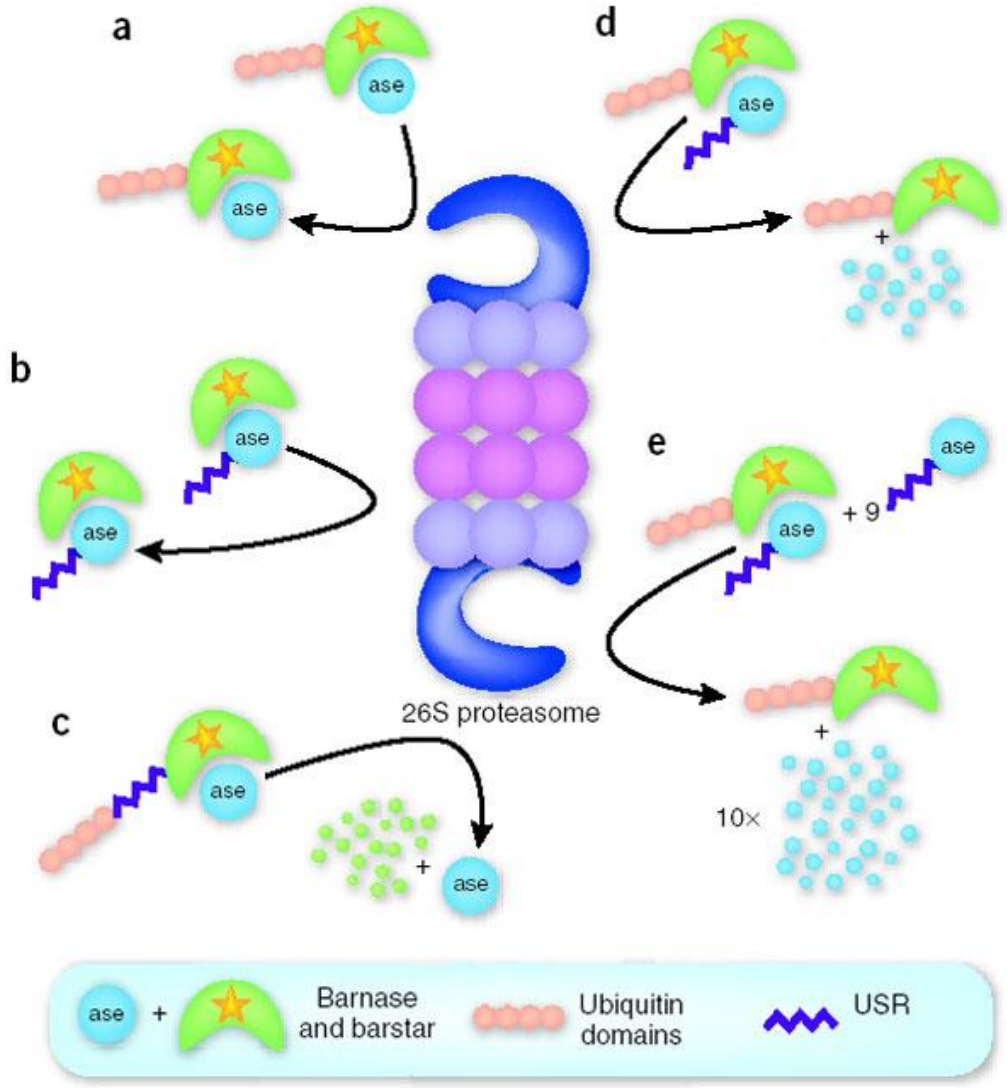

Figure 2: Schematic representation of the bimolecular complexes, designed and tested by Prakash et al [15], as substrate for the proteasome and their outcome. Barnase and/or Barstar are equipped with ubiquitin molecules and /or an unstructured region (USR). (a**) Barnase lacking a USR is stable when presented to the proteasome by ubiquitinated barstar. (**b**) Barnase displaying a USR is not degraded if barstar is not ubiquitinated. (**c**) Ubiquitinated barstar displaying a USR is degraded by the proteasome, but barnase is stable. (**d,e**) When ubiquitinated barstar delivers a USR-displaying barnase to the proteasome, the barnase is proteolyzed but the ubiquitinated barstar is spared (**d**). Ubiquitinated barstar was capable of 'turning over' multiple copies of a USR-displaying barnase (in 1o-fold excess) for proteasome-mediated degradation (**e**). Adapted from [16].**

Several protein knock-out techniques were developed (as reviewed in the introduction of Chapter 3), but despite their promises, engineered degradation has so far been successfully applied to very few proteins only, and every time redesigned case by case. As almost all of them were limited by the lack of known binding motifs, we chose to use a common binding scaffold, DARPins, for the engineering of diverse effector proteins, meant to degrade a target protein. Furthermore, we wanted to design effector proteins, which would only minimally interfere with the cell metabolism (by not relying on existing molecules), and would be able to lead any kind of target protein to the proteasome. By choosing MBP, an exogenous stable protein as target protein, we wanted to further assess the potential of protein knock-out.

The chimeric F-box strategy (described in Chapter 1) showed only limited success in yeast. As expected, the chimeric F-box protein seemed to be functional as it was mediating degradation of the target protein and, was itself degraded by the proteasome, like natural F-box proteins. To circumvent the ubiquitination step, which might have been too restrictive for "foreign" substrate, another strategy relying on DARPin-degron constructs (described in Chapter 2 and 3) was established. These molecules were efficiently recognized and degraded by the proteasome, but they failed to co-lead a target protein for degradation. Our results were thus not as convincing as those earlier described by the different groups, who had developed similar techniques but for however only very specific cases, not allowing any generality.

A very recent study might partially explain why our attempts to increase the capacity of protein knock-out, were not awarded. Prakash et al [17] proposed earlier that the presence of an unstructured region (USR) in a proteasome substrate serves as inititation site for protein degradation and could also be a second component of the targeting signal, in addition to the ubiquitin chain. Recently, Prakash and colleagues [15], further assessed the importance of these two structural features for the proteasome when selecting substrates in a protein complex. They used a bimolecular complex made of barnase and barstar as substrate, and appended to these molecules either an ubiquitin signal and/or an unstructured region (USR), and monitor their fate in the presence of reticulocyte lysate or purified yeast proteasome (Fig. 3). A single protein bearing only one sort of signal was stable but with both signals, it was efficiently degraded (Fig. 3a,b,c). The USR could lead a target protein to degradation, but only if associated with an ubiquitin signal, present on the target protein itself or carried by the binding partner (Fig. 3c,d). Strikingly, the co-degradation of the ubiquitinated binding partner was occurring only, when an USR was also present in its sequence. In other words, they demonstrated that an ubiquitinated member of a complex could act in trans and catalytically (Fig. 3e), like an adaptor for the proteasome, leading multiple copies of USR-containing partner to degradation, but only if it did not contain itself an initiation site. In such a complex, the substrate specificity was then determined primarily by the presence of an initiation site, rather than by the location of the ubiquitin modification. Additionally, the chemical properties of the initiation site added another substrate selectivity level as certain unstructured regions were more favorable [15, 18].

These latter results would explain why MBP, a tightly folded protein, was not co-degraded with a DARPin-degron construct. It is likely that both proteins could form a complex, which was brought to the proteasome but that the DARPin-degron construct was a much more favorable substrate for the

proteasome, which then spared the MBP. It cannot also be excluded that our chimeric F-box protein, which was also degraded by the proteasome, and even more readily than MBP, might even have been competing with MBP and decreasing its degradation. In other words, the chimeric F-box protein could have, after mediating MBP ubiquitination and thus promoting its recognition by the proteasome, inhibiting its degradation in a second step.

Protein degradation represents an underexamined dimension of proteomics. All data, which can be gathered regarding the ubiquitination machineries, the protesomal degradation mechanism and the requirements for an appropriate substrate, are urgently needed and will be determinant for better understanding this highly elaborated turnover system. Even so, as more and more information has emerged since the discovery of the ubiquitin proteasome pathway by Aaron Ciechanover, Avram Hershko and Irwin Rose, all awarded by the chemistry Nobel prize in 2004, the difficulty lies in assembling it in a comprehensible manner. Mixed signals do emerge from varying studies, it is thus likely that all substrates are not handled similarly by the proteasome, making it even more challenging to draw conclusions.

However, the potential of protein knock-out has been long known and exploited by viruses. Since the observation that HPV E6 targets p53 for ubiquitination, numerous other viral proteins have been identified, which induce degradation of cellular proteins in order to better escape the immune response and ease their progragation [19, 20]. To achieve degradation, viral proteins can manipulate the host ubiquitination machinery [21]or bypass it and go directly to the proteasome [22]. Interestingly, while already working on our chimeric F-box protein strategy, poxviruses appeared to have evolved a unique class of F-box proteins, based on the use of the ANK repeat motif for the substrate recognition domain [23]. Their design is close to ours, except that the domain orientation is inverted, the ANK domain lies N-terminally while the F-box domain lies C-terminally, and is shorter than other cellular F-box motifs (approximately 30 residues instead of 45). Poxvirus ankyrin repeat proteins can interact with the host SCF ubiquitin ligase complex and most likely use it to redirect the degradation of specific cellular proteins [24, 25]. Substrates have not been identified yet but one of these F-box proteins was shown to colocalize with NF-κB and interfere with inflammation [24].

To conclude, it appears that reaching the gate of the proteasome, via a polyubiquitin signal or a degron sequence, might not be enough for accessing its safe chamber. A few candidates might success, escape the controls and be rewarded but most of them will be driven back, if they are not structurally adapted. Other stratagems may be developed, but the future potential of protein knock-out techniques will be most likely restricted to a certain type of protein substrates.

References

1. Paul, S., *Dysfunction of the ubiquitin-proteasome system in multiple disease conditions: therapeutic approaches.* Bioessays, 2008. **30**(11-12): p. 1172-84.
2. Schwartz, A.L. and A. Ciechanover, *Targeting proteins for destruction by the ubiquitin system: implications for human pathobiology.* Annu Rev Pharmacol Toxicol, 2009. **49**: p. 73-96.
3. Iwakuma, T. and G. Lozano, *MDM2, an introduction.* Mol Cancer Res, 2003. **1**(14): p. 993-1000.
4. Bond, G.L., et al., *A single nucleotide polymorphism in the MDM2 promoter attenuates the p53 tumor suppressor pathway and accelerates tumor formation in humans.* Cell, 2004. **119**(5): p. 591-602.
5. Bond, G.L., W. Hu, and A.J. Levine, *MDM2 is a central node in the p53 pathway: 12 years and counting.* Curr Cancer Drug Targets, 2005. **5**(1): p. 3-8.
6. Frescas, D. and M. Pagano, *Deregulated proteolysis by the F-box proteins SKP2 and beta-TrCP: tipping the scales of cancer.* Nat Rev Cancer, 2008. **8**(6): p. 438-49.
7. Hattori, N. and Y. Mizuno, *Pathogenetic mechanisms of parkin in Parkinson's disease.* Lancet, 2004. **364**(9435): p. 722-4.
8. Xiong, H., et al., *Parkin, PINK1, and DJ-1 form a ubiquitin E3 ligase complex promoting unfolded protein degradation.* J Clin Invest, 2009. **119**(3): p. 650-60.
9. Nalepa, G., M. Rolfe, and J.W. Harper, *Drug discovery in the ubiquitin-proteasome system.* Nat Rev Drug Discov, 2006. **5**(7): p. 596-613.
10. Imarisio, S., et al., *Huntington's disease: from pathology and genetics to potential therapies.* Biochem J, 2008. **412**(2): p. 191-209.
11. Venkatraman, P., et al., *Eukaryotic proteasomes cannot digest polyglutamine sequences and release them during degradation of polyglutamine-containing proteins.* Mol Cell, 2004. **14**(1): p. 95-104.
12. Hoeller, D. and I. Dikic, *Targeting the ubiquitin system in cancer therapy.* Nature, 2009. **458**(7237): p. 438-44.
13. Verma, R., et al., *Ubistatins inhibit proteasome-dependent degradation by binding the ubiquitin chain.* Science, 2004. **306**(5693): p. 117-20.
14. Hjerpe, R. and M.S. Rodriguez, *Alternative UPS drug targets upstream the 26S proteasome.* Int J Biochem Cell Biol, 2008. **40**(6-7): p. 1126-40.
15. Prakash, S., et al., *Substrate selection by the proteasome during degradation of protein complexes.* Nat Chem Biol, 2009. **5**(1): p. 29-36.
16. Wandless, T.J., *The proteasome makes sense of mixed signals.* Nat Chem Biol, 2009. **5**(1): p. 3-4.
17. Prakash, S., et al., *An unstructured initiation site is required for efficient proteasome-mediated degradation.* Nat Struct Mol Biol, 2004. **11**(9): p. 830-7.
18. Verhoef, L.G., et al., *Minimal length requirement for proteasomal degradation of ubiquitin-dependent substrates.* Faseb J, 2009. **23**(1): p. 123-33.
19. Barry, M. and K. Fruh, *Viral modulators of cullin RING ubiquitin ligases: culling the host defense.* Sci STKE, 2006. **2006**(335): p. pe21.
20. Zeng, L.R., et al., *Ubiquitination-mediated protein degradation and modification: an emerging theme in plant-microbe interactions.* Cell Res, 2006. **16**(5): p. 413-26.
21. Yu, X., et al., *Induction of APOBEC3G ubiquitination and degradation by an HIV-1 Vif-Cul5-SCF complex.* Science, 2003. **302**(5647): p. 1056-60.
22. Isono, O., et al., *Human T-cell leukemia virus type 1 HBZ protein bypasses the targeting function of ubiquitination.* J Biol Chem, 2008. **283**(49): p. 34273-82.

23. Mercer, A.A., S.B. Fleming, and N. Ueda, *F-box-like domains are present in most poxvirus ankyrin repeat proteins.* Virus Genes, 2005. **31**(2): p. 127-33.
24. Sonnberg, S., et al., *Poxvirus ankyrin repeat proteins are a unique class of F-box proteins that associate with cellular SCF1 ubiquitin ligase complexes.* Proc Natl Acad Sci U S A, 2008. **105**(31): p. 10955-60.
25. van Buuren, N., et al., *Ectromelia virus encodes a novel family of F-box proteins that interact with the SCF complex.* J Virol, 2008. **82**(20): p. 9917-27.

Acknowledgements

I want to thank Prof. Dr. Andreas Plückthun for his trust, by allowing me to start my own project and giving me the complete liberty to lead it and shape it as I wanted. Thanks for the valuable discussions and support throughout these five years.

I wish to thank Prof. Dr. Matthias Peter for giving me the opportunity to work in his laboratory, learn all the fundamental yeast techniques and being part of my thesis committee. I also want to thank many of his previous collaborators for their readiness to help and to answer questions, especially Brian Luke, Sarah Luke-Glaser, Fabian Rudolf and Michael Olma.

I am also grateful to Prof. Dr.Peter Sonderegger and especially to Dr. Olivier Coux, the two other members of my thesis committee for taking the time to follow and assess my work during the entire thesis.

I want to acknowledge Dr. Peter Lindner, our indispensable “lab manager” and Dr. Birgit Dreier for facilitating our daily work by carefully organizing the “AP unit”.

Big thanks to ALL previous and current Plückies! I really enjoyed working and participating to extra-work activities with you. I don’t think one can go through a Ph.D without the support of its labmates. I really met a lot of nice people during these five years…. from Reto, Manca, Ernsti, Holgi, Petra and others who welcomed me so warmly in the AP group ….to Karola, Igor and Mark, with whom I had an awesome time in M94, what a “ CONSTANT very nice atmosphere”, it was! I will definitely miss our up-to-date-gossip-sessions and our laughing times. I also want to thank Jonas, for his positive energy and Fabio for being not only a supportive labmate but also a good friend. Apparently we were meant to work once in the same group.

Finally I want to thank my relatives and friends who were kind enough to ask about the progress of my thesis at the beginning and smart enough for not asking any more after the third year. I am grateful to my mother who blindly supported me and all my friends who helped me to balance my work life with lots of fun times, especially to Maud, Sandra, Delph, Seb, Erica, Peter and Sarah. Last but not least, I want to thank Thibault for endlessly believing in me and cheering me up. This thesis was also yours; we went through it together, even despite the distance, …merci!

Curriculum vitae

Myriam Vincent

Born 28th December 1978, in Besançon (France)
Citizenship: French

EDUCATION

2004-2009	Molecular Life Sciences PhD program Subject: Designed degradation of a specific protein in the cell Laboratory of Prof. Andreas Plueckthun Department. of Biochemistry, University of Zuerich, Switzerland
1999-2002	Engineer degree in biotechnology (Dipl.Biotech) (5th out of 40) and D.E.A. degree (validating the first year of a Ph.D.program in biotechnology) Ecole Supérieure de Biotechnologie de Strasbourg Louis Pasteur University, Strasbourg, France
1998-1999	Licence de biochimie (4th out of 89) (biochemistry degree) Franche-Comté University, Besançon, France
1996-1998	DEUG de biologie cellulaire (1st out of 130) (validating the first 2 years of university) Franche-Comté University, Besançon, France
1996	Baccalauréaut scientifique, passed with distinction (equivalent to A-levels) Lycée Jean-Michel, Lons-Le-Saunier, France

TRAINING

2002-2004	New England Biolabs Inc., Beverly, Massachusetts, USA Research Associate in the research and development department Development of a new patented technology: Helicase Dependent Amplification of Nucleic Acids, on which was launched the spin-off company: Biohelix Corporation
2002	New England Biolabs, Inc., Beverly, Massachusetts, USA Intern (M.S. thesis) in the research and development department (8 months) Establishment of a new Nucleic Acid Amplification Technique
2001	Institut de Génétique et Biologie Moléculaire et Cellulaire, Strasbourg, France Intern at the Microarray Platform (1 month) Validation of a new DNA chips

2001 bioMerieux S.A., Marcy l'Etoile, France
Technician in the department of immunoassays (5 weeks)
Optimization of an ELISA test for the toxoplasmosis

2000 University of Basel, Biozentrum, Dept. of Molecular Microbiology, Switzerland
Internship in the Laboratory of Prof. Peter Philippsen (6 weeks)
Construction of knock-out mutants for genes involved in the nuclear migration of *A.gossypii*

1999 bioMerieux S.A., Marcy l'Etoile, France
Intern in the department of immunoassays (3 months)
Optimization of an ELISA test with cardiac markers

PUBLICATIONS AND PATENTS

Jianbin Wang, Yan Jiang, **Myriam Vincent**, Yongqiao Sun, Hong Yu, Jing Wang, Qiyu Bao, Huimin Kong and Songnian Hu.
Complete genome sequence of bacteriophage T5.(2005). *Virology*, 332, 45-65.

Myriam Vincent, Yan Xu and Huimin Kong
Helicase-dependent isothermal DNA amplification. (2004). *EMBO reports*, 5, 8, 795-800.

Helicase dependent amplification of nucleic acids.
Patent Cooperation Treaty international publication number: WO 2004, 20040058378
Huimin Kong, **Myriam Vincent**, Yan Xu

GRANTS

Recipient of the Forschungskredit of the University of Zürich from November 2005 to October 2007